UNIVERSITY OF CALIFORNIA
RIVERSIDE

Extensions of the Standard Model with Dark Matter in Some Explicit Examples

A Dissertation submitted in partial satisfaction
of the requirements for the degree of

Doctor of Philosophy

in

Physics

by

Mohammadreza Zakeri Niasar

September 2017

Dissertation Committee:

Dr. Ernest Ma, Chairperson
Dr. Hai-Bo Yu
Dr. Philip Tanedo

The Dissertation of Mohammadreza Zakeri Niasar is approved:

Committee Chairperson

University of California, Riverside

Acknowledgments

I wish to thank all my teachers who contributed to my education.

I would like to thank my advisor, Dr. Ernest Ma for his guidance. I am also very grateful to Dr. Hai-Bo Yu and Dr. Flip Tanedo for their support and dedication.

I would also like to thank Dr. Sean Fraser for being patiently helpful during my PhD, and Dr. Alexander Natale for sharing his knowledge with our research group.

I am deeply indebted to my lovely girlfriend Ashley, Mom, Dad, and my sisters Sahar & Negar for their ceaseless support. I especially thank Ashley for the enlightening discussions which helped me in having a better understanding of myself and the world around me.

I like to thank all my friends in Riverside with whom I had joyful memories that I will never forget.

This thesis is based on previously published papers, in collaboration with S. Fraser [1–3], E. Ma [1–8], O. Popov [3, 5, 7, 8], C. Kownacki [3, 6–8], N. Pollard [3–8], and R. Srivastava [4].

I humbly dedicate this thesis to my caring parents, Mahbobeh & Mohsen for all their support.

ABSTRACT OF THE DISSERTATION

Extensions of the Standard Model with Dark Matter in Some Explicit Examples

by

Mohammadreza Zakeri Niasar

Doctor of Philosophy, Graduate Program in Physics
University of California, Riverside, September 2017
Dr. Ernest Ma, Chairperson

The compelling astrophysical evidence for dark matter on one hand and the experimental evidence for neutrino masses on the other, demands modifications beyond the Standard Model. Therefore, building new models by extending the symmetries and particle content of the Standard Model is being pursued to remedy these problems. In this thesis, various models along with their predictions are presented. First, a gauge $SU(2)_N$ extension of the Standard Model, under which all of the Standard Model particles are singlet is introduced. The inverse seesaw mechanism is implemented for neutrino mass, with the new gauge boson as a dark matter candidate. The second paper is a gauge B-L extension of the Standard Model which breaks down to $\mathbb{Z}_3$, and it includes a long-lived dark matter candidate. The next model assumes that leptons do not couple directly to Higgs, and one loop mass generation is considered with important consequences, including Higgs decay, muon anomalous magnetic moment, etc. We then look at a U(1) gauge extension of the supersymmetric Standard Model, which has no μ term, and the Higgs boson's mass supersymmetric constraint is relaxed. The next model is a gauge B-L extension of the Standard

Model with radiative seesaw neutrino mass and multipartite dark matter. We then consider another gauge U(1) extension under which quarks and leptons of each family may transform differently, while flavor-changing interactions are suitably suppressed. The next paper has an unbroken gauge SU(2) symmetry, which becomes confining at keV scale. We discuss the cosmological constraints and the implications for future e^+e^- colliders. Finally, an alternative left-right model is proposed with an automatic residual $Z_2 \times Z_3$ symmetry, such that dark matter has two components, i.e., one Dirac fermion and one complex scalar.

Contents

List of Figures

List of Tables

Chapter 1

Introduction

This thesis is divided into three parts. First, a short introduction to the Standard Model and models beyond this framework is presented. Second part is the main part of the thesis, which covers detailed description of various models. The last part includes the conclusions, the bibliography, and the appendices.

We start by a brief historical introduction, followed by a short description of the Standard Model, a summary of neutrino mass and oscillation, and dark matter physics. The two latter subjects are the main focus of this thesis.

1.1 Historical Introduction

Radioactivity in uranium was discovered by H. Becquerel in 1896 [9]. Later in 1899, E. Rutherford classified radioactive emissions based on penetration of objects into two types: alpha and beta. Beta rays could penetrate several millimeters of aluminum.

In 1900, Becquerel found the mass-to-charge ratio (m/e) to be the same as cathode rays, which suggests that beta rays are also electrons.

Two puzzling issues arose during the following years of studying beta decay spectrum. These were the violation of conservation of energy and angular momentum. In 1930, W. Pauli postulated [10] the existence of light neutral (spin 1/2) particles which he called "neutron", as a "desperate remedy" to the beta decay issues. One year later in 1931, E. Fermi renamed Pauli's "neutron" to neutrino[1]. In 1933, Fermi proposed an explanation for the beta-decay [11]. This was the first theory of the weak interaction, known as Fermi's interaction. Beta decay could be explained by a four-fermion interaction, involving a contact force with no range. This theory was successful in describing the weak interactions at low energies (less than ~ 100 GeV). However, the calculated cross-section grows as the square of the energy (without bound), which suggested a more complete theory (UV completion) was needed.

In 1927, P. A. M. Dirac published his theory of the interaction of electromagnetic waves with atoms. In his paper [12], Dirac was able to compute the Einstein's coefficients of spontaneous emission of an atom. In the following years, Many physicists contributed to the formulation of quantum electrodynamics. In 1937, F. Bloch and A. Nordsieck discussed the infinite low frequency corrections to the transition probabilities [13]. These corrections are logarithmically divergent with no classical counterpart ("infrared catastrophe"). Two years

[1]Two years after Pauli's proposal, neutrons were discovered by J. Chadwick. In 1934, when Fermi was explaining his theory of beta-decay, he clarified that he was talking about a different particle. He referred to it as neutrino ("little neutral one").

later in 1939, V. Weisskopf discussed the physical significance of the logarithmic divergence in the self-energy of the electron [14]. The difficulties with the theory persisted during the following years. In 1947, Lamb and Rutherford have shown [15] that the fine structure of the second quantum state of hydrogen does not agree with the prediction of the Dirac theory. In the same year, H. Bethe derived the Lamb shift by proposing a way [16] to absorb the infinities in the definition of the mass of electron ("renormalization"). Subsequent works by S. Tomonaga [17], J. Schwinger [18,19], R. Feynman [20–22] and F. Dyson [23,24] resulted in fully covariant formulations that were finite at any order in a perturbation series of quantum electrodynamics ("QED")[2].

Along with the invention of bubble chamber by D. A. Glaser [28] in 1952, a large number of new particles ("hadrons") were discovered. It seemed implausible that all these particles were fundamental. In 1961, M. Gell-Mann [29] organized spin-$\frac{1}{2}$ baryons into an octet, i.e., an eight-dimensional irreducible representation of SU(3). He was able to predict the existence of another baryon (Ω^-), which was later discovered in 1964 [30]. In the same year and independently of Gell-Mann, Y. Ne'eman [31] suggested a representation for the baryons, based on the SU(3) symmetry. He generated the strong interactions from a gauge invariance principle, involving eight vector bosons. The quark model was independently proposed by Gell-Mann [32] and G. Zweig [33, 34] to explain the structure of the symmetries in hadrons. According to quark model, all hadrons are made up of three flavors of smaller particles inside them, called quarks. Ω^- has strangeness -3, and spin-$\frac{3}{2}$, i.e., it must be composed of three strange quarks with parallel spins. This violates the Pauli ex-

[2]For the proof of renormalizability of YangMills theories see Refs. [25–27].

clusion principle, unless quarks have an additional quantum number ("color")[3] [37, 38]. In 1969, R. Feynman proposed the parton model [39] to explain the high-energy hadron collisions. In parton model, hadrons are composed of point-like constituents called "partons" with a distribution of position or momentum. In 1969, J. D. Bjorken showed [40] that in electron-nucleon deep inelastic scattering, the ratio of cross-section over Mott cross-section[4] ($\sigma_{\rm DIS}/\sigma_0$) is independent of the momentum transfer[5] in parton model. Results from a series of experiments, performed from 1967 through 1973 by a collaboration of scientists from MIT and SLAC, verified the approximate scaling behavior [41], thereby the quark model was established.

The success of QED as a gauge theory, motivated the further development of the theory of weak interactions based on gauge interactions. During the 1960s, S. L. Glashow [42], A. Salam [43] and S. Weinberg [44], independently constructed the gauge-invariant theory of electroweak interactions.

1.2 The Standard Model

We now take a look at the construction of the Standard Model of particle physics. Quarks and leptons are divided into three families (flavors) as follows

$$\text{Quarks:} \quad \begin{pmatrix} u \\ d \end{pmatrix}, \begin{pmatrix} c \\ s \end{pmatrix}, \begin{pmatrix} t \\ b \end{pmatrix}, \qquad \text{Leptons:} \quad \begin{pmatrix} e \\ \nu_e \end{pmatrix}, \begin{pmatrix} \mu \\ \nu_\mu \end{pmatrix}, \begin{pmatrix} \tau \\ \nu_\tau \end{pmatrix}. \tag{1.1}$$

[3] Similar situation occurs with Δ^{++}, which is composed of three up quarks with parallel spins. In 1964, Greenberg [35] and in 1965, Han-Nambu [36] independently resolved this problem by proposing that quarks possess a SU(3) color degree of freedom.

[4] Mott cross-section is for scattering of a lepton (e.g. an electron) on a point-like charged particle.

[5] This behavior is called "Bjorken Scaling".

We would like to assign particles to different representations of gauge group(s). We start by noting that since charged lepton flavor violation processes have not yet been discovered, electron and muon should not be in the same representation of the gauge group, etc. Furthermore, the particles in the same representation of the gauge group should have the same Lorentz transformation. It is then natural to introduce a left-handed doublet (ν_L, e_L) and a right-handed singlet e_R, with a gauge symmetry given by[6]

$$\mathrm{G_{EW}} = \mathrm{SU}(2)_L \times \mathrm{U}(1)_Y. \tag{1.2}$$

If we also add the quarks to our theory, we need to include the SU(3) gauge symmetry, and the complete gauge group of the Standard Model becomes

$$\mathrm{G_{SM}} = \mathrm{SU}(3)_C \times \mathrm{SU}(2)_L \times \mathrm{U}(1)_Y \tag{1.3}$$

Table 1.1: Particle assignments under the SM gauge groups. Note that i is the family index and runs from 1 to 3.

Particle	$\mathrm{SU}(3)_C$	$\mathrm{SU}(2)_L$	$\mathrm{U}(1)_Y$
$Q_{iL} = (u, d)_{iL}$	3	2	1/6
u_{iR}	3	1	2/3
d_{iR}	3	1	$-1/3$
$L_{iL} = (\nu, l)_{iL}$	1	2	$-1/2$
l_{iR}	1	1	-1
$\Phi = (\phi^+, \phi^0)$	1	2	1/2

The transformation of each particle in the Standard Model is given in Table 1.1. There are eight massless vector particles ("gluons") transforming as adjoint representation

[6] In fact the largest gauge symmetry that can be written based on this assignment is $\mathrm{SU}(2)_L \times \mathrm{U}(1)_L \times \mathrm{U}(1)_R$, but it can be shown that one linear combination of the generators of $\mathrm{U}(1)_L \times \mathrm{U}(1)_R$ should be excluded based on empirical reasons. Check section 21.3 of Weinberg's book [45] for detailed discussion of the electroweak theory.

under $\mathrm{SU}(3)_C$. The vector bosons mediating weak force are short-range, and therefore massive, while electromagnetic interactions are mediated by long-range photons. This means the gauge symmetry in Eq. (1.3) should be broken as

$$\mathrm{SU}(3)_C \times \mathrm{SU}(2)_L \times \mathrm{U}(1)_Y \qquad \longrightarrow \qquad \mathrm{SU}(3)_C \times \mathrm{U}(1)_{\mathrm{EM}} \tag{1.4}$$

where the gauge symmetry is spontaneously[7] broken via Higgs mechanism [46–48]. The Higgs particle was discovered in 2012, at the ATLAS [49] and CMS [50] experiments at CERN. The last row in Table 1.1 contains the Higgs field (h), i.e.,

$$\phi^0 = \frac{1}{\sqrt{2}}\,(h + i\,A + v)\,, \quad \text{where} \quad \langle \phi^0 \rangle = \frac{v}{\sqrt{2}}, \quad \text{and} \quad v = 246\,\mathrm{GeV}. \tag{1.5}$$

The charged-lepton masses are generated by the following Yukawa terms

$$-\,\frac{\sqrt{2}\,m_l}{v}\left[\left(\bar{\nu}_L, \bar{l}_L\right) \cdot \Phi \cdot l_R + \mathrm{h.c.}\right] \in \mathcal{L}_{\mathrm{Yuk}}, \tag{1.6}$$

where neutrinos remain massless.

1.3 Neutrino

Neutrinos are spin-$\frac{1}{2}$ neutral light[8] particles. They interact only weakly in the Standard Model. Different flavors are identified based on the charged lepton that accompanies them, i.e., ν_e is the neutrino which is produced with e^+, etc. It is also well-known from the existing data that neutrinos (anti-neutrinos) are always produced in a left-handed (LH) (right-handed (RH)) state. Currently, there is no evidence for the existence of right-handed (left-handed) neutrinos (anti-neutrinos). If they exist, their interaction should be much

[7] In spontaneous symmetry breaking, the Hamiltonian remains invariant under the symmetry, but the ground state is not invariant, e.g. as in ferromagnetism.

[8] With masses less than ~ 0.5 eV.

weaker than the weak interactions, which is why they are called "sterile" or "inert".

The experiments with solar, atmospheric, reactor and accelerator neutrinos have provided compelling evidences for the existence of neutrino oscillations [51, 52]. Neutrino oscillations are transitions between the different flavors of neutrinos ν_e, ν_μ, ν_τ, caused by non-zero neutrino masses and neutrino mixing. Therefore, we can write down the transformation between the mass-eigenstates (ν_{jL}) and the flavor-eigenstates (ν_{lL}) as

$$\nu_{lL} = \sum_{j=1}^{3} U_{lj} \nu_{jL}, \tag{1.7}$$

where U_{lj} is a three dimensional[9] unitary matrix, which is often called the Pontecorvo-Maki-Nakagawa-Sakata (PMNS) mixing matrix and it can be parameterized as

$$U = \begin{bmatrix} c_{12}c_{13} & s_{12}c_{13} & s_{13}e^{-i\delta} \\ -s_{12}c_{23} - c_{12}s_{23}s_{13}e^{i\delta} & c_{12}c_{23} - s_{12}s_{23}s_{13}e^{i\delta} & s_{23}c_{13} \\ s_{12}s_{23} - c_{12}c_{23}s_{13}e^{i\delta} & -c_{12}s_{23} - s_{12}c_{23}s_{13}e^{i\delta} & c_{23}c_{13} \end{bmatrix} \cdot \begin{bmatrix} 1 & 0 & 0 \\ 0 & e^{i\frac{\alpha_{21}}{2}} & 0 \\ 0 & 0 & e^{i\frac{\alpha_{31}}{2}} \end{bmatrix}, \tag{1.8}$$

where $c_{ij} \equiv \cos(\theta_{ij})$, $s_{ij} \equiv \sin(\theta_{ij})$, and $\theta_{ij} \in [0, \pi/2]$. The phases are: one "Dirac phase", $\delta \in [0, 2\pi]$, and two "Majorana phases", α_{21} and α_{31}. The Majorana phases are non-zero, if neutrinos are Majorana particles.

The angles θ_{12}, θ_{23}, and θ_{13} can be written in terms of the elements of the neutrino mixing matrix U_{ij}. The best-fit values of these angles derived from the current neutrino oscillation data [54] is $\theta_{13} \approx 0.15$, $\theta_{12} \approx 0.58$, and $\theta_{23} \approx 0.72(0.85)$[10]. The Dirac phase

[9] The invisible decay width of the Z boson is compatible with only three light neutrinos [53].

[10] For $\Delta m^2 > 0 (< 0)$, where $\Delta m^2 \equiv m_3^2 - (m_2^2 + m_1^2)/2$. Note that we are assuming $m_1 < m_2$, and that $\Delta m_{21}^2 \equiv m_2^2 - m_1^2$ is the smaller of the two neutrino mass squared differences.

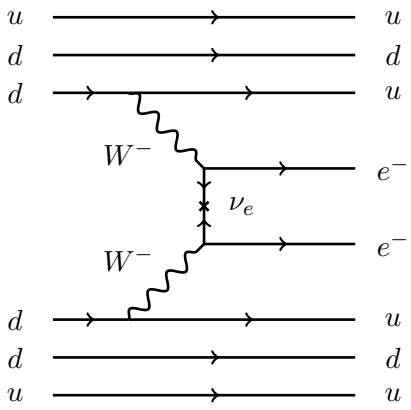

Figure 1.1: Neutrinoless double beta decay process for Majorana neutrinos.

(δ), generates CP violating effects, such that the probabilities of the processes $\nu_l \to \nu_{l'}$ and $\bar{\nu}_l \to \bar{\nu}_{l'}$ ($l \neq l'$) are different. This CP violation is parameterized by the rephasing invariant $J_{\rm CP}$ [55]:

$$J_{\rm CP} \equiv \text{Im}\left(U_{\mu 3} U^*_{e3} U_{e2} U^*_{\mu 2}\right) = \frac{1}{8} \cos\theta_{13} \sin 2\theta_{12} \sin 2\theta_{23} \sin 2\theta_{13} \sin\delta. \tag{1.9}$$

The current best-fit for the Dirac phase is $\delta \approx 3\pi/2$ [54]. The flavor neutrino oscillation probabilities don't depend on the Majorana phases [56, 57]. However, observation of processes like neutrinoless double beta decay (Fig. 1.1[11]) would be evidence for Majorana nature of neutrinos. The amplitude for this process ($0\nu\beta\beta$) is proportional to the effective Majorana mass

$$m_{ee} = |m_1 U^2_{e1} + m_2 U^2_{e2} + m_3 U^2_{e3}|. \tag{1.10}$$

The current limits on m_{ee} depend on the hierarchy of the neutrino mass spectrum[12].

[11] Some of the diagrams in this thesis are generated using tikzfeynman by F. Tanedo, which is based on the TikZ package written by T. Tantau.

[12] For numerical values and a more detailed analysis check [58].

As mentioned before neutrinos remain massless in the Standard Model framework. In the case of Majorana neutrinos, S. Weinberg showed [59] that neutrino mass can be generated via

$$\mathcal{L}_5 = -\frac{f_{ij}}{2\Lambda}\left(\nu_i\phi^0 - l_i\phi^+\right)\left(\nu_j\phi^0 - l_j\phi^+\right) + \text{H.c.} \tag{1.11}$$

where Λ is the scale of the new physics. This effective operator can be UV-completed at tree-level via three different seesaw[13] [60, 61] mechanisms. We can easily see this by noting that there are only three ways [62] that we can combine $\psi_i = (\nu_i, l_i)$, and $\Phi = \left(\phi^+, \phi^0\right)$[14].

1.3.1 Seesaw Type (I)

In this type of models ψ_i and Φ form a fermion singlet. Therefore, the intermediate heavy particle is a fermion singlet (N) as shown in Fig. 1.2, with $\Lambda = M_N$. Note, that in order to generate masses of all (three) families of neutrinos we need three N's.

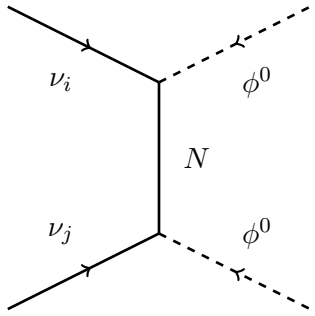

Figure 1.2: Tree-level seesaw with heavy fermion singlet (Type I).

[13] Seesaw mechanism is a generic model used to generate a small mass for neutrinos.
[14] At tree-level and using only renormalizable interactions.

1.3.2 Seesaw Type (II)

In this type of models ψ_i and ψ_j form a scalar triplet [63]. Therefore, the intermediate particle is a heavy scalar triplet, i.e, $\xi = \left(\xi^{++}, \xi^{+}, \xi^{0}\right)$ as shown in Fig. 1.3, with $\Lambda = M^2/2\mu$. Here, μ is the $\xi\phi^0\phi^0$ coupling and M is the mass of the heavy scalar (ξ). In this case only one scalar is enough to generate mass for all neutrinos.

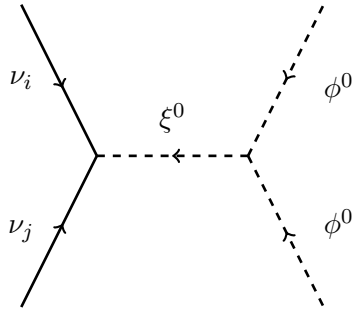

Figure 1.3: Tree-level seesaw with heavy scalar triplet (Type II).

1.3.3 Seesaw Type (III)

In this type of models ψ_i and Φ form a fermion triplet [64]. Therefore, the intermediate particle is a heavy Majorana fermion triplet, i.e, $\Sigma = \left(\Sigma^{+}, \Sigma^{0}, \Sigma^{-}\right)$ as shown in Fig. 1.4.

1.3.4 Scotogenic Model

The effective operator in Eq. (1.11) can also be realized radiatively. Radiative mass generation for neutrinos (and other particles) is one of the main focuses of this thesis, and

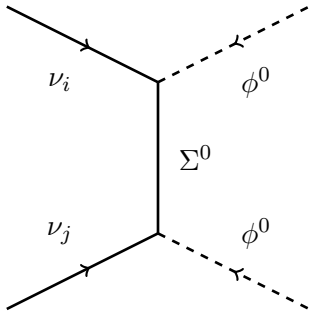

Figure 1.4: Tree-level seesaw with heavy fermion triplet (Type III).

it will be explained in depth in each model [15]. One famous framework is the "scotogenic" model [66], which is a minimal extension of the Standard Model, where neutrinos obtain naturally small Majorana masses from a one-loop radiative (see Fig. 1.5) seesaw mechanism. Three neutral fermions ($N_{1,2,3}$) are added along with a single SU(2) doublet (η), both of which are odd[16] under an additional $\mathbb{Z}_2$ symmetry. This discrete symmetry allows N_i[17] or η to be a stable dark matter candidate. Therefore, tree-level neutrino mass terms are forbidden and a loop-level Majorana mass is generated.

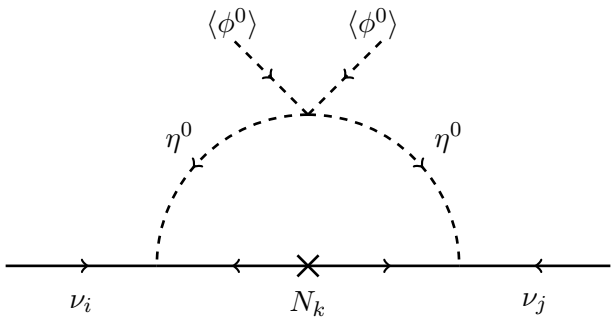

Figure 1.5: Scotogenic mechanism of radiative neutrino mass.

[15] For a brief review of radiative quark and lepton masses, see Ref. [65], and for the Majorana seesaw realizations by E. Ma, see Ref. [62].

[16] The Standard Model particles are even under $\mathbb{Z}_2$.

[17] The lightest mass eigenstate.

1.4 Dark Matter

The first[18] explicit mention of "dark matter" came from H. Poincaré in 1906 [68–70]. He argued that the amount of dark matter was likely to be less than or similar to that of visible matter, based on the velocity dispersion of the stars in the Milky Way predicted by B. Kelvin [71]. Later In 1933, F. Zwicky studied the redshifts of various galaxy clusters, and used the virial theorem in order to estimate the mass of the Coma Cluster [72,73]. In his analysis, he found a high mass-to-light ratio which points to the existence of dark matter. Currently, there are various evidences for the existence of dark matter from rotation curves of spiral galaxies [74–76], strong and weak gravitational lensing [77–80], data from the cosmic microwave background (CMB) [81,82], and from dwarf spheroidal galaxies [83,84].

Throughout this thesis, the assumption is that dark matter is a particle. Dark matter interacts gravitationally, and therefore it must have mass. There are models of dark matter with masses ranging from 10^{-31} GeV [85] to 10^{16} GeV [86]. There are several direct detection experiments for dark matter (e.g., Ref. [87–90]), but so far we haven't detected a signal. Therefore, its interaction with the rest of the Standard Model particles is constrained by these null results.

Dark matter must be stable (as it's usually assumed), or else its life-time should be longer than the age of the Universe. The models with dark matter candidates should predict the correct amount of dark matter today (known as the "relic abundance"). We will

[18] For a historical account of dark matter see Ref. [67].

see how this can sometimes be in conflict with the direct detection null results, and require us to change the model.

One of the most studied classes of dark matter candidates is the Weakly Interacting Massive Particle ("WIMP"). In this scenario, the dark matter candidate was in thermal contact with the cosmic plasma at high temperatures, but as the temperature dropped below its mass it experienced "freeze-out". Freeze-out occurs when the annihilations can't keep the particle in equilibrium[19]. If the annihilation rates were always kept in equilibrium, the relic abundance of dark matter would be suppressed by $e^{-m/T}$, and we would not have dark matter in the Universe now. If we solve the Boltzmann equations for the WIMP scenario, we find that the cross-section of annihilation that (naturally) produces the right amount of dark matter is $\sim 10^{-39}$ cm^2. There is another important theory that predicts the existence of particles with this cross-section, i.e., supersymmetry. In supersymmetry, each boson (fermion) has a fermion (boson) partner with the same mass. Since we haven't observed any of the supersymmetric (SUSY) partners of the Standard Model particles, this symmetry must be broken in nature. These SUSY particles can then be heavy, which explains why they haven't been detected yet. However, experiments have significantly reduced the parameter space for WIMP models. Thereby, shifting the focus away from WIMP paradigm to other dark matter scenarios (e.g., Ref. [91]).

[19] When the rate of annihilations (Γ) falls below Hubble expansion rate (H).

Chapter 2

$\mathbf{SU(2)}_N$ Model of Vector Dark Matter with a Leptonic Connection

2.1 Introduction

Despite the compelling evidence for dark matter, its nature remains unknown. It is usually assumed to be a single particle, but it may also be more than one [92]. In specific models, it is often considered to be a fermion or scalar. However, vector dark matter is certainly also possible [93–100]. In this paper we consider a variant of an $SU(2)_N$ model proposed previously [96,97]. The difference is that in our present study, all standard-model (SM) fermions are singlets under $SU(2)_N$, whereas in the earlier work, that was not the case.

2.2 Model

The new particles of our model are the three neutral gauge bosons $X_{1,2,3}$ of $SU(2)_N$, three copies of a neutral Dirac fermion $SU(2)_N$ doublet $(n_1, n_2)_{L,R}$, a neutral scalar $SU(2)_N$ doublet (χ_1, χ_2), and a scalar bidoublet

$$\zeta = \begin{pmatrix} \zeta_1^0 & \zeta_2^0 \\ \zeta_1^- & \zeta_2^- \end{pmatrix},$$

which transform (vertically) under $SU(2)_L \times U(1)$ and (horizontally) under $SU(2)_N$. The allowed Yukawa and trilinear scalar couplings are

$$(\bar{\nu}_L \zeta_1^0 + \bar{e}_L \zeta_1^-) n_{1R} + (\bar{\nu}_L \zeta_2^0 + \bar{e}_L \zeta_2^-) n_{2R}, \tag{2.1}$$

$$(\phi^0 \zeta_1^0 - \phi^+ \zeta_1^-) \chi_1 + (\phi^0 \zeta_2^0 - \phi^+ \zeta_2^-) \chi_2. \tag{2.2}$$

In analogy to the earlier work [96, 97], we impose a global $U(1)$ symmetry S' on the new particles so that n and χ have $S' = 1/2$ and ζ has $S' = -1/2$. As χ_2 breaks $SU(2)_N$ completely, $T_{3N} + S' = S$ remains exact, under which $n_1, \chi_1 \sim +1$, $n_2, \chi_2, \zeta_2 \sim 0$, and $\zeta_1 \sim -1$. As for the vector gauge bosons, $X(\bar{X}) = (X_1 \mp i X_2)/\sqrt{2} \sim \pm 1$ and $Z' = X_3 \sim 0$. Note that S' distinguishes the bidoublet ζ from its dual $\tilde{\zeta} = \sigma_2 \zeta^* \sigma_2$, and forbids certain terms in the Lagrangian which would be otherwise allowed. In Refs. [96, 97], the residual $U(1)$ symmetry S is broken explicitly to $(-1)^S$. Here it remains exact up to possible Planck scale corrections, but for the stability of dark matter on the scale of the lifetime of the Universe, this is not a serious concern. Note that without ζ, the dark sector would only communicate with the SM through the Higgs portal. Here ζ serves another purpose, i.e. neutrino mass. This connection is of course an assumption of the model, but once chosen, it leads naturally to an inverse seesaw mechanism for neutrino mass [101–103].

2.3 Neutrino Mass

Consider first the neutrino mass matrix spanning $(\bar{\nu}_L, n_{2R}, \bar{n}_{2L})$, i.e.

$$\mathcal{M}_{\nu n} = \begin{pmatrix} 0 & m_D & 0 \\ m_D & 0 & M \\ 0 & M & 0 \end{pmatrix}, \tag{2.3}$$

where m_D comes from $\langle \zeta_2^0 \rangle$ and M is an allowed invariant mass. It is clear that this results in one heavy Dirac fermion and one massless neutrino corresponding to $\cos\theta \nu_L - \sin\theta n_{2L}$, where $\tan\theta = m_D/M$. As such, lepton number L is conserved, with $n_{1,2}$ also having $L = 1$

To obtain a nonzero neutrino mass, a scalar triplet Δ under $SU(2)_N$ is required. Let

$$\Delta = \begin{pmatrix} \Delta_2/\sqrt{2} & \Delta_3 \\ \Delta_1 & -\Delta_2/\sqrt{2} \end{pmatrix}, \tag{2.4}$$

with $S' = -1$, then the terms

$$n_1 n_1 \Delta_1 + (n_1 n_2 + n_2 n_1)\Delta_2/\sqrt{2} - n_2 n_2 \Delta_3, \tag{2.5}$$

where each nn denotes either $n_L n_L$ or $n_R n_R$, break L to $(-1)^L$ with a nonzero $\langle \Delta_3 \rangle$, without breaking S. Note that whereas $\langle \Delta_1 \rangle$ as well as $\langle \Delta_3 \rangle$ must be nonzero (and large) in the model of Ref. [97], thus breaking S to $(-1)^S$, only $\langle \Delta_3 \rangle$ is nonzero here and it is very small for the implementation of the inverse seesaw [101–103]:

$$\mathcal{M}_{\nu n} = \begin{pmatrix} 0 & m_D & 0 \\ m_D & m_2' & M \\ 0 & M & m_2 \end{pmatrix}, \tag{2.6}$$

where m_2 comes from $\langle \Delta_3^* \rangle$ and m_2' from $\langle \Delta_3 \rangle$. This means that an inverse seesaw neutrino mass is obtained:

$$m_\nu \simeq \frac{m_D^2 m_2}{M^2}. \tag{2.7}$$

2.4 Gauge Sector

Let $\langle \phi^0 \rangle = v_1$, $\langle \zeta_2^0 \rangle = v_2$, $\langle \chi_2 \rangle = u_2$, $\langle \Delta_3 \rangle = u_3$, with g_N the $SU(2)_N$ gauge coupling, then the masses of the vector gauge bosons of this model are

$$m_W^2 = \frac{1}{2} g_2^2 (v_1^2 + v_2^2), \qquad m_X^2 = \frac{1}{2} g_N^2 (u_2^2 + v_2^2 + 2u_3^2), \tag{2.8}$$

$$m_{Z,Z'}^2 = \frac{1}{2} \begin{pmatrix} (g_1^2 + g_2^2)(v_1^2 + v_2^2) & -g_N \sqrt{(g_1^2 + g_2^2)} v_2^2 \\ -g_N \sqrt{(g_1^2 + g_2^2)} v_2^2 & g_N^2 (u_2^2 + v_2^2 + 4u_3^2) \end{pmatrix}, \tag{2.9}$$

where X_3 has been renamed Z'. In this model, all the SM fermions obtain masses from v_1, except for the neutrinos which require v_2, i.e. m_D in Eqs. (2.6) and (2.7). We assume v_2 (which causes $Z - Z'$ mixing) and u_3 (which breaks L to $(-1)^L$) to be small. Note that the Z' of this model does not couple directly to SM particles, this means that it is not easily observable at the Large Hadron Collider (LHC) as other Z' bosons which are produced by quarks and decay into lepton pairs. This issue will be studied in more detail elsewhere.

2.5 Scalar Sector

We now supply the details of this model. The Higgs potential is given by

$$\begin{aligned} V &= \mu_\zeta^2 Tr(\zeta^\dagger\zeta) + \mu_\Phi^2 \Phi^\dagger\Phi + \mu_\chi^2 \chi^\dagger\chi + \mu_\Delta^2 Tr(\Delta^\dagger\Delta) + (\mu_1 \tilde{\Phi}^\dagger \zeta\chi + \mu_2 \tilde{\chi}^\dagger \Delta\chi + H.c.) \\ &+ \frac{1}{2}\lambda_1[Tr(\zeta^\dagger\zeta)]^2 + \frac{1}{2}\lambda_2(\Phi^\dagger\Phi)^2 + \frac{1}{2}\lambda_3 Tr(\zeta^\dagger\zeta\zeta^\dagger\zeta) + \frac{1}{2}\lambda_4(\chi^\dagger\chi)^2 + \frac{1}{2}\lambda_5[Tr(\Delta^\dagger\Delta)]^2 \\ &+ \frac{1}{4}\lambda_6 Tr(\Delta^\dagger\Delta - \Delta\Delta^\dagger)^2 + f_1 \chi^\dagger\tilde{\zeta}^\dagger\tilde{\zeta}\chi + f_2 \chi^\dagger\zeta^\dagger\zeta\chi + f_3 \Phi^\dagger\zeta\zeta^\dagger\Phi + f_4 \Phi^\dagger\tilde{\zeta}\tilde{\zeta}^\dagger\Phi \\ &+ f_5(\Phi^\dagger\Phi)(\chi^\dagger\chi) + f_6(\chi^\dagger\chi)Tr(\Delta^\dagger\Delta) + f_7\chi^\dagger(\Delta\Delta^\dagger - \Delta^\dagger\Delta)\chi + f_8(\Phi^\dagger\Phi)Tr(\Delta^\dagger\Delta) \\ &+ f_9 Tr(\zeta^\dagger\zeta)Tr(\Delta^\dagger\Delta) + f_{10} Tr[\zeta(\Delta^\dagger\Delta - \Delta\Delta^\dagger)\zeta^\dagger], \end{aligned} \tag{2.10}$$

where

$$\tilde{\Phi}^\dagger = (\phi^0, -\phi^+), \quad \tilde{\chi}^\dagger = (\chi_2, -\chi_1), \quad \tilde{\zeta} = \begin{pmatrix} \zeta_2^+ & -\zeta_1^+ \\ -\bar{\zeta}_2^0 & \bar{\zeta}_1^0 \end{pmatrix}. \tag{2.11}$$

It is the same as that of Ref. [97] but with two fewer terms. The reason is that S is conserved in our model, whereas S breaks to $(-1)^S$ in Ref. [97]

The spontaneous symmetry breaking of $SU(2)_N$ is mainly through $\langle\chi_2\rangle = u_2$, where

$$u_2^2 \simeq \frac{-\mu_\chi^2}{\lambda_4}. \tag{2.12}$$

As previously mentioned, this breaks both $SU(2)_N$ and S', but the combination $T_{3N}+S' = S$ remains exact. The further breaking of $SU(2)_N$ by $\langle\Delta_3\rangle = u_3$ is assumed to be small for the implementation of the inverse seesaw mechanism, i.e.

$$u_3 \simeq \frac{-\mu_2 u_2^2}{\mu_\Delta^2 + (f_6 - f_7)u_2^2}. \tag{2.13}$$

This also does not break S, but it breaks L to $(-1)^L$ because of Eq. (2.5). The spontaneous

symmetry breaking of $SU(2)_L \times U(1)_Y$ is mainly through $\langle \phi^0 \rangle = v_1$, where

$$v_1^2 \simeq \frac{-\mu_\Phi^2 - f_5 u_2^2}{\lambda_2}. \tag{2.14}$$

The further breaking of $SU(2)_L \times U(1)_Y \times SU(2)_N$ through $\langle \zeta_2^0 \rangle = v_2$ is assumed small, i.e.

$$v_2 \simeq \frac{-\mu_1 v_1 u_2}{\mu_\zeta^2 + f_2 u_2^2}. \tag{2.15}$$

This also does not break S. The resulting physical scalar particles of this model have the following masses:

$$m^2(\sqrt{2} Re\chi_2) \simeq 2\lambda_4 u_2^2, \qquad m^2(\sqrt{2} Re\phi^0) \simeq 2\lambda_2 v_1^2, \tag{2.16}$$

$$m^2(\zeta_2^0) \simeq \mu_\zeta^2 + f_2 u_2^2 + f_4 v_1^2, \qquad m^2(\zeta_2^-) \simeq \mu_\zeta^2 + f_2 u_2^2 + f_3 v_1^2, \tag{2.17}$$

$$m^2(\zeta_1^0) \simeq \mu_\zeta^2 + f_1 u_2^2 + f_4 v_1^2, \qquad m^2(\zeta_1^-) \simeq \mu_\zeta^2 + f_1 u_2^2 + f_3 v_1^2, \tag{2.18}$$

$$m^2(\Delta_3) \simeq \mu_\Delta^2 + (f_6 - f_7) u_2^2 + f_8 v_1^2, \quad m^2(\Delta_2) \simeq \mu_\Delta^2 + f_6 u_2^2 + f_8 v_1^2, \tag{2.19}$$

$$m^2(\Delta_1) \simeq \mu_\Delta^2 + (f_6 + f_7) u_2^2 + f_8 v_1^2. \tag{2.20}$$

2.6 Dark Sector

Another important difference is that whereas the $X_{1,2}$ relic abundance is determind by their annihilation cross section to standard-model (SM) particles in Ref. [97], it is determined by $X\bar{X} \to \zeta_2 \zeta_2^\dagger$ here. Thermalization with SM particles is maintained through $\zeta_2 \zeta_2^\dagger \to l^- l^+$, etc. Of all the particles having nonzero S, i.e. $\zeta_1^0, \zeta_1^-, \Delta_2, \Delta_1, n_1$ and X, we assume that X is the lightest. Of all the new particles having zero S, i.e. $\zeta_2^0, \zeta_2^-, \Delta_3, \sqrt{2} Re\chi_2, n_2$ and Z', we assume that ζ_2^0, ζ_2^- are lighter than X so that $X\bar{X} \to \zeta_2^0 \bar{\zeta}_2^0 + \zeta_2^- \zeta_2^+$ is kinematically allowed. Since Δ_1 has $S = -2$, if $m(\Delta_3) < 2m_X$, it is also stable and may become

a significant second component [92] of dark matter. We will explore this very interesting possibility elsewhere.

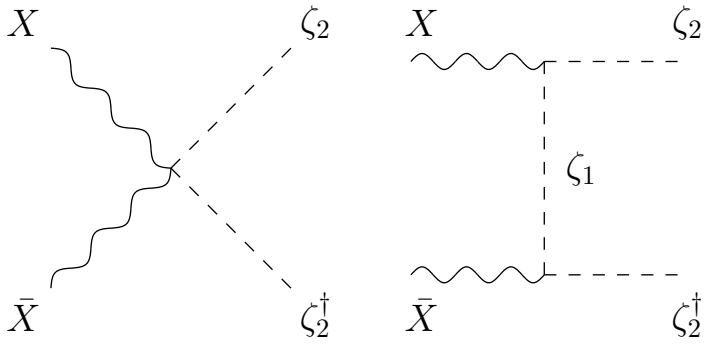

Figure 2.1: Annihilation of $X\bar{X}$ to $\zeta_2\zeta_2^\dagger$.

The annihilation of $X\bar{X} \to \zeta_2\zeta_2^\dagger$ proceeds via the diagrams of Fig. 2.1. The relevant terms for this process are given by

$$\begin{aligned}\mathcal{L} \supset & \frac{i\,g_N}{\sqrt{2}} X \left[\overline{\zeta_2^0}\partial_\mu\zeta_1^0 - \zeta_1^0\partial_\mu\overline{\zeta_2^0}\right] + \frac{i\,g_N}{\sqrt{2}}\bar{X}\left[\overline{\zeta_1^0}\partial_\mu\zeta_2^0 - \zeta_2^0\partial_\mu\overline{\zeta_1^0}\right] \\ & + \frac{i\,g_N}{\sqrt{2}} X \left[\zeta_2^+\partial_\mu\zeta_1^- - \zeta_1^-\partial_\mu\zeta_2^+\right] + \frac{i\,g_N}{\sqrt{2}}\bar{X}\left[\zeta_1^+\partial_\mu\zeta_2^- - \zeta_2^-\partial_\mu\overline{\zeta_1^+}\right] \\ & + \frac{g_N^2}{2}\left[\zeta_1^0\overline{\zeta_1^0} + \zeta_2^0\overline{\zeta_2^0} + \zeta_1^-\zeta_1^+ + \zeta_2^-\zeta_2^+\right] X\bar{X}\end{aligned} \tag{2.21}$$

Assuming X and $\bar{X}$ to be at rest, this amplitude is given by

$$\mathcal{A} = \frac{g_N^2}{2}\left[\vec{\epsilon}_1\cdot\vec{\epsilon}_2 + \frac{4(\vec{\epsilon}_1\cdot\vec{k})(\vec{\epsilon}_2\cdot\vec{k})}{m_{\zeta_1}^2 + m_X^2 - m_{\zeta_2}^2}\right], \tag{2.22}$$

where $\vec{k}$ is the three-momentum of ζ_2, and $\epsilon_{1,2}$ are the polarizations of X and $\bar{X}$. Summing over ζ_2^0 and ζ_2^-, and averaging over the spins of X and $\bar{X}$, the corresponding cross section $\times$ their relative velocity is given by

$$\sigma \times v_{rel} = \frac{g_N^4}{576\pi m_X^2}\sqrt{1 - \frac{m_{\zeta_2}^2}{m_X^2}}\left(2 + \left[1 + \frac{4(m_X^2 - m_{\zeta_2}^2)}{m_{\zeta_1}^2 + m_X^2 - m_{\zeta_2}^2}\right]^2\right), \tag{2.23}$$

where we used Eqs. (2.24)-(2.26) in our calculations:

$$\begin{aligned}\sum_{\epsilon} g_{\alpha\beta}g_{\mu\nu}\,\epsilon_\lambda^\alpha(p_1)^*\epsilon_\rho^\beta(p_2)\,\epsilon_\lambda^\mu(p_1)\epsilon_\rho^\nu(p_2)^* &= g_{\alpha\beta}g_{\mu\nu}\left[g^{\alpha\mu}-\frac{p_1^\alpha p_1^\mu}{m_X^2}\right]\left[g^{\beta\nu}-\frac{p_2^\beta p_2^\nu}{m_X^2}\right]\\ &=\left[g_{\beta\nu}-\frac{p_{1,\beta}p_{1,\nu}}{m_X^2}\right]\left[g^{\beta\nu}-\frac{p_2^\beta p_2^\nu}{m_X^2}\right]\\ &=4-1-1+\frac{(p_1.p_2)(p_1.p_2)}{m_X^4}=3,\end{aligned} \tag{2.24}$$

$$\begin{aligned}\sum_{\epsilon} k_\mu\epsilon_\lambda^\mu(p_1)\,k_\nu\epsilon_\rho^\nu(p_2)k_\alpha\epsilon_\lambda^\alpha(p_1)^*\,k_\beta\epsilon_\rho^\beta(p_2)^* &= k_\mu k_\nu k_\alpha k_\beta\left[g^{\alpha\mu}-\frac{p_1^\alpha p_1^\mu}{m_X^2}\right]\left[g^{\beta\nu}-\frac{p_2^\beta p_2^\nu}{m_X^2}\right]\\ &=\left[k^2-\frac{(p_1.k)^2}{m_X^2}\right]\left[k^2-\frac{(p_2.k)^2}{m_X^2}\right]\\ &=\left[m_{\zeta_2}^2-m_X^2\right]^2,\end{aligned} \tag{2.25}$$

$$\begin{aligned}&\sum_{\epsilon} g_{\alpha\beta}\,\epsilon_\lambda^\alpha(p_1)^*\epsilon_\rho^\beta(p_2)k_\mu\epsilon_\lambda^\mu(p_1)\,k_\nu\epsilon_\rho^\nu(p_2) = k_\mu k_\nu g_{\alpha\beta}\left[g^{\alpha\mu}-\frac{p_1^\alpha p_1^\mu}{m_X^2}\right]\left[g^{\beta\nu}-\frac{p_2^\beta p_2^\nu}{m_X^2}\right]\\ &=\left[k_\beta-\frac{p_{1,\beta}(p_1.k)}{m_X^2}\right]\left[k^\beta-\frac{p_2^\beta(p_2.k)}{m_X^2}\right]\\ &=\left[m_{\zeta_2}^2-\frac{(p_2.k)^2}{m_X^2}-\frac{(p_1.k)^2}{m_X^2}+\frac{(p_1.p_2)(p_1.k)(p_2.k)}{m_X^4}\right]=\left[m_{\zeta_2}^2-m_X^2\right].\end{aligned} \tag{2.26}$$

Since $m_{\zeta_1} > m_X$ by assumption, the above expression is bounded from below by $m_{\zeta_1} \to \infty$ and from above by $m_{\zeta_1} = m_X$. We plot in Fig. 2.2[1] the allowed region for m_X/g_N^2 as a function of $r = m_{\zeta_2}^2/m_X^2$ for the optimum value [105] of $\sigma \times v_{rel} = 4.4 \times 10^{-26}$ cm^3 s^{-1} implied by the observed relic abundance of dark matter in the Universe, taking into account that X is a complex vector field.

To detect X in underground experiments using elastic scattering off nuclei, the only possible connection is through $\phi^0 - \chi_2$ mixing. The 125 GeV particle h discovered [49, 50] at the LHC is a linear combination of $\sqrt{2}Re\phi^0$, $\sqrt{2}Re\zeta_2^0$, and $\sqrt{2}Re\chi_2$. The induced $hX\bar{X}$ interaction is approximately given by $(g_N^2 v_1/\sqrt{2})(f_5/\lambda_4)$. Since h interacts with quarks

[1] All of the plots in this thesis are generated using Mathematica [104].

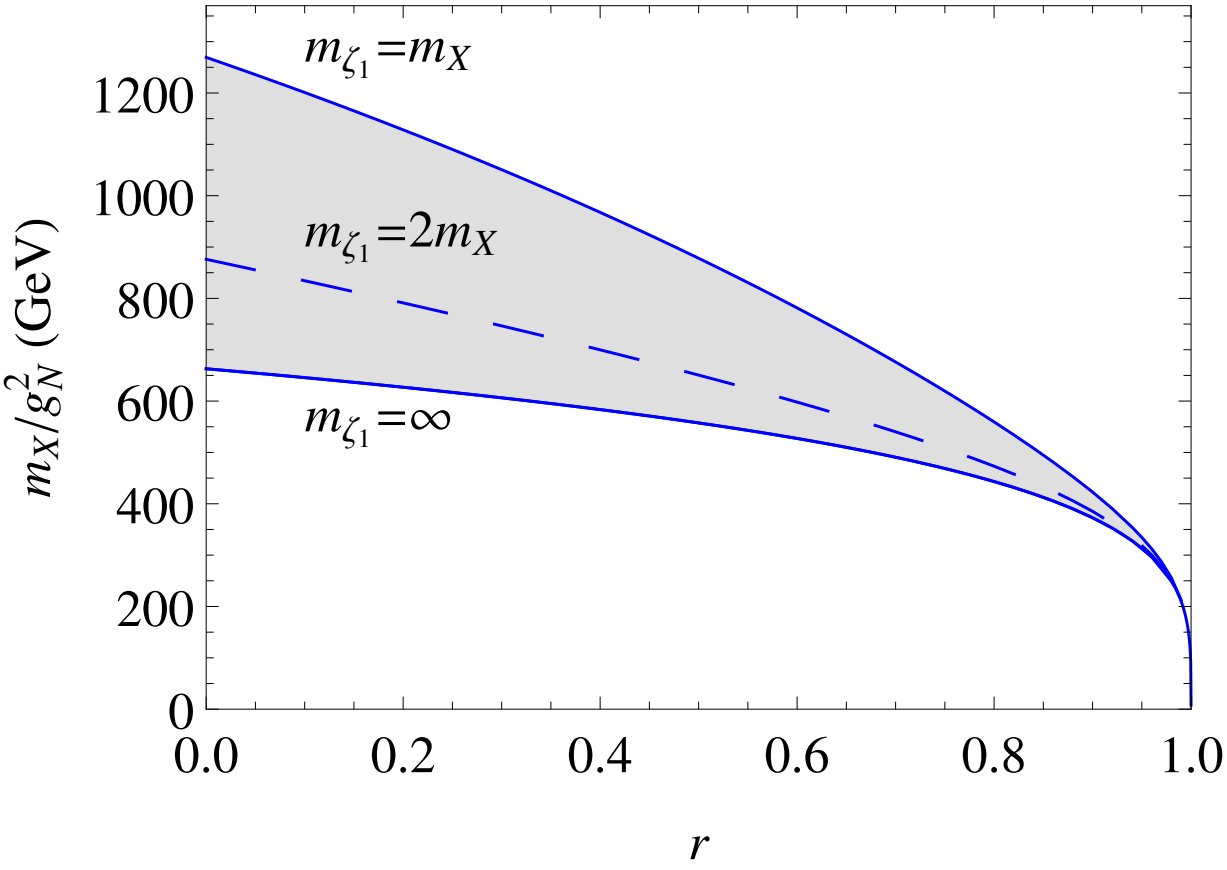

Figure 2.2: Allowed values of m_X/g_N^2 plotted against $r = m_{\zeta_2}^2/m_X^2$ from relic abundance.

through $\sqrt{2}Re\phi^0$ according to $(m_q/\sqrt{2}v_1)\bar{q}q$, there is a small cross section for X to be detected in such experiments. Following Ref. [106], we obtain

$$\frac{f_p}{m_p} = -0.075\left[\frac{g_N^2(f_5/\lambda_4)}{4m_\phi^2}\right] - 0.925(3.51)\left[\frac{g_N^2(f_5/\lambda_4)}{54m_\phi^2}\right], \tag{2.27}$$

$$\frac{f_n}{m_n} = -0.078\left[\frac{g_N^2(f_5/\lambda_4)}{4m_\phi^2}\right] - 0.922(3.51)\left[\frac{g_N^2(f_5/\lambda_4)}{54m_\phi^2}\right], \tag{2.28}$$

with the spin-independent elastic cross section for X scattering off a nucleus of Z protons and $A-Z$ neutrons normalized to one nucleon given by

$$\sigma_0 = \frac{1}{\pi}\left(\frac{m_N}{m_X + Am_N}\right)^2 \left|\frac{Zf_p + (A-Z)f_n}{A}\right|^2. \tag{2.29}$$

Using the LUX data [107], we plot in Fig. 2.3 the maximum allowed value of $g_N^2(f_5/\lambda_4)$ as a function of m_X using $m_\phi = 125$ GeV. We also plot the allowed regions of g_N^2 versus m_X for $r = 0.2$ and $r = 0.8$ from Fig. 2.2. We see that for moderate values of m_X, future improvement in direct detection will probe the allowed region from relic abundance if f_5/λ_4 is not too small.

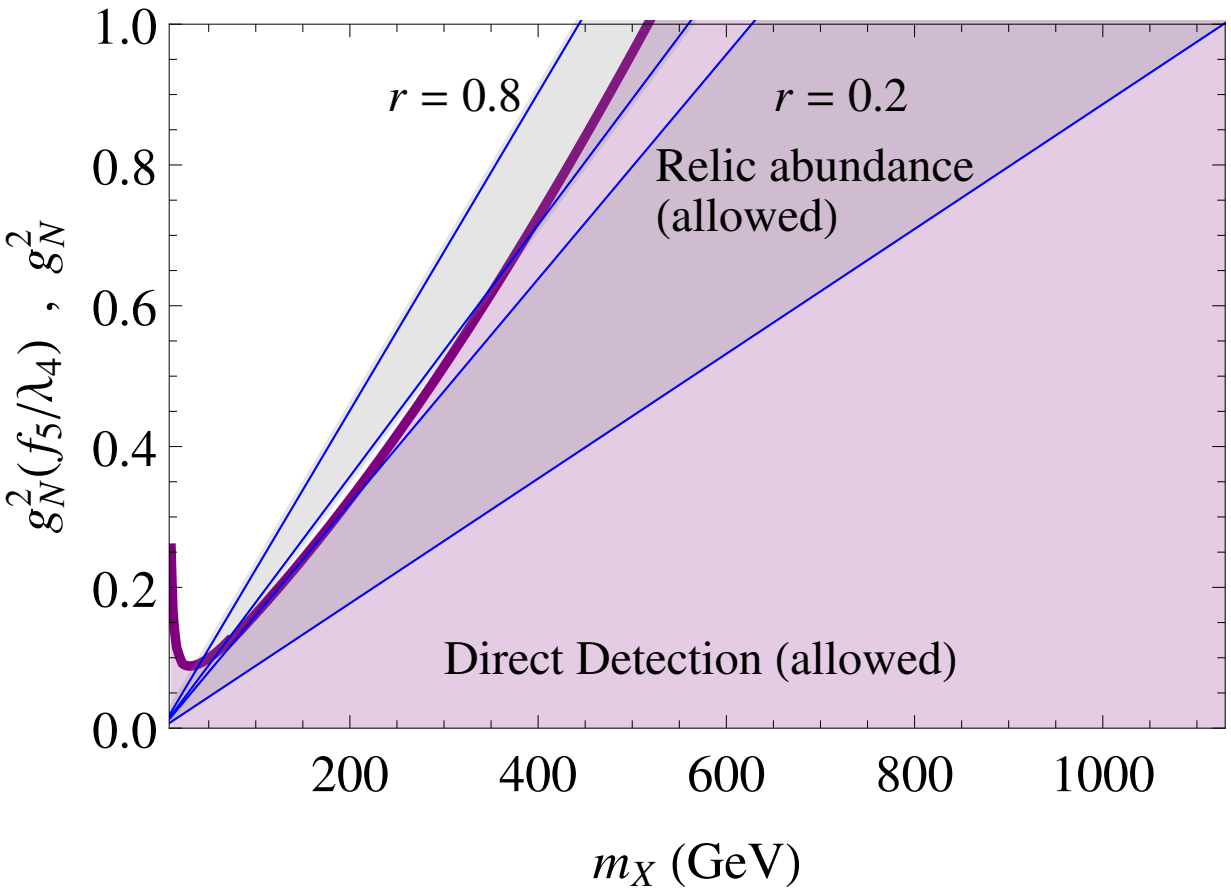

Figure 2.3: Allowed values of g_N^2 from relic abundance and $g_N^2(f_5/\lambda_4)$ from LUX, plotted against m_X.

2.7 Conclusion

In conclusion, we have discussed in this paper a simple and realistic model of vector dark matter based on $SU(2)_N$. It has a leptonic connection which is a natural framework for the inverse seesaw mechanism to generate a small Majorana neutrino mass. It also accommodates a standard-model Higgs boson which mixes only slightly with its $SU(2)_N$ counterpart, which does not couple directly to any standard-model particle. Thus the observed 125 GeV particle behaves as the one Higgs boson of the standard model for all practical purposes. The scalar particle content of this model may also allow a stable second component of dark matter, because of kinematics, and not because the dark symmetry is extended. This is the first explicit example of how such a general situation may occur, a topic we will explore in another paper. The $SU(2)_N$ gauge symmetry is also suitable to be embedded in an $SU(7)$ model unfifying matter and dark matter, as outlined in Ref. [108].

Chapter 3

Gauge $B - L$ Model with Residual Z_3 Symmetry

3.1 Introduction

Lepton number L is a familiar concept. It is usually defined as a global U(1) symmetry, under which the leptons of the standard model (SM), i.e. e, μ, τ together with their neutrinos ν_e, ν_μ, ν_τ have $L = 1$, and all other SM particles have $L = 0$. In the case of nonzero Majorana neutrino masses, this continuous symmetry is broken to a discrete Z_2 symmetry, i.e. $(-1)^L$ or lepton parity. In this paper, we consider a gauge $B - L$ extension of the SM, such that a residual Z_3 symmetry remains after the spontaneous breaking of $B - L$. This is then a realization of the unusual notion of Z_3 lepton symmetry. It has specific phenomenological consequences, including the possibility of a long-lived particle as a dark-matter candidate.

3.2 Neutrino Mass

The conventional treatment of gauge $B-L$ has three right-handed singlet neutrinos $\nu_{R1}, \nu_{R2}, \nu_{R3}$ transforming as $-1, -1, -1$ under $B-L$. It is well-known that this assignment satisfies all the anomaly-free conditions for $U(1)_{B-L}$. However, another assignment [109]

$$\nu_{R1}, \nu_{R2}, \nu_{R3} \sim 5, -4, -4 \tag{3.1}$$

works as well, because

$$5 - 4 - 4 = -3, \quad (5)^3 - (4)^3 - (4)^3 = -3. \tag{3.2}$$

To obtain a realistic model with this assignment, it was proposed [110] that three additional neutral singlet Dirac fermions $N_{1,2,3}$ be added with $B - L = -1$, together with a singlet scalar χ_3 with $B - L = 3$. Consequently, the tree-level Yukawa couplings $\bar{\nu}_L N_R \bar{\phi}^0$ and $\bar{N}_L \nu_{R2} \chi_3$, $\bar{N}_L \nu_{R3} \chi_3$ are allowed, where $\Phi = (\phi^+, \phi^0)$ is the one Higgs doublet of the SM. Together with the invariant $\bar{N}_L N_R$ mass terms, the 6×5 neutrino mass matrix linking $(\bar{\nu}_L, \bar{N}_L)$ to (ν_R, N_R) is of the form

$$\mathcal{M}_{\nu N} = \begin{pmatrix} 0 & \mathcal{M}_0 \\ \mathcal{M}_3 & \mathcal{M}_N \end{pmatrix}, \tag{3.3}$$

where $\mathcal{M}_0$ and $\mathcal{M}_N$ are 3×3 mass matrices and $\mathcal{M}_3$ is 3×2 because ν_{R1} has no tree-level Yukawa coupling. This means that one linear combination of ν_L is massless. Of course, if the dimension-five term $\bar{\nu}_{R1} N_L \chi_3^2$ also exists, then $\mathcal{M}_3$ is 3×3 and $\mathcal{M}_{\nu N}$ is 6×6. The form of $\mathcal{M}_{\nu N}$ allows nonzero seesaw Dirac neutrino masses for ν [111], i.e.

$$\mathcal{M}_\nu \simeq \mathcal{M}_0 \mathcal{M}_N^{-1} \mathcal{M}_3. \tag{3.4}$$

Without the implementation of a flavor symmetry, any 3×3 $\mathcal{M}_\nu$ is possible. Although the gauge $B-L$ is broken, a residual global L symmetry remains in this model with ν, l, N all having $L=1$. Because the pairing of any two neutral fermions of the same chirality always results in a nonzero $B-L$ charge not divisible by 3 units in this model, it is impossible to construct an operator of any dimension for a Majorana mass term which violates $B-L$. Hence the neutrinos are indeed exactly Dirac. We now add two more scalar singlets: χ_2 with $B-L=2$ and χ_6 with $B-L=-6$. The important new terms in the Lagrangian are

$$\bar{N}_L \nu_{R1} \chi_6, \quad \chi_2 N_L N_L, \quad \chi_2 N_R N_R, \quad \chi_2^3 \chi_6, \quad \chi_3^2 \chi_6. \tag{3.5}$$

Now $B-L$ is broken by $\langle \chi_3 \rangle = u_3$ as well as $\langle \chi_6 \rangle = u_6$, and all neutrinos become massive. The cubic term χ_2^3 implies that a Z_3 residual symmetry remains, such that χ_2 and all leptons transform as $\omega = \exp(2\pi i/3)$ under Z_3. This is thus the first example of a lepton symmetry which is not Z_2 (for Majorana neutrinos), nor $U(1)$ or Z_4 [112, 113] (for Dirac neutrinos). Note that Z_3 is also sufficient to guarantee that all the neutrinos remain Dirac.

3.3 Gauge Sector

In this model, there is of course a gauge boson Z' which couples to $B-L$. Its production at the Large Hadron Collider (LHC) is due to its couplings to quarks. Once produced, it decays into quarks and leptons. In the conventional $B-L$ assignment for ν_R, its branching fractions to quarks, charged leptons, and neutrinos are 1/4, 3/8, and 3/8 respectively. In this model, the ν_R charges are $(5,-4,-4)$, hence their resulting partial widths are very large. Assuming that Z' decays also into χ_2, the respective branching fractions into quarks, charged leptons, neutrinos, and χ_2 as dark matter are then 1/18,

1/12, 5/6, and 1/36. This means Z' has an 86% invisible width. Using the production of Z' via $u\bar{u}$ and $d\bar{d}$ initial states at the LHC and its decay into e^-e^+ or $\mu^-\mu^+$ as signature, the bound on $m_{Z'}$ assuming $g' = g$, i.e. the $SU(2)_L$ gauge coupling of the SM, is about 3 TeV, based on LHC data [114, 115]. However, because the branching fraction into l^-l^+ is reduced by a factor of 2/9 in our $B - L$ model, this bound is reduced to about 2.5 TeV, again for $g' = g$.

3.4 Dark Sector

Although there is no stabilizing symmetry here for dark matter, χ_2 has very small couplings to two neutrinos through the Yukawa terms of Eq. (3.5) from the mixing implied by Eq. (3.3). This means that χ_2 may have a long enough lifetime to be suitable for dark matter, as shown below. Consider for simplicity the coupling of χ_2 to just one N, with the interaction

$$\mathcal{L}_{int} = \frac{1}{2} f_L \chi_2 N_L N_L + \frac{1}{2} f_R \chi_2 N_R N_R + H.c. \tag{3.6}$$

Let the $\nu_L - N_L$ mixing be $\zeta_0 = m_0/m_N$ and $\nu_R - N_R$ mixing be $\zeta_3 = m_3/m_N$, then the decay rate of χ_2 is

$$\Gamma(\chi_2 \to \bar{\nu}\bar{\nu}) = \frac{m_\chi}{32\pi}(f_L^2\zeta_0^4 + f_R^2\zeta_3^4). \tag{3.7}$$

If we set this equal to the age of the Universe (13.75×10^9 years), and assuming $m_\chi = 100$ GeV, $f_L = f_R$ and $\zeta_0 = \zeta_3$, then $f\zeta^2 = 8.75 \times 10^{-22}$. Hence

$$\sqrt{f}\zeta << 3 \times 10^{-11} \tag{3.8}$$

would guarantee the stability of χ_2 to the present day, and allow it to be a dark-matter candidate. This sets the scale of m_N at about 10^{13} GeV, which is also the usual mass scale

for the heavy Majorana singlet neutrino in the canonical seesaw mechanism.

Since χ_2 interacts with nuclei through Z', there is also a significant constraint from dark-matter direct-search experiments. The cross section per nucleon is given by

$$\sigma_0 = \frac{1}{\pi}\left(\frac{m_\chi m_n}{m_\chi + A m_n}\right)^2 \left(\frac{2g'^2}{m_{Z'}^2}\right)^2, \tag{3.9}$$

where A is the number of nucleons in the target and m_n is the nucleon mass. Consider for example $m_\chi = 100$ GeV, then $\sigma_0 < 1.25 \times 10^{-45}$ cm^2 from the LUX data [107]. This implies $m_{Z'}/g' > 16.2$ TeV, as shown in Fig. 3.1. If $g' = g$, then $m_{Z'} > 10.6$ TeV. This limit is

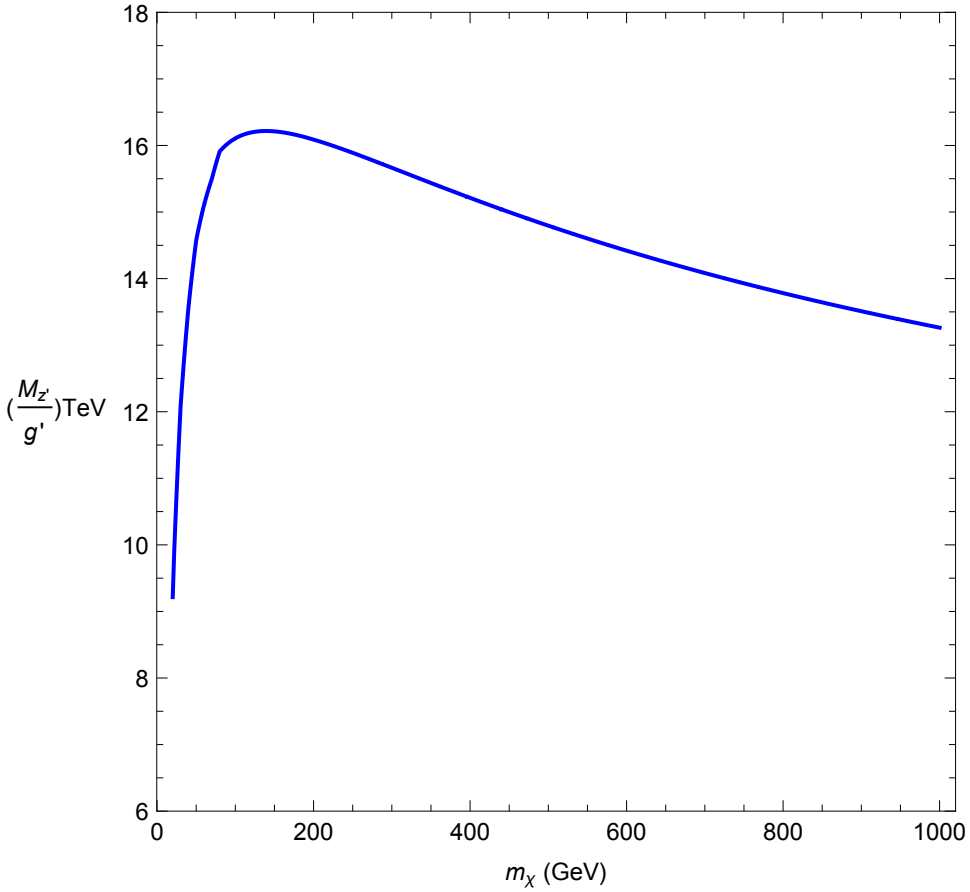

Figure 3.1: Lower bound on $m_{Z'}/g'$ versus m_χ from LUX data.

thus much more severe than the LHC bound of 2.5 TeV. If $g' < g$, then both the LHC and LUX bounds on $m_{Z'}$ are relaxed. However, it also means that it is unlikely that Z' would be discovered at the LHC even with the 14 TeV run.

Consider now the annihilation cross section of $\chi_2\chi_2^*$ for obtaining its thermal relic abundance. The process $\chi_2\chi_2^* \to Z' \to$ SM particles is p-wave suppressed and is unlikely to be strong enough for this purpose. We may then consider the well-studied process $\chi_2\chi_2^* \to h \to$ SM particles, where h is the SM Higgs boson. If this is assumed to account for all of the dark-matter relic abundance of the Universe, then it has been shown [116] that the required strength of this interaction is in conflict with LUX data except for a small region near $m_\chi = m_h/2$. In this paper, we will consider the following alternative scenario.

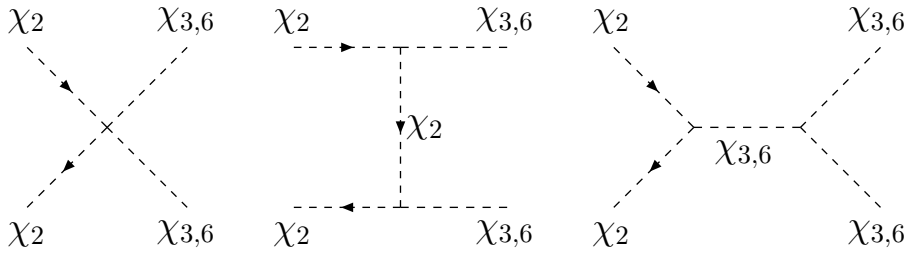

Figure 3.2: $\chi_2\chi_2^\dagger$ annihilation to $\chi_{3,6}$ final states.

We assume that the $h\chi_2\chi_2^*$ interaction is negligible, so that neither Higgs nor Z' exchange is important for $\chi_2\chi_2^*$ annihilation. Instead we invoke the new interactions of Fig. 3.2. Since $\chi_{3,6}$ may interact freely with h, thermal equilibrium is maintained with the other SM particles. This scenario requires of course that m_χ to be greater than at least one physical

mass eigenvalue in the $\chi_{3,6}$ sector.

To summarize, $\chi_2 \sim \omega$ under Z_3 and decays into two antineutrinos, but its lifetime is much longer than the age of the Universe. It is thus an example of Z_3 dark matter [117–121]. It is also different from previous Z_2 proposals [122, 123] based on Ref. [109]. It has significant elastic interactions with nuclei through Z' and Higgs exchange and may be discovered in direct-search experiments. On the other hand, its relic abundance is determined not by Z' or Higgs interactions, but by its annihilation to other scalars of this model which maintain thermal equilibrium with the SM particles through the SM Higgs boson. Note that this is also the mechanism used in a proposed model of vector dark matter [1].

3.5 Scalar Sector

We now discuss the details of the scalar sector of this model. Consider the scalar potential

$$\begin{aligned} V &= -\mu_0^2(\Phi^\dagger\Phi) + m_2^2(\chi_2^*\chi_2) - \mu_3^2(\chi_3^*\chi_3) - \mu_6^2(\chi_6^*\chi_6) \\ &+ \frac{1}{2}\lambda_0(\Phi^\dagger\Phi)^2 + \frac{1}{2}\lambda_2(\chi_2^*\chi_2)^2 + \frac{1}{2}\lambda_3(\chi_3^*\chi_3)^2 + \frac{1}{2}\lambda_6(\chi_6^*\chi_6)^2 + \lambda_{02}(\chi_2^*\chi_2)(\Phi^\dagger\Phi) \\ &+ \lambda_{03}(\chi_3^*\chi_3)(\Phi^\dagger\Phi) + \lambda_{06}(\chi_6^*\chi_6)(\Phi^\dagger\Phi) + \lambda_{23}(\chi_2^*\chi_2)(\chi_3^*\chi_3) + \lambda_{26}(\chi_2^*\chi_2)(\chi_6^*\chi_6) \\ &+ \lambda_{36}(\chi_3^*\chi_3)(\chi_6^*\chi_6) + [\frac{1}{2}f_{36}(\chi_3^2\chi_6) + \text{H.c.}] + [\frac{1}{6}\lambda'_{26}(\chi_2^3\chi_6) + \text{H.c.}]. \end{aligned} \tag{3.10}$$

Let $\langle\phi^0\rangle = v$, $\langle\chi_3\rangle = u_3$, $\langle\chi_6\rangle = u_6$, then the minimum of V is determined by

$$\mu_0^2 = \lambda_0 v^2 + \lambda_{03}u_3^2 + \lambda_{06}u_6^2, \tag{3.11}$$

$$\mu_3^2 = \lambda_3 u_3^2 + \lambda_{03}v^2 + \lambda_{36}u_6^2 + f_{36}u_6, \tag{3.12}$$

$$\mu_6^2 = \lambda_6 u_6^2 + \lambda_{06}v^2 + \lambda_{36}u_3^2 + \frac{f_{36}u_3^2}{2u_6}. \tag{3.13}$$

There is one dark-matter scalar boson χ_2 with mass given by

$$m_\chi^2 = m_2^2 + \lambda_{02} v^2 + \lambda_{23} u_3^2 + \lambda_{26} u_6^2. \tag{3.14}$$

There is one physical pseudoscalar boson

$$A = \sqrt{2} Im(2u_6 \chi_3 + u_3 \chi_6)/\sqrt{u_3^2 + 4u_6^2} \tag{3.15}$$

with mass given by

$$m_A^2 = -f_{36}(u_3^2 + 4u_6^2)/2u_6. \tag{3.16}$$

There are three physical scalar bosons spanning the basis $[h, \sqrt{2}Re(\chi_3), \sqrt{2}Re(\chi_6)]$, with 3×3 mass-squared matrix given by

$$M^2 = \begin{pmatrix} 2\lambda_0 v^2 & 2\lambda_{03} u_3 v & 2\lambda_{06} u_6 v \\ 2\lambda_{03} u_3 v & 2\lambda_3 u_3^2 & 2\lambda_{36} u_3 u_6 + f_{36} u_3 \\ 2\lambda_{06} u_6 v & 2\lambda_{36} u_3 u_6 + f_{36} u_3 & 2\lambda_6 u_6^2 - f_{36} u_3^2/2u_6 \end{pmatrix}. \tag{3.17}$$

For illustration, we consider the special case $\lambda_{03} = \lambda_{06} = 0$, so that h decouples from $\chi_{3,6}$. It then becomes identical to that of the SM, and may be identified with the 125 GeV particle discovered [49, 50] at the LHC. We now look for a solution with

$$S = \sqrt{2} Re(-u_3 \chi_3 + 2u_6 \chi_6)/\sqrt{u_3^2 + 4u_6^2}, \tag{3.18}$$

$$S' = \sqrt{2} Re(2u_6 \chi_3 + u_3 \chi_6)/\sqrt{u_3^2 + 4u_6^2}, \tag{3.19}$$

as mass eigenstates. This is easily accomplished for example with

$$u_3 = 2u_6, \qquad 4\lambda_3 = \lambda_6 - f_{36}/u_6. \tag{3.20}$$

In this case,

$$S = -Re\chi_3 + Re\chi_6, \qquad m_S^2 = 2\lambda_6 u_6^2 - 4\lambda_{36} u_6^2 - 4 f_{36} u_6, \tag{3.21}$$

$$S' = Re\chi_3 + Re\chi_6, \qquad m_{S'}^2 = 2\lambda_6 u_6^2 + 4\lambda_{36} u_6^2, \tag{3.22}$$

$$A = Im\chi_3 + Im\chi_6, \qquad m_A^2 = -4 f_{36} u_6, \tag{3.23}$$

$$m_{Z'} = 12 g' u_6. \tag{3.24}$$

The couplings of $\chi_2\chi_2^*$ to S and S' are given by

$$\chi_2\chi_2^*[u_6(\lambda_{26} - 2\lambda_{23})S + u_6(\lambda_{26} + 2\lambda_{23})S']. \tag{3.25}$$

Since S plays the same role in breaking $B - L$ as the Higgs boson h does in breaking $SU(2)_L \times U(1)_Y$, it is expected to be massive of order $\sqrt{u_3^2 + 4u_6^2} = 2\sqrt{2}u_6$. This allows $m_{S'}$ to be adjusted to be very small, then it may serve as a light scalar mediator for χ_2 as self-interacting dark matter [124]. For $m_{S'} \simeq 0$, we need $\lambda_{36} = -\lambda_6/2$. In that case, using Eq. (3.20), we find

$$m_S^2 = 16\lambda_3 u_6^2, \quad m_A^2 = m_S^2 - 4\lambda_6 u_6^2. \tag{3.26}$$

We assume that the relic density of χ_2 is dominated by the $\chi_2\chi_2^*$ annihilation to $S'S'$. For illustration, we set to zero the $\chi_2\chi_2^*S'S'$ coupling, i.e. $\lambda_{23} + \lambda_{26} = 0$, as well as the $SS'S'$ coupling, i.e. $-12\lambda_3 + 6\lambda_6 + 2\lambda_{36} - f_{36}/u_6 = 0$. This implies $\lambda_3 = \lambda_6/2$ so that the $S'S'S'$ coupling is also zero and $m_A^2 = m_S^2/2$. This choice of parameters means that only the middle diagram of Fig. 3.2 contributes to the $\chi_2\chi_2^*$ annihilation cross section with

$$\sigma \times v_{rel} = \frac{1}{64\pi m_\chi^2} \left| \frac{\lambda_{26}^2 u_6^2}{m_\chi^2} \right|^2. \tag{3.27}$$

Equating this to the optimal value [105] of 4.4×10^{-26} cm^3 s^{-1} for the correct dark-matter

relic density of the Universe, we find for $m_\chi = 100$ GeV

$$\lambda_{26} = 0.0295 \left(\frac{1 \text{ TeV}}{u_6} \right). \tag{3.28}$$

We assume of course that $m_A > 2m_\chi$.

For S' to be in thermal equilibrium with the SM particles, we need to have nonzero values of λ_{03} and λ_{06}. This is possible in our chosen parameter space if $2\lambda_{03} + \lambda_{06} \simeq 0$, so that the $S'h$ mixing is very small and yet the $S'S'h$ coupling $\lambda_{06}v/4\sqrt{2}$ and $S'S'hh$ coupling $\lambda_{06}/16$ may be significant. Note that the Sh mixing is now fixed at $(\lambda_{06}/\lambda_6)(v/2\sqrt{2}u_6)$ which may yet be suitably suppressed for h to be essentially the one Higgs boson of the SM. The $h \to S'S'$ decay width is given by

$$\Gamma(h \to S'S') = \frac{\lambda_{06}^2 v^2}{256\pi m_h} = \left(\frac{\lambda_{06}}{0.04} \right)^2 0.5 \text{ MeV}. \tag{3.29}$$

It is invisible at the LHC because S' decays slowly to e^-e^+ only through its mixing with h, if $m_{S'} \sim 10$ MeV for S' as a light mediator for the self-interacting dark matter χ_2.

3.6 Conclusion

In conclusion, we have considered the unusual case of a gauge $B - L$ symmetry which is spontaneously broken to Z_3 lepton number. Neutrinos are Dirac fermions transforming as $\omega = \exp(2\pi i/3)$ under Z_3. A complex neutral scalar χ_2 exists which also transforms as ω. It is not absolutely stable, but decays to two antineutrinos with a lifetime much greater than that of the Universe. It is thus an example of Z_3 dark matter. In addition to the one Higgs boson h of the SM, there are three neutral scalars S, S', A and one

heavy vector gauge boson Z'. From direct-search experiments, $m_{Z'}/g'$ is constrained to be very large, thus making it impossible to discover Z' at the LHC even with the current run. The relic abundance of χ_2 is determined by its annihilation into S' which is a candidate for the light mediator by which χ_2 obtains its long-range self-interaction.

Chapter 4

Verifiable Associated Processes from Radiative Lepton Masses with Dark Matter

4.1 Introduction

The idea that lepton masses are induced in one loop has been around for a long time. Some models have been proposed [125–127] where the particles in the loop are distinguished from ordinary matter by an unbroken symmetry so that the lightest neutral particle among them may be the dark matter of the Universe. As an example, consider the specific proposal of Ref. [127] for generating charged-lepton masses. This model assumes the non-Abelian discrete symmetry A_4 under which the three families of leptons transform

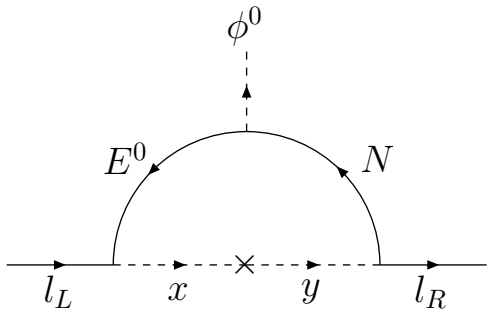

Figure 4.1: One-loop generation of charged-lepton mass.

as

$$(\nu_i, l_i)_L \sim \underline{3}, \quad l_{iR} \sim \underline{1}, \underline{1}', \underline{1}''. \tag{4.1}$$

With only the one Higgs doublet (ϕ^+, ϕ^0) of the standard model (SM) transforming as $\underline{1}$, a tree-level lepton mass is forbidden. To obtain one-loop radiative lepton masses, the following new particles are added, all of which are odd under an unbroken dark Z_2 symmetry:

$$(E^0, E^-)_{L,R} \sim \underline{1}, \quad N_{L,R} \sim \underline{1}, \quad x_i^- \sim \underline{3}, \quad y_i^- \sim \underline{1}, \underline{1}', \underline{1}'', \tag{4.2}$$

where $(E^0, E^-), N$ are fermions and x^-, y^- are charged scalars. Note that in supersymmetry, there are also similar new particles, i.e. left and right charged sleptons and doublet Higgsinos. The soft breaking of A_4 to Z_3 lepton triality [128, 129] is encoded in the scalar off-diagonal mass-squared $x_i y_j^*$ terms. In this paper we will study the phenomenological consequences of this proposal, including the deviation of the Higgs to charged-lepton decay from the SM, the muon anomalous magnetic moment, $\mu \to e\gamma$, $\mu \to eee$, as well as the structure of its dark sector.

4.2 Radiative Lepton Masses

The mass matrix linking $(\bar{N}_L, \bar{E}^0_L)$ to (N_R, E^0_R) is given by

$$\mathcal{M}_{N,E} = \begin{pmatrix} m_N & m_D \\ m_F & m_E \end{pmatrix}, \tag{4.3}$$

where m_N, m_E are invariant mass terms, and m_D, m_F come from the Higgs Yukawa terms $f_D \bar{N}_L E^0_R \bar{\phi}^0$, $f_F \bar{E}^0_L N_R \phi^0$ with vacuum expectation value $\langle \phi^0 \rangle = v/\sqrt{2}$. As a result, N and E^0 mix to form two Dirac fermion eigenstates

$$n_{1(L,R)} = \cos\theta_{L,R} N_{L,R} - \sin\theta_{L,R} E^0_{L,R}, \quad n_{2(L,R)} = \sin\theta_{L,R} N_{L,R} + \cos\theta_{L,R} E^0_{L,R}, \tag{4.4}$$

of masses $m_{1,2}$, with mixing angles

$$m_D m_E + m_F m_N = \sin\theta_L \cos\theta_L (m_1^2 - m_2^2), \tag{4.5}$$

$$m_D m_N + m_F m_E = \sin\theta_R \cos\theta_R (m_1^2 - m_2^2). \tag{4.6}$$

With the A_4 assignment of Eq. (4.2), and the soft breaking to Z_3 of the term $x_i y_j^*$, i.e.

$$U_\omega \begin{pmatrix} \mu_e^2 & 0 & 0 \\ 0 & \mu_\mu^2 & 0 \\ 0 & 0 & \mu_\tau^2 \end{pmatrix} = \frac{1}{\sqrt{3}} \begin{pmatrix} 1 & 1 & 1 \\ 1 & \omega & \omega^2 \\ 1 & \omega^2 & \omega \end{pmatrix} \begin{pmatrix} \mu_e^2 & 0 & 0 \\ 0 & \mu_\mu^2 & 0 \\ 0 & 0 & \mu_\tau^2 \end{pmatrix}, \tag{4.7}$$

where $\omega = \exp(2\pi i/3) = -1/2 + i\sqrt{3}/2$, and U_ω is the familiar [130] unitary matrix derivable from A_4, the charged-lepton mass matrix is given by

$$\mathcal{M}_l = U_\omega^\dagger \begin{pmatrix} m_e & 0 & 0 \\ 0 & m_\mu & 0 \\ 0 & 0 & m_\tau \end{pmatrix}, \tag{4.8}$$

with

$$m_e = -if' f_e \mu_e^2 \int \frac{d^4k}{(2\pi)^4} \frac{1}{(k^2 - m_{1e}^2)(k^2 - m_{2e}^2)} \left[\frac{m_1 \cos\theta_R \sin\theta_L}{k^2 - m_1^2} - \frac{m_2 \cos\theta_L \sin\theta_R}{k^2 - m_2^2} \right], \tag{4.9}$$

where f' is the $E_L^0 l_L x^*$ Yukawa coupling, f_e is the $N_R e_R y_1^*$ Yukawa coupling, and $m_{1e,2e}$ are the mass eigenvalues of the 2×2 mass-squared matrix

$$\mathcal{M}_{xy_1}^2 = \begin{pmatrix} m_x^2 & \mu_e^2 \\ \mu_e^2 & m_{y_1}^2 \end{pmatrix}, \tag{4.10}$$

with $\mu_e^2 = \sin\theta_e \cos\theta_e (m_{1e}^2 - m_{2e}^2)$, and similarly for m_μ and m_τ. It is clear that the residual Z_3 triality [128, 129] remains exact with $e, \mu, \tau \sim 1, \omega^2, \omega$, and the Higgs coupling matrix as well as the anomalous magnetic moment matrix are diagonal, as far as Fig. 4.1 is concerned. In other words, flavor is not violated in Higgs decays and $\mu \to e\gamma$ is not mediated by the new particles of Eq. (4.2).

4.3 Anomalous Higgs Yukawa Couplings

One immediate consequence of a radiative charged-lepton mass is that the Higgs Yukawa coupling $h\bar{l}l$ is no longer exactly m_l/v as in the SM. Its deviation is not suppressed by the usual one-loop factor of $16\pi^2$ and may be large enough to be observable [131]. Moreover, this deviation is finite and calculable exactly in one loop. For discussion, compare our proposal to the usual consideration of the deviation of the Higgs coupling from m_l/v from new physics in terms of higher-dimensional operators, i.e.

$$-\mathcal{L} = f_l \bar{l}_L l_R \phi^0 \left(1 + \frac{\Phi^\dagger \Phi}{\Lambda^2} \right), \tag{4.11}$$

where $\Lambda^2 >> v^2$. This implies $m_l = (f_l v/\sqrt{2})(1 + v^2/2\Lambda^2)$, whereas the Higgs coupling is $(f_l/\sqrt{2})(1 + 3v^2/2\Lambda^2) \simeq (m_l/v)(1 + v^2/\Lambda^2)$. However, this approach is only valid for $v^2 << \Lambda^2$, which guarantees the effect to be small. In the present case, if our result is interpreted as an expansion in powers of v^2, then it is a sum of infinite number of terms for both m_l and the Higgs coupling, but each sum is finite. Their ratio is not necessarily small because some particles in the loop could be light, as shown below.

There are three contributions to the $h\bar{l}l$ coupling: (1) the Yukawa terms $(f_D/\sqrt{2})h\bar{N}_L E^0_R$ and $(f_F/\sqrt{2})h\bar{E}^0_L N_R$, (2) the scalar trilinear $(\lambda_x v)hx^*x$ term, and (3) the scalar trilinear $(\lambda_y v)hy^*y$ term. In the following expressions, the couplings $f_{D,F}$ do not appear explicitly because they have been expressed in terms of the fermion masses $m_{1,2}$ and angles $\theta_{L,R}$. Consider $h\bar{\tau}\tau$. The detailed calculation of effective Higgs Yukawa coupling is presented in appendix B. The first contribution is given by

$$f^{(1)}_\tau = \frac{f' f_\tau \sin 2\theta_\tau}{32\pi^2 v}\big[c_R s_L T_1 + s_L s_R T_2 + c_L c_R T_3 + c_L s_R T_4\big], \tag{4.12}$$

where $x_{ij} = (\frac{m_{i\tau}}{m_j})^2$, $s_{L,R} = \sin\theta_{L,R}$, $c_{L,R} = \cos\theta_{L,R}$ and

$$\begin{aligned}
F_N(x) &= \frac{x(1+x)\ln x}{(1-x)^2} + \frac{2}{1-x}, \quad H(x) = \frac{x}{x-1}\ln x \\
T_1 &= [2m_2 s_L c_L s_R c_R - m_1(s^2_L c^2_R + c^2_L s^2_R)][F_N(x_{11}) - F_N(x_{21})], \\
T_2 &= m_2 s_L c_L (c^2_R - s^2_R)[H(x_{22}) - H(x_{12})] - m_1 s_R c_R (c^2_L - s^2_L)[H(x_{21}) - H(x_{11})], \\
T_3 &= m_1 s_L c_L (c^2_R - s^2_R)[H(x_{21}) - H(x_{11})] - m_2 s_R c_R (c^2_L - s^2_L)[H(x_{22}) - H(x_{12})], \\
T_4 &= [2m_1 c_L c_R s_L s_R - m_2(s^2_L c^2_R + c^2_L s^2_R)][F_N(x_{12}) - F_N(x_{22})].
\end{aligned} \tag{4.13}$$

The second contribution is given by

$$f_\tau^{(2)} = \frac{\lambda_x v f' f_\tau \sin 2\theta_\tau s_L c_L}{32\pi^2 m_1 m_2}\left[c_\tau^2 T_1' + s_\tau^2 T_2'\right], \tag{4.14}$$

where $c_\tau = \cos\theta_\tau$, $s_\tau = \sin\theta_\tau$ and

$$\begin{aligned} F(x,y) &= \frac{1}{x-y}\left[\frac{x}{x-1}\ln x - \frac{y}{y-1}\ln y\right] \quad x \neq y, \quad F(x,x) = \frac{1}{x-1} - \frac{\ln x}{(x-1)^2}, \\ T_1' &= m_2[F(x_{11},x_{11}) - F(x_{11},x_{21})] - m_1[F(x_{12},x_{12}) - F(x_{12},x_{22})], \\ T_2' &= m_2[F(x_{11},x_{21}) - F(x_{21},x_{21})] - m_1[F(x_{12},x_{22}) - F(x_{22},x_{22})]. \end{aligned} \tag{4.15}$$

The third contribution is given by

$$f_\tau^{(3)} = \frac{\lambda_y v f' f_\tau \sin 2\theta_\tau s_L c_L}{32\pi^2 m_1 m_2}\left[s_\tau^2 T_1' + c_\tau^2 T_2'\right]. \tag{4.16}$$

Combining all three contributions and using Eq. (4.9) for the tau mass, the effective Higgs Yukawa coupling $\tilde{f}_\tau$ is given by

$$\begin{aligned} \frac{\tilde{f}_\tau v}{m_\tau} &= \frac{[f_\tau^{(1)} + f_\tau^{(2)} + f_\tau^{(3)}]v}{m_\tau} \\ &= \frac{c_R s_L T_1 + s_L s_R T_2 + c_L c_R T_3 + c_L s_R T_4 + \frac{v^2 s_L c_L}{m_1 m_2}[(\lambda_x c_\tau^2 + \lambda_y s_\tau^2)T_1' + (\lambda_x s_\tau^2 + \lambda_y c_\tau^2)T_2']}{s_L c_R m_1[H(x_{21}) - H(x_{11})] + s_R c_L m_2[H(x_{12}) - H(x_{22})]}. \end{aligned} \tag{4.17}$$

To simplify the analysis, we focus on $\theta_L = \theta_R$, in which case $f_D = f_F$. We use the relation $f_D v/\sqrt{2} = s_L c_L(m_1 - m_2) = s_L c_L m_1(1 - m_2/m_1)$ from fermion mixing to define m_1 as a function of θ_L for a constant ratio $m_2/m_1 = 2.2$ and coupling $f_D/\sqrt{4\pi} = -0.19$. In this parameterization, the combination $s_L c_L m_1$ remains constant, and also appears in the radiative mass formula for each charged lepton. In addition, we use the value $f'/\sqrt{4\pi} =$

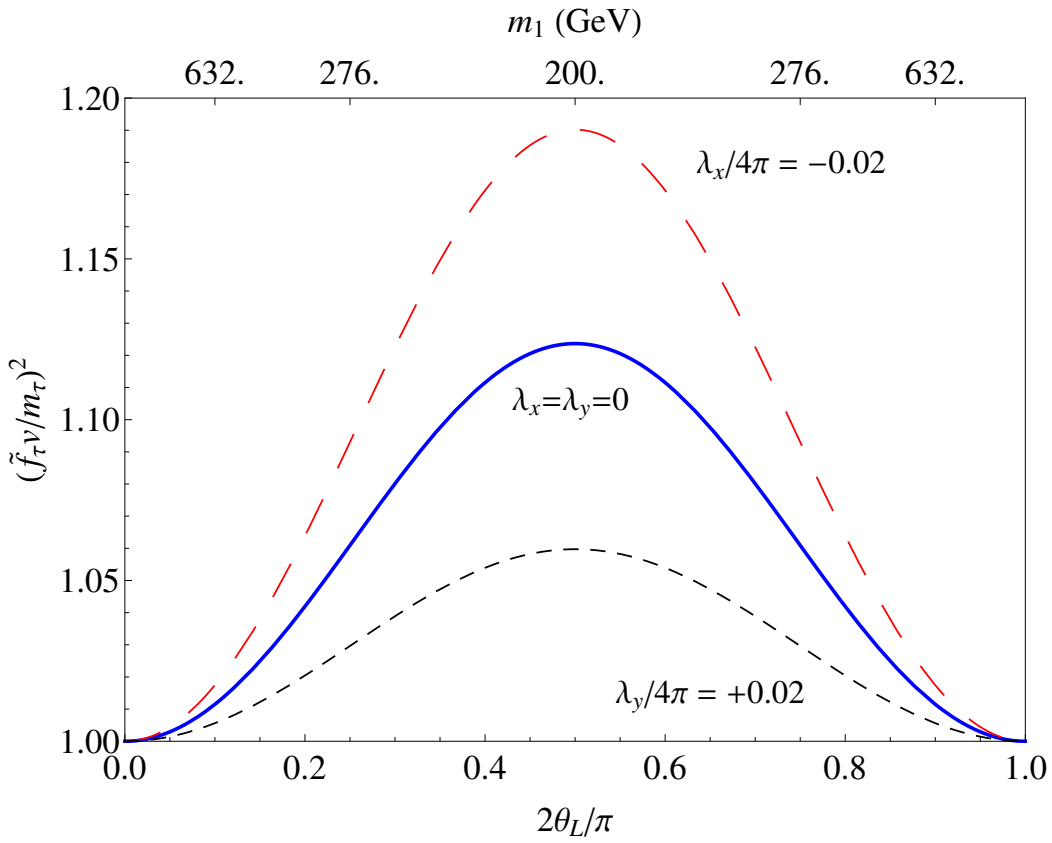

Figure 4.2: The ratio $(\tilde{f}_\tau v/m_\tau)^2$ plotted against θ_L with various $\lambda_{x,y}$ for the case $\theta_L = \theta_R$.

-0.6. For the scalars in the tau sector, we choose fixed mass ratios $m_{1\tau}/m_1 = 5.7$ and $m_{2\tau}/m_1 = 1.1$. To satisfy the mass formula, we verify that the product $f_\tau \sin 2\theta_\tau$ is not too large. We have checked that the values used here also allow solutions for the muon and electron radiative masses. In Fig. 4.2 we plot the effective Yukawa coupling from Eq. (4.17) as a function of θ_L, using the values $f_\tau/\sqrt{4\pi} = -0.54$, $\theta_\tau = 0.8$ for the $\lambda_{x,y}$ curves. We see that a significant deviation from the SM prediction is possible.

4.4 Muon Anomalous Magnetic Moment

Another important consequence of a radiative charged-lepton mass is that the same particles which generate m_l also contribute to its anomalous magnetic moment. This differs from the usual contribution of new physics, because there is again no $16\pi^2$ suppression. There are three contributions to the anomalous magnetic moment. The main contribution is given by (see appendix A)

$$\Delta a_\mu = \frac{m_\mu^2}{m_1 m_2}\left\{\frac{s_L c_R m_2[G(x_{11})-G(x_{21})]+s_R c_L m_1[G(x_{22})-G(x_{12})]}{s_L c_R m_1[H(x_{11})-H(x_{21})]+s_R c_L m_2[H(x_{22})-H(x_{12})]}\right\}, \tag{4.18}$$

where $x_{ij}=(\frac{m_{i\mu}}{m_j})^2$ and

$$G(x)=\frac{2x\ln x}{(x-1)^3}-\frac{x+1}{(x-1)^2}. \tag{4.19}$$

In the simplifying case we are considering, Eq. (4.18) is independent of $\theta_L=\theta_R$. In Fig. 4.3 we plot $m_{1\mu}$ against m_1 for various ratios $m_{2\mu}/m_{1\mu}$ in order to show the values of m_1 and $m_{1,2\mu}$ which can account for the discrepancy between the experimental measurement [132] and the SM prediction [133]

$$\Delta a_\mu = 39.35 \pm 5.21_{\rm th} \pm 6.3_{\rm exp} \times 10^{-10} \tag{4.20}$$

We have combined the experimental and theoretical uncertainties in quadrature, which corresponds to the curved limits of the shaded regions. The lower limit of 200 GeV for m_1 corresponds to $\theta_L=\pi/4$.

The subdominant contributions to Δa_μ from f'^2 , and f_μ^2 are negative as expected

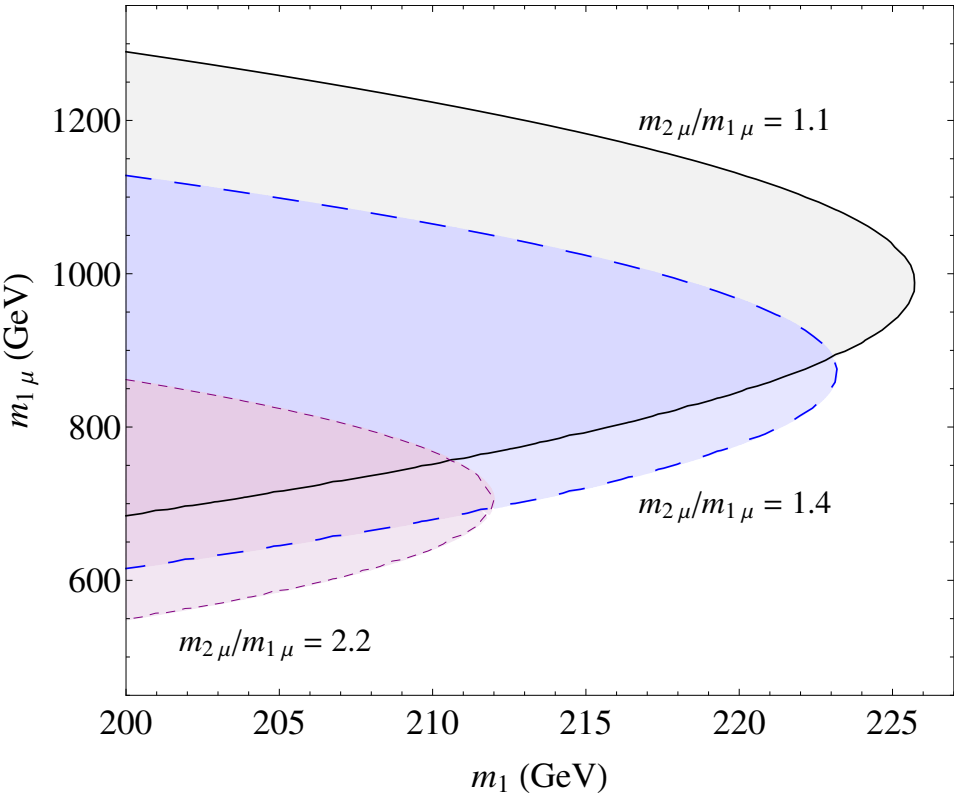

Figure 4.3: Values of m_1 and $m_{1,2\mu}$ which can explain Δa_μ for the case $\theta_L = \theta_R$.

, i.e.

$$(\Delta a_\mu)' = \frac{-m_\mu^2}{32\pi^2}\Bigg\{ \quad f'^2\left[\frac{s_L^2}{m_1^2}\left(c_\mu^2 J(x_{11}) + s_\mu^2 J(x_{21})\right) + \frac{c_L^2}{m_2^2}\left(c_\mu^2 J(x_{12}) + s_\mu^2 J(x_{22})\right)\right] \\ + f_\mu^2\Bigg[\quad \frac{c_R^2}{m_1^2}\left(s_\mu^2 J(x_{11}) + c_\mu^2 J(x_{21})\right) + \frac{s_R^2}{m_2^2}\left(s_\mu^2 J(x_{12}) + c_\mu^2 J(x_{22})\right)\Bigg]\Bigg\}, \quad (4.21)$$

where

$$J(x) = \frac{x\ln x}{(x-1)^4} + \frac{x^2 - 5x - 2}{6(x-1)^3}. \quad (4.22)$$

The third contribution is from s exchange which will be introduced in the next section and is given by

$$(\Delta a_\mu)'' = \sum_{i=1}^{3} \frac{-f^2 |U_{\mu i}|^2 m_\mu^2}{16\pi^2 m_E^2} G_\gamma(x_i), \quad (4.23)$$

where $x_i = \frac{m_{s_i}^2}{m_E^2}$ and

$$G_\gamma(x) = \frac{2x^3 + 3x^2 - 6x^2 \ln x - 6x + 1}{6(x-1)^4} < \frac{1}{6}. \tag{4.24}$$

The mass of E^- has a lower limit of $m_E \simeq 300$ GeV, which is numerically equivalent to $G_F m_E^2 \simeq 1$ used in the following section, due to our parameterization for the fermion mixing of N and E^0. Hence $(\Delta a_\mu)''$ is less than $10^{-10} f^2$, which for $f < 1$ is below the present experimental sensitivity of 10^{-9} and thus can be neglected.

4.5 Rare Lepton Decays

Whereas Z_3 lepton triality is exact in Fig. 4.1, the corresponding diagram for neutrino mass breaks it, as shown below. The new particles are three real scalars $s_{1,2,3} \sim \underline{3}$

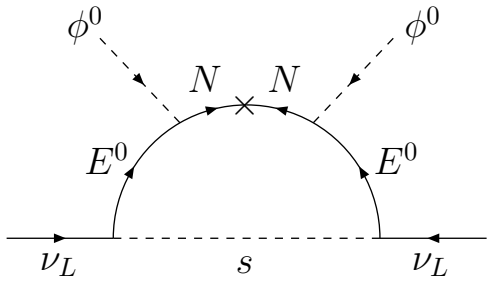

Figure 4.4: One-loop generation of neutrino mass.

under A_4. To connect the loop, Majorana mass terms $(m_L/2)N_L N_L$ and $(m_R/2)N_R N_R$ are assumed. Since both E and N may be defined to carry lepton number, these new terms violate lepton number softly and may be naturally small. Using the Yukawa interaction

$fs\bar{E}^0_R\nu_L$, the one-loop Majorana neutrino mass is given by

$$\begin{aligned} m_\nu &= f^2 m_R \sin^2\theta_R \cos^2\theta_R (m_1^2 - m_2^2)^2 \int \frac{d^4k}{(2\pi)^4} \frac{k^2}{(k^2-m_s^2)} \frac{1}{(k^2-m_1^2)^2} \frac{1}{(k^2-m_2^2)^2} \\ &+ f^2 m_L m_1^2 \sin^2\theta_L \cos^2\theta_R \int \frac{d^4k}{(2\pi)^4} \frac{1}{(k^2-m_s^2)} \frac{1}{(k^2-m_1^2)^2} \\ &+ f^2 m_L m_2^2 \sin^2\theta_R \cos^2\theta_L \int \frac{d^4k}{(2\pi)^4} \frac{1}{(k^2-m_s^2)} \frac{1}{(k^2-m_2^2)^2} \\ &- 2f^2 m_L m_1 m_2 \sin\theta_L \sin\theta_R \cos\theta_L \cos\theta_R \int \frac{d^4k}{(2\pi)^4} \frac{1}{(k^2-m_s^2)} \frac{1}{(k^2-m_1^2)} \frac{1}{(k^2-m_2^2)}. \end{aligned} \tag{4.25}$$

This formula holds for s as a mass eigenstate. If A_4 is unbroken, then $s_{1,2,3}$ all have the same mass and $\mathcal{M}_\nu$ is proportional to the identity matrix. However, if A_4 is softly broken by the necessarily real $s_i s_j$ mass terms, then the neutrino mass matrix is given by

$$\mathcal{M}_\nu = \mathcal{O} \begin{pmatrix} m_{\nu 1} & 0 & 0 \\ 0 & m_{\nu 2} & 0 \\ 0 & 0 & m_{\nu 3} \end{pmatrix} \mathcal{O}^T, \tag{4.26}$$

where $\mathcal{O}$ is an orthogonal matrix and $\mathcal{O} \neq 1$ breaks Z_3 lepton triality explicitly. Now each $m_{\nu i}$ may be complex because f, m_L, m_R may be complex, but a common unphysical phase, say for ν_1, may be rotated away, leaving just two relative Majorana phases for ν_2 and ν_3, owing to the relative phase between m_L and m_R with different $s_{1,2,3}$ masses. Hence $\mathcal{M}_\nu$ is diagonalized by $\mathcal{O}$, which is all that is required to obtain cobimaximal mixing [134], i.e. $\theta_{23} = \pi/4$ and $\delta_{CP} = \pm\pi/2$, once U_ω is applied, as explained in Ref. [127].

The companion interaction to $fs\bar{E}^0_R\nu_L$ is $fs\bar{E}^-_R l_L$, which induces the radiative process $l_i \to l_j + \gamma$. In the limit of exact Z_3 lepton triality, this amplitude is zero. Here it is proportional to $\sum_k U_{ik} U^*_{jk} F_k$ where $F_{1,2,3}$ refer to functions of $m^2_{s_{1,2,3}}$, and U_{ik} is the neutrino mixing matrix. Clearly, it is also zero if $F_1 = F_2 = F_3$. The amplitude for $\mu \to e\gamma$

is given by

$$A_{\mu e} = \frac{ef^2 m_\mu}{32\pi^2 m_E^2} \sum_i U_{ei}^* U_{\mu i} G_\gamma(x_i), \tag{4.27}$$

Using the bound on $\mu \to e\gamma$ [135], this branching fraction is constrained by

$$B = \frac{12\pi^2 |A_{\mu e}|^2}{m_\mu^2 G_F^2} < 5.7 \times 10^{-13}. \tag{4.28}$$

For small x_i and $x_1 \simeq x_2$,

$$|\sum_i U_{ei}^* U_{\mu i} G_\gamma(x_i)| = \frac{s_{13} c_{13}}{3\sqrt{2}} |x_3 - x_2|, \tag{4.29}$$

where $s_{13} = \sin\theta_{13}$, $c_{13} = \cos\theta_{13}$, and $\sin\theta_{23} = 1/\sqrt{2}$ has been assumed. Hence

$$B = \frac{\alpha s_{13}^2 c_{13}^2}{384\pi} \left(\frac{f^2 |x_3 - x_2|}{G_F m_E^2} \right)^2. \tag{4.30}$$

Let $G_F m_E^2 \simeq 1$, $f = 0.2$, $|x_3 - x_2| \simeq 0.05$, then $B = 5.6 \times 10^{-13}$, just below the experimental constraint.

Another possible rare decay is $\mu \to eee$, which comes from $\mu \to e(\gamma, Z) \to eee$ as well as directly through a box diagram as shown below. The amplitude for the former

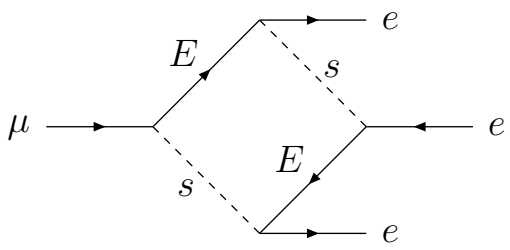

Figure 4.5: Box diagram for $\mu \to eee$.

process with a virtual photon is given by

$$\begin{aligned}\mathcal{M}_\gamma &= \frac{-e^2 f^2}{32\pi^2 m_E^2}\sum_i^3 U_{ei}^* U_{\mu i}\bar{u}(p_1)\left[G_e(x_i)\left(\gamma^\alpha - \frac{q^\alpha \not{q}}{q^2}\right)P_L - i m_\mu G_\gamma(x_i)\frac{\sigma^{\alpha\beta}q_\beta}{q^2}P_R\right]\mathcal{O} \\ &- (p_1 \leftrightarrow p_2),\end{aligned} \tag{4.31}$$

where $\mathcal{O} \equiv u_\mu(p)\bar{u}(p_2)\gamma_\alpha v(p_3)$, $P_{L,R} = (1 \mp \gamma_5)/2$, $q = p - p_1$ and

$$G_e(x) = \frac{7 - 36x + 45x^2 - 16x^3 + 6x^2(2x-3)\ln x}{18(x-1)^4}. \tag{4.32}$$

The amplitude for the process with a virtual Z boson has a similar form because $E_{L,R}$ is vector-like, but it is further suppressed by m_Z^2. The amplitude for the box diagram is given by

$$i\mathcal{M}_B = \frac{if^4[\bar{u}(p_1)\gamma_\alpha P_L u_\mu(p)\bar{u}(p_2)\gamma^\alpha P_L v(p_3) - (p_1 \leftrightarrow p_2)]}{64\pi^2 m_E^2}\sum_{i,j=1}^3 U_{\mu i}U_{ej}^*[U_{ei}U_{ej}^* - U_{ej}U_{ei}^*]B_{ij}, \tag{4.33}$$

where

$$B_{ij} = \frac{B(x_i) - B(x_j)}{x_i - x_j} \quad i \neq j, \quad B_{ii} = \frac{x_i^2 - 2x_i\ln x_i - 1}{(x_i-1)^3}, \quad B(x) = \frac{x^2\ln x}{(x-1)^2} - \frac{1}{x-1}. \tag{4.34}$$

With the same specific choice of parameters as in Eq. (4.29) we find that the box diagram contribution is dominant. Hence the $\mu \to eee$ branching fraction is

$$B' = \frac{f^8}{2(8\pi)^4 m_E^4 G_F^2}\left|\sum_{i,j=1}^3 U_{\mu i}U_{ej}^*[U_{ei}U_{ej}^* - U_{ej}U_{ei}^*]B_{ij}\right|^2. \tag{4.35}$$

Using the bound [136] on $\mu \to eee$ decay and for small x_i we have

$$B' = \frac{f^8}{2(8\pi)^4 m_E^4 G_F^2}\frac{\sin^2(4\theta_{13})}{8} < 1.0 \times 10^{-12}. \tag{4.36}$$

This constraint is easily satisfied for $G_F m_E^2 \simeq 1$, $f = 0.2$, which yields $B' = 1.35 \times 10^{-13}$.

4.6 Dark Matter

As for dark matter, there is a one-to-one correlation of the neutrino mass eigenstates to the $s_{1,2,3}$ mass eigenstates, the lightest of which is dark matter. Due to the presence of the A_4 symmetry, the dark matter parity of this model is also derivable from lepton parity [137]. Under lepton parity, let the new particles $(E^0, E^-), N$ be even and s, x, y be odd, then the same Lagrangian is obtained. As a result, dark parity is simply given by $(-1)^{L+2j}$, which is odd for all the new particles and even for all the SM particles. Note that the tree-level Yukawa coupling $\bar{l}_L l_R \phi^0$ would be allowed by lepton parity alone, but is forbidden here because of the A_4 symmetry.

If the Yukawa coupling f of s to leptons is small, its relic density and elastic cross section off nuclei are both controlled by the interaction $\lambda v h s^2$. As such, an analysis [116] claims that the resulting allowed parameter space is limited to a small region near $m_s < m_h/2$. To evade this constraint, the mechanism of Ref. [121] may be invoked. Add a complex neutral singlet scalar $\chi \sim \underline{1}'$ under A_4 with Z_2 even. The dimension-four terms of the Lagrangian are of course required to be invariant under A_4. We assume that the dimension-three terms are also invariant: χ^3, $(\chi^\dagger)^3$, $(s_1^2 + \omega^2 s_2^2 + \omega s_3^2)\chi$, and $(s_1^2 + \omega s_2^2 + \omega^2 s_3^2)\chi^\dagger$. The symmetry A_4 is broken only by the dimension-two terms: χ^2, $(\chi^\dagger)^2$, and $s_i s_j$. As a result, χ is split into χ_R and χ_I, each mixing with h radiatively. In the physical basis, the dark matter s has residual $s^2 \chi_{R,I}$ interactions which contribute to its annihilation cross section, but do not affect its scattering off nuclei through h exchange.

Let us denote the $\chi_{R,I}$ masses with $m_{R,I}$. For illustration, we assume $m_R < m_s < m_I$, and take the $\chi_I \chi_R^2$ coupling to be zero, so that the annihilations shown in Fig. 4.6 are

controlled by the interaction terms

$$-\mathcal{L}_{int} = \frac{\lambda'}{4} s^2 \chi_R^2 + \frac{g}{2} s^2 \chi_R + \frac{g'}{3!} \chi_R^3 \tag{4.37}$$

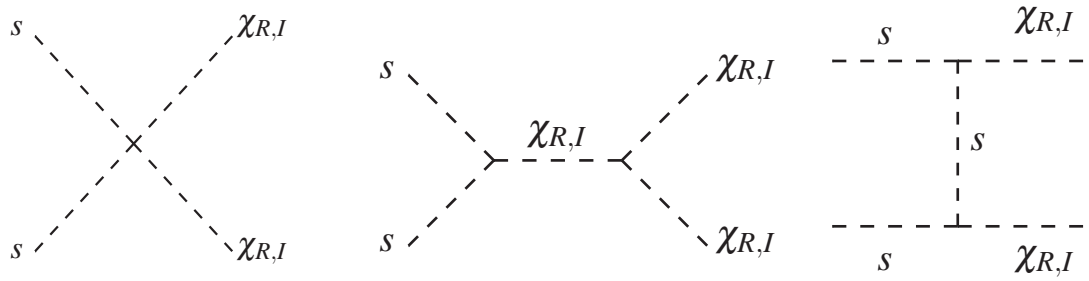

Figure 4.6: $s\,s$ annihilation to $\chi_{R,I}$ mass eigenstates.

As a result, the annihilation cross section times relative velocity is given by

$$\sigma \times v_{rel} = \frac{\sqrt{1-(m_R/m_s)^2}}{64\pi m_s^2} \left(\lambda' + \frac{g'g}{4m_s^2 - m_R^2} - \frac{g^2}{2m_s^2 - m_R^2} \right)^2 . \tag{4.38}$$

Setting this equal to $2.2 \times 10^{-26}\,\mathrm{cm^3 s^{-1}}$, with $m_s = 200$ GeV and $m_R = 150$ GeV, we find

$$\lambda' + 0.073 \left(\frac{\sqrt{g'g}}{100\,\mathrm{GeV}} \right)^2 - 0.174 \left(\frac{g}{100\,\mathrm{GeV}} \right)^2 = 0.1514. \tag{4.39}$$

Note that χ_R decays to SM particles through its mixing with h. As mentioned earlier, the spin-independent elastic cross section proceeds through h exchange, with

$$\sigma_{SI} = \frac{\lambda^2 f_N^2 \mu^2 m_N^2}{\pi m_h^4 m_s^2}, \tag{4.40}$$

where $\mu = m_N m_s/(m_N + m_s)$ is the DM-nucleon reduced mass, $m_N = (m_p + m_n)/2 = 938.95\,\mathrm{MeV}$ is the nucleon mass, and $f_N = 0.3$ is the Higgs-nucleon coupling factor [138]. The LUX bound [139] for $m_s = 200\,\mathrm{GeV}$ is $\sigma \approx 1.5$ zb , which implies

$$\lambda < 3.3 \times 10^{-4}. \tag{4.41}$$

4.7 Conclusion

In conclusion, in the context of a specific A_4 scotogenic (dark-matter-induced) model of radiative neutrino and charged-lepton masses with the one Higgs boson of the standard model, we study finite calculable anomalous Higgs couplings with possible large deviations from the SM predictions. We show that the observed discrepancy in the muon anomalous magnetic moment may be explained by new particles in the TeV mass range, with predictions for the lepton flavor violating processes $\mu \to e\gamma$ and $\mu \to eee$. We also discuss the nature of the expected dark matter in this scenario.

Chapter 5

Phenomenology of the Utilitarian Supersymmetric Standard Model

5.1 Introduction

In 2002, a model was proposed [140] which extends the supersymmetric standard model by a new $U(1)_X$ gauge symmetry. It replaces the μ term with a singlet scalar superfield which also couples to heavy color-triplet superfields which are electroweak singlets. The latter are not *ad hoc* inventions, but are necessary for the cancellation of axial-vector anomalies. It was shown in Ref. [140] how this was accomplished by the remarkable exact factorization of the sum of eleven cubic terms, resulting in two generic classes of solutions [141]. Both are able to enforce the conservation of baryon number and lepton number up to dimension-five terms. As such, the scalar singlet and the vectorlike quarks are indispensible ingredients of this 2002 model. In 2010 [142], a specific version was discussed,

which will be the subject of this paper as well. An important byproduct of this study is the discovery of relaxed supersymmetric constraints on the Higgs boson's mass of 125 GeV.

In 2015, ATLAS [143] and CMS [144] announced a diphoton excess around 750 GeV. At that point, numerous papers [145] have appeared, explaining its presence or discussing its implications. In this paper, we study the phenomenology of the 2002 model, which has exactly all the necessary and sufficient particles and interactions for this purpose. Of course, they were there for solving other issues in particle physics. The observed diphoton excess could have been a first revelation [146] of this model, including its connection to dark matter. However, this excess was absent in data collected in 2016, suggesting that the diphoton excess was a statistical fluctuation [147, 148].

5.2 Model

Consider the gauge group $SU(3)_C \times SU(2)_L \times U(1)_Y \times U(1)_X$ with the particle content of Ref. [140]. For $n_1 = 0$ and $n_4 = 1/3$ in Solution (A), the various superfields transform as shown in Table 5.1. There are three copies of $Q, u^c, d^c, L, e^c, N^c, S_1, S_2$; two copies of U, U^c, S_3; and one copy of ϕ_1, ϕ_2, D, D^c. The only allowed terms of the superpotential are thus trilinear, i.e.

$$Qu^c\phi_2, \quad Qd^c\phi_1, \quad Le^c\phi_1, \quad LN^c\phi_2, \quad S_3\phi_1\phi_2, \quad N^cN^cS_1, \tag{5.1}$$

$$S_3UU^c, \quad S_3DD^c, \quad u^cN^cU, \quad u^ce^cD, \quad d^cN^cD, \quad QLD^c, \quad S_1S_2S_3. \tag{5.2}$$

The absence of any bilinear term means that all masses come from soft supersymmetry breaking, thus explaining why the $U(1)_X$ and electroweak symmetry breaking scales are not

Table 5.1: Particle content of proposed model.

Superfield	$SU(3)_C$	$SU(2)_L$	$U(1)_Y$	$U(1)_X$
$Q = (u, d)$	3	2	1/6	0
u^c	3^*	1	$-2/3$	1/2
d^c	3^*	1	1/3	1/2
$L = (\nu, e)$	1	2	$-1/2$	1/3
e^c	1	1	1	1/6
N^c	1	1	0	1/6
ϕ_1	1	2	$-1/2$	$-1/2$
ϕ_2	1	2	1/2	$-1/2$
S_1	1	1	0	$-1/3$
S_2	1	1	0	$-2/3$
S_3	1	1	0	1
U	3	1	2/3	$-2/3$
D	3	1	$-1/3$	$-2/3$
U^c	3^*	1	$-2/3$	$-1/3$
D^c	3^*	1	1/3	$-1/3$

far from that of supersymmetry breaking. As $S_{1,2,3}$ acquire nonzero vacuum expectation values (VEVs), the exotic (U, U^c) and (D, D^c) fermions obtain Dirac masses from $\langle S_3 \rangle$, which also generates the μ term. The singlet N^c fermion gets a large Majorana mass from $\langle S_1 \rangle$, so that the neutrino ν gets a small seesaw mass in the usual way. The singlet $S_{1,2,3}$ fermions themselves get Majorana masses from their scalar counterparts $\langle S_{1,2,3} \rangle$ through the $S_1 S_2 S_3$ terms. The only massless fields left are the usual quarks and leptons. They then become massive as $\phi^0_{1,2}$ acquire VEVs, as in the minimal supersymmetric standard model (MSSM).

Because of $U(1)_X$, the structure of the superpotential conserves both B and $(-1)^L$, with $B = 1/3$ for Q, U, D, and $B = -1/3$ for u^c, d^c, U^c, D^c; $(-1)^L$ odd for $L, e^c, N^c, U, U^c, D, D^c$, and even for all others. Hence the exotic U, U^c, D, D^c scalars are leptoquarks and decay into ordinary quarks and leptons. The R parity of the MSSM is defined here in the same

way, i.e. $R \equiv (-)^{2j+3B+L}$, and is conserved. Note also that the quadrilinear terms $QQQL$ and $u^c u^c d^c e^c$ (allowed in the MSSM) as well as $u^c d^c d^c N^c$ are forbidden by $U(1)_X$. Proton decay is thus strongly suppressed. It may proceed through the quintilinear term $QQQLS_1$ as the S_1 fields acquire VEVs, but this is a dimension-six term in the effective Lagrangian, which is suppressed by two powers of a very large mass, say the Planck mass, and may safely be allowed.

5.3 Gauge Sector

The new Z_X gauge boson of this model becomes massive through $\langle S_{1,2,3} \rangle = u_{1,2,3}$, whereas $\langle \phi^0_{1,2} \rangle = v_{1,2}$ contribute to both Z and Z_X. The resulting 2×2 mass-squared matrix is given by [149]

$$\mathcal{M}^2_{Z,Z_X} = \begin{pmatrix} (1/2) g_Z^2 (v_1^2 + v_2^2) & (1/2) g_Z g_X (v_2^2 - v_1^2) \\ (1/2) g_Z g_X (v_2^2 - v_1^2) & 2 g_X^2 [(1/9) u_1^2 + (4/9) u_2^2 + u_3^2 + (1/4)(v_1^2 + v_2^2)] \end{pmatrix}. \quad (5.3)$$

Since precision electroweak measurements require $Z - Z_X$ mixing to be very small [150], $v_1 = v_2$, i.e. $\tan\beta = 1$, is preferred. With the 2012 discovery [49, 50] of the 125 GeV particle, and identified as the one Higgs boson h responsible for electroweak symmetry breaking, $\tan\beta = 1$ is not compatible with the MSSM, but is perfectly consistent here, as shown already in Ref. [142] and in more detail in the next section.

Consider the decay of Z_X to the usual quarks and leptons. Each fermionic partial width is given by

$$\Gamma(Z_X \to \bar{f} f) = \frac{g_X^2 M_{Z_X}}{24\pi} [c_L^2 + c_R^2], \quad (5.4)$$

where $c_{L,R}$ can be read off under $U(1)_X$ from Table 5.1. Thus

$$\frac{\Gamma(Z_X \to \bar{t}t)}{\Gamma(Z_X \to \mu^+\mu^-)} = \frac{\Gamma(Z_X \to \bar{b}b)}{\Gamma(Z_X \to \mu^+\mu^-)} = \frac{27}{5}. \tag{5.5}$$

This will serve to distinguish it from other Z' models [151].

At the LHC, limits on the mass of any Z' boson depend on its production by u and d quarks times its branching fraction to e^-e^+ and $\mu^-\mu^+$. In a general analysis of Z' couplings to u and d quarks,

$$\mathcal{L} = \frac{g'}{2} Z'_\mu \bar{f} \gamma_\mu (g_V - g_A \gamma_5) f, \tag{5.6}$$

where $f = u, d$. The c_u, c_d coefficients used in an experimental search [114, 152] of Z' are then given by

$$c_u = \frac{g'^2}{2}[(g_V^u)^2 + (g_A^u)^2] B(Z' \to l^- l^+), \quad c_d = \frac{g'^2}{2}[(g_V^d)^2 + (g_A^d)^2] B(Z' \to l^- l^+), \tag{5.7}$$

where $l = e, \mu$. In this model

$$c_u = c_d = \frac{g_X^2}{4} B(Z' \to l^- l^+). \tag{5.8}$$

To estimate $B(Z' \to l^- l^+)$, we assume Z_X decays to all SM quarks and leptons with effective zero mass, all the scalar leptons with effective mass of 500 GeV, all the scalar quarks with effective mass of 800 GeV, the exotic U, D fermions with effective mass of 400 GeV (needed to explain the diphoton excess), and one pseudo-Dirac fermion from combining $\tilde{S}_{1,2}$ (the dark matter candidate to be discussed) with mass of 200 GeV. We find $B(Z' \to l^- l^+) = 0.04$, and for $g_X = 0.53$, a lower bound of 2.85 TeV on m_{Z_X} is obtained from the LHC data based on the 7 and 8 TeV runs.

5.4 Scalar Sector

Consider the scalar potential consisting of $\phi_{1,2}$ and $S_{1,2,3}$, where only the $S_{1,2,3}$ scalars with VEVs are included. The superpotential linking the corresponding superfields is

$$W = fS_3\phi_1\phi_2 + hS_3S_2S_1. \tag{5.9}$$

Its contribution to the scalar potential is

$$V_F = f^2(\Phi_1^\dagger\Phi_1 + \Phi_2^\dagger\Phi_2)S_3^*S_3 + h^2(S_1^*S_1 + S_2^*S_2)S_3^*S_3 + |f\Phi_1^\dagger\Phi_2 + hS_1S_2|^2, \tag{5.10}$$

where ϕ_1 has been redefined to $\Phi_1 = (\phi_1^+, \phi_1^0)$. The gauge contribution is

$$\begin{aligned} V_D &= \frac{1}{8}g_2^2[(\Phi_1^\dagger\Phi_1)^2 + (\Phi_2^\dagger\Phi_2)^2 + 2(\Phi_1^\dagger\Phi_1)(\Phi_2^\dagger\Phi_2) - 4(\Phi_1^\dagger\Phi_2)(\Phi_2^\dagger\Phi_1)] \\ &+ \frac{1}{8}g_1^2[-(\Phi_1^\dagger\Phi_1) + (\Phi_2^\dagger\Phi_2)]^2 \\ &+ \frac{1}{2}g_X^2\left[-\frac{1}{2}\Phi_1^\dagger\Phi_1 - \frac{1}{2}\Phi_2^\dagger\Phi_2 - \frac{1}{3}S_1^*S_1 - \frac{2}{3}S_2^*S_2 + S_3^*S_3\right]^2. \end{aligned} \tag{5.11}$$

The soft supersymmetry-breaking terms are

$$\begin{aligned} V_{soft} &= \mu_1^2\Phi_1^\dagger\Phi_1 + \mu_2^2\Phi_2^\dagger\Phi_2 + m_3^2S_3^*S_3 + m_2^2S_2^*S_2 + m_1^2S_1^*S_1 \\ &+ [m_{12}S_2^*S_1^2 + A_f fS_3\Phi_1^\dagger\Phi_2 + A_h hS_3S_2S_1 + H.c.]. \end{aligned} \tag{5.12}$$

In addition, there is an important one-loop contribution from the t quark and its supersymmetric scalar partners:

$$V_t = \frac{1}{2}\lambda_2(\Phi_2^\dagger\Phi_2)^2, \tag{5.13}$$

where

$$\lambda_2 = \frac{6G_F^2m_t^4}{\pi^2}\ln\left(\frac{m_{\tilde{t}_1}m_{\tilde{t}_2}}{m_t^2}\right) \tag{5.14}$$

is the well-known correction which allows the Higgs mass to exceed m_Z.

Let $\langle \phi^0_{1,2} \rangle = v_{1,2}$ and $\langle S_{1,2,3} \rangle = u_{1,2,3}$, we study the conditions for obtaining a minimum of the scalar potential $V = V_F + V_D + V_{soft} + V_t$. We look for the solution $v_1 = v_2 = v$ which implies that

$$\mu_1^2 = \mu_2^2 + \lambda_2 v^2 \tag{5.15}$$

$$0 = \mu_1^2 + A_f f u_3 + f^2(u_3^2 + v^2) + \frac{1}{2} g_X^2 \left(v^2 + \frac{1}{3} u_1^2 + \frac{2}{3} u_2^2 - u_3^2 \right) + f h u_1 u_2. \tag{5.16}$$

We then require that this solution does not mix the $Re(\phi_{1,2})$ and $Re(S_{1,2,3})$ sectors. The additional conditions are

$$0 = A_f f + (2f^2 - g_X^2) u_3, \tag{5.17}$$

$$0 = \frac{1}{3} g_X^2 u_1 + f h u_2, \tag{5.18}$$

$$0 = \frac{2}{3} g_X^2 u_2 + f h u_1. \tag{5.19}$$

Hence

$$u_1 = \sqrt{2} u_2, \quad fh = \frac{-\sqrt{2} g_X^2}{3}. \tag{5.20}$$

The 2×2 mass-squared matrix spanning $[\sqrt{2} Re(\phi_1^0), \sqrt{2} Re(\phi_2^0)]$ is

$$\mathcal{M}_\phi^2 = \begin{pmatrix} \kappa + g_X^2 v^2/2 & -\kappa + g_X^2 v^2/2 + 2f^2 v^2 \\ -\kappa + g_X^2 v^2/2 + 2f^2 v^2 & \kappa + g_X^2 v^2/2 + 2\lambda_2 v^2 \end{pmatrix}, \tag{5.21}$$

where

$$\kappa = (2f^2 - g_X^2) u_3^2 + \frac{2}{3} g_X^2 u_2^2 + \frac{1}{2} (g_1^2 + g_2^2) v^2. \tag{5.22}$$

For $\lambda_2 v^2 << \kappa$, the Higgs boson $h \simeq Re(\phi_1^0 + \phi_2^0)$ has a mass given by

$$m_h^2 \simeq \left(g_X^2 + 2f^2 + \lambda_2 \right) v^2, \tag{5.23}$$

whereas its heavy counterpart $H \simeq Re(-\phi_1^0 + \phi_2^0)$ has a mass given by

$$m_H^2 \simeq (4f^2 - 2g_X^2)u_3^2 + \frac{4}{3}g_X^2 u_2^2 + (g_1^2 + g_2^2 - 2f^2 + \lambda_2)v^2. \tag{5.24}$$

The conditions for obtaining the minimum of V in the $S_{1,2,3}$ directions are

$$\begin{aligned}
0 &= m_3^2 + g_X^2 u_3^2 + \left(3h^2 - \frac{4}{3}g_X^2\right)u_2^2 + \frac{\sqrt{2}A_h h u_2^2}{u_3}, &(5.25)\\
0 &= m_2^2 + 2m_{12}u_2 + \left(2h^2 + \frac{8}{9}g_X^2\right)u_2^2 + \left(h^2 - \frac{2}{3}g_X^2\right)u_3^2 + \sqrt{2}A_h h u_3, &(5.26)\\
0 &= m_1^2 + 2m_{12}u_2 + \left(h^2 + \frac{4}{9}g_X^2\right)u_2^2 + \left(h^2 - \frac{1}{3}g_X^2\right)u_3^2 + \frac{1}{\sqrt{2}}A_h h u_3. &(5.27)
\end{aligned}$$

The 3×3 mass-squared matrix spanning $[\sqrt{2}Re(S_1), \sqrt{2}Re(S_2), \sqrt{2}Re(S_3)]$ is given by

$$\begin{aligned}
m_{11}^2 &= \frac{4}{9}g_X^2 u_2^2 - \frac{1}{\sqrt{2}}A_h h u_3 + \frac{1}{3}g_X^2 v^2, \quad m_{22}^2 = 2m_{11}^2 - 2m_{12}u_2, &(5.28)\\
m_{12}^2 &= m_{21}^2 = 2\sqrt{2}m_{12}u_2 + A_h h u_3 + 2\sqrt{2}\left(h^2 + \frac{2}{9}g_X^2\right)u_2^2 - \frac{\sqrt{2}}{3}g_X^2 v^2, &(5.29)\\
m_{33}^2 &= 2g_X^2 u_3^2 - \sqrt{2}A_h h u_2^2/u_3 + (2f^2 - g_X^2)v^2, &(5.30)\\
m_{13}^2 &= m_{31}^2 = A_h h u_2 + 2\sqrt{2}\left(h^2 - \frac{1}{3}g_X^2\right)u_3 u_2, &(5.31)\\
m_{23}^2 &= m_{32}^2 = \sqrt{2}A_h h u_2 + 2\left(h^2 - \frac{2}{3}g_X^2\right)u_3 u_2. &(5.32)
\end{aligned}$$

The 5×5 mass-squared matrix spanning $[\sqrt{2}Im(\phi_1^0), \sqrt{2}Im(\phi_2^0), \sqrt{2}Im(S_1), \sqrt{2}Im(S_2), \sqrt{2}Im(S_3)]$ has two zero eigenvalues, corresponding to the would-be Goldstone modes

$$(1,1,0,0,0) \quad \text{and} \quad (v/2, -v/2, -\sqrt{2}u_2/3, -2u_2/3, u_3), \tag{5.33}$$

for the Z and Z_X gauge bosons. One exact mass eigenstate is $A_{12} = [2Im(S_1) - \sqrt{2}Im(S_2)]/\sqrt{3}$ with mass given by

$$m_{A_{12}}^2 = -6m_{12}u_2. \tag{5.34}$$

Assuming that $v^2 << u_{2,3}^2$, the other two mass eigenstates are $A \simeq -Im(\phi_1^0) + Im(\phi_2^0)$ and $A_S \simeq [u_3 Im(S_1) + \sqrt{2} u_3 Im(S_2) + \sqrt{2} u_2 Im(S_3)]/\sqrt{u_2^2 + 3u_3^2/2}$ with masses given by

$$m_A^2 \simeq (4f^2 - 2g_X^2)u_3^2 + \frac{4}{3} g_X^2 u_2^2, \tag{5.35}$$

$$m_{A_S}^2 \simeq -A_h h \left(\frac{3u_3}{\sqrt{2}} + \frac{\sqrt{2}u_2^2}{u_3} \right), \tag{5.36}$$

respectively. The charged scalar $H^\pm = (-\phi_1^\pm + \phi_2^\pm)/\sqrt{2}$ has a mass given by

$$m_{H^\pm}^2 = (4f^2 - 2g_X^2)u_3^2 + \frac{4}{3} g_X^2 u_2^2 + (g_2^2 - 2f^2)v^2. \tag{5.37}$$

5.5 Physical Scalars and Pseudoscalars

In the MSSM without radiative corrections,

$$m_{H^\pm}^2 = m_A^2 + m_W^2, \tag{5.38}$$

$$m_{h,H}^2 = \frac{1}{2} \left(m_A^2 + m_Z^2 \mp \sqrt{(m_A^2 + m_Z^2)^2 - 4 m_Z^2 m_A^2 \cos^2 2\beta} \right), \tag{5.39}$$

where $\tan\beta = v_2/v_1$. For $v_1 = v_2$ as in this model, m_h would be zero. There is of course the important radiative correction from Eq. (14), but that alone will not reach 125 GeV. Hence the MSSM requires both large $\tan\beta$ and large radiative correction, but a significant tension remains in accommodating all data. In this model, as Eq. (23) shows, $m_h^2 \simeq (g_X^2 + 2f^2 + \lambda_2)v^2$, where $v = 123$ GeV. This is a very interesting and important result, allowing the Higgs boson mass to be determined by the gauge $U(1)_X$ coupling g_X in addition to the Yukawa coupling f which replaces the μ parameter, i.e. $\mu = f u_3$. There is no tension between $m_h = 125$ GeV and the superparticle mass spectrum. Since $\lambda_2 \simeq 0.25$ for $\tilde{m}_t \simeq 1$ TeV, we have the important constraint

$$\sqrt{g_X^2 + 2f^2} \simeq 0.885. \tag{5.40}$$

For illustration, we have already chosen $g_X = 0.53$. Hence $f = 0.5$ and for $u_3 = 2$ TeV, $fu_3 = 1$ TeV is the value of the μ parameter of the MSSM. Let us choose $u_2 = 4$ TeV, then $m_{Z_X} = 2.87$ TeV, which is slightly above the present experimental lower bound of 2.85 TeV using $g_X = 0.53$ discussed earlier.

As for the heavy Higgs doublet, the four components $(H^\pm, H, A)$ are all degenerate in mass, i.e. $m^2 \simeq (4f^2 - 2g_X^2)u_3^2 + (4/3)g_X^2 u_2^2$ up to v^2 corrections. Each mass is then about 2.78 TeV. In more detail, as shown in Eq. (37), $m^2_{H^\pm}$ is corrected by $g_2^2 v^2 = m_W^2$ plus a term due to f. As shown in Eq. (24), m_H^2 is corrected by $(g_1^2 + g_2^2)v^2 = m_Z^2$ plus a term due to f and λ_2. These are exactly in accordance with Eqs. (38) and (39).

In the $S_{1,2,3}$ sector, the three physical scalars are mixtures of all three $Re(S_i)$ components, whereas the physical pseudoscalar A_{12} has no $Im(S_3)$ component. Since only S_3 couples to UU^c, DD^c, and $\phi_1\phi_2$, a candidate for the 750 GeV diphoton resonance must have an S_3 component. It could be one of the three scalars or the pseudoscalar A_S, or the other S_3 without VEV. In the following, we will consider the last option, specifically a pseudoscalar χ with a significant component of this other S_3. This allows the χUU^c, χDD^c and $\chi\phi_1\phi_2$ couplings to be independent of the masses of U, D, and the charged higgsino. The other scalars and pseudoscalars are assumed to be much heavier, and yet to be discovered.

5.6 Diphoton Excess

In this model, other than the addition of N^c for seesaw neutrino masses, the only new particles are U, U^c, D, D^c and $S_{1,2,3}$, which would be exactly the ingredients needed

to explain the diphoton excess[1] at the LHC. The allowed $S_3 UU^c$ and $S_3 DD^c$ couplings enable the one-loop gluon production of S_3 in analogy to that of h. The one-loop decay

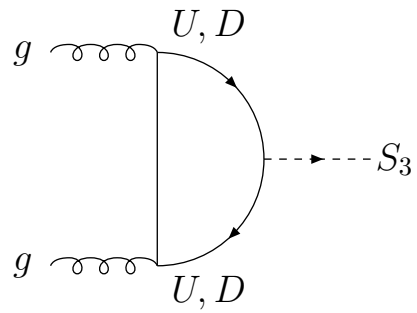

Figure 5.1: One-loop production of S_3 by gluon fusion.

of S_3 to two photons comes from these couplings as well as $S_3 \phi_1 \phi_2$. In addition, the

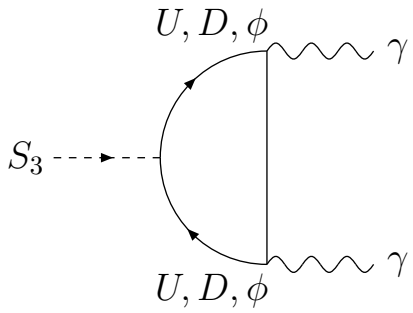

Figure 5.2: One-loop decay of S_3 to two photons.

direct $S_1 S_2 S_3$ couplings enable the decay of S_3 to other final states, including those of the dark sector, which contribute to its total width. The fact that the exotic U, U^c, D, D^c scalars are leptoquarks is also very useful for understanding [153] other possible LHC flavor anomalies. In a nutshell, a desirable comprehensive picture of possible new physics beyond

[1]Note that the 2015 diphoton excess disappeared in the more recent analyses in 2016. Nevertheless, the analysis here may be instructive for possible signals in the future.

the standard model is encapsulated by this existing model. In the following, we assume that the pseudoscalar χ is the 750 GeV particle, and show how its production and decay are consistent with the 2015 data.

The production cross section through gluon fusion is given by

$$\hat{\sigma}(gg \to \chi) = \frac{\pi^2}{8m_\chi^2}\Gamma(\chi \to gg)\delta(\hat{s} - m_\chi^2). \tag{5.41}$$

For the LHC at 13 TeV, the diphoton cross section is roughly [154]

$$\sigma(gg \to \chi \to \gamma\gamma) \simeq (100 \text{ pb}) \times (\lambda_g \text{ TeV})^2 \times B(\chi \to \gamma\gamma), \tag{5.42}$$

where λ_g is the effective coupling of χ to two gluons, normalized by

$$\Gamma(\chi \to gg) = \frac{\lambda_g^2}{8\pi} m_\chi^3. \tag{5.43}$$

Let the $\chi\bar{Q}Q$ coupling be f_Q, then

$$\lambda_g = \frac{\alpha_s}{\pi m_\chi} \sum_Q f_Q F(m_Q^2/m_\chi^2), \tag{5.44}$$

where [155]

$$F(x) = 2\sqrt{x}\left[\arctan\left(\frac{1}{\sqrt{4x-1}}\right)\right]^2, \tag{5.45}$$

which has the maximum value of $\pi^2/4 = 2.47$ as $x \to 1/4$. Let $f_Q^2/4\pi = 0.21$ and $F(m_Q^2/m_\chi^2) = 2.0$ (i.e. $m_Q = 380$ GeV) for all $Q = U, U, D$, then $\lambda_g = 0.49$ TeV^{-1}. For the corresponding

$$\Gamma(\chi \to \gamma\gamma) = \frac{\lambda_\gamma^2}{64\pi} m_\chi^3, \tag{5.46}$$

the $\phi^\pm$ higgsino contributes as well as U, D. However, its mass is roughly $fu_3 = 1$ TeV, so $F(x_\phi) = 0.394$, and

$$\lambda_\gamma = \frac{2\alpha}{\pi m_\chi} \sum_\psi N_\psi Q_\psi^2 f_\psi F(x_\psi), \tag{5.47}$$

where $\psi = U, U, D, \phi^\pm$ and N_ψ is the number of copies of ψ. Using $f_\phi^2/4\pi = 0.21$ as well, $\lambda_\gamma = 0.069$ TeV^{-1} is obtained. We then have $\Gamma(\chi \to \gamma\gamma) = 10$ MeV and $\Gamma(\chi \to gg) = 4.0$ GeV. If $B(\chi \to \gamma\gamma) = 2.5 \times 10^{-4}$, then $\sigma = 6$ fb, and the total width of χ is 40 GeV, in good agreement with data [143, 144].

As mentioned earlier, there are 2 copies of S_3 and 3 copies each of $S_{1,2}$. In addition to the ones with VEVs in their scalar components, there are 5 other superfields. One pair $\tilde{S}_{1,2}$ may form a pseudo-Dirac fermion, and be the lightest particle with odd R parity. It will couple to χ, say with strength f_S which is independent of all other couplings that we have discussed, then the tree-level decay $\chi \to \tilde{S}_1 \tilde{S}_2$ dominates the total width of χ and is invisible.

$$\Gamma(\chi \to \tilde{S}_1 \tilde{S}_2) = \frac{f_S^2}{8\pi} \sqrt{m_\chi^2 - 4m_S^2}. \tag{5.48}$$

For $m_\chi = 750$ GeV and $m_S = 200$ GeV, we find $\Gamma = 36$ GeV if $f_S = 1.2$. These numbers reinforce our numerical analysis to support the claim that χ could be a possible candidate for the 750 GeV diphoton excess. Note also that λ_g and λ_γ have scalar contributions which we have not considered. Adding them will allow us to reduce the fermion contributions we have assumed and still get the same final reuslts.

If we disregard the decay to dark matter ($f_S = 0$), then the total width of χ is dominated by $\Gamma(\chi \to gg)$, which is then less than a GeV. Assuming that the cross section for the diphoton resonance is 6.2 ± 1 fb [154], we plot the allowed values of $f_Q^2/4\pi$ versus m_Q for both $f_S = 1.2$ which gives a total width of about 40 GeV for χ, and $f_S = 0$ which requires much smaller values of $f_Q^2/4\pi$. Since χ must also decay into two gluons, we show the diject exclusion upper limits (~ 2 pb) from the 8 TeV data in each case as well.

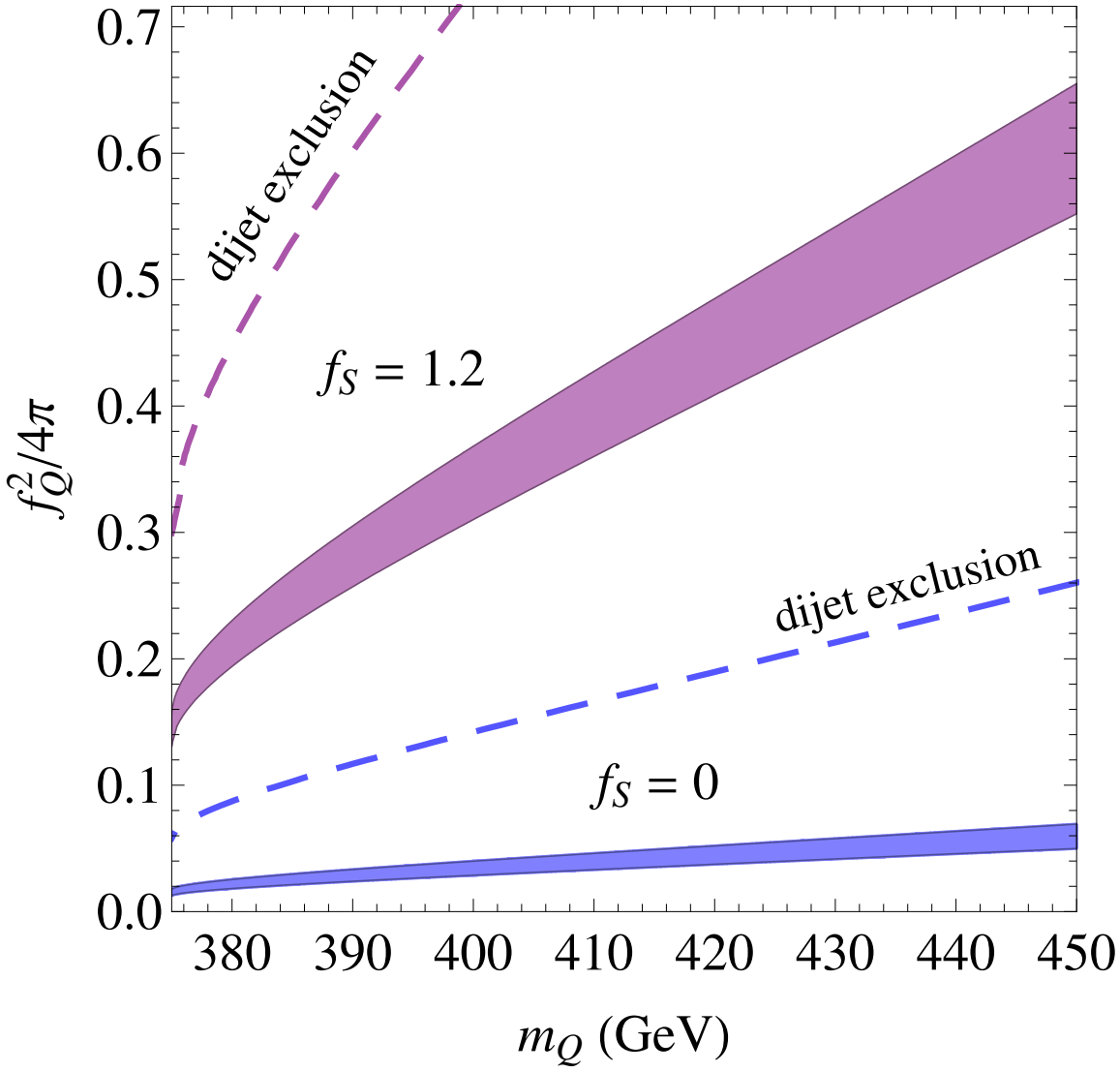

Figure 5.3: Allowed region for diphoton cross section of 6.2 ± 1 fb.

5.7 Scalar Neutrino and Neutralino Sectors

In the neutrino sector, the 2×2 mass matrix spanning (ν, N^c) per family is given by the well-known seesaw structure:

$$\mathcal{M}_\nu = \begin{pmatrix} 0 & m_D \\ m_D & m_N \end{pmatrix}, \tag{5.49}$$

where m_D comes from v_2 and m_N from u_1. There are two neutral complex scalars with odd R parity per family, i.e. $\tilde{\nu} = (\tilde{\nu}_R + i\tilde{\nu}_I)/\sqrt{2}$ and $\tilde{N}^c = (\tilde{N}^c_R + i\tilde{N}^c_I)/\sqrt{2}$. The 4×4 mass-squared matrix spanning $(\tilde{\nu}_R, \tilde{\nu}_I, \tilde{N}^c_R, \tilde{N}^c_I)$ is given by

$$\mathcal{M}^2_{\tilde{\nu},\tilde{N}^c} = \begin{pmatrix} m^2_{\tilde{\nu}} & 0 & A_D m_D & 0 \\ 0 & m^2_{\tilde{\nu}} & 0 & -A_D m_D \\ A_D m_D & 0 & m^2_{\tilde{N}^c} + A_N m_N & 0 \\ 0 & -A_D m_D & 0 & m^2_{\tilde{N}^c} - A_N m_N \end{pmatrix}. \tag{5.50}$$

In the MSSM, $\tilde{\nu}$ is ruled out as a dark-matter candidate because it interacts elastically with nuclei through the Z boson. Here, the A_N term allows a mass splitting between the real and imaginary parts of the scalar fields, and avoids this elastic-scattering constraint by virtue of kinematics. However, we still assume their masses to be heavier than that of $\tilde{S}_{1,2}$, discussed in the previous section.

In the neutralino sector, in addition to the 4×4 mass matrix of the MSSM spanning

$(\tilde{B}, \tilde{W}_3, \tilde{\phi}_1^0, \tilde{\phi}_2^0)$ with the μ parameter replaced by fu_3, i.e.

$$\mathcal{M}_0 = \begin{pmatrix} M_1 & 0 & -g_1 v_1/\sqrt{2} & g_1 v_2/\sqrt{2} \\ 0 & M_2 & g_2 v_1/\sqrt{2} & -g_2 v_2/\sqrt{2} \\ -g_1 v_1/\sqrt{2} & g_2 v_1/\sqrt{2} & 0 & -f u_3 \\ g_1 v_2/\sqrt{2} & -g_2 v_2/\sqrt{2} & -f u_3 & 0 \end{pmatrix}, \tag{5.51}$$

there is also the 4×4 mass matrix spanning $(\tilde{X}, \tilde{S}_3, \tilde{S}_2, \tilde{S}_1)$, i.e.

$$\mathcal{M}_S = \begin{pmatrix} M_X & \sqrt{2} g_X u_3 & -2\sqrt{2} g_X u_2/3 & -\sqrt{2} g_X u_1/3 \\ \sqrt{2} g_X u_3 & 0 & h u_1 & h u_2 \\ -2\sqrt{2} g_X u_2/3 & h u_1 & 0 & h u_3 \\ -\sqrt{2} g_X u_1/3 & h u_2 & h u_3 & 0 \end{pmatrix}. \tag{5.52}$$

The two are connected through the 4×4 matrix

$$\mathcal{M}_{0S} = \begin{pmatrix} 0 & 0 & 0 & 0 \\ 0 & 0 & 0 & 0 \\ -g_x v_1/\sqrt{2} & -f v_2 & 0 & 0 \\ -g_X v_2/\sqrt{2} & -f v_1 & 0 & 0 \end{pmatrix}. \tag{5.53}$$

These neutral fermions are odd under R parity and the lightest could in principle be a dark-matter candidate. To avoid the stringent bounds on dark matter with the MSSM alone, we assume again that all these particles are heavier than $\tilde{S}_{1,2}$, as the dark matter discussed in the previous section.

5.8 Dark Matter

The 5×5 mass matrix spanning the 5 singlet fermions $(\tilde{S}_1, \tilde{S}_2, \tilde{S}_1, \tilde{S}_2, \tilde{S}_3)$, corresponding to superfields with zero VEV for their scalar components, is given by

$$\mathcal{M}_{\tilde{S}} = \begin{pmatrix} 0 & m_0 & 0 & 0 & m_{13} \\ m_0 & 0 & 0 & 0 & m_{23} \\ 0 & 0 & 0 & M_3 & M_2 \\ 0 & 0 & M_3 & 0 & M_1 \\ m_{13} & m_{23} & M_2 & M_1 & 0 \end{pmatrix}. \tag{5.54}$$

Note that the 4×4 submatrix spanning $(\tilde{S}_1, \tilde{S}_2, \tilde{S}_1, \tilde{S}_2)$ has been diagonalized to form two Dirac fermions. We can choose m_0 to be small, say 200 GeV, and $M_{1,2,3}$ to be large, of order TeV. However, because of the mixing terms m_{13}, m_{23}, the light Dirac fermion gets split into two Majorana fermions, so it should be called a pseudo-Dirac fermion.

The dark matter with odd R parity is the lighter of the two Majorana fermions, call it $\tilde{S}$, contained in the pseudo-Dirac fermion formed out of $\tilde{S}_{1,2}$ as discussed in Sec. 6. It couples to the Z_X gauge boson, but in the nonrelativistic limit, its elastic scattering cross section with nuclei through Z_X vanishes because it is Majorana. It also does not couple directly to the Higgs boson h, so its direct detection at underground search experiments is very much suppressed. However, it does couple to A_S which couples also to quarks through the very small mixing of A_S with A. This is further suppressed because it contributes only to the spin-dependent cross section. To obtain a spin-independent cross section at tree level, the constraint of Eqs. (17) to (19) have to be relaxed so that h mixes with $S_{1,2,3}$.

Let the coupling of h to $\tilde{S}\tilde{S}$ be ϵ, then the effective interaction for elastic scattering

of $\tilde{S}$ with nuclei through h is given by

$$\mathcal{L}_{\rm eff} = \frac{\epsilon f_q}{m_h^2} \overline{\tilde{S}} \tilde{S} \bar{q} q, \tag{5.55}$$

where $f_q = m_q/2v = m_q/(246\ \text{GeV})$. The spin-independent direct-detection cross section per nucleon is given by

$$\sigma^{SI} = \frac{4\mu_{DM}^2}{\pi A^2} [\lambda_p Z + (A - Z)\lambda_n]^2, \tag{5.56}$$

where $\mu_{DM} = m_{DM} M_A/(m_{DM} + M_A)$ is the reduced mass of the dark matter. Using [156]

$$\lambda_N = \left[\sum_{u,d,s} f_q^N + \frac{2}{27} \left(1 - \sum_{u,d,s} f_q^N \right) \right] \frac{\epsilon m_N}{(246\ \text{GeV}) m_h^2}, \tag{5.57}$$

with [157]

$$f_u^p = 0.023, \quad f_d^p = 0.032, \quad f_s^p = 0.020, \tag{5.58}$$

$$f_u^n = 0.017, \quad f_d^n = 0.041, \quad f_s^n = 0.020, \tag{5.59}$$

we find $\lambda_p \simeq 3.50 \times 10^{-8}\ \text{GeV}^{-2}$, and $\lambda_n \simeq 3.57 \times 10^{-8}\ \text{GeV}^{-2}$. Using $A = 131$, $Z = 54$, and $M_A = 130.9$ atomic mass units for the LUX experiment [139], and $m_{DM} = 200$ GeV, we find for the upper limit of $\sigma^{SI} < 1.5 \times 10^{-45}\ \text{cm}^2$, the bound $\epsilon < 6.5 \times 10^{-4}$.

We have already invoked the $\chi \tilde{S}_1 \tilde{S}_2$ coupling to obtain a large invisible width for χ. Consider now the fermion counterpart of χ, call it $\tilde{S}'$, and the scalar counterparts of $\tilde{S}_{1,2}$, then the couplings $\tilde{S}' \tilde{S}_1 S_2$ and $\tilde{S}' \tilde{S}_2 S_1$ are also $f_S = 1.2$. Suppose one linear combination of $S_{1,2}$, call it ζ, is lighter than 200 GeV, then the thermal relic abundance of dark matter is determined by the annihilation $\tilde{S}\tilde{S} \to \zeta\zeta$, with a cross section times relative velocity given by

$$\sigma \times v_{rel} = \frac{f_\zeta^4 m_{S'}^2 \sqrt{1 - m_\zeta^2/m_S^2}}{16\pi (m_{S'}^2 + m_S^2 - m_\zeta^2)^2}. \tag{5.60}$$

Setting this equal to the optimal value [105] of 2.2×10^{-26} cm^3/s, we find $f_\zeta \simeq 0.62$ for $m_{S'} = 1$ TeV, $m_S = 200$ GeV, and $m_\zeta = 150$ GeV. Note that ζ stays in thermal equilibrium through its interaction with h from a term in V_D. It is also very difficult to be produced at the LHC, because it is an SM singlet, so its mass of 150 GeV is allowed.

5.9 Conclusion

The utilitarian supersymmetric $U(1)_X$ gauge extension of the Standard Model of particle interactions proposed 14 years ago [140] allows for two classes of anomaly-free models which have no μ term and conserve baryon number and lepton number automatically. A simple version [142] with leptoquark superfields is especially interesting because of existing LHC flavor anomalies.

The new Z_X gauge boson of this model has specified couplings to quarks and leptons which are distinct from other gauge extensions and may be tested at the LHC. Since S_3 couples to leptoquarks, the $S_3 \to l_i^+ l_j^-$ decay must occur at some level. As such, $S_3 \to e^+ \mu^-$ would be a very distinct signature at the LHC. Its branching fraction depends on unknown Yukawa couplings which need not be very small. Similarly, the S_3 couplings to $\phi_1 \phi_2$ as well as leptoquarks imply decays to ZZ and $Z\gamma$ with rates comparable to $\gamma\gamma$.

An important consequence of this study is the discovery of relaxed supersymmetric constraints on the Higgs boson's mass of 125 GeV. It is now given by Eq. (5.23), i.e. $m_h^2 \simeq (g_X^2 + 2f^2 + \lambda_2)v^2$, which allows it to be free of the tension encountered in the MSSM.

Chapter 6

Gauge $B - L$ Model of Radiative Neutrino Mass with Multipartite Dark Matter

6.1 Introduction

It is well-known that a gauge $B - L$ symmetry is supported by a simple extension of the standard model (SM) of quarks and leptons with the addition of one singlet right-handed neutrino per family, so that the theory is anomaly-free. For convenience in notation, let these three extra neutral fermion singlets N be left-handed, then their charges under $U(1)_{B-L}$ are (1,1,1). Their additional contributions to the axial-vector anomaly and the mixed gauge-gravitational anomaly are respectively

$$(1)^3 + (1)^3 + (1)^3 = 3, \quad (1) + (1) + (1) = 3, \tag{6.1}$$

which cancel exactly those of the SM quarks and leptons. On the other hand, it has been known for some time [109] that another set of charges are possible, i.e.

$$(-5)^3 + (4)^3 + (4)^3 = 3, \quad (-5) + (4) + (4) = 3. \tag{6.2}$$

Adding also three pairs of neutral singlet fermions with charges $(1, -1)$, naturally small seesaw Dirac masses for the known three neutrinos may be obtained [110], and a residual global $U(1)$ symmetry is maintained as lepton number. A further extension in the scalar sector allows for the unusual case of Z_3 lepton number [4] with the appearance of a scalar dark-matter candidate which is unstable but long-lived and decays to two antineutrinos. Here we consider another set of possible charges for the neutral fermion singlets, such that tree-level neutrino masses are forbidden. New scalar particles transforming under $U(1)_{B-L}$ are then added to generate one-loop Majorana neutrino masses. The breaking of $B - L$ to Z_2 results in lepton parity and thus R parity or dark parity [137] which is odd for some particles, the lightest neutral one being dark matter. A closer look st the neutral fermion singlets shows that one may be a keV sterile neutrino, and two others are heavy and stable, thus realizing the interesting scenario of multipartite dark matter. If color-triplet fermions with both B and L are added, the diphoton excess [143, 144] at 750 GeV, observed at the Large Hadron Collider (LHC) in 2015, could also be explained.

6.2 Model

The extra left-handed neutral singlet fermions have charges $(2, 2, 2, 2, -1, -1, -3)$, so that

$$4(2)^3 + 2(-1)^3 + (-3)^3 = 3, \quad 4(2) + 2(-1) + (-3) = 3. \tag{6.3}$$

Since there is no charge +1 in the above, there is no connection between them and the doublet neutrinos ν with charge -1 through the one Higgs doublet Φ which has charge zero. Neutrinos are thus massless at tree level. To generate one-loop Majorana masses, the basic mechanism of Ref. [66] is adopted, using the four fermions with charge +2, but because of the $U(1)_{B-L}$ gauge symmetry, we need both a scalar doublet (η^+, η^0) and a scalar singlet χ^0. The $U(1)_{B-L}$ gauge symmetry itself is broken by ρ_2^0 with charge -2 and

Table 6.1: Particle content of proposed model.

Particle	$SU(3)_C$	$SU(2)_L$	$U(1)_Y$	B	L	$B-L$	copies	R parity
$Q=(u,d)$	3	2	1/6	1/3	0	1/3	3	+
u^c	3^*	1	$-2/3$	$-1/3$	0	$-1/3$	3	+
d^c	3^*	1	1/3	$-1/3$	0	$-1/3$	3	+
$L=(\nu,e)$	1	2	$-1/2$	0	1	-1	3	+
e^c	1	1	1	0	-1	1	3	+
N	1	1	0	0	-2	2	4	−
S	1	1	0	0	1	-1	2	+
S'	1	1	0	0	3	-3	1	+
$\Phi=(\phi^+,\phi^0)$	1	2	1/2	0	0	0	1	+
$\eta=(\eta^+,\eta^0)$	1	2	1/2	0	1	-1	1	−
χ^0	1	1	0	0	1	-1	1	−
ρ_2^0	1	1	0	0	2	-2	1	+
ρ_4^0	1	1	0	0	4	-4	1	+
D_1	3	1	$-1/3$	1/3	1	$-2/3$	1	−
D_2	3	1	$-1/3$	1/3	-1	4/3	1	−
D_1^c	3^*	1	1/3	$-1/3$	-1	2/3	1	−
D_2^c	3^*	1	1/3	$-1/3$	1	$-4/3$	1	−

by ρ_4^0 with charge -4. The leptoquark fermions $D_{1,2}$ and $D_{1,2}^c$ are not necessary for neutrino mass, but are natural extensions of this model to accommodate the diphoton excess at 750 GeV. The complete particle content of this model is shown in Table 6.1.

6.3 Radiative Neutrino Mass

Using the four N's, radiative Majorana masses for the three ν's are generated as shown in Fig. 6.1. Note that N, η, χ all have odd R parity, so that the lightest neutral

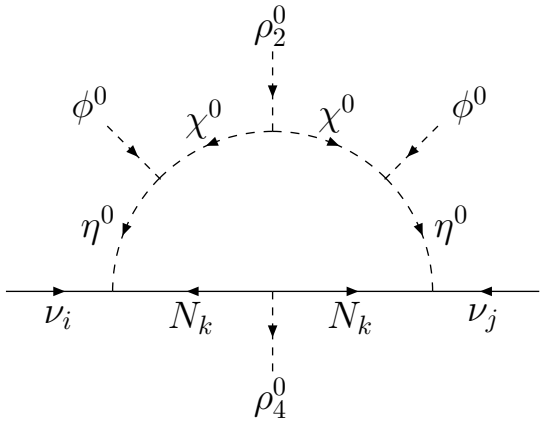

Figure 6.1: Radiative generation of neutrino mass through dark matter.

particle among them is a dark-matter candidate. This is the scotogenic mechanism, from the Greek 'scotos' meaning darkness. In addition to the $\eta^\dagger \Phi \chi$ trilinear coupling used in Fig. 6.1, there is also the $\eta^\dagger \Phi \chi^\dagger \rho_2$ quadrilinear coupling, which may also be used to complete the loop. There are 4 real scalar fields, spanning $\sqrt{2}Re(\eta^0)$, $\sqrt{2}Im(\eta^0)$, $\sqrt{2}Re(\chi^0)$, $\sqrt{2}Im(\chi^0)$. We denote their mass eigenstates as ζ_l^0 with mass m_l. Let the $\nu_i N_k \eta^0$ coupling be h_{ik}^ν, then the radiative neutrino mass matrix is given by [66]

$$(\mathcal{M}_\nu)_{ij} = \sum_k \frac{h_{ik}^\nu h_{jk}^\nu M_k}{16\pi^2} \sum_l [(y_l^R)^2 F(x_{lk}) - (y_l^I)^2 F(x_{lk})], \tag{6.4}$$

where $\sqrt{2}Re(\eta^0) = \sum_l y_l^R \zeta_l^0$, $\sqrt{2}Im(\eta^0) = \sum_l y_l^I \zeta_l^0$, with $\sum_l (y_l^R)^2 = \sum_l (y_l^I)^2 = 1$, $x_{lk} = m_l^2/M_k^2$, and the function F is given by

$$F(x) = \frac{x \ln x}{x-1}. \tag{6.5}$$

6.4 Multipartite Dark Matter

Since the only neutral particles of odd R parity are N, η^0, χ^0, there appears to be only one dark-matter candidate. However as shown below, there could be two or even four, all within the context of the existing model.

First note that $\rho^0_{2,4}$ have exactly the right $U(1)_{B-L}$ charges to make the (S, S, S') fermions massive. The corresponding 3×3 mass matrix is of the form

$$\mathcal{M}_S = \begin{pmatrix} m_{S1} & 0 & m_{13} \\ 0 & m_{S2} & m_{23} \\ m_{13} & m_{23} & 0 \end{pmatrix}, \tag{6.6}$$

where m_{S1}, m_{S2} come from $\langle \rho^0_2 \rangle = u_2$ and m_{13}, m_{23} from $\langle \rho^0_4 \rangle = u_4$. If all these entries are of order 100 GeV to a few TeV, then there are three extra heavy singlet neutrinos in this model which also have even R parity. They do not mix with the light active neutrinos ν at tree level, but do so in one loop. For example, S' mixes with ν as shown in Fig. 6.2. Similarly S will also mix with ν, using the $SN\chi^0$ Yukawa coupling. However, these terms are negligible compared to the assumed large masses for (S, S, S') and may be safely ignored.

Consider now the possibility that $m_{13}, m_{23} << m_{S1}, m_{S2}$ in $\mathcal{M}_S$, then S' obtains

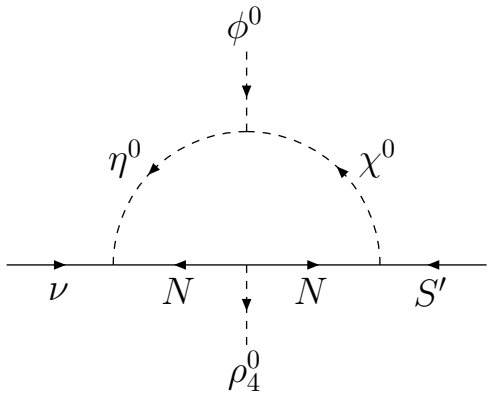

Figure 6.2: Radiative generation of $\nu - S'$ mixing.

a small seesaw mass given by

$$m_{S'} \simeq -\frac{m_{13}^2}{m_{S1}} - \frac{m_{23}^2}{m_{S2}}. \tag{6.7}$$

Let this be a few keV, then S' is a light sterile neutrino which mixes with ν only slightly through Fig. 6.2. Hence it is a candidate for warm dark matter. Whereas the usual sterile neutrino is an *ad hoc* invention, it has a natural place here in terms of its mass as well as its suppressed mixing with the active neutrinos.

We now have the interesting scenario where part of the dark matter of the Universe is cold, and the other is warm. This hybrid case was also obtained in a different radiative model of neutrino masses [158]. Within the present context, there is a third possibility. If we assign an extra Z_2 symmetry, under which $S_{1,2}$ are odd and all other particles even, then the only interactions involving $S_{1,2}$ come from their diagonal $U(1)_{B-L}$ gauge couplings and the diagonal Yukawa terms $f_1 S_1 S_1 (\rho_2^0)^*$ and $f_2 S_2 S_2 (\rho_2^0)^*$. This means that both S_1 and S_2 are stable and their relic abundances are determined by their annihilation cross sections to SM particles. In this scenario, dark matter has four components [92].

Since $S_{1,2}$ are now separated from S', the m_{13} and m_{23} terms in $\mathcal{M}_S$ are zero and there is no tree-level mass for S'. However, there is a one-loop mass as shown in Fig. 6.3. This makes it more natural for S' to be light. A detailed study of the dark-matter

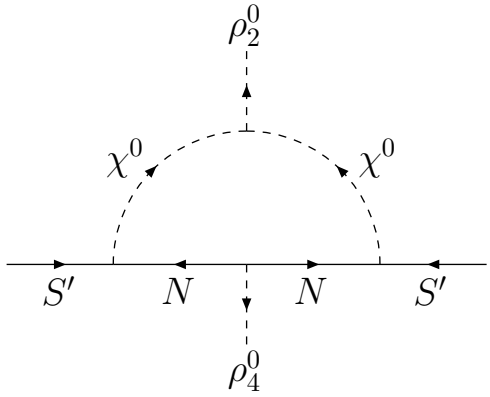

Figure 6.3: Radiative generation of S' mass.

phenomenology of this multipartite scenario will be given elsewhere.

6.5 Scalar Sector for Symmetry Breaking

In this model, there is only one Higgs doublet Φ which breaks the $SU(2)_L \times U(1)_Y$ electroweak symmetry, whereas there are two Higgs singlets ρ_2 and ρ_4 which break $U(1)_{B-L}$ to Z_2. The most general Higgs potential consisting of Φ, ρ_2, ρ_4 is given by

$$\begin{aligned} V &= \mu_0^2 \Phi^\dagger \Phi + \mu_2^2 \rho_2^* \rho_2 + \mu_4^2 \rho_4^* \rho_4 + \frac{1}{2}\mu_{24}[\rho_2^2 \rho_4^* + H.c.] + \frac{1}{2}\lambda_0 (\Phi^\dagger \Phi)^2 + \frac{1}{2}\lambda_2 (\rho_2^* \rho_2)^2 \\ &+ \frac{1}{2}\lambda_4 (\rho_4^* \rho_4)^2 + \lambda_{02} (\Phi^\dagger \Phi)(\rho_2^* \rho_2) + \lambda_{04} (\Phi^\dagger \Phi)(\rho_4^* \rho_4) + \lambda_{24} (\rho_2^* \rho_2)(\rho_4^* \rho_4). \end{aligned} \tag{6.8}$$

Let $\langle\phi^0\rangle = v$, $\langle\rho_2\rangle = u_2$, $\langle\rho_4\rangle = u_4$, then the minimum of V is determined by

$$0 = \mu_0^2 + \lambda_0 v^2 + \lambda_{02} u_2^2 + \lambda_{04} u_4^2, \tag{6.9}$$

$$0 = \mu_2^2 + \lambda_{02} v^2 + \lambda_2 u_2^2 + \lambda_{24} u_4^2 + \mu_{24} u_4, \tag{6.10}$$

$$0 = u_4(\mu_4^2 + \lambda_{04} v^2 + \lambda_{24} u_2^2 + \lambda_4 u_4^2) + \frac{1}{2}\mu_{24} u_2^2. \tag{6.11}$$

The would-be Goldstone bosons are $\phi^\pm$, $\sqrt{2}Im(\phi^0)$, corresponding to the breaking of $SU(2)_L \times U(1)_Y$ to $U(1)_{em}$, and $\sqrt{2}[u_2 Im(\rho_2) + 2u_4 Im(\rho_4)]/\sqrt{u_2^2 + 4u_4^2}$, corresponding to the breaking of $U(1)_{B-L}$ to Z_2. The linear combination orthogonal to the latter is a physical pseudoscalar A, with a mass given by

$$m_A = \frac{-\mu_{24}(u_2^2 + 4u_4^2)}{2u_4}. \tag{6.12}$$

The 3×3 mass-squared matrix of the physical scalars $[\sqrt{2}Re(\phi^0), \sqrt{2}Re(\rho_2), \sqrt{2}Re(\rho_4)]$ is given by

$$\mathcal{M}^2 = \begin{pmatrix} 2\lambda_0 v^2 & 2\lambda_{02} v u_2 & 2\lambda_{04} v u_4 \\ 2\lambda_{02} v u_2 & 2\lambda_2 u_2^2 & u_2(2\lambda_{24} u_4 + \mu_{24}) \\ 2\lambda_{04} v u_4 & u_2(2\lambda_{24} u_4 + \mu_{24}) & 2\lambda_4 u_4^2 - \mu_{24} u_2^2/2u_4 \end{pmatrix}. \tag{6.13}$$

For $v^2 << u_{2,4}^2$, $\sqrt{2}Re(\phi^0) = h$ is approximately a mass eigenstate which is identified with the 125 GeV particle discovered at the LHC.

6.6 Gauge Sector

Since ϕ^0 does not transform under $U(1)_{B-L}$ and $\rho_{2,4}$ do not transform under $SU(2)_L \times U(1)_Y$, there is no tree-level mixing between their corresponding gauge bosons Z and Z_{B-L}. In our convention, $M_{Z_{B-L}}^2 = 8g_{B-L}^2(u_2^2 + 4u_4^2)$. The LHC bound on $M_{Z_{B-L}}$

comes from the production of Z_{B-L} from u and d quarks and its subsequent decay to e^-e^+ and $\mu^-\mu^+$. If all the particles listed in Table 6.1 are possible decay products of Z_{B-L} with negligible kinematic suppression, then its branching fraction to e^-e^+ and $\mu^-\mu^+$ is about 0.061. The $c_{u,d}$ coefficients used in the LHC analysis [114, 152] are then

$$c_u = c_d = \left[\left(\frac{1}{3}\right)^2 + \left(\frac{1}{3}\right)^2\right] g_{B-L}^2 \times B(Z_{B-L} \to e^-e^+, \mu^-\mu^+) = 1.36 \times 10^{-2}\ g_{B-L}^2. \quad (6.14)$$

From LHC data based on the 7 and 8 TeV runs, a bound of about 2.5 TeV would correspond to $g_{B-L} < 0.24$.

6.7 Leptoquark Fermions

The singlet leptoquark fermions $D_{1,2}$ have charge $-1/3$ and the following possible interactions:

$$D_1 d^c \chi^*, \quad D_2 d^c \chi, \quad D_1 D_2^c \rho_2^*, \quad D_2 D_1^c \rho_2. \quad (6.15)$$

Hence they mix in a 2×2 mass matrix linking $D_{1,2}$ to $D_{1,2}^c$ with $\langle \rho_2 \rangle = u_2$, and decay to d quarks + $\chi(\chi^*)$. Now χ mixes with η^0, so it decays to neutrinos (ν) and dark matter (N), which are invisible. The search for $D_{1,2}$ at the LHC would be similar to the search for scalar quarks which decay to quarks + missing energy. However, if we assume that N has a mass of about 200 GeV, then there is no useful limit at present on the mass of $D_{1,2}$ from the LHC.

Consider now the pseudoscalar A of Eq. (6.12). Let the two mass eigenstates in the $(D_{1,2}, D_{1,2}^c)$ sector be $\psi_{1,2}$, then A couples to them according to

$$\mathcal{L}_{int} = f_1 \bar{\psi}_1 \gamma_5 \psi_1 + f_2 \bar{\psi}_2 \gamma_5 \psi_2, \quad (6.16)$$

where $f_{1,2}$ are rearranged from their original $D_1 D_2^c \rho_2^*$ and $D_2 D_1^c \rho_2$ couplings. Hence A decays to two gluons as well as to two photons in one loop through $\psi_{1,2}$. It may also decay to dark matter, say NN, at tree level. It was thus a possible candidate for explaining the 750 GeV diphoton excess observed [143,144] at the LHC in 2015. The numerical analysis of this model runs parallel to that of a proposal [3], and will not be repeated here. Note again that these leptoquark fermions are not essential for the radiative generation of neutrino masses based on $B - L$.

6.8 Conclusion

Using gauge $U(1)_{B-L}$ symmetry, we have proposed a new anomaly-free solution with exotic fermion singlets, such that neutrino mass is forbidden at tree level. We add a number of new scalars so that neutrino masses are obtained in one loop through dark matter, i.e. the scotogenic mechanism. Because of the structure of the new singlets required for anomaly cancellation, we find a possible dark-matter scenario with four components. Three are stable cold Weakly Interaction Massive Particles (WIMPs) and one a keV singlet neutrino, i.e. warm dark matter with a very long lifetime.

Chapter 7

Generalized Gauge U(1) Family Symmetry for Quarks and Leptons

7.1 Introduction

In the standard model of particle interactions, there are three families of quarks and leptons. Under its $SU(3)_C \times SU(2)_L \times U(1)_Y$ gauge symmetry, singlet right-handed neutrinos ν_R do not transform. They were thus not included in the minimal standard model which only have three massless left-handed neutrinos. Since neutrinos are now known to be massive, ν_R should be considered as additions to the standard model. In that case, the model admits a possible new family gauge symmetry $U(1)_F$, with charges $n_{1,2,3}$ for the quarks and $n'_{1,2,3}$ for the leptons as shown in Table 7.1.

To constrain $n_{1,2,3}$ and $n'_{1,2,3}$, the requirement of gauge anomaly cancellation is

Table 7.1: Fermion assignments under $U(1)_F$.

Particle	$SU(3)_C$	$SU(2)_L$	$U(1)_Y$	$U(1)_F$
$Q_{iL} = (u,d)_{iL}$	3	2	1/6	n_i
u_{iR}	3	1	2/3	n_i
d_{iR}	3	1	$-1/3$	n_i
$L_{iL} = (\nu,l)_{iL}$	1	2	$-1/2$	n'_i
l_{iR}	1	1	-1	n'_i
ν_{iR}	1	1	0	n'_i

imposed. The contributions of color triplets to the $[SU(3)]^2U(1)_F$ anomaly sum up to

$$[SU(3)]^2U(1)_F \;:\quad \frac{1}{2}\sum_{i=1}^{3}(2n_i - n_i - n_i); \tag{7.1}$$

and the contributions of $Q_{iL}, u_{iR}, d_{iR}, L_{iL}, l_{iR}$ to the $U(1)_Y[U(1)_F]^2$ anomaly sum up to

$$U(1)_Y[U(1)_F]^2 \;:\quad \sum_{i=1}^{3}\left[6\left(\frac{1}{6}\right) - 3\left(\frac{2}{3}\right) - 3\left(-\frac{1}{3}\right)\right]n_i^2 + \left[2\left(-\frac{1}{2}\right) - (-1)\right]n_i'^2. \tag{7.2}$$

Both are automatically zero, as well as the $[U(1)_F]^3$ anomaly because all fermions couple to $U(1)_F$ vectorially. The contributions of the $SU(2)_L$ doublets to the $[SU(2)]^2U(1)_F$ anomaly sum up to

$$[SU(2)]^2U(1)_F \;:\quad \frac{1}{2}\sum_{i=1}^{3}(3n_i + n'_i); \tag{7.3}$$

and the contributions to the $[U(1)_Y]^2U(1)_F$ anomaly sum up to

$$\begin{aligned}[U(1)_Y]^2U(1)_F \quad &: \quad \sum_{i=1}^{3}\left[6\left(\frac{1}{6}\right)^2 - 3\left(\frac{2}{3}\right)^2 - 3\left(-\frac{1}{3}\right)^2\right]n_i + \left[2\left(-\frac{1}{2}\right)^2 - (-1)^2\right]n'_i \\ &= \quad \sum_{i=1}^{3}\left(-\frac{3}{2}n_i - \frac{1}{2}n'_i\right).\end{aligned} \tag{7.4}$$

Both are zero if

$$\sum_{i=1}^{3}(3n_i + n'_i) = 0. \tag{7.5}$$

Table 7.2: Examples of models satisfying Eq. (7.5).

n_1	n_2	n_3	n'_1	n'_2	n'_3	Model
1/3	1/3	1/3	-1	-1	-1	$B-L$ [159]
0	0	0	0	1	-1	$L_\mu - L_\tau$ [160–163]
1/3	1/3	1/3	0	0	-3	$B-3L_\tau$ [164–167]
1/3	1/3	1/3	3	-3	-3	Ref. [168]
1	1	-2	1	1	-2	Ref. [169]
a	a	$-2a$	0	-1	1	Ref. [170]

There are many specific examples of models which satisfy this condition as shown in Table 7.2. If there are four families, then $n_{1,2,3} = 1/3$, $n_4 = -1$, and $n'_{1,2,3} = 1$, $n'_4 = -3$, would also satisfy Eq. (7.5). This may then be considered [171,172] as the separate gauging of B and L.

In this paper, we discuss two new examples which offer some insights to the structure of mixing among quarks and lepton families. Both have nontrivial connections between quarks and leptons. Their structures are shown in Table 7.3. In both cases, with only one

Table 7.3: Two new models satisfying Eq. (7.5).

n_1	n_2	n_3	n'_1	n'_2	n'_3	Model
1	1	0	0	-2	-4	A
1	1	-1	0	-1	-2	B

Higgs doublet with zero charge under $U(1)_F$, quark and lepton mass matrices are diagonal except for the first two quark families. This allows for mixing among them, but not with the third family. It is a good approximation to the 3×3 quark mixing matrix, to the extent that mixing with the third family is known to be suppressed. In the lepton sector, mixing also comes from the Majorana mass matrix of ν_R which depends on the choice of singlets

with vacuum expectation values which break $U(1)_F$. Adding a second Higgs doublet with nonzero $U(1)_F$ charge will allow mixing of the first two families of quarks with the third in both cases. As for the leptons, this will not affect Model A, but will cause mixing in the charged-lepton and Dirac neutrino mass matrices in Model B. Flavor-changing neutral currents are predicted, with interesting phenomenological consequences.

7.2 Basic structure of Model A

Consider first the structure of the 3×3 quark mass matrix $\mathcal{M}_d$ linking $(\bar{d}_L, \bar{s}_L, \bar{b}_L)$ to (d_R, s_R, b_R). Using

$$\Phi_1 = (\phi_1^+, \phi_1^0) \sim (1, 2, 1/2; 0), \tag{7.6}$$

with $\langle \phi_1^0 \rangle = v_1$, it is clear that $\mathcal{M}_d$ is block diagonal with a 2×2 submatrix which may be rotated on the left to become

$$\mathcal{M}_d = \begin{pmatrix} c_L & -s_L & 0 \\ s_L & c_L & 0 \\ 0 & 0 & 1 \end{pmatrix} \begin{pmatrix} m'_d & 0 & 0 \\ 0 & m'_s & 0 \\ 0 & 0 & m'_b \end{pmatrix}, \tag{7.7}$$

where $s_L = \sin\theta_L$ and $c_L = \cos\theta_L$. We now add a second Higgs doublet

$$\Phi_2 = (\phi_2^+, \phi_2^0) \sim (1, 2, 1/2; 1), \tag{7.8}$$

with $\langle \phi_2^0 \rangle = v_2$, so that

$$\mathcal{M}_d = \begin{pmatrix} c_L & -s_L & 0 \\ s_L & c_L & 0 \\ 0 & 0 & 1 \end{pmatrix} \begin{pmatrix} m'_d & 0 & m'_{db} \\ 0 & m'_s & m'_{sb} \\ 0 & 0 & m'_b \end{pmatrix} \tag{7.9}$$

is obtained. At the same time, $\mathcal{M}_u$ is of the form

$$\mathcal{M}_u = \begin{pmatrix} m'_u & 0 & 0 \\ 0 & m'_c & 0 \\ m'_{ut} & m'_{ct} & m'_t \end{pmatrix} \begin{pmatrix} c_R & s_R & 0 \\ -s_R & c_R & 0 \\ 0 & 0 & 1 \end{pmatrix}, \tag{7.10}$$

where it has been rotated on the right. Because of the physical mass hierarchy $m_u << m_c << m_t$, the diagonalization of Eq. (7.10) will have very small deviations from unity on the left. Hence the unitary matrix diagonalizing Eq. (7.9) on the left will be essentially the experimentally observed quark mixing matrix V_{CKM} which has three angles and one phase. Now $\mathcal{M}_d$ of Eq. (7.9) has exactly seven parameters, the three diagonal masses m'_d, m'_s, m'_b, the angle θ_L, the off-diagonal mass m'_{sb} which can be chosen real, and the off-diagonal mass m'_{db} which is complex. With the input of the three quark mass eigenvalues m_d, m_s, m_b and V_{CKM}, these seven parameters can be determined.

Consider the diagonalization of the real mass matrix

$$\begin{pmatrix} a & 0 & s_1 c \\ 0 & b & s_2 c \\ 0 & 0 & c \end{pmatrix} = V_L \begin{pmatrix} a(1-s_1^2/2) & 0 & 0 \\ 0 & b(1-s_2^2/2) & 0 \\ 0 & 0 & c(1+s_1^2/2+s_2^2/2) \end{pmatrix} V_R^\dagger, \tag{7.11}$$

where $s_{1,2} << 1$ and $a << b << c$ have been assumed. We obtain

$$V_L = \begin{pmatrix} 1-s_1^2/2 & -s_1 s_2 b^2/(b^2 - s_1^2 c^2 - a^2) & s_1 \\ s_1 s_2 a^2/(b^2 + s_2^2 c^2 - a^2) & 1-s_2^2/2 & s_2 \\ -s_1 & -s_2 & 1-s_1^2/2-s_2^2/2 \end{pmatrix}, \tag{7.12}$$

and

$$V_R^\dagger = \begin{pmatrix} 1 & s_1 s_2 ab/(b^2-a^2) & -s_1 a/c \\ -s_1 s_2 ab/(b^2-a^2) & 1 & -s_2 b/c \\ s_1 a/c & s_2 b/c & 1 \end{pmatrix}. \tag{7.13}$$

Hence

$$V_{CKM} = \begin{pmatrix} c_L & -s_L & 0 \\ s_L & c_L & 0 \\ 0 & 0 & 1 \end{pmatrix} \begin{pmatrix} e^{i\alpha} & 0 & 0 \\ 0 & 1 & 0 \\ 0 & 0 & 1 \end{pmatrix} V_L, \tag{7.14}$$

where α is the phase transferred from m'_{db}.

Comparing the above with the known values of V_{CKM} [173], we obtain

$$s_1 = 0.00886, \quad s_2 = 0.0405, \quad s_L = -0.2253, \quad e^{i\alpha} = -0.9215 + i0.3884, \tag{7.15}$$

with $m_d = m'_d$, $m_s = m'_s$, $m_b = m'_b$ to a very good approximation.

7.3 Scalar sector of Model A

In addition to $\Phi_{1,2}$, we add a scalar singlet

$$\sigma \sim (1, 1, 0; 1), \tag{7.16}$$

then the Higgs potential containing $\Phi_{1,2}$ and σ is given by

$$\begin{aligned} V &= m_1^2 \Phi_1^\dagger \Phi_1 + m_2^2 \Phi_2^\dagger \Phi_2 + m_3^2 \bar{\sigma}\sigma + [\mu \sigma \Phi_2^\dagger \Phi_1 + H.c.] \\ &+ \frac{1}{2}\lambda_1 (\Phi_1^\dagger \Phi_1)^2 + \frac{1}{2}\lambda_2 (\Phi_2^\dagger \Phi_2)^2 + \frac{1}{2}\lambda_3 (\bar{\sigma}\sigma)^2 + \lambda_{12} (\Phi_1^\dagger \Phi_1)(\Phi_2^\dagger \Phi_2) \\ &+ \lambda'_{12} (\Phi_1^\dagger \Phi_2)(\Phi_2^\dagger \Phi_1) + \lambda_{13} (\Phi_1^\dagger \Phi_1)(\bar{\sigma}\sigma) + \lambda_{23} (\Phi_2^\dagger \Phi_2)(\bar{\sigma}\sigma). \end{aligned} \tag{7.17}$$

Let $\langle \phi^0_{1,2} \rangle = v_{1,2}$ and $\langle \sigma \rangle = u$, then the minimum of V is determined by

$$0 = v_1(m_1^2 + \lambda_1 v_1^2 + (\lambda_{12} + \lambda'_{12})v_2^2 + \lambda_{13}u^2) + \mu v_2 u, \tag{7.18}$$

$$0 = v_2(m_2^2 + \lambda_2 v_2^2 + (\lambda_{12} + \lambda'_{12})v_1^2 + \lambda_{23}u^2) + \mu v_1 u, \tag{7.19}$$

$$0 = u(m_3^2 + \lambda_3 u^2 + \lambda_{13}v_1^2 + \lambda_{23}v_2^2) + \mu v_1 v_2. \tag{7.20}$$

For m_2^2 large and positive, a solution exists with $v_2^2 << v_1^2 << u^2$, i.e.

$$u^2 \simeq \frac{-m_3^2}{\lambda_3}, \quad v_1^2 \simeq \frac{-m_1^2 - \lambda_{13}u^2}{\lambda_1}, \quad v_2 \simeq \frac{-\mu v_1 u}{m_2^2 + \lambda_{23}u^2}. \tag{7.21}$$

Hence the scalar particle spectrum of Model A consists of a Higgs boson h very much like that of the SM with $m_h^2 \simeq 2\lambda_1 v_1^2$, a heavy Higgs boson which breaks $U(1)_F$ with $m_\sigma^2 \simeq 2\lambda_3 u^2$, and a heavy scalar doublet very much like Φ_2 with $m^2(\phi_2^+, \phi_2^0) \simeq m_2^2 + \lambda_{23}u^2$.

7.4 Gauge sector of Model A

With the scalar structure already considered, the $Z - Z_F$ mass-squared matrix is given by

$$\mathcal{M}^2_{Z,Z_F} = \begin{pmatrix} g_Z^2(v_1^2 + v_2^2)/4 & -g_Z g_F v_2^2/2 \\ -g_Z g_F v_2^2/2 & g_F^2(u^2 + v_2^2) \end{pmatrix}. \tag{7.22}$$

The $Z - Z_F$ mixing is then $(g_Z/2g_F)(v_2^2/u^2)$. For $v_2 \sim 10$ GeV and $u \sim 1$ TeV, this is about 10^{-4}, well within the experimentally allowed range.

Since Z_F couples to quarks and leptons according to $n_{1,2,3}$ and $n'_{1,2,3}$, its branching fractions to e^-e^+ and $\mu^-\mu^+$ are given by $2{n'_{1,2}}^2/(12\sum n_i^2 + 3\sum {n'_i}^2)$. Since $n'_1 = 0$, we need consider only the branching fraction $Z_F \to \mu^-\mu^+$ to compare against data. For Model A, it is about 2/21. The $c_{u,d}$ coefficients used in the experimental search [174, 175] of Z_F are

then

$$c_u = c_d = 2g_F^2(2/21). \tag{7.23}$$

For $g_F = 0.13$, a lower bound of about 4.0 TeV on m_{Z_F} is obtained from the Large Hadron Collider (LHC) based on the preliminary 13 TeV data by comparison with the published data from the 7 and 8 TeV runs. Note however that if $Z_F \to e^- e^+$ is ever observed, this particular model is ruled out.

7.5 Flavor-changing interactions

Whereas the SM Z boson does not mediate any flavor-changing interactions, the heavy Z_F does because it distinguishes families. For quarks,

$$\mathcal{L}_{Z_F} = g_F Z_F^\mu (\bar{u}'\gamma_\mu u' + \bar{c}'\gamma_\mu c' + \bar{d}'\gamma_\mu d' + \bar{s}'\gamma_\mu s'). \tag{7.24}$$

Using Eqs. (7.12) and (7.13) to express the above in terms of mass eigenstates for the d sector, and keeping only the leading flavor-changing terms, we find

$$\mathcal{L}'_{Z_F} = g_F Z_F^\mu [s_1(\bar{d}_L\gamma_\mu b_L + \bar{b}_L\gamma_\mu d_L) + s_2(\bar{s}_L\gamma_\mu b_L + \bar{b}_L\gamma_\mu s_L) - s_1 s_2(\bar{d}_L\gamma_\mu s_L + \bar{s}_L\gamma_\mu d_L)]. \tag{7.25}$$

From the experimental values of the $B^0 - \bar{B}^0$, $B_S^0 - \bar{B}_S^0$, and $K_L - K_S$ mass differences, severe constraints on $g_F^2/m_{Z_F}^2$ are obtained, coming from the operators

$$(\bar{d}_L\gamma_\mu b_L)^2 + H.c., \quad (\bar{s}_L\gamma_\mu b_L)^2 + H.c., \quad (\bar{d}_L\gamma_\mu s_L)^2 + H.c. \tag{7.26}$$

respectively. Using typical values of quark masses and hadronic decay and bag parameters [176], we estimate the various Wilson coefficients to find their contributions as follows:

$$\Delta M_B = 4.5 \times 10^{-2}\ s_1^2 (g_F^2/m_{Z_F}^2)\ \text{GeV}^3, \tag{7.27}$$

$$\Delta M_{B_s} = 6.4 \times 10^{-2}\ s_2^2 (g_F^2/m_{Z_F}^2)\ \text{GeV}^3, \tag{7.28}$$

$$\Delta M_K = 1.9 \times 10^{-3}\ s_1^2 s_2^2 (g_F^2/m_{Z_F}^2)\ \text{GeV}^3. \tag{7.29}$$

Using Eq. (7.15) and assuming that the above contributions are no more than 10% of their experimental values [173], we find the lower limits on m_{Z_F}/g_F to be 10.2, 9.5, 0.84 TeV respectively. This is easily satisfied for $m_{Z_F} > 4.0$ TeV with $g_F = 0.13$ from the LHC bound discussed in the previous section.

In the scalar sector, since $\Phi_{1,2}$ both contribute to $\mathcal{M}_d$, the neutral scalar field orthogonal to the SM Higgs field will also mediate flavor-changing interactions. The Yukawa interactions are

$$\mathcal{L}_Y = \frac{h_1}{\sqrt{2}v_1}(m'_d \bar{d}'_L d'_R + m'_s \bar{s}'_L s'_R + m'_b \bar{b}'_L b'_R) + \frac{h_2}{\sqrt{2}v_2}(m'_{db} \bar{d}'_L b'_R + m'_{sb} \bar{s}'_L b'_R). \tag{7.30}$$

Extracting again the leading flavor-changing terms, we obtain

$$\begin{aligned} \mathcal{L}'_Y = & \left(\frac{h_2}{\sqrt{2}v_2} - \frac{h_1}{\sqrt{2}v_1}\right)(s_1 m_b \bar{d}_L b_R + s_2 m_b \bar{s}_L b_R - s_1 s_2 m_s \bar{d}_L s_R - s_1 s_2 m_d \bar{s}_L d_R \\ & - s_1 s_2^2 m_d \bar{b}_L d_R - s_2^3 m_s \bar{b}_L s_R), \end{aligned} \tag{7.31}$$

where the physical scalar $(v_1 h_2 - v_2 h_1)/\sqrt{v_1^2 + v_2^2} = H + iA$ is a complex field, with $m_H \simeq m_A$.

Assuming negligible mixing between H or A with the SM h (identified as the 125

GeV particle observed at the LHC), we consider the following effective operators [177]:

$$\frac{s_1^2 m_b^2}{8v_2^2}\left(\frac{1}{m_H^2}-\frac{1}{m_A^2}\right)(\bar{d}_L b_R)^2 - \frac{s_1^2 s_2^2 m_b m_d}{4v_2^2}\left(\frac{1}{m_H^2}+\frac{1}{m_A^2}\right)(\bar{d}_L b_R)(\bar{d}_R b_L) + H.c., \quad (7.32)$$

$$\frac{s_2^2 m_b^2}{8v_2^2}\left(\frac{1}{m_H^2}-\frac{1}{m_A^2}\right)(\bar{s}_L b_R)^2 - \frac{s_2^4 m_b m_s}{4v_2^2}\left(\frac{1}{m_H^2}+\frac{1}{m_A^2}\right)(\bar{s}_L b_R)(\bar{s_R} b_L) + H.c., \quad (7.33)$$

$$\frac{s_1^2 s_2^2 m_s^2}{8v_2^2}\left(\frac{1}{m_H^2}-\frac{1}{m_A^2}\right)(\bar{d}_L s_R)^2 - \frac{s_1^2 s_2^2 m_s m_d}{4v_2^2}\left(\frac{1}{m_H^2}+\frac{1}{m_A^2}\right)(\bar{d}_L s_R)(\bar{d}_R s_L) + H.c. \quad (7.34)$$

The upper bounds on $(1/v_2^2)[(1/m_H^2)-(1/m_A^2)]$ from $\Delta M_B, \Delta M_{B_s}, \Delta M_K$ are then

$$(4.5\times10^{-9},\ 5.3\times10^{-9},\ 4.5\times10^{-3})\ \text{GeV}^{-4}, \quad (7.35)$$

respectively, whereas those on $(1/v_2^2)[(1/m_H^2)+(1/m_A^2)]$ are

$$(1.4\times10^{-4},\ 1.7\times10^{-5},\ 8.0\times10^{-5})\ \text{GeV}^{-4}. \quad (7.36)$$

For $v_2 = 10$ GeV, these are easily satisfied with for example $m_H = 500$ GeV and $m_A = 520$ GeV. Fig. 7.1 shows the parameter space from ΔM_{B_s} constraint.

7.6 Lepton sector of Model A

With the chosen $U(1)_F$ charges $(0,-2,-4)$ of Table 7.3, the charged-lepton and Dirac neutrino mass matrices ($\mathcal{M}_l$ and $\mathcal{M}_D$) are both diagonal. As for the 3×3 Majorana mass matrix $\mathcal{M}_R$ of ν_R, it depends on the choice of scalar singlets which break $U(1)_F$. We have already used $\sigma\sim1$ [see Eq. (7.16)] to induce a small v_2 [see Eq. (7.21)]. Call that σ_1 and add $\sigma_{2,4}\sim2,4$, with vacuum expectation values $u_{1,2,4}$ respectively. Then

$$\mathcal{M}_R = \begin{pmatrix} M_0 & M_1 & M_2 \\ M_1 & M_3 & 0 \\ M_2 & 0 & 0 \end{pmatrix}, \quad (7.37)$$

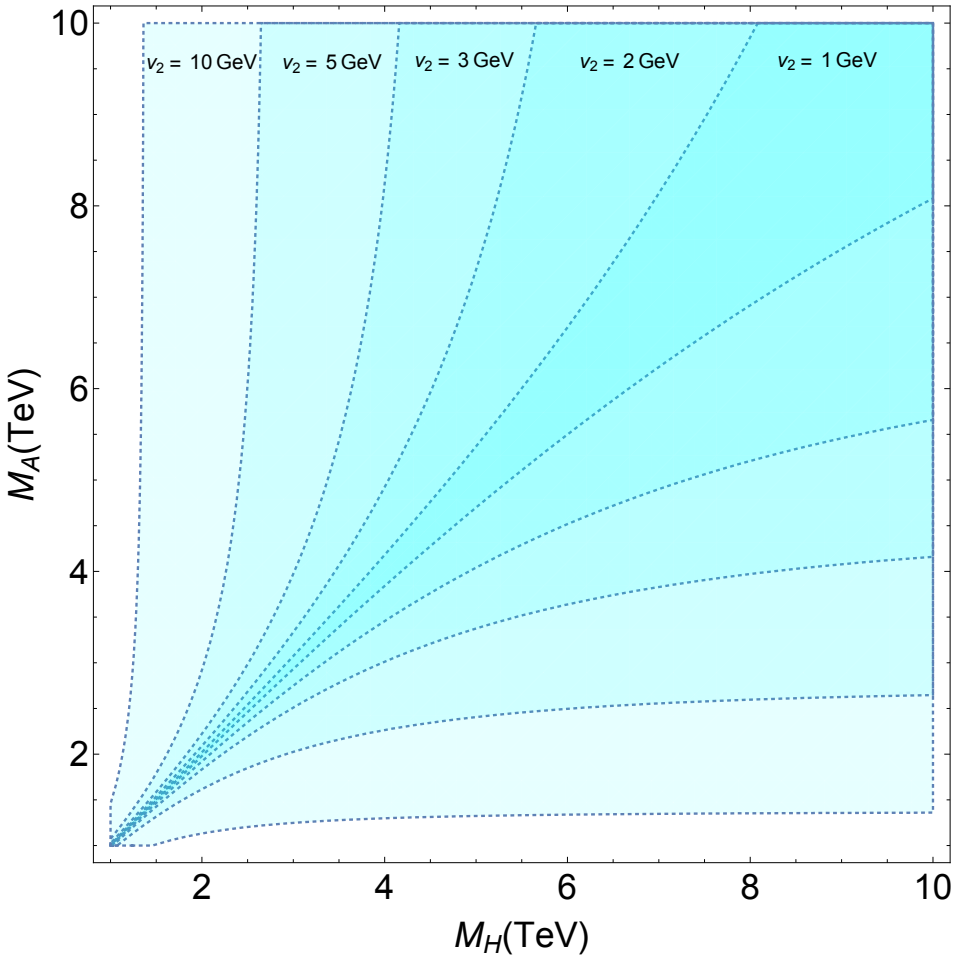

Figure 7.1: Allowed region for suppressed scalar contributions to ΔM_{B_s} for different values of v_2.

where M_0 is an allowed invariant mas term, M_1 comes from u_2, and $M_{2,3}$ from u_4. The seesaw neutrino mass matrix is then

$$\mathcal{M}_\nu = \mathcal{M}_D \mathcal{M}_R^{-1} \mathcal{M}_D^T = \begin{pmatrix} 0 & 0 & a \\ 0 & b & c \\ a & c & d \end{pmatrix}, \tag{7.38}$$

where the two texture zeros appear because of the form of $\mathcal{M}_R$ and $\mathcal{M}_D$ being diagonal [178]. This form is known to be suitable for a best-fit [179] to current neutrino-oscillation data

with normal ordering of neutrino masses. Possible neutrino mass matrix textures from seesaw mechanism are given in appendix D.

7.7 Basic structure of Model B

The quark structure of Model B is basically the same as that of Model A, with the second Higgs doublet now having two units of $U(1)_F$ charge, i.e.

$$\Phi_2 = (\phi_2^+, \phi_2^0) \sim (1, 2, 1/2; 2). \tag{7.39}$$

Hence $\sigma_2 \sim (1, 1, 0; 2)$ is needed for the $\sigma_2 \Phi_2^\dagger \Phi_1$ term in Eq. (7.17).

In the gauge sector, again $Z_F \to e^- e^+$ is zero, and the branching fraction $Z_F \to \mu^- \mu^+$ is now 2/51. The $c_{u,d}$ coefficients are then

$$c_u = c_d = 2 g_F^2 (2/51). \tag{7.40}$$

For the same choice of $g_F = 0.13$ for Model A, the present experimental lower bound from LHC data is reduced from 4.0 TeV to 3.7 TeV. For quarks,

$$\mathcal{L}_{Z_F} = g_F Z_F^\mu (\bar{u}' \gamma_\mu u' + \bar{c}' \gamma_\mu c' - \bar{t}' \gamma_\mu t' + \bar{d}' \gamma_\mu d' + \bar{s}' \gamma_\mu s' - \bar{b}' \gamma_\mu b'). \tag{7.41}$$

Using Eqs. (7.12) and (7.13) to express the above in terms of mass eigenstates for the d sector, and keeping only the leading flavor-changing terms, we find

$$\mathcal{L}'_{Z_F} = 2 g_F Z_F^\mu [-s_1 (\bar{d}_L \gamma_\mu b_L + \bar{b}_L \gamma_\mu d_L) - s_2 (\bar{s}_L \gamma_\mu b_L + \bar{b}_L \gamma_\mu s_L) + s_1 s_2 (\bar{d}_L \gamma_\mu s_L + \bar{s}_L \gamma_\mu d_L)]. \tag{7.42}$$

This differs from Eq. (7.25) only by an overall factor of -2. As for the scalar sector, Eqs. (7.30) and (7.31) remain the same. Altogether, this means that Eqs. (7.9) to (7.15) are also valid in Model B.

7.8 Lepton sector of Model B

With the chosen $U(1)_F$ charges $(0,-1,-2)$ of Table 7.3, the charged-lepton and Dirac neutrino mass matrices are given by

$$\mathcal{M}_l = \begin{pmatrix} m'_e & 0 & m'_{e\tau} \\ 0 & m_\mu & 0 \\ 0 & 0 & m'_\tau \end{pmatrix}, \quad \mathcal{M}_D = \begin{pmatrix} m'_1 & 0 & 0 \\ 0 & m'_2 & 0 \\ m'_{31} & 0 & m'_3 \end{pmatrix}. \tag{7.43}$$

Using the scalar singlets $\sigma_1 \sim 1$ as well σ_2, the ν_R Majorana mass matrix is again given by Eq. (7.37). Now even though $\mathcal{M}_D$ is not diagonal, Eq. (7.38) is still obtained, thereby guaranteeing a best-fit to current neutrino-oscillation data. The difference from Model A is the presence of $\tau - e$ transitions from the nondiagonal $\mathcal{M}_l$. The $\tau \to e\mu^-\mu^+$ decay can occur via Z_F or $h_1 - h_2$ mixing. If we parametrize this mixing by ϵ and the momenta as $\tau^-(p) \to e^-(q_1)\mu^-(q_2)\mu^+(q_3)$, then the amplitude for dominant contribution is given by

$$\mathcal{M} = \frac{-\epsilon\,(m'_{e\tau}/m'_\tau)\,m_\mu m_\tau}{2v_1 v_2 M_h^2}\,[\bar{u}_e(q_1)P_R u_\tau(p)\bar{u}_\mu(q_2)v(q_3)]\,, \tag{7.44}$$

after squaring the amplitude we have

$$|\mathcal{M}|^2 = \frac{\epsilon^2\,(m'_{e\tau}/m'_\tau)^2\,m_\mu^2 m_\tau^2}{4v_1^2 v_2^2 M_h^4}\Big[\bar{u}_e(q_1)P_R\,u_\tau(p)\bar{u}_\mu(q_2)v(q_3)\bar{v}(q_3)u_\mu(q_2)\bar{u}_\tau(p)P_L\,u_e(q_1)\Big], \tag{7.45}$$

we then average over spins of all fermions to get

$$\overline{|\mathcal{M}|^2} = \frac{\epsilon^2\,(m'_{e\tau}/m'_\tau)^2\,m_\mu^2 m_\tau^2}{8v_1^2 v_2^2 M_h^4}\Big[\mathrm{Tr}\left(\not{q}_1 P_R \not{p}\right).\mathrm{Tr}\left([\not{q}_3 - m_\mu][\not{q}_2 + m_\mu]\right)\Big], \tag{7.46}$$

if we take the traces it becomes

$$\overline{|\mathcal{M}|^2} = \frac{\epsilon^2\,(m'_{e\tau}/m'_\tau)^2\,m_\mu^2 m_\tau^2}{v_1^2 v_2^2 M_h^4}\Big[(q_1.p)(q_3.q_2 - m_\mu^2)\Big], \tag{7.47}$$

assuming $m_\mu \ll m_\tau$, we find

$$\overline{|\mathcal{M}|^2} = \frac{\epsilon^2 \left(m'_{e\tau}/m'_\tau\right)^2 m_\mu^2 m_\tau^4}{v_1^2 v_2^2 M_h^4} \Big[\frac{m_\tau E_1}{2} - E_1^2\Big], \tag{7.48}$$

the decay rate is then given by

$$\Gamma = \frac{1}{64\pi^3 m_\tau} \int_0^{\frac{m_\tau}{2}} dE_1 \int_{\frac{m_\tau}{2}-E_1}^{\frac{m_\tau}{2}} \overline{|\mathcal{M}|^2} dE_2 = \frac{\epsilon^2 \left(m'_{e\tau}/m'_\tau\right)^2 m_\mu^2}{v_1^2 v_2^2 M_h^4} \left(\frac{m_\tau^7}{3(16\pi)^3}\right), \tag{7.49}$$

and the constraint on branching ratio is

$$\mathrm{Br}(\tau^- \to e^-\mu^-\mu^+) = \frac{\epsilon^2 \left(m'_{e\tau}/m'_\tau\right)^2 m_\mu^2}{v_1^2 v_2^2 M_h^4} \left(\frac{m_\tau^7}{3(16\pi)^3}\right) \times \frac{1}{\Gamma_\tau} = 5 \times 10^{-14} < 4.1 \times 10^{-8}. \tag{7.50}$$

After plugging $m_e = 0.511$ MeV, $m_\tau = 1.776$ GeV and $\Gamma_\tau = 2.2673 \times 10^{-12}$ GeV, This bound is easily satisfied for $v_2 = 10$ GeV, $M_h = 125$ GeV and ϵ, $(m'_{e\tau}/m'_\tau) \approx 10^{-1}$.

We use the same notation to find the amplitude for the gauge mediated diagram

$$\mathcal{M} = \frac{2\left(m'_{e\tau}/m'_\tau\right) g_F^2}{M_{Z_F}^2} \left[\bar{u}_e(q_1) P_R \,\gamma_\nu\, u_\tau(p) \bar{u}_\mu(q_2)\, \gamma^\nu\, v(q_3)\right], \tag{7.51}$$

we square the amplitude to get

$$|\mathcal{M}|^2 = \frac{4\left(m'_{e\tau}/m'_\tau\right)^2 g_F^4}{M_{Z_F}^4} \Big[\bar{u}_e(q_1) P_R\, \gamma^\nu\, u_\tau(p) \bar{u}_\mu(q_2)\, \gamma_\nu\, v(q_3) \bar{v}(q_3)\, \gamma^\mu\, u_\mu(q_2) \bar{u}_\tau(p) P_R\, \gamma_\mu\, u_e(q_1)\Big], \tag{7.52}$$

after averaging over spins of all fermions we have

$$\overline{|\mathcal{M}|^2} = \frac{2\left(m'_{e\tau}/m'_\tau\right)^2 g_F^4}{M_{Z_F}^4} \Big[\mathrm{Tr}\left(\not{q}_1 \gamma^\nu \not{p} \gamma^\mu P_L\right) . \mathrm{Tr}\left([\not{q}_3 - m_\mu]\gamma_\mu [\not{q}_2 + m_\mu]\gamma_\nu\right)\Big], \tag{7.53}$$

we then take the traces to get

$$\overline{|\mathcal{M}|^2} = \frac{32\left(m'_{e\tau}/m'_\tau\right)^2 g_F^4}{M_{Z_F}^4} \Big[m_\mu^2 (q_1.p) + (q_1.q_2)(p.q_3) + (q_1.q_3)(p.q_2)\Big], \tag{7.54}$$

assuming $m_\mu, m_e \ll m_\tau$ we have

$$\overline{|\mathcal{M}|^2} = \frac{32\,(m'_{e\tau}/m'_\tau)^2\,g_F^4\,m_\tau^2}{M_{Z_F}^4}\Big[-\frac{m_\tau^2}{2}+\frac{m_\tau}{2}(3E_1+4E_2)-E_1^2-2E_1E_2-2E_2^2\Big], \quad (7.55)$$

the decay rate is then given by

$$\Gamma = \frac{1}{64\pi^3 m_\tau}\int_0^{\frac{m_\tau}{2}} dE_1 \int_{\frac{m_\tau}{2}-E_1}^{\frac{m_\tau}{2}} \overline{|\mathcal{M}|^2} dE_2 = \frac{(m'_{e\tau}/m'_\tau)^2\,g_F^4\,m_\tau^2}{M_{Z_F}^4}\left(\frac{m_\tau^3}{3(4\pi)^3}\right), \quad (7.56)$$

and if we take $(m'_{e\tau}/m'_\tau) = 10^{-1}$, $M_{Z_F} = 3.7$ TeV, and $g_F = 0.13$, the constraint on the branching ratio is given by

$$\mathrm{Br}(\tau^- \to e^-\mu^-\mu^+) = \frac{(m'_{e\tau}/m'_\tau)^2\,g_F^4}{3M_{Z_F}^4}\left(\frac{m_\tau^5}{(4\pi)^3}\right)\times\frac{1}{\Gamma_\tau} = 1.97\times10^{-11} < 4.1\times10^{-8}. \quad (7.57)$$

Therefore, we see that for $m'_{e\tau}/m'_\tau < 0.1$, the branching fraction of $\tau \to e\mu^-\mu^+$ is less than 2×10^{-11}, far below the current bound of 4.1×10^{-8}.

7.9 Application to LHC anomalies

Whereas Z_F also mediates $b \to s\mu^-\mu^+$, its effect is too small in Models A and B to explain the tentative LHC observations of $B \to K^*\mu^-\mu^+$ and the ratio of $B^+ \to K^+\mu^-\mu^+$ to $B^+ \to K^+e^-e^+$ [180]. The reason is the stringent bound on m_{Z_F} from LHC data as a function of g_F through the parameters $c_{u,d}$ of Eqs. (7.23) and (7.40). Suppose we take $n_{1,2,3} = (0,0,1)$ and $n'_{1,2,3} = (0,-3,0)$, then Z_F couples to only $\mu^-\mu^+$ and $b'\bar{b}'$, thus allowing for $b-s$ mixing, but $c_{u,d} = 0$. This evades the direct LHC bound, and may be used to explain the B anomalies if they persist. Of course, Eqs. (7.27) to (7.29) still hold, and a full analysis of the detailed structure of $B \to K^*\mu^-\mu^+$ will be required.

7.10 Conclusion

We have generalized the $B - L$ symmetry as a gauge $U(1)_F$ extension of the standard model, where quarks and leptons of each family may transform differently. We have considered two new examples (A and B), each with two Higgs doublets and restricted quark mass matrices consistent with data. The new Z_F gauge boson couples differently to each quark and lepton family, and is constrained by present data to be heavier than about 4 TeV if $g_F = 0.13$. Future data may reveal just such a Z_F belonging to this class of models. Flavor-changing interactions are suitably suppressed by the assignments of quarks and leptons under $U(1)_F$. In the leptonic sector, with the addition of a minimal set of Higgs singlets, a Majorana neutrino mass matrix of two texture zeros may be obtained, leading to a best-fit of neutrino-oscillation data with normal ordering of neutrino masses.

Chapter 8

Quartified Leptonic Color, Bound States, and Future Electron-Positron Collider

8.1 Introduction

Fundamental matter consists of quarks and leptons, but why are they so different? Both interact through the $SU(2)_L \times U(1)_Y$ electroweak gauge bosons $W^{\pm}, Z^0$ and the photon A, but only quarks interact through the strong force as mediated by the gluons of the unbroken (and confining) color $SU(3)$ gauge symmetry, called quantum chromodynamics (QCD). Suppose this is only true of the effective low-energy theory. At high energy, there may in fact be three "colors" of leptons transforming as a triplet under a leptonic color $SU(3)$ gauge symmetry. Unlike QCD, only its $SU(2)_l$ subgroup remains exact, thus confining only

two of the three "colored" leptons, called "hemions" in Ref. [181] because they have $\pm 1/2$ electric charges, leaving the third ones free as the known leptons.

The notion of leptonic color was already discussed many years ago [182, 183], and its incorporation into $[SU(3)]^4$ appeared in Ref. [184], but without full unification. Its relevance today is threefold. (1) The $[SU(3)]^4$ quartification model [181] of Babu, Ma, and Willenbrock (BMW) is non-supersymmetric, and yet achieves gauge-coupling unification at 4×10^{11} GeV without endangering proton decay. This unification of gauge couplings is only possible if the three families of hemions have masses below the TeV scale. Given the absence of experimental evidence for supersymmetry at the Large Hadron Collider (LHC) to date, this alternative scenario deserves a closer look. (2) The quartification scale determines the common gauge coupling for the $SU(2)_l$ symmetry. Its extrapolation to low energy predicts that it becomes strong at the keV scale, in analogy to that of QCD becoming strong at somewhat below the GeV scale. This may alter the thermal history of the Universe and allows the formation of gauge-boson bound states, the lightest of which is a potential warm dark-matter candidate [185]. (3) The hemions (called 'liptons' previously [183]) have $\pm 1/2$ electric charges and are confined to form bound states by the $SU(2)_l$ 'stickons' in analogy to quarks forming hadrons through the $SU(3)_C$ gluons. They have been considered previously [186] as technifermions responsible for electroweak symmetry breaking. Their electroweak production at the LHC is possible [187] but the background is large. However, in a future $e^- e^+$ collider (ILC, CEPC, FCC-ee), neutral vector resonances of their bound states (hemionia) would easily appear, in analogy to the observations of quarkonia (J/ψ, Υ) at past $e^- e^+$ colliders.

8.2 The BMW Model

Under the $[SU(3)]^4$ quartification gauge symmetry, quarks and leptons transform as $(3, \bar{3})$ in a moose chain linking $SU(3)_q$ to $SU(3)_L$ to $SU(3)_l$ to $SU(3)_R$ back to $SU(3)_q$ as depicted in Fig. 8.1.

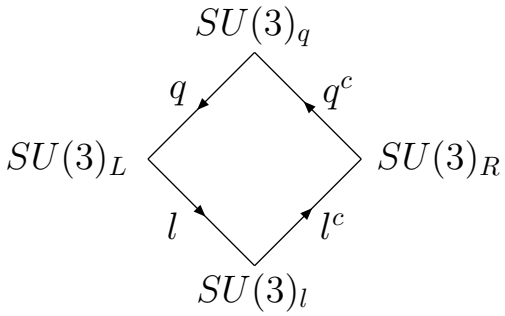

Figure 8.1: Moose diagram of $[SU(3)]^4$ quartification.

Specifically,

$$q \sim (3, \bar{3}, 1, 1) \sim \begin{pmatrix} d & u & h \\ d & u & h \\ d & u & h \end{pmatrix}, \quad l \sim (1, 3, \bar{3}, 1) \sim \begin{pmatrix} x_1 & x_2 & \nu \\ y_1 & y_2 & e \\ z_1 & z_2 & N \end{pmatrix}, \tag{8.1}$$

$$l^c \sim (1, 1, 3, \bar{3}) \sim \begin{pmatrix} x_1^c & y_1^c & z_1^c \\ x_2^c & y_2^c & z_2^c \\ \nu^c & e^c & N^c \end{pmatrix}, \quad q^c \sim (\bar{3}, 1, 1, 3) \sim \begin{pmatrix} d^c & d^c & d^c \\ u^c & u^c & u^c \\ h^c & h^c & h^c \end{pmatrix}. \tag{8.2}$$

Below the TeV energy scale, the gauge symmetry is reduced [181] to $SU(3)_C \times SU(2)_l \times SU(2)_L \times U(1)_Y$ with the particle content given in Table 8.1. The electric charge Q is given by $Q = I_{3L} + Y$ as usual. The exotic $SU(2)_l$ doublets x, y have $\pm 1/2$ charges, hence

Table 8.1: Particle content of proposed model.

particles	$SU(3)_C$	$SU(2)_l$	$SU(2)_L$	$U(1)_Y$
$(u,d)_L$	3	1	2	1/6
u_R	3	1	1	2/3
d_R	3	1	1	$-1/3$
$(x,y)_L$	1	2	2	0
x_R	1	2	1	1/2
y_R	1	2	1	$-1/2$
$(\nu,l)_L$	1	1	2	$-1/2$
ν_R	1	1	1	0
l_R	1	1	1	-1
(ϕ^+,ϕ^0)	1	1	2	1/2

the name hemions. Whereas the quarks and charged leptons must obtain masses through electroweak symmetry breaking, the hemions have invariant mass terms, i.e. $x_{1L}y_{2L} - x_{2L}y_{1L}$ and $x_{1R}y_{2R} - x_{2R}y_{1R}$. This is important because they are then allowed to be heavy without disturbing the electroweak oblique parameters S, T, U which are highly constrained experimentally. In the following, the mass terms from electroweak symmetry breaking, i.e. $\bar{x}_L x_R \bar{\phi}^0$ and $\bar{y}_L y_R \phi^0$, will be assumed negligible.

8.3 Gauge Coupling Unification and the Leptonic Color Confinement Scale

The renormalization-group evolution of the gauge couplings is dictated at leading order by

$$\frac{1}{\alpha_i(\mu)} - \frac{1}{\alpha_i(\mu')} = \frac{b_i}{2\pi} \ln\left(\frac{\mu'}{\mu}\right), \tag{8.3}$$

where b_i are the one-loop beta-function coefficients,

$$b_C = -11 + \frac{4}{3}N_F, \tag{8.4}$$

$$b_l = -\frac{22}{3} + \frac{4}{3}N_F, \tag{8.5}$$

$$b_L = -\frac{22}{3} + 2N_F + \frac{1}{6}N_\Phi, \tag{8.6}$$

$$b_Y = \frac{13}{9}N_F + \frac{1}{12}N_\Phi. \tag{8.7}$$

The number of families N_F is set to three, and the number of Higgs doublets N_Φ is set to two, as in the original BMW model. Here we make a small adjustment by separating the three hemion families into two light ones at the electroweak scale M_Z and one at a somewhat higher scale M_X. We then input the values [173]

$$\alpha_C(M_Z) = 0.1185, \tag{8.8}$$

$$\alpha_L(M_Z) = (\sqrt{2}/\pi)G_F M_W^2 = 0.0339, \tag{8.9}$$

$$\alpha_Y(M_Z) = 2\alpha_L(M_Z)\tan^2\theta_W = 0.0204, \tag{8.10}$$

where α_Y has been normalized by a factor of 2 (and b_Y by a factor of 1/2) to conform to $[SU(3)]^4$ quartification. We find

$$M_U = 4 \times 10^{11}\ \text{GeV}, \quad \alpha_U = 0.0301, \quad M_X = 486\ \text{GeV}. \tag{8.11}$$

We then use b_l to extrapolate back to M_Z and obtain $\alpha_l(M_Z) = 0.0469$. Fig. 8.2 shows the evolution of the couplings in this model. Below the electroweak scale, the evolution of α_l comes only from the stickons and it becomes strong at about 1 keV. Hence 'stickballs' are expected at this confinement mass scale. Unlike QCD where glueballs are heavier than the

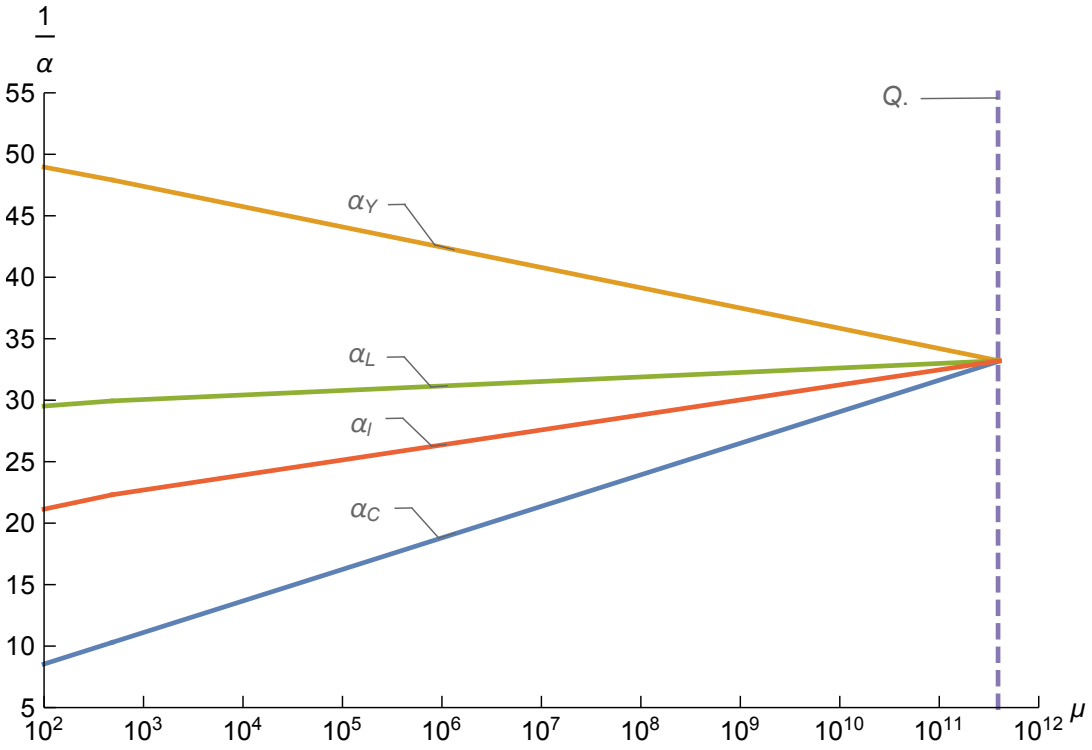

Figure 8.2: The evolution of the couplings are plotted using Eqs. (8.4)-(8.7).

π mesons so that they decay quickly, the stickballs are so light that they could decay only to lighter stickballs or to photon pairs through their interactions with hemions.

8.4 Thermal History of Stickons

At temperatures above the electroweak symmetry scale, the hemions are active and the stickons (ζ) are in thermal equilibrium with the standard-model particles. Below the hemion mass scale, the stickon interacts with photons through $\zeta\zeta \to \gamma\gamma$ scattering with a cross section

$$\sigma \sim \frac{9\alpha^2\alpha_l^2 T^6}{16 M_{\rm eff}^8}. \tag{8.12}$$

The decoupling temperature of ζ is then obtained by matching the Hubble expansion rate

$$H = \sqrt{(8\pi/3) G_N (\pi^2/30) g_* T^4} \tag{8.13}$$

to $[6\zeta(3)/\pi^2] T^3 \langle \sigma v \rangle$. Hence

$$T^{14} \sim \frac{2^8}{3^8} \left(\frac{\pi^7}{5[\zeta(3)]^2} \right) \frac{G_N g_* M_{\rm eff}^{16}}{\alpha^4 \alpha_l^4}, \tag{8.14}$$

where $6 M_{\rm eff}^{-4} = \sum (M^i_{xy})^{-4}$. For $M_{\rm eff} = 110$ GeV and $g_* = 92.25$ which includes all particles with masses up to a few GeV, $T \sim 6.66$ GeV. Hence the contribution of stickons to the effective number of neutrinos at the time of big bang nucleosynthesis (BBN) is given by [188]

$$\Delta N_\nu = \frac{8}{7}(3) \left(\frac{10.75}{92.25} \right)^{4/3} = 0.195, \tag{8.15}$$

compared to the value 0.50 ± 0.23 from an analysis [189]. PLANCK measurement [190] coming from the cosmic microwave background (CMB) is

$$N_{\rm eff} = 3.15 \pm 0.23. \tag{8.16}$$

However, at the time of photon decoupling, the stickons have disappeared, hence $N_{\rm eff} = 3.046$ as in the SM. This is discussed in more detail below. Fig. 8.3 shows the evolution of the ratio of stickon temperature to the temperature of photons.

8.5 Formation and Decay of Stickballs

As the Universe further cools below a few keV, leptonic color goes through a phase transition and stickballs are formed. If the lightest stickball ω is stable, it may be a candidate for warm dark matter. It has strong self-interactions and the $3 \to 2$ process

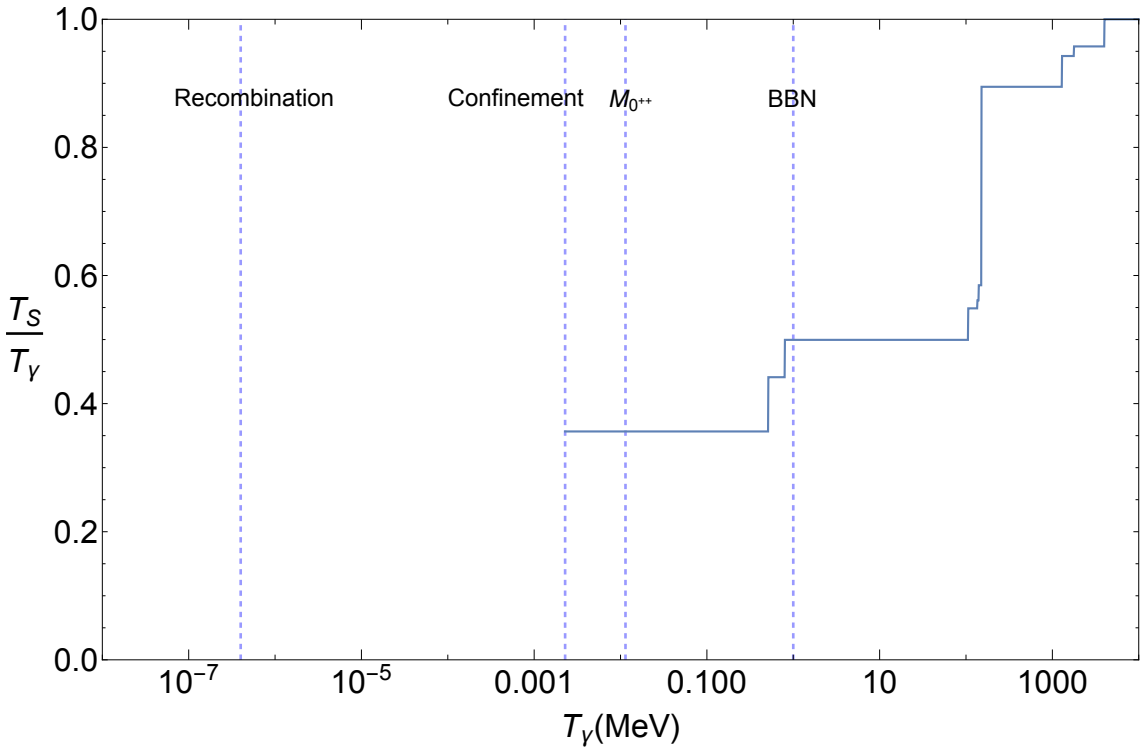

Figure 8.3: The evolution of (T_S/T_γ) after decoupling and down to the confinement scale. Each step corresponds to the decoupling of a specific particle from the photon plasma. The mass of the lightest stickball configuration, $M_{0^{++}}$ is shown as a reference.

determines its relic abundance. Following Ref. [191] and using Ref. [185], we estimate that it is overproduced by a factor of about 3. However, ω is not absolutely stable. It is allowed to mix with a scalar bound state of two hemions which would decay to two photons. We assume this mixing to be $f_\omega m_\omega / M_{xy}$, so that its decay rate is given by

$$\Gamma(\omega \to \gamma\gamma) = \frac{9\alpha^2 f_\omega^2 m_\omega^5}{64\pi^3 M_{\rm eff}^4}, \tag{8.17}$$

where $M_{\rm eff}$ is now defined by $6M_{\rm eff}^{-2} = \sum (M_{xy}^i)^{-2}$. Setting $m_\omega = 5$ keV to be above the astrophysical bound of 4 keV from Lyman α forest observations [192] and $M_{\rm eff} = 150$ GeV, its lifetime is estimated to be $4.4 \times 10^{17} s$ for $f_\omega = 1$. This is exactly the age of the Universe, and it appears that ω may be a candidate for dark matter after all. However,

CMB measurements constrain [193] a would-be dark-matter lifetime to be greater than about $10^{25}s$, and x-ray line measurements in this mass range constrain [194] it to be greater than $10^{27}s$, so this scenario is ruled out. On the other hand, if $m_\omega = 10$ keV, then the ω lifetime is $1.4 \times 10^{16}s$, which translates to a fraction of 2×10^{-14} of the initial abundance of ω to remain at the present Universe. Compared to the upper bound of 10^{-10} for a lifetime of $10^{16}s$ given in Ref. [193], this is easily satisfied, even though ω is overproduced at the leptonic color phase transition by a factor of 3.

At the time of photon decoupling, the $SU(2)_l$ sector contributes no additional relativistic degrees of freedom, hence $N_{\rm eff}$ remains the same as in the SM, i.e. 3.046, coming only from neutrinos. In this scenario, ω is not dark matter. However, there are many neutral scalars and fermions in the BMW model which are not being considered here. They are naturally very heavy, but some may be light enough and stable, and be suitable as dark matter.

8.6 Revelation of Leptonic Color at Future e^-e^+ Colliders

Unlike quarks, all hemions are heavy. Hence the lightest bound state is likely to be at least 200 GeV. Its cross section through electroweak production at the LHC is probably too small for it to be discovered. On the other hand, in analogy to the observations of J/ψ and Υ at e^-e^+ colliders of the last century, the resonance production of the corresponding neutral vector bound states (hemionia) of these hemions is expected at a future e^-e^+ collider (ILC, CEPC, FCC-ee) with sufficient reach in total center-of-mass energy. Their decays will be distinguishable from heavy quarkonia (such as toponia) experimentally.

The formation of hemion bound states is analogous to that of QCD. Instead of one-gluon exchange, the Coulomb potential binding a hemion-antihemion pair comes from one-stickon exchange. The difference is just the change in an SU(3) color factor of 4/3 to an SU(2) color factor of 3/4. The Bohr radius is then $a_0 = [(3/8)\bar{\alpha}_l m]^{-1}$, and the effective $\bar{\alpha}_l$ is defined by

$$\bar{\alpha}_l = \alpha_l(a_0^{-1}). \tag{8.18}$$

Using Eqs. (8.3) and (8.5), and $\alpha_l(M_Z) = 0.047$ with $m = 100$ GeV, we obtain $\bar{\alpha}_l = 0.059$ and $a_0^{-1} = 2.2$ GeV. Consider the lowest-energy vector bound state Ω of the lightest hemion of mass $m = 100$ GeV. In analogy to the hydrogen atom, its binding energy is given by

$$E_b = \frac{1}{4}\left(\frac{3}{4}\right)^2 \bar{\alpha}_l^2 m = 0.049 \text{ GeV}, \tag{8.19}$$

and its wavefunction at the origin is

$$|\psi(0)|^2 = \frac{1}{\pi a_0^3} = 3.4 \text{ GeV}^3. \tag{8.20}$$

Since Ω will appear as a narrow resonance at a future e^-e^+ collider, its observation depends on the integrated cross section over the energy range $\sqrt{s}$ around m_Ω:

$$\int d\sqrt{s}\, \sigma(e^-e^+ \to \Omega \to X) = \frac{6\pi^2}{m_\Omega^2} \frac{\Gamma_{ee}\Gamma_X}{\Gamma_{tot}}, \tag{8.21}$$

where Γ_{tot} is the total decay width of Ω, and Γ_{ee}, Γ_X are the respective partial widths.

Since Ω is a vector meson, it couples to both the photon and Z boson through its constituent hemions. Hence it will decay to W^-W^+, $q\bar{q}$, l^-l^+, and $\nu\bar{\nu}$. We now derive the relation of the amplitude of bound state decay to its constituent annihilation. We

work in the center-of-mass frame of the hemions. Take the amplitude for free hemion and anti-hemion annihilation to be

$$\mathcal{M}_f = \bar{v}(k_2)\,[\mathcal{O}]\,u(k_1) = \mathrm{Tr}\,[\mathcal{O}u(k_1)\bar{v}(k_2)]\,. \tag{8.22}$$

The spinors can be combined to represent definite total spin states, i.e., ${}^1S_0$ and ${}^3S_1$ as follows

$$(u\bar{v})_{{}^1S_0} = \frac{1}{\sqrt{2}}\gamma_5(\not{k}_1 - m) \quad \text{and} \quad (u\bar{v})_{{}^3S_1} = \frac{1}{\sqrt{2}}\not{\epsilon}(\not{k}_1 - m) \tag{8.23}$$

where ϵ is the polarization vector for the vector particle such that $\epsilon.k_1 = 0$. The bound state amplitude is related to the free hemion annihilations according to

$$\mathcal{M}(B \to \text{ anything}) = \sqrt{2m_\Omega}\int \frac{d^3k}{(2\pi)^3}\tilde{\psi}(k)\frac{1}{\sqrt{2m}}\frac{1}{\sqrt{2m}}\mathcal{M}(x^+x^- \to \text{anything}) \tag{8.24}$$

If we neglect the binding energy, $m_\Omega = 2m$. Furthermore, if the amplitude doesn't have momentum dependence, we can integrate over k to get:

$$\mathcal{M}(B \to \text{ anything}) = \sqrt{\frac{2}{m_\Omega}}\cdot\psi(0)\cdot\mathcal{M}(x^+x^- \to \text{anything}), \tag{8.25}$$

using Eq. (8.23) the bound state part of the amplitude becomes

$$\mathcal{M}(B_0) = \sqrt{\frac{1}{m_\Omega}}\cdot\psi(0)\cdot\mathrm{Tr}\,[\mathcal{O}\,\gamma_5\,(\not{k} - m)]\,, \tag{8.26}$$

$$\mathcal{M}(\Omega) = \sqrt{\frac{1}{m_\Omega}}\cdot\psi(0)\cdot\mathrm{Tr}\,[\mathcal{O}\not{\epsilon}\,(\not{k} - m)]\,, \tag{8.27}$$

where Ω is a vector bound state, and B_0 is a scalar. The SU(2) singlet bound state, is $(x_1y_2 - x_2y_1)/\sqrt{2}$. Therefore, we should multiply the amplitude by a color factor, i.e., $2/\sqrt{2} = \sqrt{2}$. In the special case that $\mathcal{O} = \gamma^\mu$, we have

$$\sqrt{2}\,\mathcal{M}(\Omega) = -\sqrt{2}\cdot\sqrt{4m_\Omega}\cdot\psi(0)\cdot\epsilon^\mu = -\sqrt{8\,m_\Omega}\cdot\psi(0)\cdot\epsilon^\mu, \tag{8.28}$$

and for $\mathcal{O} = \gamma^\mu\gamma^5$, it's zero. Using

$$\langle 0|\bar{x}\gamma^\mu x|\Omega\rangle = \epsilon^\mu_\Omega\sqrt{8m_\Omega}|\psi(0)|, \tag{8.29}$$

the $\Omega \to e^-e^+$ decay rate is given by

$$\Gamma(\Omega \to \gamma, Z \to e^-e^+) = \frac{2m_\Omega^2}{3\pi}(|C_V|^2 + |C_A|^2)|\psi(0)|^2, \tag{8.30}$$

where

$$C_V = \frac{e^2(1/2)(-1)}{m_\Omega^2} + \frac{g_Z^2(-\sin^2\theta_W/4)[(-1+4\sin^2\theta_W)/4]}{m_\Omega^2 - M_Z^2}, \tag{8.31}$$

$$C_A = \frac{g_Z^2(-\sin^2\theta_W/4)(1/4)}{m_\Omega^2 - M_Z^2}. \tag{8.32}$$

In the above, Ω is assumed to be composed of the singlet hemions x_R and y_R with invariant mass term $x_{1R}y_{2R} - x_{2R}y_{1R}$ (case A). Hence $\Gamma_{ee} = 43$ eV. If Ω comes instead from x_L and y_L with invariant mass term $x_{1L}y_{2L} - x_{2L}y_{1L}$ (case B), then the factor $(-\sin^2\theta_W/4)$ in C_V and C_A is replaced with $(\cos^2\theta_W/4)$ and $\Gamma_{ee} = 69$ eV. Similar expressions hold for the other fermions of the Standard Model (SM).

For $\Omega \to W^-W^+$, the triple γW^-W^+ and ZW^-W^+ vertices have the same structure. The decay rate is calculated to be

$$\Gamma(\Omega \to \gamma, Z \to W^-W^+) = \frac{m_\Omega^2(1-r)^{3/2}}{6\pi r^2}\left(4 + 20r + 3r^2\right)C_W^2|\psi(0)|^2, \tag{8.33}$$

where $r = 4M_W^2/m_\Omega^2$ and

$$C_W = \frac{e^2(1/2)}{m_\Omega^2} + \frac{g_Z^2(-\sin^2\theta_W/4)}{m_\Omega^2 - M_Z^2} \tag{8.34}$$

in case A. Because of the accidental cancellation of the two terms in the above, C_W turns out to be very small. Hence $\Gamma_{WW} = 3.2$ eV. In addition to the $s-$channel decay of Ω to

W^-W^+ through γ and Z, there is also a $t-$channel electroweak contribution in case B because x_L and y_L form an electroweak doublet. Replacing $(-\sin^2\theta_W/4)$ with $(\cos^2\theta_W/4)$ in C_W, and adding this contribution, we obtain

$$\begin{aligned}\Gamma(\Omega \to W^-W^+) &= \frac{m_\Omega^2(1-r)^{3/2}}{6\pi r^2}[(4+20r+3r^2)C_W^2 \\ &+ 2r(10+3r)C_W D_W + r(8-r)D_W^2]|\psi(0)|^2, \end{aligned} \tag{8.35}$$

where

$$D_W = \frac{-g^2}{4(m_\Omega^2 - 2M_W^2)}. \tag{8.36}$$

Thus a much larger $\Gamma_{WW} = 190$ eV is obtained. For $\Omega \to ZZ$, there is only the $t-$channel contribution, i.e.

$$\Gamma(\Omega \to ZZ) = \frac{m_\Omega^2(1-r_Z)^{5/2}}{3\pi r_Z} D_Z^2 |\psi(0)|^2, \tag{8.37}$$

where $r_Z = 4M_Z^2/m_\Omega^2$ and $D_Z = g_Z^2 \sin^4\theta_W/4(m_\Omega^2 - 2m_Z^2)$ in case A, with $\sin^4\theta_W$ replaced by $\cos^4\theta_W$ in case B. Hence Γ_{ZZ} is negligible in case A and only 2.5 eV in case B.

The Ω decay to two stickons is forbidden by charge conjugation. Its decay to three stickons is analogous to that of quarkonium to three gluons. Whereas the latter forms a singlet which is symmetric in $SU(3)_C$, the former forms a singlet which is antisymmetric in $SU(2)_l$. However, the two amplitudes are identical because the latter is symmetrized with respect to the exchange of the three gluons and the former is antisymmetrized with respect to the exchange of the three stickons. Taking into account the different color factors of $SU(2)_l$ versus $SU(3)_C$, the decay rate of Ω to three stickons and to two stickons plus a

photon are given by

$$\Gamma(\Omega \to \zeta\zeta\zeta) = \frac{16}{27}(\pi^2 - 9)\frac{\alpha_l^3}{m_\Omega^2}|\psi(0)|^2, \tag{8.38}$$

$$\Gamma(\Omega \to \gamma\zeta\zeta) = \frac{8}{9}(\pi^2 - 9)\frac{\alpha\alpha_l^2}{m_\Omega^2}|\psi(0)|^2. \tag{8.39}$$

Hence $\Gamma_{\zeta\zeta\zeta} = 4.5$ eV and $\Gamma_{\gamma\zeta\zeta} = 1.1$ eV. The integrated cross section of Eq. (8.21) for $X = \mu^-\mu^+$ is then 3.8×10^{-33} cm^2-keV in case A and 2.1×10^{-33} cm^2-keV in case B. For comparison, this number is 7.9×10^{-30} cm^2-keV for the $\Upsilon(1S)$. At a high-luminosity e^-e^+ collider, it should be feasible to make this observation. Table 8.2 summarizes all the partial decay widths.

Table 8.2: Partial decay widths of the hemionium Ω.

Channel	Width (A)	Width (B)
$\nu\bar{\nu}$	11 eV	123 eV
e^-e^+	43 eV	69 eV
$\mu^-\mu^+$	43 eV	69 eV
$\tau^-\tau^+$	43 eV	69 eV
$u\bar{u}$	50 eV	175 eV
$c\bar{c}$	50 eV	175 eV
$d\bar{d}$	10 eV	147 eV
$s\bar{s}$	10 eV	147 eV
$b\bar{b}$	10 eV	147 eV
W^-W^+	3.2 eV	190 eV
ZZ	0.02 eV	2.5 eV
$\zeta\zeta\zeta$	4.5 eV	4.5 eV
$\zeta\zeta\gamma$	1.1 eV	1.1 eV
sum	279 eV	1319 eV

8.7 Discussion and Outlook

There are important differences between QCD and QHD (quantum hemiodynamics). In the former, because of the existence of light u and d quarks, it is easy to pop up $u\bar{u}$ and $d\bar{d}$ pairs from the QCD vacuum. Hence the production of open charm in an e^-e^+ collider is described well by the fundamental process $e^-e^+ \to c\bar{c}$. In the latter, there are no light hemions. Instead it is easy to pop up the light stickballs from the QHD vacuum. As a result, just above the threshold of making the Ω resonance, the many-body production of Ω + stickballs becomes possible. This cross section is presumably also well described by the fundamental process $e^-e^+ \to x\bar{x}$. In case A, the cross section is given by

$$\begin{aligned}\sigma(e^-e^+ \to x\bar{x}) &= \frac{2\pi\alpha^2}{3}\sqrt{1-\frac{4m^2}{s}}\left[\frac{(s+2m^2)}{s^2}+\frac{x_W^2}{2(1-x_W)^2}\frac{(s-m^2)}{(s-m_Z^2)^2}\right.\\ &+ \left.\frac{x_W}{(1-x_W)}\frac{(s-m^2)}{s(s-m_Z^2)}-\frac{(1-4x_W)}{4(1-x_W)}\frac{m^2}{s(s-m_Z^2)}\right], \end{aligned} \tag{8.40}$$

where $x_W = \sin^2\theta_W$ and $s = 4E^2$ is the square of the center-of-mass energy. In case B, it is

$$\begin{aligned}\sigma(e^-e^+ \to x\bar{x}) &= \frac{2\pi\alpha^2}{3}\sqrt{1-\frac{4m^2}{s}}\left[\frac{(s+2m^2)}{s^2}+\frac{(s-m^2)}{2(s-m_Z^2)^2}\right.\\ &- \left.\frac{(s-m^2)}{s(s-m_Z^2)}+\frac{(1-4x_W)}{4x_W}\frac{m^2}{s(s-m_Z^2)}\right]. \end{aligned} \tag{8.41}$$

Using $m = 100$ GeV and $s = (250\text{ GeV})^2$ as an example, we find these cross sections to be 0.79 and 0.44 pb respectively.

In QCD, there are $q\bar{q}$ bound states which are bosons, and qqq bound states which are fermions. In QHD, there are only bound-state bosons, because the confining symmetry is $SU(2)_l$. Also, unlike baryon (or quark) number in QCD, there is no such thing as hemion

number in QHD, because y is effectively $\bar{x}$. This explains why there are no stable analog fermion in QHD such as the proton in QCD.

The SM Higgs boson h couples to the hemions, but these Yukawa couplings could be small, because hemions have invariant masses themselves as already explained. So far we have assumed these couplings to be negligible. If not, then h may decay to two photons and two stickons through a loop of hemions. This may show up in precision Higgs studies as a deviation of $h \to \gamma\gamma$ from the SM prediction. It will also imply a partial invisible width of h proportional to this deviation. Neither would be large effects and that is perfectly consistent with present data.

The absence of observations of new physics at the LHC is a possible indication that fundamental new physics may not be accessible using the strong interaction, i.e. quarks and gluons. It is then natural to think about future e^-e^+ colliders. But is there some fundamental issue of theoretical physics which may only reveal itself there? and not at hadron colliders? The BMW model is one possible answer. It assumes a quartification symmetry based on $[SU(3)]^4$. It has gauge-coupling unification without supersymmetry, but requires the existence of new half-charged fermions (hemions) under a confining $SU(2)_l$ leptonic color symmetry, with masses below the TeV scale. It also predicts the $SU(2)_l$ confining scale to be keV, so that stickball bound states of the vector gauge stickons are formed. These new particles have no QCD interactions, but hemions have electroweak couplings, so they are accessible in a future e^-e^+ collider, as described in this paper.

Chapter 9

Dark Gauge U(1) Symmetry for an Alternative Left-Right Model

9.1 Introduction

The alternative left-right model [195] of 1987 was inspired by the E_6 decomposition to the standard $SU(3)_C \times SU(2)_L \times U(1)_Y$ gauge symmetry through an $SU(2)_R$ which does not have the conventional assignments of quarks and leptons. Instead of $(u,d)_R$ and $(\nu,l)_R$ as doublets under $SU(2)_R$, a new quark h and a new lepton n per family are added so that $(u,h)_R$ and $(n,e)_R$ are the $SU(2)_R$ doublets, and h_L, d_R, n_L, ν_R are singlets.

This structure allows for the absence of tree-level flavor-changing neutral currents (unavoidable in the conventional model), as well as the existence of dark matter. The key new ingredient is a $U(1)_S$ symmetry, which breaks together with $SU(2)_R$, such that a residual global S' symmetry remains for the stabilization of dark matter. Previously [196–

198], this $U(1)_S$ was assumed to be global. We show in this paper how it may be promoted to a gauge symmetry. To accomplish this, new fermions are added to render the model free of gauge anomalies. The resulting theory has an automatic discrete Z_2 symmetry which is unbroken, as well as the global S', which is now broken to Z_3. Hence dark matter has two components [92]. They are identified as one Dirac fermion (nontrivial under both Z_2 and Z_3) and one complex scalar (nontrivial under Z_3).

9.2 Model

The particle content of our model is given in Table 9.1, where the scalar $SU(2)_L \times SU(2)_R$ bidoublet is given by

$$\eta = \begin{pmatrix} \eta_1^0 & \eta_2^+ \\ \eta_1^- & \eta_2^0 \end{pmatrix}, \tag{9.1}$$

with $SU(2)_L$ transforming vertically and $SU(2)_R$ horizontally. Without $U(1)_S$ as a gauge symmetry, the model is free of anomalies without the addition of the ψ and χ fermions. In the presence of gauge $U(1)_S$, the additional anomaly-free conditions are all satisfied by the addition of the ψ and χ fermions. The $[SU(3)_C]^2 U(1)_S$ anomaly is canceled between $(u,h)_R$ and h_L; the $[SU(2)_L]^2 U(1)_S$ anomaly is zero because $(u,d)_L$ and $(\nu,l)_L$ do not transform under $U(1)_S$; the $[SU(2)_R]^2 U(1)_S$ and $[SU(2)_R]^2 U(1)_X$ anomalies are both canceled by summing over $(u,h)_R$, $(n,l)_R$, $(\psi_1^0, \psi_1^-)_R$, and $(\psi_2^+, \psi_2^0)_R$; the addition of $\chi_R^\pm$ renders the $[U(1)_X]^2 U(1)_S$, $U(1)_X [U(1)_S]^2$, $[U(1)_X]^3$, and $U(1)_X$ anomalies zero; and the further

Table 9.1: Particle content of proposed model of dark gauge $U(1)$ symmetry.

particles	$SU(3)_C$	$SU(2)_L$	$SU(2)_R$	$U(1)_X$	$U(1)_S$
$(u,d)_L$	3	2	1	1/6	0
$(u,h)_R$	3	1	2	1/6	$-1/2$
d_R	3	1	1	$-1/3$	0
h_L	3	1	1	$-1/3$	-1
$(\nu,l)_L$	1	2	1	$-1/2$	0
$(n,l)_R$	1	1	2	$-1/2$	1/2
ν_R	1	1	1	0	0
n_L	1	1	1	0	1
(ϕ_L^+,ϕ_L^0)	1	2	1	1/2	0
(ϕ_R^+,ϕ_R^0)	1	1	2	1/2	1/2
η	1	2	2	0	$-1/2$
ζ	1	1	1	0	1
$(\psi_1^0,\psi_1^-)_R$	1	1	2	$-1/2$	2
$(\psi_2^+,\psi_2^0)_R$	1	1	2	1/2	1
χ_R^+	1	1	1	1	$-3/2$
χ_R^-	1	1	1	-1	$-3/2$
χ_{1R}^0	1	1	1	0	$-1/2$
χ_{2R}^0	1	1	1	0	$-5/2$
σ	1	1	1	0	3

addition of χ_{1R}^0 and χ_{2R}^0 kills both the $[U(1)_S]^3$ and $U(1)_S$ anomalies, i.e.

$$\begin{aligned} 0 &= 3[6(-1/2)^3 - 3(-1)^3 + 2(1/2)^3 - (1)^3] \\ &+ 2(2)^3 + 2(1)^3 + 2(-3/2)^3 + (-1/2)^3 + (-5/2)^3, \end{aligned} \tag{9.2}$$

$$\begin{aligned} 0 &= 3[6(-1/2) - 3(-1) + 2(1/2) - (1)] \\ &+ 2(2) + 2(1) + 2(-3/2) + (-1/2) + (-5/2). \end{aligned} \tag{9.3}$$

Under $T_{3R} + S$, the neutral scalars ϕ_R^0 and η_2^0 are zero, so that their vacuum expectation values do not break $T_{3R} + S$ which remains as a global symmetry. However, $\langle\sigma\rangle \neq 0$ does break $T_{3R}+S$ and gives masses to $\psi_{1R}^0\psi_{2R}^0 - \psi_{1R}^-\psi_{2R}^+$, $\chi_R^+\chi_R^-$, and $\chi_{1R}^0\chi_{2R}^0$. These exotic fermions all have half-integral charges [199] under $T_{3R} + S$ and only communicate

with the others with integral charges through $W_R^\pm$, $\sqrt{2}Re(\phi_R^0)$, ζ, and the two extra neutral gauge bosons beyond the Z. Some explicit Yukawa terms are

$$(\psi_{1R}^0\phi_R^- + \psi_{1R}^-\bar{\phi}_R^0)\chi_R^+, \quad (\psi_{2R}^+\phi_R^0 - \psi_{2R}^0\phi_R^+)\chi_R^-, \tag{9.4}$$

$$(\psi_{1R}^0\phi_R^0 - \psi_{1R}^-\phi_R^+)\chi_{2R}^0, \quad (\psi_{2R}^+\phi_R^- + \psi_{2R}^0\bar{\phi}_R^0)\chi_{1R}^0. \tag{9.5}$$

This dichotomy of particle content results in an additional unbroken symmetry of the Lagrangian, i.e. discrete Z_2 under which the exotic fermions are odd. Hence dark matter has two layers: those with nonzero $T_{3R}+S$ and even Z_2, i.e. $n, h, W_R^\pm, \phi_R^\pm, \eta_1^\pm, \eta_1^0, \bar{\eta}_1^0, \zeta$, and the underlying exotic fermions with odd Z_2. Without ζ, a global S' symmetry remains. With ζ, because of the $\zeta^3\sigma^*$ and $\chi_{1R}^0\chi_{1R}^0\zeta$ terms, the S' symmetry breaks to Z_3.

Table 9.2: Particle content of proposed model under $(T_{3R}+S)\times Z_2$.

particles	gauge $T_{3R}+S$	global S'	Z_3	Z_2
u, d, ν, l	0	0	1	$+$
$(\phi_L^+, \phi_L^0), (\eta_2^+, \eta_2^0), \phi_R^0$	0	0	1	$+$
n, ϕ_R^+, ζ	1	1	ω	$+$
$h, (\eta_1^0, \eta_1^-)$	-1	-1	ω^2	$+$
ψ_{2R}^+, χ_R^+	$3/2, -3/2$	0	1	$-$
ψ_{1R}^-, χ_R^-	$3/2, -3/2$	0	1	$-$
ψ_{1R}^0, ψ_{2R}^0	$5/2, 1/2$	$1, -1$	ω, ω^2	$-$
χ_{1R}^0, χ_{2R}^0	$-1/2, -5/2$	$1, -1$	ω, ω^2	$-$
σ	3	0	1	$+$

Let

$$\langle\phi_L^0\rangle = v_1, \quad \langle\eta_2^0\rangle = v_2, \quad \langle\phi_R^0\rangle = v_R, \quad \langle\sigma\rangle = v_S, \tag{9.6}$$

then the $SU(3)_C\times SU(2)_L\times SU(2)_R\times U(1)_X\times U(1)_S$ gauge symmetry is broken to $SU(3)_C\times U(1)_Q$ with S', which becomes Z_3, as shown in Table 9.2 with $\omega^3 = 1$. The discrete Z_2 symmetry is unbroken. Note that the global S' assignments for the exotic fermions are not

$T_{3R} + S$ because of v_S which breaks the gauge $U(1)_S$ by 3 units.

9.3 Gauge sector

Consider now the masses of the gauge bosons. The charged ones, $W_L^{\pm}$ and $W_R^{\pm}$, do not mix because of $S'(Z_3)$, as in the original alternative left-right models. Their masses are given by

$$M_{W_L}^2 = \frac{1}{2} g_L^2 (v_1^2 + v_2^2), \quad M_{W_R}^2 = \frac{1}{2} g_R^2 (v_R^2 + v_2^2). \tag{9.7}$$

Since $Q = I_{3L} + I_{3R} + X$, the photon is given by

$$A = \frac{e}{g_L} W_{3L} + \frac{e}{g_R} W_{3R} + \frac{e}{g_X} X, \tag{9.8}$$

where $e^{-2} = g_L^{-2} + g_R^{-2} + g_X^{-2}$. Let

$$Z = (g_L^2 + g_Y^2)^{-1/2} \left(g_L W_{3L} - \frac{g_Y^2}{g_R} W_{3R} - \frac{g_Y^2}{g_X} X \right), \tag{9.9}$$

$$Z' = (g_R^2 + g_X^2)^{-1/2} (g_R W_{3R} - g_X X), \tag{9.10}$$

where $g_Y^{-2} = g_R^{-2} + g_X^{-2}$, then the 3×3 mass-squared matrix spanning (Z, Z', S) has the entries:

$$
\begin{aligned}
M^2_{ZZ} &= \frac{1}{2}(g_L^2 + g_Y^2)(v_1^2 + v_2^2), && (9.11)\\
M^2_{Z'Z'} &= \frac{1}{2}(g_R^2 + g_X^2)v_R^2 + \frac{g_X^4 v_1^2 + g_R^4 v_2^2}{2(g_R^2 + g_X^2)}, && (9.12)\\
M^2_{SS} &= 18 g_S^2 v_S^2 + \frac{1}{2} g_S^2 (v_R^2 + v_2^2), && (9.13)\\
M^2_{ZZ'} &= \frac{\sqrt{g_L^2 + g_Y^2}}{2\sqrt{g_R^2 + g_X^2}}(g_X^2 v_1^2 - g_R^2 v_2^2), && (9.14)\\
M^2_{ZS} &= \frac{1}{2} g_S \sqrt{g_L^2 + g_Y^2}\, v_2^2, && (9.15)\\
M^2_{Z'S} &= -\frac{1}{2} g_S \sqrt{g_R^2 - g_X^2}\, v_R^2 - \frac{g_S g_R v_2^2}{2\sqrt{g_R^2 + g_X^2}}. && (9.16)
\end{aligned}
$$

Their neutral-current interactions are given by

$$
\begin{aligned}
\mathcal{L}_{NC} &= e A_\mu j_Q^\mu + g_Z Z_\mu (j_{3L}^\mu - \sin^2\theta_W j_Q^\mu)\\
&+ (g_R^2 + g_X^2)^{-1/2} Z'_\mu (g_R^2 j_{3R}^\mu - g_X^2 j_X^\mu) + g_S S_\mu j_S^\mu, && (9.17)
\end{aligned}
$$

where $g_Z^2 = g_L^2 + g_Y^2$ and $\sin^2\theta_W = g_Y^2/g_Z^2$.

In the limit $v_{1,2}^2 << v_R^2, v_S^2$, the mass-squared matrix spanning (Z', S) may be simplified if we assume

$$
\frac{v_S^2}{v_R^2} = \frac{(g_R^2 + g_X^2 + g_S^2)^2}{36 g_S^2 (g_R^2 + g_X^2 - g_S^2)}, \tag{9.18}
$$

and let

$$
\tan\theta_D = \frac{\sqrt{g_R^2 + g_X^2} - g_S}{\sqrt{g_R^2 + g_X^2} + g_S}, \tag{9.19}
$$

then

$$
\begin{pmatrix} D_1 \\ \\ D_2 \end{pmatrix} = \begin{pmatrix} \cos\theta_D & \sin\theta_D \\ \\ -\sin\theta_D & \cos\theta_D \end{pmatrix} \begin{pmatrix} Z' \\ \\ S \end{pmatrix}, \tag{9.20}
$$

with mass eigenvalues given by

$$M^2_{D_1} = \sqrt{g_R^2+g_X^2}\sqrt{g_R^2+g_X^2+g_S^2}\,\frac{v_R^2}{2\sqrt{2}\cos\theta_D}, \quad (9.21)$$

$$M^2_{D_2} = \sqrt{g_R^2+g_X^2}\sqrt{g_R^2+g_X^2+g_S^2}\,\frac{v_R^2}{2\sqrt{2}\sin\theta_D}. \quad (9.22)$$

In addition to the assumption of Eq. (9.18), let us take for example

$$2g_S = \sqrt{g_R^2+g_X^2}, \quad (9.23)$$

then $\sin\theta_D = 1/\sqrt{10}$ and $\cos\theta_D = 3/\sqrt{10}$. Assuming also that $g_R = g_L$, we obtain

$$\frac{g_X^2}{g_Z^2} = \frac{\sin^2\theta_W\cos^2\theta_W}{\cos 2\theta_W}, \quad \frac{g_S}{g_Z} = \frac{\cos^2\theta_W}{2\sqrt{\cos 2\theta_W}}, \quad (9.24)$$

$$\frac{v_S^2}{v_R^2} = \frac{25}{108}, \quad M^2_{D_2} = 3M^2_{D_1} = \frac{5\cos^4\theta_W}{4\cos 2\theta_W}g_Z^2 v_R^2. \quad (9.25)$$

The resulting gauge interactions of $D_{1,2}$ are given by

$$\mathcal{L}_D = \frac{g_Z}{\sqrt{10}\sqrt{\cos 2\theta_W}}\{[3\cos 2\theta_W j^\mu_{3R} - 3\sin^2\theta_W j^\mu_X + (1/2)\cos^2\theta_W j^\mu_S]D_{1\mu} + [-\cos 2\theta_W j^\mu_{3R} + \sin^2\theta_W j^\mu_X + (3/2)\cos^2\theta_W j^\mu_S]D_{2\mu}\}. \quad (9.26)$$

Since D_2 is $\sqrt{3}$ times heavier than D_1 in this example, the latter would be produced first in pp collisions at the Large Hadron Collider (LHC).

9.4 Fermion sector

All fermions obtain masses through the four vacuum expectation values of Eq. (9.6) except ν_R which is allowed to have an invariant Majorana mass. This means that neutrino masses may be small from the usual canonical seesaw mechanism. The various Yukawa

terms for the quark and lepton masses are

$$\begin{aligned} -\mathcal{L}_Y &= \frac{m_u}{v_2}[\bar{u}_R(u_L\eta_2^0 - d_L\eta_2^+) + \bar{h}_R(-u_L\eta_2^- + d_L\eta_1^0)] \\ &+ \frac{m_d}{v_1}(\bar{u}_L\phi_L^+ + \bar{d}_L\phi_L^0)d_R + \frac{m_h}{v_R}(\bar{u}_R\phi_R^+ + \bar{h}_R\phi_R^0)h_L \\ &+ \frac{m_l}{v_2}[(\bar{\nu}_L\eta_1^0 + \bar{l}_L\eta_1^-)n_R + (\bar{\nu}_L\eta_2^+ + \bar{l}_L\eta_2^0)l_R] \\ &+ \frac{m_D}{v_1}\bar{\nu}_R(\nu_L\phi_L^0 - l_L\phi_L^+) + \frac{m_n}{v_R}\bar{n}_L(n_R\phi_R^0 - l_R\phi_R^-) + H.c. \end{aligned} \tag{9.27}$$

These terms show explicitly that the assignments of Tables 9.1 and 9.2 are satisfied.

As for the exotic ψ and χ fermions, they have masses from the Yukawa terms of Eqs. (9.4) and (9.5), as well as

$$(\phi_{1R}^0\psi_{2R}^0 - \psi_{1R}^-\psi_{2R}^+)\sigma^*, \quad \chi_R^-\chi_R^+\sigma, \quad \chi_{1R}^0\chi_{2R}^0\sigma. \tag{9.28}$$

As a result, two neutral Dirac fermions are formed from the matrix linking χ_{1R}^0 and ψ_{1R}^0 to χ_{2R}^0 and ψ_{2R}^0. Let us call the lighter of these two Dirac fermions χ_0, then it is one component of dark matter of our model. The other will be the scalar ζ, to be discussed later. Note that χ_0 communicates with ζ through the allowed $\chi_{1R}^0\chi_{1R}^0\zeta$ interaction. Note also that the allowed Yukawa terms

$$\bar{d}_R h_L\zeta, \quad \bar{n}_L\nu_R\zeta \tag{9.29}$$

enable the dark fermions h and n to decay into ζ.

9.5 Scalar sector

Consider the most general scalar potential consisting of $\Phi_{L,R}$, η, and σ. Let

$$\eta = \begin{pmatrix} \eta_1^0 & \eta_2^+ \\ \eta_1^- & \eta_2^0 \end{pmatrix}, \quad \tilde{\eta} = \sigma_2\eta^*\sigma_2 = \begin{pmatrix} \bar{\eta}_2^0 & -\eta_1^+ \\ -\eta_2^- & \bar{\eta}_1^0 \end{pmatrix}, \tag{9.30}$$

then

$$
\begin{aligned}
V &= -\mu_L^2 \Phi_L^\dagger \Phi_L - \mu_R^2 \Phi_R^\dagger \Phi_R - \mu_\sigma^2 \sigma^* \sigma - \mu_\eta^2 Tr(\eta^\dagger \eta) + [\mu_3 \Phi_L^\dagger \eta \Phi_R + H.c.] \\
&+ \frac{1}{2}\lambda_L (\Phi_L^\dagger \Phi_L)^2 + \frac{1}{2}\lambda_R (\Phi_R^\dagger \Phi_R)^2 + \frac{1}{2}\lambda_\sigma (\sigma^* \sigma)^2 + \frac{1}{2}\lambda_\eta [Tr(\eta^\dagger \eta)]^2 + \frac{1}{2}\lambda'_\eta Tr(\eta^\dagger \eta \eta^\dagger \eta) \\
&+ \lambda_{LR} (\Phi_L^\dagger \Phi_L)(\Phi_R^\dagger \Phi_R) + \lambda_{L\sigma} (\Phi_L^\dagger \Phi_L)(\sigma^* \sigma) + \lambda_{R\sigma} (\Phi_R^\dagger \Phi_R)(\sigma^* \sigma) + \lambda_{\sigma\eta} (\sigma^* \sigma) Tr(\eta^\dagger \eta) \\
&+ \lambda_{L\eta} \Phi_L^\dagger \eta \eta^\dagger \Phi_L + \lambda'_{L\eta} \Phi_L^\dagger \tilde{\eta} \tilde{\eta}^\dagger \Phi_L + \lambda_{R\eta} \Phi_R^\dagger \eta^\dagger \eta \Phi_R + \lambda'_{R\eta} \Phi_R^\dagger \tilde{\eta}^\dagger \tilde{\eta} \Phi_R. \qquad (9.31)
\end{aligned}
$$

Note that

$$
\begin{aligned}
2|det(\eta)|^2 &= [Tr(\eta^\dagger \eta)]^2 - Tr(\eta^\dagger \eta \eta^\dagger \eta), \qquad (9.32) \\
(\Phi_L^\dagger \Phi_L) Tr(\eta^\dagger \eta) &= \Phi_L^\dagger \eta \eta^\dagger \Phi_L + \Phi_L^\dagger \tilde{\eta} \tilde{\eta}^\dagger \Phi_L, \qquad (9.33) \\
(\Phi_R^\dagger \Phi_R) Tr(\eta^\dagger \eta) &= \Phi_R^\dagger \eta^\dagger \eta \Phi_R + \Phi_R^\dagger \tilde{\eta}^\dagger \tilde{\eta} \Phi_L. \qquad (9.34)
\end{aligned}
$$

The minimum of V satisfies the conditions

$$
\begin{aligned}
\mu_L^2 &= \lambda_L v_1^2 + \lambda_{L\eta} v_2^2 + \lambda_{LR} v_R^2 + \lambda_{L\sigma} v_S^2 + \mu_3 v_2 v_R / v_1, \qquad (9.35) \\
\mu_\eta^2 &= (\lambda_\eta + \lambda'_\eta) v_2^2 + \lambda_{L\eta} v_1^2 + \lambda_{R\eta} v_R^2 + \lambda_{\sigma\eta} v_S^2 + \mu_3 v_1 v_R / v_2, \qquad (9.36) \\
\mu_R^2 &= \lambda_R v_R^2 + \lambda_{LR} v_1^2 + \lambda_{R\eta} v_2^2 + \lambda_{R\sigma} v_S^2 + \mu_3 v_1 v_2 / v_R, \qquad (9.37) \\
\mu_\sigma^2 &= \lambda_\sigma v_S^2 + \lambda_{L\sigma} v_1^2 + \lambda_{\sigma\eta} v_2^2 + \lambda_{R\sigma} v_R^2. \qquad (9.38)
\end{aligned}
$$

The 4×4 mass-squared matrix spanning $\sqrt{2} Im(\phi_L^0, \eta_2^0, \phi_R^0, \sigma)$ is then given by

$$
\mathcal{M}_I^2 = \mu_3 \begin{pmatrix}
-v_2 v_R / v_1 & v_R & v_2 & 0 \\
v_R & -v_1 v_R / v_2 & v_1 & 0 \\
v_2 & v_1 & -v_1 v_2 / v_R & 0 \\
0 & 0 & 0 & 0.
\end{pmatrix} \qquad (9.39)
$$

and that spanning $\sqrt{2}Re(\phi_L^0, \eta_2^0, \phi_R^0, \sigma)$ is

$$\mathcal{M}_R^2 = \mathcal{M}_I^2 + 2 \begin{pmatrix} \lambda_L v_1^2 & \lambda_{L\eta} v_1 v_2 & \lambda_{LR} v_1 v_R & \lambda_{L\sigma} v_1 v_S \\ \lambda_{L\eta} v_1 v_2 & (\lambda_\eta + \lambda'_\eta) v_2^2 & \lambda_{R\eta} v_2 v_R & \lambda_{\sigma\eta} v_2 v_S \\ \lambda_{LR} v_1 v_R & \lambda_{R\eta} v_2 v_R & \lambda_R v_R^2 & \lambda_{R\sigma} v_R v_S \\ \lambda_{L\sigma} v_1 v_S & \lambda_{\sigma\eta} v_2 v_S & \lambda_{R\sigma} v_R v_S & \lambda_\sigma v_S^2 \end{pmatrix}. \tag{9.40}$$

Hence, there are three zero eigenvalues in $\mathcal{M}_I^2$ with one nonzero eigenvalue $-\mu_3[v_1 v_2/v_R + v_R(v_1^2 + v_2^2)/v_1 v_2]$ corresponding to the eigenstate $(-v_1^{-1}, v_2^{-1}, v_R^{-1}, 0)/\sqrt{v_1^{-2} + v_2^{-2} + v_R^{-2}}$. In $\mathcal{M}_R^2$, the linear combination $H = (v_1, v_2, 0, 0)/\sqrt{v_1^2 + v_2^2}$, is the standard-model Higgs boson, with

$$m_H^2 = 2[\lambda_L v_1^4 + (\lambda_\eta + \lambda'_\eta) v_2^4 + 2\lambda_{L\eta} v_1^2 v_2^2]/(v_1^2 + v_2^2). \tag{9.41}$$

The other three scalar bosons are much heavier, with suppressed mixing to H, which may all be assumed to be small enough to avoid the constraints from dark-matter direct-search experiments. The addition of the scalar ζ introduces two important new terms:

$$\zeta^3 \sigma^*, \quad (\eta_1^0 \eta_2^0 - \eta_1^- \eta_2^+)\zeta. \tag{9.42}$$

The first term breaks global S' to Z_3, and the second term mixes ζ with η_1^0 through v_2. We assume the latter to be negligible, so that the physical dark scalar is mostly ζ.

9.6 Present phenomenological constraints

Many of the new particles of this model interact with those of the standard model. The most important ones are the neutral $D_{1,2}$ gauge bosons, which may be produced at the LHC through their couplings to u and d quarks, and decay to charged leptons ($e^- e^+$ and

$\mu^-\mu^+$). As noted previously, in our chosen example, D_1 is the lighter of the two. Hence current search limits for a Z' boson are applicable [152, 174]. The $c_{u,d}$ coefficients used in the data analysis are

$$c_u = (g_{uL}^2 + g_{uR}^2)B = 0.0273\ B, \quad c_d = (g_{dL}^2 + g_{dR}^2)B = 0.0068\ B, \tag{9.43}$$

where B is the branching fraction of Z' to e^-e^+ and $\mu^-\mu^+$. Assuming that D_1 decays to all the particles listed in Table 9.2, except for the scalars which become the longitudinal components of the various gauge bosons, we find $B = 1.2 \times 10^{-2}$. Based on the 2016 LHC 13 TeV data set, this translates to a bound of about 4 TeV on the D_1 mass.

The would-be dark-matter candidate n is a Dirac fermion which couples to $D_{1,2}$ which also couples to quarks. Hence severe limits exist on the masses of $D_{1,2}$ from underground direct-search experiments as well. The annihilation cross section of n through $D_{1,2}$ would then be too small, so that its relic abundance would be too big for it to be a dark-matter candidate. Its annihilation at rest through s-channel scalar exchange is p-wave suppressed and does not help. As for the t-channel diagrams, they also turn out to be too small. Previous studies where n is chosen as dark matter are now ruled out.

9.7 Dark sector

Dark matter is envisioned to have two components. One is a Dirac fermion χ_0 which is a mixture of the four neutral fermions of odd Z_2, and the other is a complex scalar boson which is mostly ζ. The annihilation $\chi_0\bar{\chi}_0 \to \zeta\zeta^*$ determines the relic abundance of χ_0, and the annihilation $\zeta\zeta^* \to HH$, where H is the standard-model Higgs boson, determines that of ζ. The direct $\zeta\zeta^*H$ coupling is assumed small to avoid the severe constraint in

direct-search experiments.

Let the interaction of ζ with χ_0 be $f_0 \zeta \chi_{0R} \chi_{0R} + H.c.$, then the annihilation cross section of $\chi_0 \bar{\chi}_0$ to $\zeta \zeta^*$ times relative velicity is given by

$$\langle \sigma \times v_{rel} \rangle_\chi = \frac{f_0^4}{4\pi m_{\chi_0}} \frac{(m_{\chi_0}^2 - m_\zeta^2)^{3/2}}{(2m_{\chi_o}^2 - m_\zeta^2)^2}. \tag{9.44}$$

Let the effective interaction strength of $\zeta \zeta^*$ with HH be λ_0, then the annihilation cross section of $\zeta \zeta^*$ to HH times relative velicity is given by

$$\langle \sigma_\zeta \times v_{rel} \rangle_\zeta = \frac{\lambda_0^2}{16\pi} \frac{(m_\zeta^2 - m_H^2)^{1/2}}{m_\zeta^3}. \tag{9.45}$$

Note that λ_0 is the sum over several interactions. The quartic coupling $\lambda_{\zeta H}$ is assumed negligible, to suppress the trilinear $\zeta \zeta^* H$ coupling which contributes to the elastic ζ scattering cross section off nuclei. However, the trilinear couplings $\zeta \zeta^* Re(\phi_R^0)$ and $Re(\phi_R^0) HH$ are proportional to v_R, and the trilinear couplings $\zeta \zeta^* Re(\sigma)$ and $Re(\sigma) HH$ are proportional to v_S. Hence their effective contributions to λ_0 are proportional to $v_R^2/m^2[\sqrt{2} Re(\phi_R^0)]$ and $v_S^2/m^2[\sqrt{2} Re(\sigma)]$, which are not suppressed.

As a rough estimate, we will assume that

$$\langle \sigma \times v_{rel} \rangle_\chi^{-1} + \langle \sigma_\zeta \times v_{rel} \rangle_\zeta^{-1} = (4.4 \times 10^{-26}\ cm^3/s)^{-1} \tag{9.46}$$

to satisfy the condition of dark-matter relic abundance [105] of the Universe. For given values of m_ζ and m_{χ_0}, the parameters λ_0 and f_0 are thus constrained. We show in Fig. 9.1 the plots of λ_0 versus f_0 for $m_\zeta = 150$ GeV and various values of m_{χ_0}. Since m_ζ is fixed at 150 GeV, λ_0 is also fixed for a given fraction of $\Omega_\zeta / \Omega_{DM}$. To adjust for the rest of dark matter, f_0 must then vary as a function of m_{χ_0} according to Eq. (9.44).

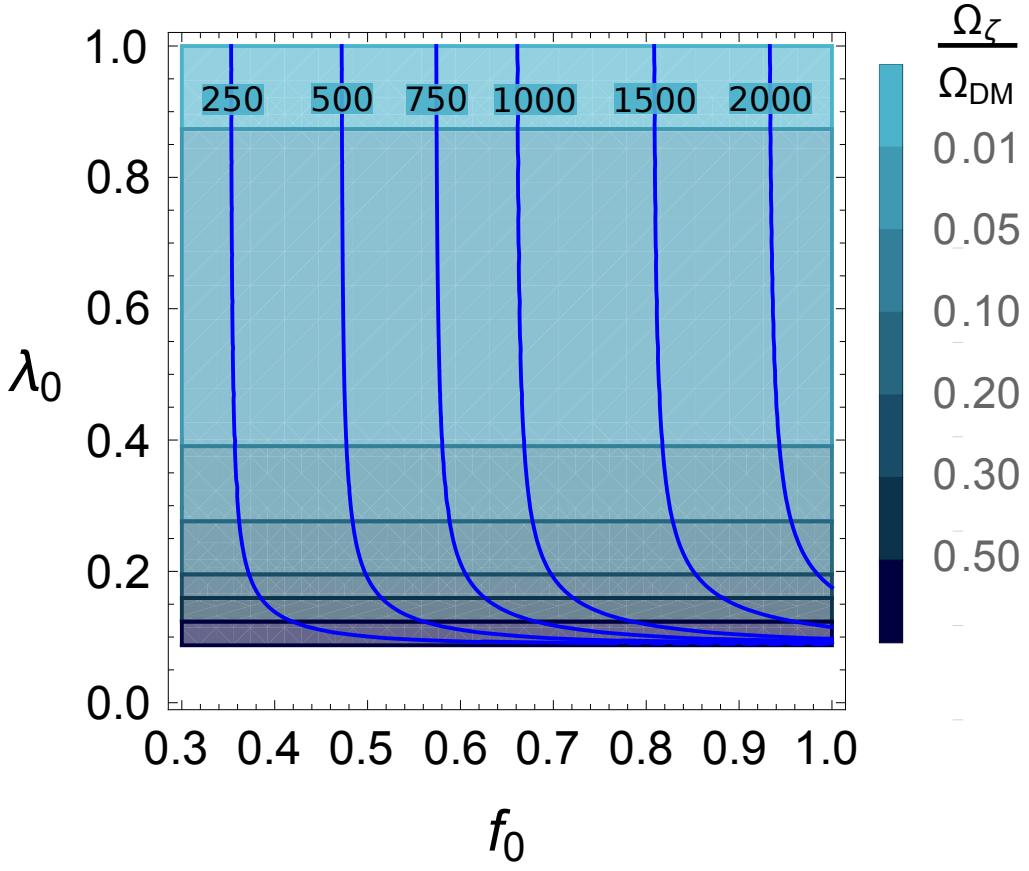

Figure 9.1: Relic-abundance constraints on λ_0 and f_0 for $m_\zeta = 150$ GeV and various values of m_{χ_0}.

As for direct detection, both χ_0 and ζ have possible interactions with quarks through the gauge bosons $D_{1,2}$ and the standard-model Higgs boson H. They are suppressed by making the $D_{1,2}$ masses heavy, and the H couplings to χ_0 and ζ small. In our example with $m_\zeta = 150$ GeV, let us choose $m_{\chi_0} = 500$ Gev and the relic abundances of both to be equal. From Fig. 9.1, these choices translate to $\lambda_0 = 0.12$ and $f_0 = 0.56$.

Consider first the $D_{1,2}$ interactions. Using Eq. (9.26), we obtain

$$g_u^V(D_1) = 0.0621, \quad g_d^V(D_1) = 0.0184, \quad g_\zeta(D_1) = 0.1234, \tag{9.47}$$

$$g_u^V(D_2) = -0.1235, \quad g_d^V(D_2) = -0.0062, \quad g_\zeta(D_2) = 0.3701. \tag{9.48}$$

The effective ζ elastic scattering cross section through $D_{1,2}$ is then completely determined as a function of the D_1 mass (because $M_{D_2} = \sqrt{3} M_{D_1}$ in our example), i.e.

$$\mathcal{L}_{\zeta q}^V = \frac{(\zeta^* \partial_\mu - \zeta \partial_\mu \zeta^*)}{M_{D_1}^2} [(-7.57 \times 10^{-3}) \bar{u} \gamma^\mu u + (1.51 \times 10^{-3}) \bar{d} \gamma^\mu d]. \tag{9.49}$$

Using the latest LUX result [87] and and Eq. (9.25), we obtain $v_R > 35$ TeV which translates to $M_{D_1} > 18$ TeV.

The $\bar{\chi}_0 \gamma_\mu \chi_0$ couplings to $D_{1,2}$ depend on the 2×2 mass matrix linking (χ_1, ψ_1) to (χ_2, ψ_2) which has two mixing angles and two mass eigenvalues, the lighter one being m_{χ_0}. By adjusting these parameters, it is possible to make the effective χ_0 interaction with xenon negligibly small. Hence there is no useful limit on the D_1 mass in this case.

Direct search also constrains the coupling of the Higgs boson to ζ (through a possible trilinear $\lambda_{\zeta H} \sqrt{2} v_H \zeta^* \zeta$ interaction) or χ_0 (through an effective Yukawa coupling ϵ from H mixing with σ_R and ϕ_R^0). Let their effective interactions with quarks through H exchange be given by

$$\mathcal{L}_{\zeta q}^S = \frac{\lambda_{\zeta H} m_q}{m_H^2} \zeta^* \zeta \bar{q} q + \frac{\epsilon f_q}{m_H^2} \bar{\chi}_0 \chi_0 \bar{q} q, \tag{9.50}$$

where $f_q = m_q / \sqrt{2} v_H = m_q / (246 \text{ GeV})$. The spin-independent direct-detection cross section per nucleon in the former is given by

$$\sigma^{SI} = \frac{\mu_\zeta^2}{\pi A^2} [\lambda_p Z + (A - Z) \lambda_n]^2, \tag{9.51}$$

where $\mu_\zeta = m_\zeta M_A/(m_\zeta + M_A)$ is the reduced mass of the dark matter, and [156]

$$\lambda_N = \left[\sum_{u,d,s} f_q^N + \frac{2}{27}\left(1 - \sum_{u,d,s} f_q^N\right)\right] \frac{\lambda_{\zeta H} m_N}{2 m_\zeta m_H^2}, \tag{9.52}$$

with [157]

$$f_u^p = 0.023, \quad f_d^p = 0.032, \quad f_s^p = 0.020, \tag{9.53}$$

$$f_u^n = 0.017, \quad f_d^n = 0.041, \quad f_s^n = 0.020. \tag{9.54}$$

For $m_\zeta = 150$ GeV, we have

$$\lambda_p = 2.87 \times 10^{-8} \lambda_{\zeta H} \text{ GeV}^{-2}, \quad \lambda_n = 2.93 \times 10^{-8} \lambda_{\zeta H} \text{ GeV}^{-2}. \tag{9.55}$$

Using $A = 131$, $Z = 54$, and $M_A = 130.9$ atomic mass units for the LUX experiment [87], , and twice the bound of 2×10^{-46} cm^2 (because ζ is assumed to account for only half of the dark matter) at this mass, we find

$$\lambda_{\zeta H} < 9.1 \times 10^{-4}. \tag{9.56}$$

As noted earlier, this is negligible for considering the annihilation cross section of ζ to H.

For the H contribution to the χ_0 elastic cross section off nuclei, we replace m_ζ with $m_{\chi_0} = 500$ GeV in Eq. (9.51) and $\lambda_{\zeta H}/2m_\zeta$ with $\epsilon/\sqrt{2}v_H$ in Eq. (9.52). Using the experimental data at 500 GeV, we obtain the bound.

$$\epsilon < 9.6 \times 10^{-4}. \tag{9.57}$$

From the above discussion, it is clear that our model allows for the discovery of dark matter in direct-search experiments in the future if these bounds are only a little above the actual values of $\lambda_{\zeta H}$ and ϵ.

9.8 Conclusion and outlook

In the context of the alternative left-right model, a new gauge $U(1)_S$ symmetry has been proposed to stabilize dark matter. This is accomplished by the addition of a few new fermions to cancel all the gauge anomalies, as shown in Table 9.1. As a result of this particle content, an automatic unbroken Z_2 symmetry exists on top of $U(1)_S$ which is broken to a conserved residual Z_3 symmetry. Thus dark matter has two components. One is the Dirac fermion $\chi_0 \sim (\omega, -)$ and the other the complex scalar $\zeta \sim (\omega, +)$ under $Z_3 \times Z_2$. We have shown how they may account for the relic abundance of dark matter in the Universe, and satisfy present experimental search bounds.

Whereas we have no specific prediction for discovery in direct-search experiments, our model will be able to accommodate any positive result in the future, just like many other existing proposals. To single out our model, many additional details must also be confirmed. Foremost are the new gauge bosons $D_{1,2}$. Whereas the LHC bound is about 4 TeV, the direct-search bound is much higher provided that ζ is a significant fraction of dark matter. If χ_0 dominates instead, the adjustment of free parameters of our model can lower this bound to below 4 TeV. In that case, future $D_{1,2}$ observations are still possible at the LHC as more data become available.

Another is the exotic h quark which is easily produced if kinematically allowed. It would decay to d and ζ through the direct $\bar{d}_R h_L \zeta$ coupling of Eq. (9.29). Assuming that this branching fraction is 100%, the search at the LHC for 2 jets plus missing energy puts a limit on m_h of about 1.0 TeV, as reported by the CMS Collaboration [200] based on the $\sqrt{s} = 13$ TeV data at the LHC with an integrated luminosity of 35.9 fb^{-1} for a single scalar

quark.

If the $\bar{d}_R h_L \zeta$ coupling is very small, then h may also decay significantly to u and a virtual W_R^-, with W_R^- becoming $\bar{n} l^-$, and $\bar{n}$ becoming $\bar{\nu}\zeta^*$. This has no analog in the usual searches for supersymmetry or the fourth family because W_R is heavy (> 16 TeV). To be specific, the final states of 2 jets plus $l_1^- l_2^+$ plus missing energy should be searched for. As more data are accumulated at the LHC, such events may become observable.

Chapter 10

Conclusions

Various extensions of the Standard Model were presented in this thesis, to accommodate the neutrino mass and dark matter. A brief review of these models follows.

In the second chapter, we introduced a vector dark matter based on $\mathrm{SU}(2)_N$, under which all of the Standard Model particles are singlet. A small Majorana neutrino mass is generated via inverse seesaw mechanism. The scalar sector of this model may also allow a stable second component of dark matter.

We then considered a gauge B$-$L extension of the Standard Model, which is spontaneously broken to $\mathbb{Z}_3$ lepton number. Neutrinos are Dirac fermions. A complex neutral scalar (χ_2) is the dark matter candidate. It is not absolutely stable, and it decays to two antineutrinos with a lifetime much greater than that of the Universe. It is impossible to discover Z' at the LHC with the current run, because of the stringent constraint on m'_Z/g'

from direct-search experiments.

The next model which was introduced in chapter four, is a scotogenic model of radiative neutrino and charged lepton masses. We studied anomalous Higgs couplings with possible large deviations from the Standard Model predictions. We showed that the observed discrepancy in the muon anomalous magnetic moment may be explained by new particles in this model. We also checked the bounds from the lepton flavor violating processes, such as $\mu \to e\gamma$ and $\mu \to eee$.

In chapter five, a gauge $U(1)_X$ extension of the supersymmetric Standard Model was presented to solve the μ-problem of the MSSM. In this model, we replaced the μ term with a singlet scalar superfield which also couples to heavy color-triplet superfields. These electroweak singlets were necessary for the cancellation of axial-vector anomalies. Therefore, they were perfect ingredients for accommodating the 750 GeV diphoton excess which was observed in 2015[1]. An important product of our study is the discovery of relaxed supersymmetric constraints on the Higgs boson's mass, which depends on the $U(1)_X$ gauge coupling and it's free of the tension encountered in the MSSM.

One way to resolve the small structure issues of the cold dark matter models is to have a mixed[2] dark matter. Chapter six contains a B−L gauge extension of the standard model, where a light sterile neutrino and cold dark matter candidates are naturally

[1] It was absent in the more recent analysis.
[2] A mixture of cold and warm dark matter.

generated. Neutrino masses were generated in one loop through the dark matter, i.e., the scotogenic mechanism, while the keV sterile neutrino obtains its mass by seesaw mechanism. It was shown that we can have up to four dark matter candidates assuming an extra $\mathbb{Z}_2$ symmetry. Three are stable cold Weakly Interaction Massive Particles (WIMP), and one a keV singlet neutrino with a very long life-time.

In chapter seven, another gauge extension of the standard model with new charge assignments to leptons and quarks was introduced. This model offered some insights to the structure of mixing among quark and lepton families, together with their possible verification at the Large Hadron Collider. Meson-anitmeson oscillations data was used to constrain the parameters of our model. A Majorana neutrino mass matrix of two texture zeros may be obtained in this model, which leads to a best-fit of neutrino oscillation data with normal ordering of neutrino masses.

The low energy phenomenology of the Babu-Ma-Willenbrock (BMW) model was studied in chapter eight. The gauge symmetry of this model is based on $[\mathrm{SU}(3)]^4$, which breaks down to the usual Standard Model gauge symmetry and an unbroken $\mathrm{SU}(2)_l$ (leptonic color) gauge symmetry. This model has gauge-coupling unification without supersymmetry. This required the addition of new half-charged fermions (hemions) under the $\mathrm{SU}(2)_l$ leptonic color symmetry. Also, we saw that their masses have to be below the TeV scale. The $\mathrm{SU}(2)_l$ symmetry becomes confining at M scale, such that stickball bound states of the vector gauge stickons are formed. Note that these new particles have no QCD interactions,

but hemions can interact electroweakly. Therefore, hemions are accessible in a future e^-e^+ collider.

Finally, an alternative left-right model was presented, with a new gauge $\mathrm{U}(1)_S$ symmetry which stabilizes the dark matter candidate. A few new fermions were added to cancel all the gauge anomalies. An automatic unbroken $\mathbb{Z}_2$ symmetry exists on top of $\mathrm{U}(1)_S$ which is broken to a residual $\mathbb{Z}_3$ symmetry. Therefore, dark matter has two components, a Dirac fermion (χ_0) and one complex scalar (ξ). It was shown how they can account for the relic abundance of dark matter in the Universe, and satisfy the present experimental search bounds.

Bibliography

[1] S. Fraser, E. Ma, and M. Zakeri, "$SU(2)_N$ model of vector dark matter with a leptonic connection," *Int. J. Mod. Phys.* **A30** no. 03, (2015) 1550018, arXiv:1409.1162 [hep-ph].

[2] S. Fraser, E. Ma, and M. Zakeri, "Verifiable Associated Processes from Radiative Lepton Masses with Dark Matter," *Phys. Rev.* **D93** no. 11, (2016) 115019, arXiv:1511.07458 [hep-ph].

[3] S. Fraser, C. Kownacki, E. Ma, N. Pollard, O. Popov, and M. Zakeri, "Phenomenology of the Utilitarian Supersymmetric Standard Model," *Nucl. Phys.* **B909** (2016) 644–656, arXiv:1603.04778 [hep-ph].

[4] E. Ma, N. Pollard, R. Srivastava, and M. Zakeri, "Gauge $B-L$ Model with Residual Z_3 Symmetry," *Phys. Lett.* **B750** (2015) 135–138, arXiv:1507.03943 [hep-ph].

[5] E. Ma, N. Pollard, O. Popov, and M. Zakeri, "Gauge $B-L$ model of radiative neutrino mass with multipartite dark matter," *Mod. Phys. Lett.* **A31** no. 27, (2016) 1650163, arXiv:1605.00991 [hep-ph].

[6] C. Kownacki, E. Ma, N. Pollard, and M. Zakeri, "Generalized Gauge U(1) Family Symmetry for Quarks and Leptons," *Phys. Lett.* **B766** (2017) 149–152, arXiv:1611.05017 [hep-ph].

[7] C. Kownacki, E. Ma, N. Pollard, O. Popov, and M. Zakeri, "Quartified leptonic color, bound states, and future electronpositron collider," *Phys. Lett.* **B769** (2017) 267–271, arXiv:1701.07043 [hep-ph].

[8] C. Kownacki, E. Ma, N. Pollard, O. Popov, and M. Zakeri, "Dark Gauge U(1) Symmetry for an Alternative Left-Right Model," arXiv:1706.06501 [hep-ph].

[9] H. Becquerel, "On the rays emitted by phosphorescence," *Compt. Rend. Hebd. Seances Acad. Sci.* **122** no. 8, (1896) 420–421.

[10] W. Pauli, "Dear radioactive ladies and gentlemen," *Phys. Today* **31N9** (1978) 27.

[11] E. Fermi, "Tentativo di una teoria dell'emissione dei raggi beta," *Ric. Sci.* **4** (1933) 491–495.

[12] P. A. M. Dirac, "Quantum theory of emission and absorption of radiation," *Proc. Roy. Soc. Lond.* **A114** (1927) 243.

[13] F. Bloch and A. Nordsieck, "Note on the radiation field of the electron," *Phys. Rev.* **52** (Jul, 1937) 54–59. https://link.aps.org/doi/10.1103/PhysRev.52.54.

[14] V. F. Weisskopf, "On the self-energy and the electromagnetic field of the electron," *Phys. Rev.* **56** (Jul, 1939) 72–85. https://link.aps.org/doi/10.1103/PhysRev.56.72.

[15] W. E. Lamb and R. C. Retherford, "Fine structure of the hydrogen atom by a microwave method," *Phys. Rev.* **72** (Aug, 1947) 241–243. https://link.aps.org/doi/10.1103/PhysRev.72.241.

[16] H. A. Bethe, "The electromagnetic shift of energy levels," *Phys. Rev.* **72** (Aug, 1947) 339–341. https://link.aps.org/doi/10.1103/PhysRev.72.339.

[17] S. Tomonaga, "On a relativistically invariant formulation of the quantum theory of wave fields," *Progress of Theoretical Physics* **1** no. 2, (1946) 27. http://dx.doi.org/10.1143/PTP.1.27.

[18] J. Schwinger, "On quantum-electrodynamics and the magnetic moment of the electron," *Phys. Rev.* **73** (Feb, 1948) 416–417. https://link.aps.org/doi/10.1103/PhysRev.73.416.

[19] J. Schwinger, "Quantum electrodynamics. i. a covariant formulation," *Phys. Rev.* **74** (Nov, 1948) 1439–1461. https://link.aps.org/doi/10.1103/PhysRev.74.1439.

[20] R. P. Feynman, "Space-time approach to quantum electrodynamics," *Phys. Rev.* **76** (Sep, 1949) 769–789. https://link.aps.org/doi/10.1103/PhysRev.76.769.

[21] R. P. Feynman, "The theory of positrons," *Phys. Rev.* **76** (Sep, 1949) 749–759. https://link.aps.org/doi/10.1103/PhysRev.76.749.

[22] R. P. Feynman, "Mathematical formulation of the quantum theory of electromagnetic interaction," *Phys. Rev.* **80** (Nov, 1950) 440–457. https://link.aps.org/doi/10.1103/PhysRev.80.440.

[23] F. J. Dyson, "The radiation theories of tomonaga, schwinger, and feynman," *Phys. Rev.* **75** (Feb, 1949) 486–502. https://link.aps.org/doi/10.1103/PhysRev.75.486.

[24] F. J. Dyson, "The s matrix in quantum electrodynamics," *Phys. Rev.* **75** (Jun, 1949) 1736–1755. https://link.aps.org/doi/10.1103/PhysRev.75.1736.

[25] G. 't Hooft, "Renormalizable Lagrangians for Massive Yang-Mills Fields," *Nucl. Phys.* **B35** (1971) 167–188.

[26] G. 't Hooft, "Renormalization of Massless Yang-Mills Fields," *Nucl. Phys.* **B33** (1971) 173–199.

[27] G. 't Hooft and M. J. G. Veltman, "Regularization and Renormalization of Gauge Fields," *Nucl. Phys.* **B44** (1972) 189–213.

[28] D. A. Glaser, "Some effects of ionizing radiation on the formation of bubbles in liquids," *Phys. Rev.* **87** (Aug, 1952) 665–665. https://link.aps.org/doi/10.1103/PhysRev.87.665.

[29] M. Gell-Mann, *THE EIGHTFOLD WAY: A THEORY OF STRONG INTERACTION SYMMETRY*. Mar, 1961. http://www.osti.gov/scitech/servlets/purl/4008239.

[30] V. E. Barnes, P. L. Connolly, D. J. Crennell, B. B. Culwick, W. C. Delaney, W. B. Fowler, P. E. Hagerty, E. L. Hart, N. Horwitz, P. V. C. Hough, J. E. Jensen, J. K. Kopp, K. W. Lai, J. Leitner, J. L. Lloyd, G. W. London, T. W. Morris, Y. Oren, R. B. Palmer, A. G. Prodell, D. Radojičić, D. C. Rahm, C. R. Richardson, N. P. Samios, J. R. Sanford, R. P. Shutt, J. R. Smith, D. L. Stonehill, R. C. Strand, A. M. Thorndike, M. S. Webster, W. J. Willis, and S. S. Yamamoto, "Observation of a hyperon with strangeness minus three," *Phys. Rev. Lett.* **12** (Feb, 1964) 204–206. https://link.aps.org/doi/10.1103/PhysRevLett.12.204.

[31] Y. Ne'eman, "Derivation of strong interactions from a gauge invariance," *Nuclear Physics* **26** no. 2, (1961) 222 – 229. http://www.sciencedirect.com/science/article/pii/0029558261901341.

[32] M. Gell-Mann, "A schematic model of baryons and mesons," *Physics Letters* **8** no. 3, (1964) 214 – 215. http://www.sciencedirect.com/science/article/pii/S0031916364920013.

[33] G. Zweig, "An su(3) model for strong interaction symmetry and its breaking; version 2,". http://cds.cern.ch/record/570209. Version 1 is CERN preprint 8182/TH.401, Jan. 17, 1964.

[34] G. Zweig, "An su(3) model for strong interaction symmetry and its breaking,". http://cds.cern.ch/record/352337/files/CERN-TH-401.pdf. CERN Report No.8182/TH.401.

[35] O. W. Greenberg, "Spin and unitary-spin independence in a paraquark model of baryons and mesons," *Phys. Rev. Lett.* **13** (Nov, 1964) 598–602. https://link.aps.org/doi/10.1103/PhysRevLett.13.598.

[36] M. Y. Han and Y. Nambu, "Three-triplet model with double SU(3) symmetry," *Phys. Rev.* **139** (Aug, 1965) B1006–B1010. https://link.aps.org/doi/10.1103/PhysRev.139.B1006.

[37] B. Struminsky, "Magnetic moments of baryons in the quark model (in russian)," *JINR* (1965) 1939.

[38] B. S. N.N. Bogolyubov and A. Tavkhelidze, "On the composite models in theories of elementary particles," *JINR* (1965) 1968.

[39] R. P. Feynman, "The behavior of hadron collisions at extreme energies," *Conf. Proc.* **C690905** (1969) 237–258.

[40] J. D. Bjorken, "Asymptotic sum rules at infinite momentum," *Phys. Rev.* **179** (Mar, 1969) 1547–1553. https://link.aps.org/doi/10.1103/PhysRev.179.1547.

[41] J. I. Friedman and H. W. Kendall, "Deep inelastic electron scattering," *Annu. Rev. Nucl. Sci.* **22** (Dec, 1972) 203–254. https://doi.org/10.1146/annurev.ns.22.120172.001223.

[42] S. L. Glashow, "Partial Symmetries of Weak Interactions," *Nucl. Phys.* **22** (1961) 579–588.

[43] A. Salam, "Weak and Electromagnetic Interactions," *Conf. Proc.* **C680519** (1968) 367–377.

[44] S. Weinberg, "A model of leptons," *Phys. Rev. Lett.* **19** (Nov, 1967) 1264–1266. https://link.aps.org/doi/10.1103/PhysRevLett.19.1264.

[45] S. Weinberg, *The quantum theory of fields. Vol. 2: Modern applications*. Cambridge University Press, 2013.

[46] F. Englert and R. Brout, "Broken symmetry and the mass of gauge vector mesons," *Phys. Rev. Lett.* **13** (Aug, 1964) 321–323. https://link.aps.org/doi/10.1103/PhysRevLett.13.321.

[47] G. S. Guralnik, C. R. Hagen, and T. W. B. Kibble, "Global conservation laws and massless particles," *Phys. Rev. Lett.* **13** (Nov, 1964) 585–587. https://link.aps.org/doi/10.1103/PhysRevLett.13.585.

[48] P. W. Higgs, "Broken symmetries and the masses of gauge bosons," *Phys. Rev. Lett.* **13** (Oct, 1964) 508–509. https://link.aps.org/doi/10.1103/PhysRevLett.13.508.

[49] **ATLAS** Collaboration, G. Aad *et al.*, "Observation of a new particle in the search for the Standard Model Higgs boson with the ATLAS detector at the LHC," *Phys. Lett.* **B716** (2012) 1–29, arXiv:1207.7214 [hep-ex].

[50] **CMS** Collaboration, S. Chatrchyan *et al.*, "Observation of a new boson at a mass of 125 GeV with the CMS experiment at the LHC," *Phys. Lett.* **B716** (2012) 30–61, arXiv:1207.7235 [hep-ex].

[51] B. Pontecorvo, "Mesonium and anti-mesonium," *Zh. Eksp. Teor. Fiz.* **33** (Feb, 1957) 549551. http://www.jetp.ac.ru/cgi-bin/dn/e_006_02_0429.pdf.

[52] Z. Maki, M. Nakagawa, and S. Sakata, "Remarks on the unified model of elementary particles," *Progress of Theoretical Physics* **28** no. 5, (1962) 870. http://dx.doi.org/10.1143/PTP.28.870.

[53] **Particle Data Group** Collaboration, J. Beringer *et al.*, "Review of Particle Physics (RPP)," *Phys. Rev.* **D86** (2012) 010001.

[54] F. Capozzi, E. Lisi, A. Marrone, D. Montanino, and A. Palazzo, "Neutrino masses and mixings: Status of known and unknown 3ν parameters," *Nucl. Phys.* **B908** (2016) 218–234, arXiv:1601.07777 [hep-ph].

[55] P. Krastev and S. Petcov, "Resonance amplification and t-violation effects in three-neutrino oscillations in the earth," *Physics Letters B* **205** no. 1, (1988) 84 – 92. http://www.sciencedirect.com/science/article/pii/0370269388904042.

[56] S. Bilenky, J. Hoek, and S. Petcov, "On the oscillations of neutrinos with dirac and majorana masses," *Physics Letters B* **94** no. 4, (1980) 495 – 498. http://www.sciencedirect.com/science/article/pii/0370269380909272.

[57] P. Langacker, S. Petcov, G. Steigman, and S. Toshev, "Implications of the mikheyev-smirnov-wolfenstein (msw) mechanism of amplification of neutrino oscillations in matter," *Nuclear Physics B* **282** (1987) 589 – 609. http://www.sciencedirect.com/science/article/pii/0550321387906997.

[58] S. P. K. Nakamura, "Neutrino Mass, Mixing, and Oscillations," (2016) . http://pdg.ihep.su/2017/reviews/rpp2016-rev-neutrino-mixing.pdf.

[59] S. Weinberg, "Baryon- and lepton-nonconserving processes," *Phys. Rev. Lett.* **43** (Nov, 1979) 1566–1570. https://link.aps.org/doi/10.1103/PhysRevLett.43.1566.

[60] M. Gell-Mann, P. Ramond, and R. Slansky, "Complex Spinors and Unified Theories," *Conf. Proc.* **C790927** (1979) 315–321, arXiv:1306.4669 [hep-th].

[61] T. Yanagida, "HORIZONTAL SYMMETRY AND MASSES OF NEUTRINOS," *Conf. Proc.* **C7902131** (1979) 95–99.

[62] E. Ma, "Pathways to naturally small neutrino masses," *Phys. Rev. Lett.* **81** (1998) 1171–1174, arXiv:hep-ph/9805219 [hep-ph].

[63] E. Ma and U. Sarkar, "Neutrino masses and leptogenesis with heavy Higgs triplets," *Phys. Rev. Lett.* **80** (1998) 5716–5719, arXiv:hep-ph/9802445 [hep-ph].

[64] R. Foot, H. Lew, X. G. He, and G. C. Joshi, "See-saw neutrino masses induced by a triplet of leptons," *Zeitschrift für Physik C Particles and Fields* **44** no. 3, (Sep, 1989) 441–444. http://dx.doi.org/10.1007/BF01415558.

[65] K. S. Babu and E. Ma, "Radiative Mechanisms for Generating Quark and Lepton Masses: Some Recent Developments," *Mod. Phys. Lett.* **A4** (1989) 1975.

[66] E. Ma, "Verifiable radiative seesaw mechanism of neutrino mass and dark matter," *Phys. Rev.* **D73** (2006) 077301, arXiv:hep-ph/0601225 [hep-ph].

[67] G. Bertone and D. Hooper, "A History of Dark Matter," *Submitted to: Rev. Mod. Phys.* (2016) , arXiv:1605.04909 [astro-ph.CO].

[68] H. Poincare, 1906.

[69] H. Poincare, 1906.

[70] H. Poincare and H. Vergne, 1911.

[71] B. Kelvin, William Thomson, *Baltimore lectures on molecular dynamics and the wave theory of light*. London : C. J. Clay and sons; Baltimore, Publication agency of the Johns Hopkins university, 1904.

[72] F. Zwicky, "Die Rotverschiebung von extragalaktischen Nebeln," *Helvetica Physica Acta* **6** (1933) 110–127.

[73] F. Zwicky, "On the Masses of Nebulae and of Clusters of Nebulae," *Astrophys. J.* **86** (Oct., 1937) 217.

[74] W. J. G. de Blok, S. S. McGaugh, A. Bosma, and V. C. Rubin, "Mass density profiles of LSB galaxies," *Astrophys. J.* **552** (2001) L23–L26, arXiv:astro-ph/0103102 [astro-ph].

[75] P. Salucci and A. Borriello, "The intriguing distribution of dark matter in galaxies," *Lect. Notes Phys.* **616** (2003) 66–77, arXiv:astro-ph/0203457 [astro-ph].

[76] D. Reed, F. Governato, L. Verde, J. Gardner, T. R. Quinn, J. Stadel, D. Merritt, and G. Lake, "Evolution of the density profiles of dark matter halos," *Mon. Not. Roy. Astron. Soc.* **357** (2005) 82–96, arXiv:astro-ph/0312544 [astro-ph].

[77] L. V. E. Koopmans and T. Treu, "The structure and dynamics of luminous and dark matter in the early-type lens galaxy of 0047-281 at z=0.485," *Astrophys. J.* **583** (2003) 606–615, arXiv:astro-ph/0205281 [astro-ph].

[78] R. B. Metcalf, L. A. Moustakas, A. J. Bunker, and I. R. Parry, "Spectroscopic gravitational lensing and limits on the dark matter substructure in Q2237+0305," *Astrophys. J.* **607** (2004) 43–59, arXiv:astro-ph/0309738 [astro-ph].

[79] H. Hoekstra, H. Yee, and M. Gladders, "Current status of weak gravitational lensing," *New Astron. Rev.* **46** (2002) 767–781, arXiv:astro-ph/0205205 [astro-ph].

[80] L. A. Moustakas and R. B. Metcalf, "Detecting dark matter substructure spectroscopically in strong gravitational lenses," *Mon. Not. Roy. Astron. Soc.* **339** (2003) 607, arXiv:astro-ph/0206176 [astro-ph].

[81] **Planck** Collaboration, P. A. R. Ade *et al.*, "Planck 2015 results. XIII. Cosmological parameters," *Astron. Astrophys.* **594** (2016) A13, arXiv:1502.01589 [astro-ph.CO].

[82] C. L. Bennett, D. Larson, J. L. Weiland, N. Jarosik, G. Hinshaw, N. Odegard, K. M. Smith, R. S. Hill, B. Gold, M. Halpern, E. Komatsu, M. R. Nolta, L. Page, D. N. Spergel, E. Wollack, J. Dunkley, A. Kogut, M. Limon, S. S. Meyer, G. S. Tucker, and E. L. Wright, "Nine-year wilkinson microwave anisotropy probe (wmap) observations: Final maps and results," *The Astrophysical Journal Supplement Series* **208** no. 2, (2013) 20. http://stacks.iop.org/0067-0049/208/i=2/a=20.

[83] S. S. Vogt, M. Mateo, E. W. Olszewski, and M. J. Keane, "Internal kinematics of the Leo II dwarf spherodial galaxy," *Astrophys. J.* **109** (Jan., 1995) 151–163.

[84] M. Mateo, "Dwarf galaxies of the Local Group," *Ann. Rev. Astron. Astrophys.* **36** (1998) 435–506, arXiv:astro-ph/9810070 [astro-ph].

[85] W. Hu, R. Barkana, and A. Gruzinov, "Cold and fuzzy dark matter," *Phys. Rev. Lett.* **85** (2000) 1158–1161, arXiv:astro-ph/0003365 [astro-ph].

[86] E. W. Kolb, D. J. H. Chung, and A. Riotto, "WIMPzillas!," in *Trends in theoretical physics II. Proceedings, 2nd La Plata Meeting, Buenos Aires, Argentina, November 29-December 4, 1998*, pp. 91–105. 1998. arXiv:hep-ph/9810361 [hep-ph]. http://lss.fnal.gov/cgi-bin/find_paper.pl?conf-98-325. [,91(1998)].

[87] **LUX Collaboration** Collaboration, D. S. Akerib, S. Alsum, H. M. Araújo, X. Bai, A. J. Bailey, J. Balajthy, P. Beltrame, E. P. Bernard, A. Bernstein, T. P. Biesiadzinski, E. M. Boulton, R. Bramante, P. Brás, D. Byram, S. B. Cahn, M. C. Carmona-Benitez, C. Chan, A. A. Chiller, C. Chiller, A. Currie, J. E. Cutter, T. J. R. Davison, A. Dobi, J. E. Y. Dobson, E. Druszkiewicz, B. N. Edwards, C. H. Faham, S. Fiorucci, R. J. Gaitskell, V. M. Gehman, C. Ghag, K. R. Gibson, M. G. D. Gilchriese, C. R. Hall, M. Hanhardt, S. J. Haselschwardt, S. A. Hertel, D. P. Hogan, M. Horn, D. Q. Huang, C. M. Ignarra, M. Ihm, R. G. Jacobsen, W. Ji, K. Kamdin, K. Kazkaz, D. Khaitan, R. Knoche, N. A. Larsen, C. Lee, B. G. Lenardo, K. T. Lesko, A. Lindote, M. I. Lopes, A. Manalaysay, R. L. Mannino, M. F. Marzioni, D. N. McKinsey, D.-M. Mei, J. Mock, M. Moongweluwan, J. A. Morad, A. S. J. Murphy, C. Nehrkorn, H. N. Nelson, F. Neves, K. O'Sullivan, K. C. Oliver-Mallory, K. J. Palladino, E. K. Pease, P. Phelps, L. Reichhart, C. Rhyne, S. Shaw, T. A. Shutt, C. Silva, M. Solmaz, V. N. Solovov, P. Sorensen, S. Stephenson, T. J. Sumner, M. Szydagis, D. J. Taylor, W. C. Taylor, B. P. Tennyson, P. A. Terman, D. R. Tiedt, W. H. To, M. Tripathi, L. Tvrznikova, S. Uvarov, J. R. Verbus, R. C. Webb, J. T. White, T. J. Whitis, M. S. Witherell, F. L. H. Wolfs, J. Xu, K. Yazdani, S. K. Young, and C. Zhang, "Results from a search for dark matter in the complete lux exposure," *Phys. Rev. Lett.* **118** (Jan, 2017) 021303. https://link.aps.org/doi/10.1103/PhysRevLett.118.021303.

[88] **PandaX-II** Collaboration, A. Tan *et al.*, "Dark Matter Results from First 98.7 Days of Data from the PandaX-II Experiment," *Phys. Rev. Lett.* **117** no. 12, (2016) 121303, arXiv:1607.07400 [hep-ex].

[89] **SuperCDMS** Collaboration, R. Agnese *et al.*, "Search for Low-Mass Weakly Interacting Massive Particles with SuperCDMS," *Phys. Rev. Lett.* **112** no. 24, (2014) 241302, arXiv:1402.7137 [hep-ex].

[90] **XENON** Collaboration, E. Aprile *et al.*, "First Dark Matter Search Results from the XENON1T Experiment," arXiv:1705.06655 [astro-ph.CO].

[91] J. L. Feng and J. Kumar, "The WIMPless Miracle: Dark-Matter Particles without Weak-Scale Masses or Weak Interactions," *Phys. Rev. Lett.* **101** (2008) 231301, arXiv:0803.4196 [hep-ph].

[92] Q.-H. Cao, E. Ma, J. Wudka, and C. P. Yuan, "Multipartite dark matter," arXiv:0711.3881 [hep-ph].

[93] G. Servant and T. M. P. Tait, "Is the lightest Kaluza-Klein particle a viable dark matter candidate?," *Nucl. Phys.* **B650** (2003) 391–419, arXiv:hep-ph/0206071 [hep-ph].

[94] J. Hubisz and P. Meade, "Phenomenology of the littlest Higgs with T-parity," *Phys. Rev.* **D71** (2005) 035016, arXiv:hep-ph/0411264 [hep-ph].

[95] T. Hambye, "Hidden vector dark matter," *JHEP* **01** (2009) 028, arXiv:0811.0172 [hep-ph].

[96] J. L. Diaz-Cruz and E. Ma, "Neutral SU(2) Gauge Extension of the Standard Model and a Vector-Boson Dark-Matter Candidate," *Phys. Lett.* **B695** (2011) 264–267, arXiv:1007.2631 [hep-ph].

[97] S. Bhattacharya, J. L. Diaz-Cruz, E. Ma, and D. Wegman, "Dark Vector-Gauge-Boson Model," *Phys. Rev.* **D85** (2012) 055008, arXiv:1107.2093 [hep-ph].

[98] T. Abe, M. Kakizaki, S. Matsumoto, and O. Seto, "Vector WIMP Miracle," *Phys. Lett.* **B713** (2012) 211–215, arXiv:1202.5902 [hep-ph].

[99] Y. Farzan and A. R. Akbarieh, "VDM: A model for Vector Dark Matter," *JCAP* **1210** (2012) 026, arXiv:1207.4272 [hep-ph].

[100] S. Baek, P. Ko, W.-I. Park, and E. Senaha, "Higgs Portal Vector Dark Matter : Revisited," *JHEP* **05** (2013) 036, arXiv:1212.2131 [hep-ph].

[101] D. Wyler and L. Wolfenstein, "Massless neutrinos in left-hand symmetric models," *Nuclear Physics B* **218** no. 1, (1983) 205 – 214. http://www.sciencedirect.com/science/article/pii/0550321383904820.

[102] R. N. Mohapatra and J. W. F. Valle, "Neutrino mass and baryon-number nonconservation in superstring models," *Phys. Rev. D* **34** (Sep, 1986) 1642–1645. https://link.aps.org/doi/10.1103/PhysRevD.34.1642.

[103] E. Ma, "Lepton-number nonconservation in e6 superstring models," *Physics Letters B* **191** no. 3, (1987) 287 – 289. http://www.sciencedirect.com/science/article/pii/0370269387902565.

[104] Wolfram Research, Inc., "Mathematica." https://www.wolfram.com.

[105] G. Steigman, B. Dasgupta, and J. F. Beacom, "Precise Relic WIMP Abundance and its Impact on Searches for Dark Matter Annihilation," *Phys. Rev.* **D86** (2012) 023506, arXiv:1204.3622 [hep-ph].

[106] J. Hisano, K. Ishiwata, N. Nagata, and M. Yamanaka, "Direct Detection of Vector Dark Matter," *Prog. Theor. Phys.* **126** (2011) 435–456, arXiv:1012.5455 [hep-ph].

[107] **LUX** Collaboration, D. S. Akerib *et al.*, "First results from the LUX dark matter experiment at the Sanford Underground Research Facility," *Phys. Rev. Lett.* **112** (2014) 091303, arXiv:1310.8214 [astro-ph.CO].

[108] E. Ma, "Unified Framework for Matter, Dark Matter, and Radiative Neutrino Mass," *Phys. Rev.* **D88** no. 11, (2013) 117702, arXiv:1307.7064 [hep-ph].

[109] J. C. Montero and V. Pleitez, "Gauging U(1) symmetries and the number of right-handed neutrinos," *Phys. Lett.* **B675** (2009) 64–68, arXiv:0706.0473 [hep-ph].

[110] E. Ma and R. Srivastava, "Dirac or inverse seesaw neutrino masses with $B - L$ gauge symmetry and S_3 flavor symmetry," *Phys. Lett.* **B741** (2015) 217–222, arXiv:1411.5042 [hep-ph].

[111] P. Roy and O. Shanker, "Observable neutrino dirac mass and supergrand unification," *Phys. Rev. Lett.* **52** (Feb, 1984) 713–716. https://link.aps.org/doi/10.1103/PhysRevLett.52.713.

[112] J. Heeck and W. Rodejohann, "Neutrinoless Quadruple Beta Decay," *Europhys. Lett.* **103** (2013) 32001, arXiv:1306.0580 [hep-ph].

[113] J. Heeck, "Leptogenesis with Lepton-Number-Violating Dirac Neutrinos," *Phys. Rev.* **D88** (2013) 076004, arXiv:1307.2241 [hep-ph].

[114] **ATLAS** Collaboration, G. Aad *et al.*, "Search for high-mass dilepton resonances in pp collisions at $\sqrt{s} = 8$TeV with the ATLAS detector," *Phys. Rev.* **D90** no. 5, (2014) 052005, arXiv:1405.4123 [hep-ex].

[115] **CMS** Collaboration, V. Khachatryan *et al.*, "Search for physics beyond the standard model in dilepton mass spectra in proton-proton collisions at $\sqrt{s} = 8$ TeV," *JHEP* **04** (2015) 025, arXiv:1412.6302 [hep-ex].

[116] L. Feng, S. Profumo, and L. Ubaldi, "Closing in on singlet scalar dark matter: LUX, invisible Higgs decays and gamma-ray lines," *JHEP* **03** (2015) 045, arXiv:1412.1105 [hep-ph].

[117] E. Ma, "Z(3) Dark Matter and Two-Loop Neutrino Mass," *Phys. Lett.* **B662** (2008) 49–52, arXiv:0708.3371 [hep-ph].

[118] G. Belanger, K. Kannike, A. Pukhov, and M. Raidal, "Z_3 Scalar Singlet Dark Matter," *JCAP* **1301** (2013) 022, arXiv:1211.1014 [hep-ph].

[119] P. Ko and Y. Tang, "Self-interacting scalar dark matter with local Z_3 symmetry," *JCAP* **1405** (2014) 047, arXiv:1402.6449 [hep-ph].

[120] J. Guo, Z. Kang, P. Ko, and Y. Orikasa, "Accidental dark matter: Case in the scale invariant local B-L model," *Phys. Rev.* **D91** no. 11, (2015) 115017, arXiv:1502.00508 [hep-ph].

[121] E. Ma, "Radiative Mixing of the One Higgs Boson and Emergent Self-Interacting Dark Matter," *Phys. Lett.* **B754** (2016) 114–117, arXiv:1506.06658 [hep-ph].

[122] B. L. Snchez-Vega, J. C. Montero, and E. R. Schmitz, "Complex Scalar DM in a B-L Model," *Phys. Rev.* **D90** no. 5, (2014) 055022, arXiv:1404.5973 [hep-ph].

[123] B. L. Snchez-Vega and E. R. Schmitz, "Fermionic dark matter and neutrino masses in a B-L model," *Phys. Rev.* **D92** (2015) 053007, arXiv:1505.03595 [hep-ph].

[124] S. Tulin, "Self-interacting dark matter," *AIP Conference Proceedings* **1604** no. 1, (2014) 121–127, http://aip.scitation.org/doi/pdf/10.1063/1.4883420. http://aip.scitation.org/doi/abs/10.1063/1.4883420.

[125] E. Ma, "Radiative Origin of All Quark and Lepton Masses through Dark Matter with Flavor Symmetry," *Phys. Rev. Lett.* **112** (2014) 091801, arXiv:1311.3213 [hep-ph].

[126] E. Ma, "Syndetic Model of Fundamental Interactions," *Phys. Lett.* **B741** (2015) 202–204, arXiv:1411.6679 [hep-ph].

[127] E. Ma, "Transformative A_4 mixing of neutrinos with CP violation," *Phys. Rev.* **D92** no. 5, (2015) 051301, arXiv:1504.02086 [hep-ph].

[128] E. Ma, "Quark and Lepton Flavor Triality," *Phys. Rev.* **D82** (2010) 037301, arXiv:1006.3524 [hep-ph].

[129] Q.-H. Cao, A. Damanik, E. Ma, and D. Wegman, "Probing Lepton Flavor Triality with Higgs Boson Decay," *Phys. Rev.* **D83** (2011) 093012, arXiv:1103.0008 [hep-ph].

[130] E. Ma and G. Rajasekaran, "Softly broken A(4) symmetry for nearly degenerate neutrino masses," *Phys. Rev.* **D64** (2001) 113012, arXiv:hep-ph/0106291 [hep-ph].

[131] S. Fraser and E. Ma, "Anomalous Higgs Yukawa Couplings," *Europhys. Lett.* **108** no. 1, (2014) 11002, arXiv:1402.6415 [hep-ph].

[132] **Muon g-2** Collaboration, G. W. Bennett *et al.*, "Final Report of the Muon E821 Anomalous Magnetic Moment Measurement at BNL," *Phys. Rev.* **D73** (2006) 072003, arXiv:hep-ex/0602035 [hep-ex].

[133] M. Benayoun, P. David, L. DelBuono, and F. Jegerlehner, "An Update of the HLS Estimate of the Muon g-2," *Eur. Phys. J.* **C73** (2013) 2453, arXiv:1210.7184 [hep-ph].

[134] E. Ma, "Neutrino mixing: A_4 variations," *Phys. Lett.* **B752** (2016) 198–200, arXiv:1510.02501 [hep-ph].

[135] **MEG** Collaboration, J. Adam *et al.*, "New constraint on the existence of the $\mu^+ \to e^+\gamma$ decay," *Phys. Rev. Lett.* **110** (2013) 201801, arXiv:1303.0754 [hep-ex].

[136] U. Bellgardt, G. Otter, R. Eichler, L. Felawka, C. Niebuhr, H. Walter, W. Bertl, N. Lordong, J. Martino, S. Egli, R. Engfer, C. Grab, M. Grossmann-Handschin, E. Hermes, N. Kraus, F. Muheim, H. Pruys, A. V. D. Schaaf, and D. Vermeulen, "Search for the decay + e+e+e," *Nuclear Physics B* **299** no. 1, (1988) 1 – 6. http://www.sciencedirect.com/science/article/pii/0550321388904622.

[137] E. Ma, "Derivation of Dark Matter Parity from Lepton Parity," *Phys. Rev. Lett.* **115** no. 1, (2015) 011801, arXiv:1502.02200 [hep-ph].

[138] J. M. Cline, K. Kainulainen, P. Scott, and C. Weniger, "Update on scalar singlet dark matter," *Phys. Rev.* **D88** (2013) 055025, arXiv:1306.4710 [hep-ph]. [Erratum: Phys. Rev.D92,no.3,039906(2015)].

[139] **LUX** Collaboration, D. S. Akerib *et al.*, "Improved Limits on Scattering of Weakly Interacting Massive Particles from Reanalysis of 2013 LUX Data," *Phys. Rev. Lett.* **116** no. 16, (2016) 161301, arXiv:1512.03506 [astro-ph.CO].

[140] E. Ma, "New U(1) gauge extension of the supersymmetric standard model," *Phys. Rev. Lett.* **89** (2002) 041801, arXiv:hep-ph/0201083 [hep-ph].

[141] E. Ma, "Compendium of models from a gauge U(1) framework," *Mod. Phys. Lett.* **A31** no. 18, (2016) 1650112, arXiv:1601.01400 [hep-ph].

[142] E. Ma, "Utilitarian Supersymmetric Gauge Model of Particle Interactions," *Phys. Rev.* **D81** (2010) 097701, arXiv:1004.0192 [hep-ph].

[143] T. A. collaboration, "Search for resonances decaying to photon pairs in 3.2 fb^{-1} of pp collisions at $\sqrt{s} = 13$ TeV with the ATLAS detector,".

[144] **CMS** Collaboration, C. Collaboration, "Search for new physics in high mass diphoton events in proton-proton collisions at 13TeV,".

[145] "There are already some 200 papers on the arXiv since December 15, 2015.,".

[146] E. Ma, "Diphoton Revelation of the Utilitarian Supersymmetric Standard Model," arXiv:1512.09159 [hep-ph].

[147] **CMS Collaboration** Collaboration, "Search for resonant production of high mass photon pairs using 12.9 fb^{-1} of proton-proton collisions at $\sqrt{s} = 13$ TeV and combined interpretation of searches at 8 and 13 TeV," Tech. Rep. CMS-PAS-EXO-16-027, CERN, Geneva, 2016. https://cds.cern.ch/record/2205245.

[148] **ATLAS** Collaboration, T. A. collaboration, "Search for scalar diphoton resonances with 15.4 fb^{-1} of data collected at $\sqrt{s}$=13 TeV in 2015 and 2016 with the ATLAS detector,".

[149] E. Keith and E. Ma, "Generic consequences of a supersymmetric U(1) gauge factor at the TeV scale," *Phys. Rev.* **D56** (1997) 7155–7165, arXiv:hep-ph/9704441 [hep-ph].

[150] J. Erler, P. Langacker, S. Munir, and E. Rojas, "Improved Constraints on Z-prime Bosons from Electroweak Precision Data," *JHEP* **08** (2009) 017, arXiv:0906.2435 [hep-ph].

[151] S. Godfrey and T. A. W. Martin, "Identification of Extra Neutral Gauge Bosons at the LHC Using b- and t-Quarks," *Phys. Rev. Lett.* **101** (2008) 151803, arXiv:0807.1080 [hep-ph].

[152] **CMS** Collaboration, V. Khachatryan *et al.*, "Search for physics beyond the standard model in dilepton mass spectra in proton-proton collisions at $\sqrt{s} = 8$ TeV," *JHEP* **04** (2015) 025, arXiv:1412.6302 [hep-ex].

[153] M. Bauer and M. Neubert, "Flavor anomalies, the 750 GeV diphoton excess, and a dark matter candidate," *Phys. Rev.* **D93** no. 11, (2016) 115030, arXiv:1512.06828 [hep-ph].

[154] J. Ellis, S. A. R. Ellis, J. Quevillon, V. Sanz, and T. You, "On the Interpretation of a Possible $\sim$ 750 GeV Particle Decaying into $\gamma\gamma$," *JHEP* **03** (2016) 176, arXiv:1512.05327 [hep-ph].

[155] Y. Hamada, H. Kawai, K. Kawana, and K. Tsumura, "Models of the LHC diphoton excesses valid up to the Planck scale," *Phys. Rev.* **D94** no. 1, (2016) 014007, arXiv:1602.04170 [hep-ph].

[156] G. Belanger, F. Boudjema, A. Pukhov, and A. Semenov, "Dark matter direct detection rate in a generic model with micrOMEGAs 2.2," *Comput. Phys. Commun.* **180** (2009) 747–767, arXiv:0803.2360 [hep-ph].

[157] H. Ohki, H. Fukaya, S. Hashimoto, T. Kaneko, H. Matsufuru, J. Noaki, T. Onogi, E. Shintani, and N. Yamada, "Nucleon sigma term and strange quark content from lattice QCD with exact chiral symmetry," *Phys. Rev.* **D78** (2008) 054502, arXiv:0806.4744 [hep-lat].

[158] R. Adhikari, D. Borah, and E. Ma, "New U(1) Gauge Model of Radiative Lepton Masses with Sterile Neutrino and Dark Matter," *Phys. Lett.* **B755** (2016) 414–417, arXiv:1512.05491 [hep-ph].

[159] R. Marshak and R. Mohapatra, "Quark-lepton symmetry and b l as the u(1) generator of the electroweak symmetry group," *Physics Letters B* **91** no. 2, (1980) 222 – 224. http://www.sciencedirect.com/science/article/pii/0370269380904360.

[160] X. G. He, G. C. Joshi, H. Lew, and R. R. Volkas, "NEW Z-prime PHENOMENOLOGY," *Phys. Rev.* **D43** (1991) 22–24.

[161] E. Ma, D. P. Roy, and S. Roy, "Gauged L(mu) - L(tau) with large muon anomalous magnetic moment and the bimaximal mixing of neutrinos," *Phys. Lett.* **B525** (2002) 101–106, arXiv:hep-ph/0110146 [hep-ph].

[162] W. Altmannshofer, S. Gori, M. Pospelov, and I. Yavin, "Quark flavor transitions in $L_\mu - L_\tau$ models," *Phys. Rev.* **D89** (2014) 095033, arXiv:1403.1269 [hep-ph].

[163] J. Heeck, M. Holthausen, W. Rodejohann, and Y. Shimizu, "Higgs $\to \mu\tau$ in Abelian and non-Abelian flavor symmetry models," *Nucl. Phys.* **B896** (2015) 281–310, arXiv:1412.3671 [hep-ph].

[164] E. Ma, "Gauged B - 3L(tau) and radiative neutrino masses," *Phys. Lett.* **B433** (1998) 74–81, arXiv:hep-ph/9709474 [hep-ph].

[165] E. Ma and U. Sarkar, "Gauged B - 3L(tau) and baryogenesis," *Phys. Lett.* **B439** (1998) 95–102, arXiv:hep-ph/9807307 [hep-ph].

[166] E. Ma and D. P. Roy, "Phenomenology of the B - 3L(τ) gauge boson," *Phys. Rev.* **D58** (1998) 095005, arXiv:hep-ph/9806210 [hep-ph].

[167] X.-J. Bi, X.-G. He, E. Ma, and J. Zhang, "Cosmic $e^\pm$, $\bar{p}$, γ and neutrino rays in leptocentric dark matter models," *Phys. Rev.* **D81** (2010) 063522, arXiv:0910.0771 [hep-ph].

[168] H.-S. Lee and E. Ma, "Gauged $B - x_i L$ origin of R Parity and its implications," *Phys. Lett.* **B688** (2010) 319–322, arXiv:1001.0768 [hep-ph].

[169] J.-Y. Liu, Y. Tang, and Y.-L. Wu, "Searching for $Z^{'}$ Gauge Boson in an Anomaly-Free U(1)$'$ Gauge Family Model," *J. Phys.* **G39** (2012) 055003, arXiv:1108.5012 [hep-ph].

[170] A. Crivellin, G. D'Ambrosio, and J. Heeck, "Addressing the LHC flavor anomalies with horizontal gauge symmetries," *Phys. Rev.* **D91** no. 7, (2015) 075006, arXiv:1503.03477 [hep-ph].

[171] R. Foot, G. C. Joshi, and H. Lew, "Gauged baryon and lepton numbers," *Phys. Rev. D* **40** (Oct, 1989) 2487–2489. https://link.aps.org/doi/10.1103/PhysRevD.40.2487.

[172] P. Fileviez Perez and M. B. Wise, "Baryon and lepton number as local gauge symmetries," *Phys. Rev.* **D82** (2010) 011901, arXiv:1002.1754 [hep-ph]. [Erratum: Phys. Rev.D82,079901(2010)].

[173] C. Patrignani and P. D. Group, "Review of particle physics," *Chinese Physics C* **40** no. 10, (2016) 100001. http://stacks.iop.org/1674-1137/40/i=10/a=100001.

[174] **ATLAS** Collaboration, G. Aad *et al.*, "Search for high-mass dilepton resonances in pp collisions at $\sqrt{s} = 8$TeV with the ATLAS detector," *Phys. Rev.* **D90** no. 5, (2014) 052005, arXiv:1405.4123 [hep-ex].

[175] **CMS** Collaboration, V. Khachatryan *et al.*, "Search for physics beyond the standard model in dilepton mass spectra in proton-proton collisions at $\sqrt{s} = 8$ TeV," *JHEP* **04** (2015) 025, arXiv:1412.6302 [hep-ex].

[176] M. Antonelli *et al.*, "Flavor Physics in the Quark Sector," *Phys. Rept.* **494** (2010) 197–414, arXiv:0907.5386 [hep-ph].

[177] E. Ma and B. Melic, "Updated S_3 model of quarks," *Phys. Lett.* **B725** (2013) 402–406, arXiv:1303.6928 [hep-ph].

[178] E. Ma, "Connection between the neutrino seesaw mechanism and properties of the Majorana neutrino mass matrix," *Phys. Rev.* **D71** (2005) 111301, arXiv:hep-ph/0501056 [hep-ph].

[179] J. Liao, D. Marfatia, and K. Whisnant, "Texture and Cofactor Zeros of the Neutrino Mass Matrix," *JHEP* **09** (2014) 013, arXiv:1311.2639 [hep-ph].

[180] T. Hurth, F. Mahmoudi, and S. Neshatpour, "On the anomalies in the latest LHCb data," *Nucl. Phys.* **B909** (2016) 737–777, arXiv:1603.00865 [hep-ph].

[181] K. S. Babu, E. Ma, and S. Willenbrock, "Quark lepton quartification," *Phys. Rev.* **D69** (2004) 051301, arXiv:hep-ph/0307380 [hep-ph].

[182] R. Foot and H. Lew, "QUARK - LEPTON SYMMETRIC MODEL," *Phys. Rev.* **D41** (1990) 3502.

[183] R. Foot, H. Lew, and R. R. Volkas, "Phenomenology of quark - lepton symmetric models," *Phys. Rev.* **D44** (1991) 1531–1546.

[184] G. C. Joshi and R. R. Volkas, "Extended weak isospin and fermion masses in a unified model," *Phys. Rev.* **D45** (1992) 1711–1719.

[185] A. Soni and Y. Zhang, "Hidden SU(N) Glueball Dark Matter," *Phys. Rev.* **D93** no. 11, (2016) 115025, arXiv:1602.00714 [hep-ph].

[186] R. Foot, H. Lew, and R. R. Volkas, "NATURAL GENERALIZATION OF THE STANDARD MODEL INCORPORATING CHARGE +-1/2 TECHNIFERMIONS," *Phys. Rev.* **D42** (1990) 1851–1854.

[187] J. D. Clarke, R. Foot, and R. R. Volkas, "Quark-lepton symmetric model at the LHC," *Phys. Rev.* **D85** (2012) 074012, arXiv:1112.3405 [hep-ph].

[188] K. S. Jeong and F. Takahashi, "Self-interacting Dark Radiation," *Phys. Lett.* **B725** (2013) 134, arXiv:1305.6521 [hep-ph].

[189] K. M. Nollett and G. Steigman, "BBN And The CMB Constrain Neutrino Coupled Light WIMPs," *Phys. Rev.* **D91** no. 8, (2015) 083505, arXiv:1411.6005 [astro-ph.CO].

[190] **Planck** Collaboration, P. A. R. Ade *et al.*, "Planck 2015 results. XIII. Cosmological parameters," *Astron. Astrophys.* **594** (2016) A13, arXiv:1502.01589 [astro-ph.CO].

[191] E. D. Carlson, M. E. Machacek, and L. J. Hall, "Self-interacting dark matter," *Astrophys. J.* **398** (1992) 43–52.

[192] J. Baur, N. Palanque-Delabrouille, C. Yche, C. Magneville, and M. Viel, "Lyman-alpha Forests cool Warm Dark Matter," *JCAP* **1608** no. 08, (2016) 012, arXiv:1512.01981 [astro-ph.CO].

[193] T. R. Slatyer and C.-L. Wu, "General Constraints on Dark Matter Decay from the Cosmic Microwave Background," *Phys. Rev.* **D95** no. 2, (2017) 023010, arXiv:1610.06933 [astro-ph.CO].

[194] Y. Mambrini, S. Profumo, and F. S. Queiroz, "Dark Matter and Global Symmetries," *Phys. Lett.* **B760** (2016) 807–815, arXiv:1508.06635 [hep-ph].

[195] E. Ma, "Particle dichotomy and left-right decomposition of e_6 superstring models," *Phys. Rev. D* **36** (Jul, 1987) 274–276. https://link.aps.org/doi/10.1103/PhysRevD.36.274.

[196] S. Khalil, H.-S. Lee, and E. Ma, "Generalized lepton number and dark left-right gauge model," *Phys. Rev. D* **79** (Feb, 2009) 041701. https://link.aps.org/doi/10.1103/PhysRevD.79.041701.

[197] S. Khalil, H.-S. Lee, and E. Ma, "Bound on $Z^{'}$ mass from cdms ii in the dark left-right gauge model ii," *Phys. Rev. D* **81** (Mar, 2010) 051702. https://link.aps.org/doi/10.1103/PhysRevD.81.051702.

[198] S. Bhattacharya, E. Ma, and D. Wegman, "Supersymmetric left–right model with radiative neutrino mass and multipartite dark matter," *The European Physical Journal C* **74** no. 6, (2014) 2902. http://dx.doi.org/10.1140/epjc/s10052-014-2902-7.

[199] C. Kownacki and E. Ma, "Gauge $U(1)$ dark symmetry and radiative light fermion masses," *Phys. Lett.* **B760** (2016) 59–62, arXiv:1604.01148 [hep-ph].

[200] **CMS Collaboration** Collaboration, "Search for new physics in the all-hadronic final state with the MT2 variable," Tech. Rep. CMS-PAS-SUS-16-036, CERN, Geneva, 2017. http://cds.cern.ch/record/2256872.

[201] L. J. Hall, K. Jedamzik, J. March-Russell, and S. M. West, "Freeze-In Production of FIMP Dark Matter," *JHEP* **03** (2010) 080, arXiv:0911.1120 [hep-ph].

Appendix A

Muon Anomalous Magnetic Moment Calculation

A.1 Dominant Contributions

Anomalous magnetic moment can be generated dominantly through the diagrams in Figs. A.1. Let's assume the general vertex form

$$i\mathcal{M} = ie^2[\bar{u}(p')\Gamma^{\mu}(p,p')u(p)]\frac{1}{q^2}[\bar{u}(k')\gamma^{\mu}u(k'')], \tag{A.1}$$

The amplitude for the first diagram in Fig. A.1 is given by

$$\begin{aligned}\bar{u}(p')\Gamma^{1,1,\nu}_{L,R}(p,p')u(p) &= \int \frac{d^4k}{(2\pi)^4}\bar{u}(p+q)\left(if^*_{\mu}P_L\cos\theta_R\right)\frac{i(\not{p}-\not{k}+m_{n_1})}{(p-k)^2-m^2_{n_1}+i\epsilon}\left(-if'\sin\theta_L P_L\right)\\ &\quad\times(\sin\theta_{\mu}\cos\theta_{\mu})\frac{i}{k^2-m^2_{s_1}+i\epsilon}(2k^{\nu}+q^{\nu})\frac{i}{(k+q)^2-m^2_{s_1}+i\epsilon}u(p)\\ &= A^{1,1}_{L,R}\int\frac{d^4k}{(2\pi)^4}\frac{\bar{u}(p+q)\left[(2k^{\nu}+q^{\nu})P_L\right]u(p)}{\left[(p-k)^2-m^2_{n_1}+i\epsilon\right]\left[k^2-m^2_{s_1}+i\epsilon\right]\left[(k+q)^2-m^2_{s_1}+i\epsilon\right]},\end{aligned} \tag{A.2}$$

with,

$$A^{1,1}_{L,R} \equiv -if' f^*_\mu m_{n_1} \sin\theta_L \cos\theta_R \sin\theta_\mu \cos\theta_\mu. \tag{A.3}$$

The amplitudes for all of the diagrams in the left column of Fig. A.1 have the same form as in Eq. (A.2), with the following coefficients

$$A^{1,1}_{L,R} = -if' f^*_\mu m_{n_1} \sin\theta_L \cos\theta_R \sin\theta_\mu \cos\theta_\mu, \tag{A.4}$$

$$A^{1,2}_{L,R} = +if' f^*_\mu m_{n_1} \sin\theta_L \cos\theta_R \sin\theta_\mu \cos\theta_\mu, \tag{A.5}$$

$$A^{2,1}_{L,R} = +if' f^*_\mu m_{n_2} \cos\theta_L \sin\theta_R \sin\theta_\mu \cos\theta_\mu, \tag{A.6}$$

$$A^{2,2}_{L,R} = -if' f^*_\mu m_{n_2} \cos\theta_L \sin\theta_R \sin\theta_\mu \cos\theta_\mu. \tag{A.7}$$

For the diagrams in the right column of Fig. A.1, P_L should be replaced by P_R, and the coeficients are

$$A^{1,1}_{R,L} = -if'^* f_\mu m_{n_1} \sin\theta_L \cos\theta_R \sin\theta_\mu \cos\theta_\mu = -A^{1,1\ *}_{L,R}, \tag{A.8}$$

$$A^{1,2}_{R,L} = +if'^* f_\mu m_{n_1} \sin\theta_L \cos\theta_R \sin\theta_\mu \cos\theta_\mu = -A^{1,2\ *}_{L,R}, \tag{A.9}$$

$$A^{2,1}_{R,L} = +if'^* f_\mu m_{n_2} \cos\theta_L \sin\theta_R \sin\theta_\mu \cos\theta_\mu = -A^{2,1\ *}_{L,R}, \tag{A.10}$$

$$A^{2,2}_{R,L} = -if'^* f_\mu m_{n_2} \cos\theta_L \sin\theta_R \sin\theta_\mu \cos\theta_\mu = -A^{2,2\ *}_{L,R}. \tag{A.11}$$

We ignore the terms proportional to γ^5, and we add the amplitudes (A.4) & (A.8), (A.5) & (A.9), (A.6) & (A.10), (A.7) & (A.11) to get

$$\bar{u}(p')\Gamma^{i,j,\nu}(p,p')u(p) = \int \frac{d^4k}{(2\pi)^4} \frac{i\mathrm{Im}(A^{i,j}_{L,R})\,\bar{u}(p+q)\left[2k^\nu + q^\nu\right]u(p)}{\left[(p-k)^2 - m^2_{n_i} + i\epsilon\right]\left[k^2 - m^2_{s_j} + i\epsilon\right]\left[(k+q)^2 - m^2_{s_j} + i\epsilon\right]} \tag{A.12}$$

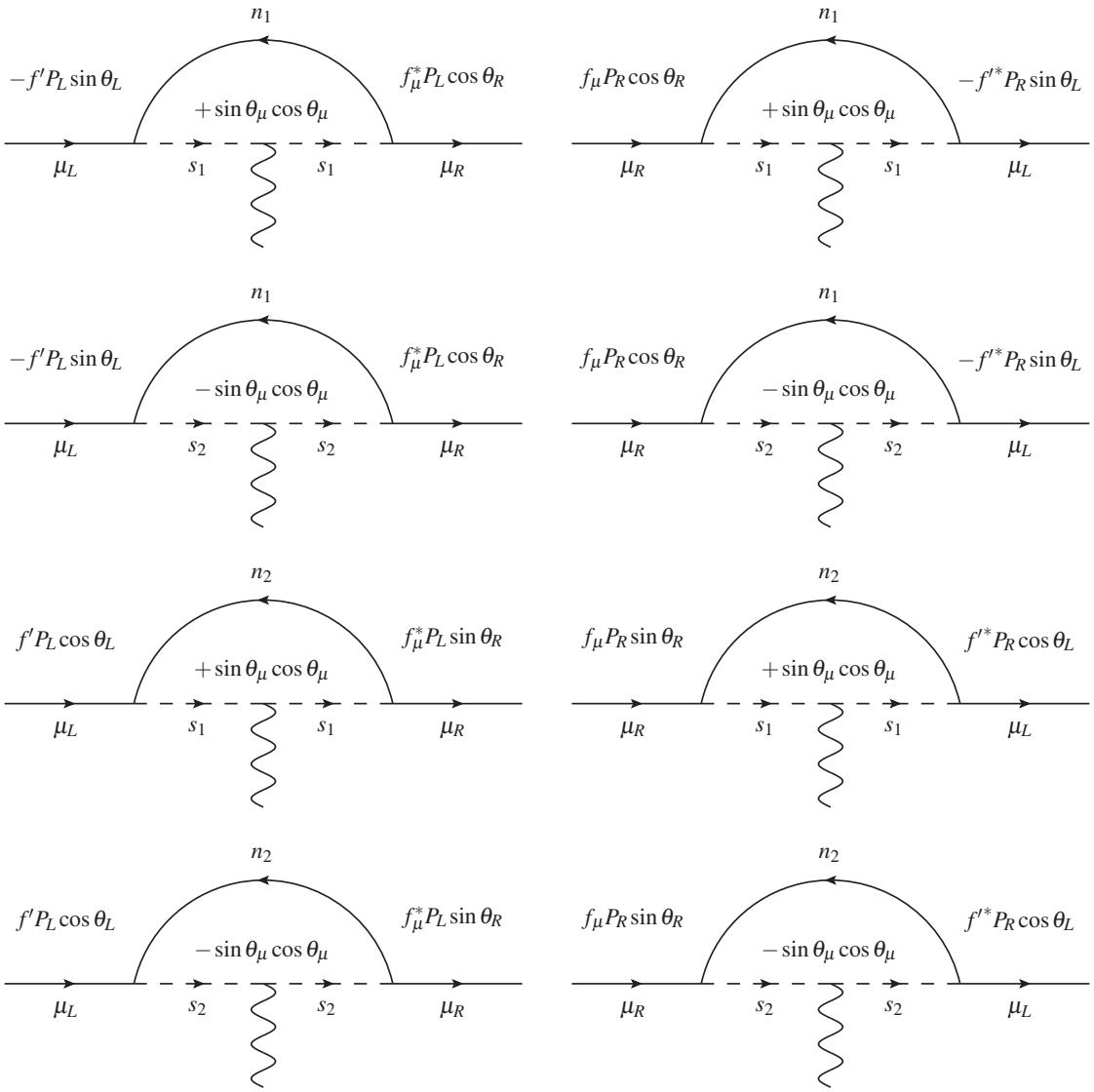

Figure A.1: Dominant diagrams contributing to muon $g-2$.

We now focus on doing the integral (A.13) using the feynman parameters:

$$\begin{aligned} I^{\nu}(m_n, m_s) &= \int \frac{d^4k}{(2\pi)^4} \frac{2k^{\nu} + q^{\nu}}{[(p-k)^2 - m_n^2 + i\epsilon]\,[k^2 - m_s^2 + i\epsilon]\,[(k+q)^2 - m_s^2 + i\epsilon]} \\ &= \int \frac{d^4k}{(2\pi)^4} \frac{2k^{\nu} + q^{\nu}}{ABC}, \end{aligned} \tag{A.13}$$

where we can write

$$\frac{1}{ABC} = \iiint dxdydz\delta(x+y+z-1)\frac{2}{D^3}, \quad D = xA + yB + zC, \tag{A.14}$$

such that

$$\frac{1}{[(p-k)^2 - m_n^2 + i\epsilon]\,[k^2 - m_s^2 + i\epsilon]\,[(k+q)^2 - m_s^2 + i\epsilon]} = \iiint dxdydz\delta(x+y+z-1)\frac{2}{D^3}, \tag{A.15}$$

with $D = x\left[(p-k)^2 - m_n^2 + i\epsilon\right] + y\left[k^2 - m_s^2 + i\epsilon\right] + z\left[(k+q)^2 - m_s^2 + i\epsilon\right]$.

$$\begin{aligned} D &= x\left[k^2 + p^2 - 2k.p - m_n^2\right] + yk^2 - ym_s^2 + z\left[k^2 + q^2 + 2k.q\right] - zm_s^2 + i\epsilon \\ &= k^2 + 2(zq - xp).k + (p^2 - m_n^2)x - ym_s^2 + z(q^2 - m_s^2) + i\epsilon \end{aligned} \tag{A.16}$$

Therefore, D can be written in terms of l and Δ as follows

$$D = l^2 - \Delta + i\epsilon, \tag{A.17}$$

$$l^{\mu} \equiv k^{\mu} + zq^{\mu} - xp^{\mu}, \tag{A.18}$$

$$\Delta \equiv z^2q^2 - z(q^2 - m_s^2) + x^2p^2 - 2xz(p.q) - x(p^2 - m_n^2) + ym_s^2. \tag{A.19}$$

The numerator in Eq. (A.13) can be written as

$$\begin{aligned} 2k^{\nu} + q^{\nu} &= 2l^{\nu} - 2zq^{\nu} + q^{\nu} + 2xp^{\nu} \\ &= 2l^{\nu} + (1 - x - 2z)q^{\nu} + x(p + p')^{\nu} \\ &= 2l^{\nu} + (y - z)q^{\nu} + (1 - y - z)(p + p')^{\nu}. \end{aligned} \tag{A.20}$$

Note that the term containing q^ν in the integral vanishes, since the denominator is even under $y \leftrightarrow z$, while the numerator is odd. Also, the integral of l^ν is zero, since the denominator depends only on l^2. Therefore, the only non-zero contribution to Eq. (A.13) comes from

$$\int \frac{d^4l}{(2\pi)^4} \iint dydz \frac{2(p+p')^\nu(1-y-z)}{\left(l^2-\Delta+i\epsilon\right)^3} = \iint dydz[2(p+p')^\nu(1-y-z)] \times \int \frac{d^4l}{(2\pi)^4} \frac{1}{\left(l^2-\Delta+i\epsilon\right)^3}. \tag{A.21}$$

Using Wick's rotation: $l^0 \equiv il_E^0$, $\vec{l} \equiv \vec{l_E}$ we have

$$\int \frac{d^4l}{(2\pi)^4} \frac{1}{\left(l^2-\Delta+i\epsilon\right)^3} = \frac{i(-1)^3}{(4\pi)^2} \frac{1}{(3-1)(3-2)} \frac{1}{\Delta^{(3-2)}} = \frac{-i}{2(4\pi)^2} \frac{1}{\Delta}. \tag{A.22}$$

Using Gordon identity : $\bar{u}(p')\left[p+p'\right]^\mu u(p) = \bar{u}(p')\left[2m\gamma^\mu - i\sigma^{\mu\nu}q_\nu\right]u(p)$ we can now write Eq. (A.12) as

$$\begin{aligned}\bar{u}(p')\Gamma^{i,j,\nu}(p,p')u(p) &= i\mathrm{Im}(A_{L,R}^{i,j}) \left(\frac{-i}{2(4\pi)^2}\right) \iint \frac{1}{\Delta} dydz \left[\bar{u}(p')2(p+p')^\nu(1-y-z)u(p)\right] \\ &= \mathrm{Im}(A_{L,R}^{i,j}) \left(\frac{1}{16\pi^2}\right) \iint \frac{1-y-z}{\Delta} dydz \left[\bar{u}(p')\left(2m_\mu\gamma^\nu - i\sigma^{\nu\alpha}q_\alpha\right)u(p)\right].\end{aligned} \tag{A.23}$$

Also, using $x+y+z=1$, and rewriting Δ in terms of y and z we get

$$\begin{aligned}\Delta &= z^2q^2 - z(q^2-m_s^2) + (1-y-z)^2p^2 - 2(1-y-z)z(p.q) - (1-y-z)(p^2-m_n^2) + ym_s^2 \\ &= z^2(q^2+p^2+2p.q) + z(m_s^2-q^2-2p^2-2p.q+p^2-m_n^2) + p^2y^2 + (m_s^2+p^2-m_n^2-2p^2)y \\ &+ (2p^2+2p.q)yz + (p^2-p^2+m_n^2) \\ &= m_\mu^2(z^2+y^2) + (m_s^2-m_n^2-m_\mu^2)(y+z) + 2(m_\mu^2+p.q)yz + m_n^2 \\ &= m_\mu^2(z^2+y^2) + (m_s^2-m_n^2-m_\mu^2)(y+z) + 2(m_\mu^2-\frac{q^2}{2})yz + m_n^2.\end{aligned} \tag{A.24}$$

In the non-relativistic limit we have $q^2 \to 0$, and (A.24) becomes

$$\Delta\big|_{q^2=0} = m_\mu^2(z^2+y^2) + (m_s^2 - m_n^2 - m_\mu^2)(y+z) + 2m_\mu^2 yz + m_n^2. \tag{A.25}$$

If we assume $m_\mu \ll m_n, m_s$, and after performing the integrals over y and z we get

$$\int_0^1 dz \int_0^{1-z} \frac{1-y-z}{\Delta} dy \approx \frac{m_n^4 - m_s^4 + 2m_s^2 m_n^2 \ln\left(\frac{m_s^2}{m_n^2}\right)}{2(m_n^2 - m_s^2)^3}, \tag{A.26}$$

Therefore, Eq. (A.23) becomes

$$\bar{u}(p')\Gamma^{i,j,\nu}(p,p')u(p) = \frac{\mathrm{Im}(A_{L,R}^{i,j})}{16\pi^2}\left(\frac{m_{n_i}^4 - m_{s_j}^4 + 2m_{s_j}^2 m_{n_i}^2 \ln(\frac{m_{s_j}^2}{m_{n_i}^2})}{2(m_{n_i}^2 - m_{s_j}^2)^3}\right)\left[\bar{u}(p')(2m_\mu\gamma^\nu - i\sigma^{\nu\alpha}q_\alpha)u(p)\right] \tag{A.27}$$

We now define $x_{ij} \equiv \left(\frac{m_{s_j}}{m_{n_i}}\right)^2$, and $G(x) \equiv \frac{2x\ln x}{(x-1)^3} - \frac{x+1}{(x-1)^2}$, such that Eq. (A.27) can now be written as

$$\bar{u}(p')\Gamma^{i,j,\nu}(p,p')u(p) = \mathrm{Im}(A_{L,R}^{i,j})\left(\frac{1}{16\pi^2}\right)\left[-\frac{G(x_{ij})}{2m_{n_i}^2}\right]\left[\bar{u}(p')(2m_\mu\gamma^\nu - i\sigma^{\nu\alpha}q_\alpha)u(p)\right] \tag{A.28}$$

After comparing Eq. (A.28) to $\Gamma^\mu = \gamma^\mu F_1(q^2) + \frac{i\sigma^{\mu\nu}q_\nu}{2m}F_2(q^2)$ we see that

$$F_2^{(1)}(q^2=0) = \sum_{i,j=1}^{2} \mathrm{Im}(A_{L,R}^{i,j})\left(\frac{1}{16\pi^2}\right)\left[\frac{m_\mu}{m_{n_i}^2}G(x_{ij})\right] \tag{A.29}$$

This is the contribution from the diagrams in Fig. A.1.

A.2 Subdominant Contributions

The subdominant contributions to muon anomalous magnetic moment are generated by the diagrams in Fig. A.2. We start by writing the amplitude for the first diagram

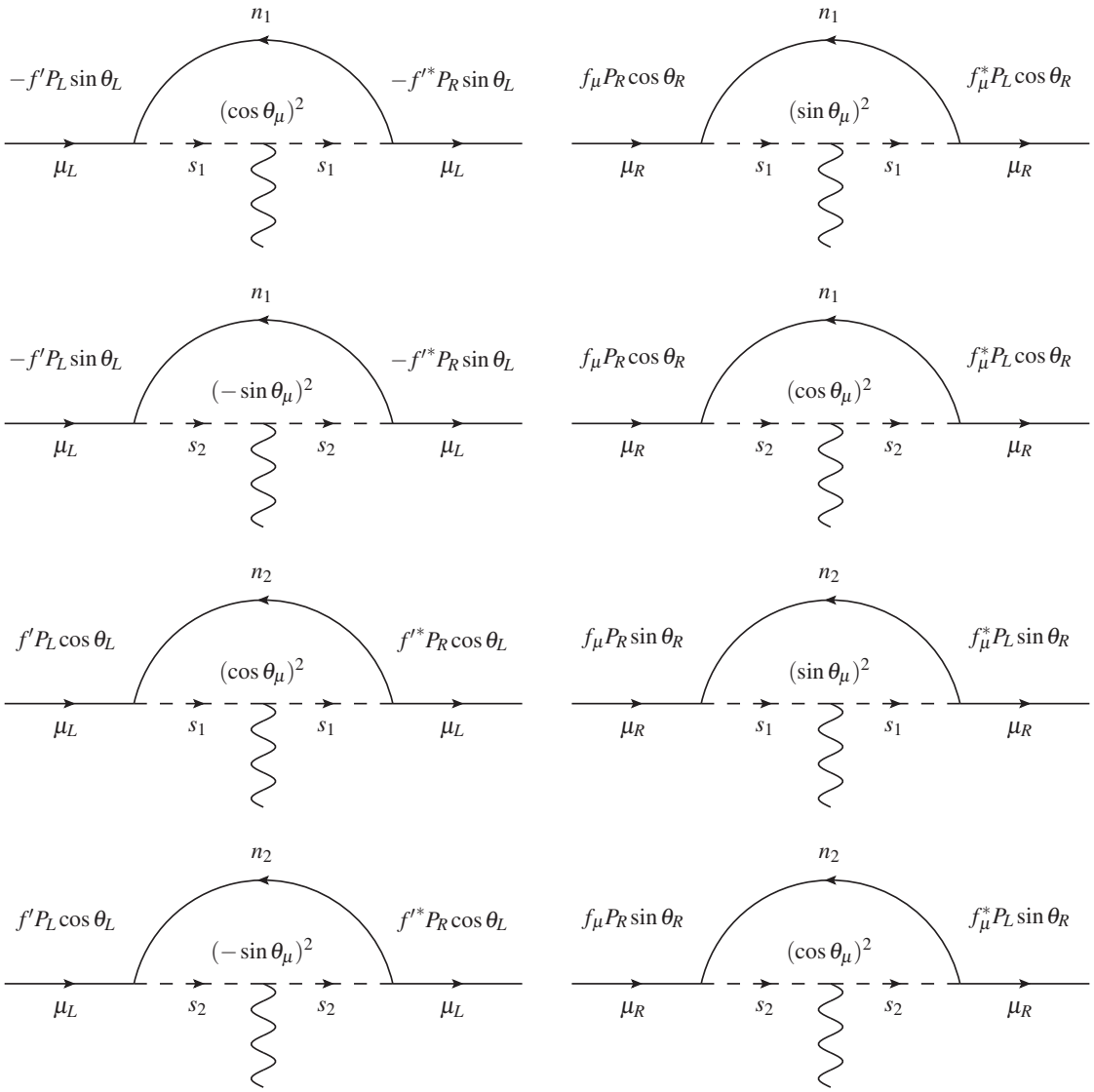

Figure A.2: Subdominant diagrams contributing to muon $g-2$.

in Fig. A.2.

$$\begin{aligned}\bar{u}(p')\Gamma^{1,1,\nu}_{L,L}(p,p')u(p) = &\int \frac{d^4k}{(2\pi)^4}\bar{u}(p+q)\left(-if'^{*}P_R\sin\theta_L\right)\frac{i\left(\not{p}-\not{k}+m_{n_1}\right)}{(p-k)^2-m_{n_1}^2+i\epsilon}\left(-if'\sin\theta_L P_L\right)\\ &\times(\cos\theta_\mu)^2\frac{i}{k^2-m_{s_1}^2+i\epsilon}\left(2k^\nu+q^\nu\right)\frac{i}{(k+q)^2-m_{s_1}^2+i\epsilon}u(p)\\ = A^{1,1}_{L,L}&\int\frac{d^4k}{(2\pi)^4}\frac{\bar{u}(p+q)\left[(\not{p}-\not{k})(2k^\nu+q^\nu)P_L\right]u(p)}{\left[(p-k)^2-m_{n_1}^2+i\epsilon\right]\left[k^2-m_{s_1}^2+i\epsilon\right]\left[(k+q)^2-m_{s_1}^2+i\epsilon\right]},\end{aligned} \tag{A.30}$$

with,

$$A^{1,1}_{L,L}\equiv if'f'^{*}\sin^2\theta_L\cos^2\theta_\mu. \tag{A.31}$$

Furthermore the amplitudes for all of the diagrams in the left column of Fig. A.2 have the same form as in Eq. (A.30) with the following coefficients

$$A^{1,1}_{L,L} = if'f'^{*}\sin^2\theta_L\cos^2\theta_\mu, \tag{A.32}$$

$$A^{1,2}_{L,L} = if'f'^{*}\sin^2\theta_L\sin^2\theta_\mu, \tag{A.33}$$

$$A^{2,1}_{L,L} = if'f'^{*}\cos^2\theta_L\cos^2\theta_\mu, \tag{A.34}$$

$$A^{2,2}_{L,L} = if'f'^{*}\cos^2\theta_L\sin^2\theta_\mu. \tag{A.35}$$

For the diagrams in the right column of Fig. A.2, P_L should be replaced by P_R and the coeficients are

$$A^{1,1}_{R,R} = if_\mu f^{*}_\mu\cos^2\theta_R\sin^2\theta_\mu, \tag{A.36}$$

$$A^{1,2}_{R,R} = if_\mu f^{*}_\mu\cos^2\theta_R\cos^2\theta_\mu, \tag{A.37}$$

$$A^{2,1}_{R,R} = if_\mu f^{*}_\mu\sin^2\theta_R\sin^2\theta_\mu, \tag{A.38}$$

$$A^{2,2}_{R,R} = if_\mu f^{*}_\mu\sin^2\theta_R\cos^2\theta_\mu. \tag{A.39}$$

We ignore the terms proportional to γ^5, and we add the amplitudes (A.32) & (A.36), (A.33) & (A.37), (A.34) & (A.38), (A.35) & (A.39) to get

$$\bar{u}(p')\Gamma^{i,j,\nu}(p,p')u(p) = \int \frac{d^4k}{2(2\pi)^4} \frac{\left(A^{i,j}_{L,L} + A^{i,j}_{R,R}\right)\, \bar{u}(p+q)\left[(\not{p}-\not{k})(2k^\nu + q^\nu)\right] u(p)}{\left[(p-k)^2 - m^2_{n_i} + i\epsilon\right]\left[k^2 - m^2_{s_j} + i\epsilon\right]\left[(k+q)^2 - m^2_{s_j} + i\epsilon\right]} \tag{A.40}$$

Since the denominator is the same as before, we have the same feynman parameters with the following integral

$$\begin{aligned} I^\nu(m_n, m_s) &= \int \frac{d^4k}{(2\pi)^4} \frac{(\not{p}-\not{k})(2k^\nu + q^\nu)}{\left[(p-k)^2 - m_n^2 + i\epsilon\right]\left[k^2 - m_s^2 + i\epsilon\right]\left[(k+q)^2 - m_s^2 + i\epsilon\right]} \\ &= \int \frac{d^4k}{(2\pi)^4} \frac{\left(\not{p}-\not{k}\right)(2k^\nu + q^\nu)}{ABC} \end{aligned} \tag{A.41}$$

We rewrite the numerator using Eq. (A.18)

$$\not{k} = \not{l} + (x+z)\not{p} - z\not{p}' \longrightarrow \not{p} - \not{k} = -\not{l} - (x+z-1)\not{p} + z\not{p}' \tag{A.42}$$

From Dirac equation we have

$$\begin{cases} \not{p}u(p) = m_\mu u(p) & \text{(A.43a)} \\ \bar{u}(p')\not{p}' = \bar{u}(p)m_\mu & \text{(A.43b)} \end{cases}$$

Therefore, Eq. (A.42) becomes

$$\bar{u}(p')\left[\not{p}-\not{k}\right]u(p) = \bar{u}(p')\left[-\not{l} - (x+z-1)m_\mu + zm_\mu\right]u(p) = \bar{u}(p')\left[-\not{l} + (y+z)m_\mu\right]u(p). \tag{A.44}$$

Also, after using Eq. (A.20) we have

$$\left(\not{p}-\not{k}\right)(2k^\nu + q^\nu) = \left[-\not{l} + (y+z)m_\mu\right]\left[2l^\nu + (y-z)q^\nu + (1-y-z)(p+p')^\nu\right]. \tag{A.45}$$

Note that we can use the same symmetry argument as in the previous section and the integral of the term involving q^ν vanishes. Using Gordon identity the only non-vanishing

terms in the numerator are

$$-2\not{l}l^{\nu}+m_{\mu}(y+z)(1-y-z)(p+p')^{\nu}=-2\not{l}l^{\nu}+m_{\mu}(y+z)(1-y-z)\left(2m\gamma^{\nu}-i\sigma^{\nu\alpha}q_{\alpha}\right). \quad \text{(A.46)}$$

Since we are only interested in the coefficient of $\sigma^{\nu\alpha}$, we ignore all other terms. We get the same integral over l as in the previous section and a different integral over feynman parameters. From Eq. (A.22) we have

$$\bar{u}(p')\Gamma^{i,j,\nu}(p,p')u(p)=\frac{i\left(A^{i,j}_{L,L}+A^{i,j}_{R,R}\right)}{32\pi^2}\iint\frac{m_{\mu}(y+z)(1-y-z)dydz}{\Delta}\bar{u}(p')[i\sigma^{\nu\alpha}q_{\alpha}]u(p). \quad \text{(A.47)}$$

Assuming $m_{\mu}\ll m_n, m_s$, $q^2=0$, and after performing the integrals over y and z we get

$$\int_0^1 dz\int_0^{1-z}\frac{(y+z)(y+z-1)}{\Delta}dy=\frac{m_n^2\left(5m_s^2-m_n^2(x^2-2)\right)}{6\left(m_n^2-m_s^2\right)^3}+\frac{m_n^4m_s^2}{\left(m_n^2-m_s^2\right)^4}\ln\left(\frac{m_s^2}{m_n^2}\right). \quad \text{(A.48)}$$

After defining $J(x)\equiv\dfrac{x\ln x}{(x-1)^4}+\dfrac{x^2-5x-2}{6(x-1)^3}$ Eq. (A.48) becomes

$$\frac{m_n^2\left(5m_s^2-m_n^2(x^2-2)\right)}{6\left(m_n^2-m_s^2\right)^3}+\frac{m_n^4m_s^2}{\left(m_n^2-m_s^2\right)^4}\ln\left(\frac{m_s^2}{m_n^2}\right)=\frac{J(x)}{m_n^2}, \quad \text{(A.49)}$$

and Eq. (A.47) can now be written as

$$\bar{u}(p')\Gamma^{i,j,\nu}(p,p')u(p)=\frac{i\left(A^{i,j}_{L,L}+A^{i,j}_{R,R}\right)}{32\pi^2}\left[\frac{m_{\mu}}{m_{n_i}^2}J(x_{ij})\right]\bar{u}(p')\left[i\sigma^{\nu\alpha}q_{\alpha}\right]u(p). \quad \text{(A.50)}$$

By comparison we find that

$$F_2^{(2)}(q^2=0)=\sum_{i,j=1}^{2}i\left(\frac{A^{i,j}_{L,L}+A^{i,j}_{R,R}}{16\pi^2}\right)\left[\frac{m_{\mu}^2}{m_{n_i}^2}J(x_{ij})\right]. \quad \text{(A.51)}$$

In order to find the total correction to $g-2$ we add Eqs. (A.29) and (A.51)

$$F_2(q^2=0)=\sum_{i,j=1}^{2}i\left(\frac{A^{i,j}_{L,L}+A^{i,j}_{R,R}}{16\pi^2}\right)\left[\frac{m_{\mu}^2}{m_{n_i}^2}J(x_{ij})\right]+\sum_{i,j=1}^{2}\frac{\mathrm{Im}(A^{i,j}_{L,R})}{16\pi^2}\left[\frac{m_{\mu}}{m_{n_i}^2}G(x_{ij})\right], \quad \text{(A.52)}$$

and therefore

$$g-2 = 2F_2(q^2=0) = \frac{m_\mu}{8\pi^2}\sum_{i,j=1}^{2}\left[\mathrm{Im}(A_{L,R}^{i,j})\frac{G(x_{ij})}{m_{n_i}^2} + i\left(\frac{A_{L,L}^{i,j}+A_{R,R}^{i,j}}{2}\right)\frac{m_\mu}{m_{n_i}^2}J(x_{ij})\right]. \tag{A.53}$$

The dominant contribution to $g-2$ is given by

$$g-2\Big|_{\text{Dom.}} = \frac{m_\mu}{8\pi^2}\sum_{i,j=1}^{2}\mathrm{Im}(A_{L,R}^{i,j})\frac{G(x_{ij})}{m_{n_i}^2}. \tag{A.54}$$

Assuming that f' and f_μ are real couplings, we can expand Eq. (A.54)

$$g-2\Big|_{\text{Dom.}} = \frac{m_\mu}{8\pi^2}\left[\mathrm{Im}(A_{L,R}^{1,1})\frac{G(x_{11})}{m_{n_1}^2} + \mathrm{Im}(A_{L,R}^{1,2})\frac{G(x_{12})}{m_{n_1}^2} + \mathrm{Im}(A_{L,R}^{2,1})\frac{G(x_{21})}{m_{n_2}^2} + \mathrm{Im}(A_{L,R}^{2,2})\frac{G(x_{22})}{m_{n_2}^2}\right]. \tag{A.55}$$

Since $A_{L,R}^{1,2} = -A_{L,R}^{1,1}$ and $A_{L,R}^{2,2} = -A_{L,R}^{2,1}$ we can write Eq. (A.55) as

$$g-2\Big|_{\text{Dom.}} = \frac{m_\mu}{8\pi^2}\left[\mathrm{Im}(A_{L,R}^{1,1})\frac{G(x_{11})-G(x_{12})}{m_{n_1}^2} + \mathrm{Im}(A_{L,R}^{2,2})\frac{G(x_{22})-G(x_{21})}{m_{n_2}^2}\right]$$

$$= \frac{-f' f_\mu m_\mu \sin(2\theta_\mu)}{16\pi^2}\left[\frac{G(x_{11})-G(x_{12})}{m_{n_1}}\sin\theta_L\cos\theta_R + \frac{G(x_{22})-G(x_{21})}{m_{n_2}}\sin\theta_R\cos\theta_L\right] \tag{A.56}$$

A.3 Muon Mass

Muon acquires rediative mass through loop diagrams in Fig. A.3, where the amplitude for the first diagram is given by

$$\begin{aligned} i\mathcal{M} =& \int \frac{d^4k}{(2\pi)^4}\bar{u}(p)\,(if_\mu^* P_L\cos\theta_R)\frac{i(\not{p}-\not{k}+m_{n_1})}{(p-k)^2-m_{n_1}^2+i\epsilon}(-if'\sin\theta_L P_L)(\sin\theta_\mu\cos\theta_\mu) \\ &\times\frac{i}{k^2-m_{s_1}^2+i\epsilon}\,u(p) \\ =& M_{L,R}^{1,1}\int\frac{d^4k}{(2\pi)^4}\frac{\bar{u}(p)P_L u(p)}{[(p-k)^2-m_{n_1}^2+i\epsilon][k^2-m_{s_1}^2+i\epsilon]}, \end{aligned} \tag{A.57}$$

with,

$$M_{L,R}^{1,1} \equiv -f' f_\mu^* m_{n_1} \sin\theta_L \cos\theta_R \sin\theta_\mu \cos\theta_\mu. \tag{A.58}$$

Notice that if we assume that f and f_μ are real then $M_{L,R}^{i,j} = M_{R,L}^{i,j}$. Therefore, we can add their contributions. Furthermore, if we ignore the terms proportional to γ^5, the combined amplitude for diagrams in the first row of Fig. A.3 becomes

$$i\mathcal{M} = M^{1,1}\bar{u}(p)\left[\int \frac{d^4k}{(2\pi)^4} \frac{1}{\left[(p-k)^2 - m_{n_1}^2 + i\epsilon\right]\left[k^2 - m_{s_1}^2 + i\epsilon\right]}\right] u(p) \tag{A.59}$$

We now focus on doing the integral in Eq. (A.59) using the feynman parameters

$$\begin{aligned} I(m_n, m_s) &= \int \frac{d^4k}{(2\pi)^4} \frac{1}{\left[(p-k)^2 - m_{n_1}^2 + i\epsilon\right]\left[k^2 - m_{s_1}^2 + i\epsilon\right]} \\ &= \int \frac{d^4k}{(2\pi)^4} \frac{1}{AB} \end{aligned} \tag{A.60}$$

We then write

$$\frac{1}{AB} = \iint dx\, dy\, \delta(x+y-1)\frac{1}{D^2}, \quad D = xA + yB, \tag{A.61}$$

with $D = x\left[(p-k)^2 - m_n^2 + i\epsilon\right] + y\left[k^2 - m_s^2 + i\epsilon\right]$.

$$\begin{aligned} D &= x\left[k^2 + p^2 - 2k.p - m_n^2\right] + yk^2 - ym_s^2 + i\epsilon \\ &= k^2 - 2xp.k + \left(p^2 - m_n^2\right)x - ym_s^2 + i\epsilon, \end{aligned} \tag{A.62}$$

so D can be written in terms of l and Δ as follows

$$D = l^2 - \Delta + i\epsilon, \tag{A.63}$$

$$l^\mu \equiv k^\mu - xp^\mu, \tag{A.64}$$

$$\Delta \equiv x^2p^2 - x\left(p^2 - m_n^2\right) + ym_s^2. \tag{A.65}$$

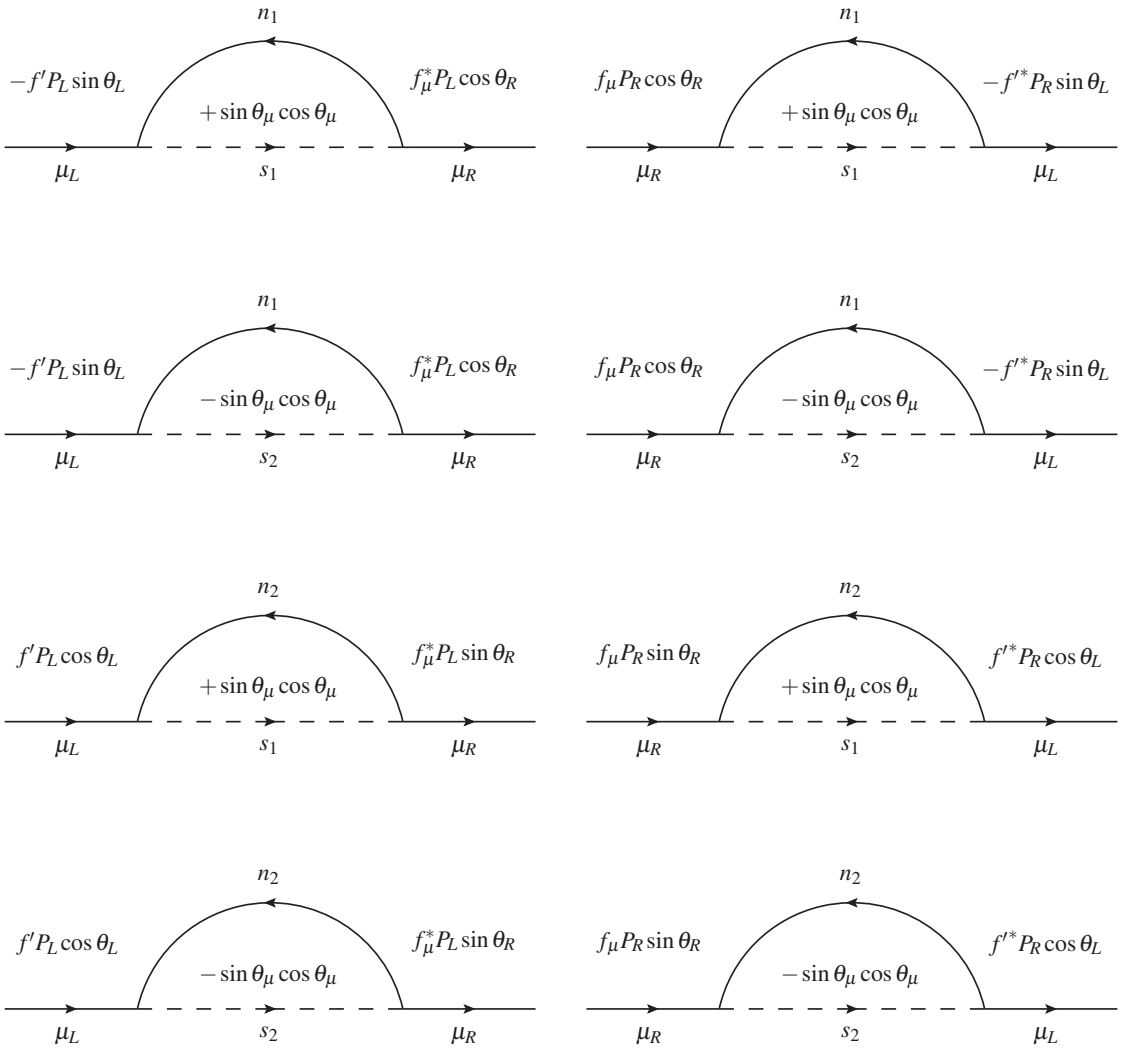

Figure A.3: Diagrams contributing to the muon mass.

Such that Eq. (A.60) becomes

$$I(m_n, m_s) = \iint dx\, dy\, \delta(x+y-1) \int \frac{d^4l}{(2\pi)^4} \frac{1}{\left(l^2 - \Delta + i\epsilon\right)^2}, \tag{A.66}$$

which is divergent, but we can combine the integrals from s_1 and s_2 and the sum will come out to be finite. Notice that there is a relative minus sign between them so that

$$\begin{aligned} &I(m_n,m_{s_1}) + I(m_n, m_{s_2}) = \\ &\iint dx\, dy\, \delta(x+y-1) \int \frac{d^4l}{(2\pi)^4} \left[\frac{1}{\left(l^2 - \Delta_{s_1} + i\epsilon\right)^2} - \frac{1}{\left(l^2 - \Delta_{s_2} + i\epsilon\right)^2} \right]. \end{aligned} \tag{A.67}$$

We now use Wick's rotation: $l^0 \equiv i l_E^0$, $\vec{l} \equiv \vec{l_E}$

$$\begin{aligned} \int \frac{d^4l}{(2\pi)^4} \frac{1}{\left(l^2 - \Delta + i\epsilon\right)^2} &= \frac{i}{(-1)^2} \int \frac{d^4l_E}{(2\pi)^4} \frac{1}{\left(l_E^2 + \Delta + i\epsilon\right)^2} = \frac{i}{(2\pi)^4} \int \frac{d^4l_E}{\left(l_E^2 + \Delta + i\epsilon\right)^2} \\ &= \frac{i}{(2\pi)^4} \int d\Omega_4 \int_0^\infty dl_E \frac{l_E^3}{\left(l_E^2 + \Delta + i\epsilon\right)^2}, \end{aligned} \tag{A.68}$$

where we first integrate over l from 0 to Λ

$$\int_0^\Lambda dl_E \frac{l_E^3}{(l_E^2 + \Delta + i\epsilon)^2} = \frac{-1}{2}(1 + \ln \Delta) + \frac{\Delta + (\Lambda^2 + \Delta)\ln(\Lambda^2 + \Delta)}{2(\Lambda^2 + \Delta)}, \tag{A.69}$$

and subsequently, we take the limit $\Lambda \to \infty$

$$\lim_{\Lambda\to\infty} \int_0^\Lambda dl_E \left[\frac{l_E^3}{(l_E^2 + \Delta_{s_1} + i\epsilon)^2} - \frac{l_E^3}{(l_E^2 + \Delta_{s_2} + i\epsilon)^2} \right] = \frac{1}{2} \ln\left(\frac{\Delta_{s_2}}{\Delta_{s_1}}\right). \tag{A.70}$$

The integral over l in Eq. (A.67) becomes

$$\begin{aligned} \int \frac{d^4l}{(2\pi)^4} \left[\frac{1}{(l^2 - \Delta_{s_1} + i\epsilon)^2} - \frac{1}{(l^2 - \Delta_{s_2} + i\epsilon)^2} \right] &= \frac{2i\pi^2}{(2\pi)^4} \frac{1}{2} \ln\left(\frac{\Delta_{s_2}}{\Delta_{s_1}}\right) \\ &= \frac{i}{16\pi^2} \ln\left(\frac{\Delta_{s_2}}{\Delta_{s_1}}\right). \end{aligned} \tag{A.71}$$

We now take the integral over the feynman parameters in Eq. (A.67)

$$I(m_n, m_{s_1}) + I(m_n, m_{s_2}) = \iint dx\, dy\, \delta(x+y-1) \frac{i}{16\pi^2} \ln\left(\frac{\Delta_{s_2}}{\Delta_{s_1}}\right). \tag{A.72}$$

The integral over y is done easily by setting $y = 1 - x$ in Δ_{s_1} and Δ_{s_2}

$$\frac{i}{16\pi^2}\int_0^1 dx \ln(\frac{\Delta_{s_2}}{\Delta_{s_1}}) = \frac{i}{16\pi^2}\left[\frac{m_{s_2}^2}{m_n^2 - m_{s_2}^2}\ln\left(\frac{m_n^2}{m_{s_2}^2}\right) - \frac{m_{s_1}^2}{m_n^2 - m_{s_1}^2}\ln\left(\frac{m_n^2}{m_{s_1}^2}\right)\right]. \tag{A.73}$$

Let us define $x_{ij} \equiv \left(\frac{m_{s_j}}{m_{n_i}}\right)^2$ so we have: $\frac{m_{s_j}^2}{m_{n_i}^2 - m_{s_j}^2}\ln\left(\frac{m_{n_i}^2}{m_{s_j}^2}\right) = \frac{x_{ij}}{x_{ij}-1}\ln x_{ij} \equiv H(x_{ij})$.

Eq. (A.73) can now be written as

$$I(m_{n_i}, m_{s_1}) + I(m_{n_i}, m_{s_2}) = \frac{i}{16\pi^2}\left[H(x_{i2}) - H(x_{i1})\right], \tag{A.74}$$

and the total amplitude from all the diagrams is given by

$$\begin{aligned} i\mathcal{M} &= \bar{u}(p)\left(M^{1,1}\frac{i}{16\pi^2}\left[H(x_{12}) - H(x_{11})\right] + M^{2,1}\frac{i}{16\pi^2}\left[H(x_{22}) - H(x_{21})\right]\right)u(p) \\ &= \bar{u}(p)\left(\frac{i}{16\pi^2}\right)\left(M^{1,1}\left[H(x_{12}) - H(x_{11})\right] + M^{2,1}\left[H(x_{22}) - H(x_{21})\right]\right)u(p) \qquad \text{(A.75)} \\ &= -im_{eff}\bar{u}(p)u(p), \\ \longrightarrow m_{eff} &= \left(\frac{1}{16\pi^2}\right)\left(M^{1,1}\left[H(x_{11}) - H(x_{12})\right] + M^{2,1}\left[H(x_{21}) - H(x_{22})\right]\right). \qquad \text{(A.76)} \end{aligned}$$

We now plug $M^{1,1}$ from Eq. (A.58) and evaluate $M^{2,1}$ for the last row of in Fig. A.3. We also assume that the couplings are real, so we get

$$\begin{aligned} m_\mu = \left(\frac{f' f_\mu \sin(2\theta_\mu)}{32\pi^2}\right)\big(&\sin\theta_L\cos\theta_R m_{n_1}\left[H(x_{12}) - H(x_{11})\right] \\ &+ \sin\theta_R\cos\theta_L m_{n_2}\left[H(x_{21}) - H(x_{22})\right]\big). \end{aligned} \tag{A.77}$$

We then solve for $\frac{f' f_\mu \sin(2\theta_\mu)}{16\pi^2}$ using Eq. (A.77)

$$\frac{-f' f_\mu \sin(2\theta_\mu)}{16\pi^2} = \frac{2m_\mu}{\sin\theta_L\cos\theta_R m_{n_1}[H(x_{11}) - H(x_{12})] + \sin\theta_R\cos\theta_L m_{n_2}[H(x_{22}) - H(x_{21})]}. \tag{A.78}$$

Eq. (A.56) can now be rewritten as

$$g-2\Big|_{\text{Dom.}} = \frac{2m_\mu^2\left(\frac{G(x_{11}) - G(x_{12})}{m_{n_1}}\sin\theta_L\cos\theta_R + \frac{G(x_{22}) - G(x_{21})}{m_{n_2}}\sin\theta_R\cos\theta_L\right)}{\sin\theta_L\cos\theta_R m_{n_1}\left[H(x_{11}) - H(x_{12})\right] + \sin\theta_R\cos\theta_L m_{n_2}\left[H(x_{22}) - H(x_{21})\right]}. \tag{A.79}$$

Appendix B

Higgs Yukawa Anomalous Coupling

The following Yukawa and trilinear terms are relevant for the Higgs interactions

$$\mathcal{L} \supset \frac{f_D}{\sqrt{2}} h \overline{N_L} E_R^0 + \frac{f_F}{\sqrt{2}} h \overline{E_L^0} N_R + \frac{f_D}{\sqrt{2}} h \overline{E_R^0} N_L + \frac{f_F}{\sqrt{2}} h \overline{N_R} E_L^0 + (\lambda_x v)\ h \left(x^* x + x'^* x' + x''^* x'' \right) + (\lambda_{y_1} v)\ h y_1^* y_1 + (\lambda_{y_2} v)\ h y_2^* y_2 + (\lambda_{y_3} v)\ h y_3^* y_3 \tag{B.1}$$

Using Eq. (B.2), we can write the trilinear terms in the mass eigenstate basis

$$\begin{pmatrix} x'' \\ y_3 \end{pmatrix} = \begin{pmatrix} \cos\theta_\tau & -\sin\theta_\tau \\ \sin\theta_\tau & \cos\theta_\tau \end{pmatrix} \begin{pmatrix} \xi_{1\tau} \\ \xi_{2\tau} \end{pmatrix} \tag{B.2}$$

The terms for third family becomes

$$\begin{aligned}(\lambda_x v)\ h\left(x''^* x''\right) + (\lambda_{y_3} v)\, h y_3^* y_3 &= (\lambda_x v)\ h\left(\cos\theta_\tau \xi_1^* - \sin\theta_\tau \xi_2^*\right)\left(\cos\theta_\tau \xi_1 - \sin\theta_\tau \xi_2\right) \\ &\quad + (\lambda_{y_3} v)\ h\left(\sin\theta_\tau \xi_1^* + \cos\theta_\tau \xi_2^*\right)\left(\sin\theta_\tau \xi_1 + \cos\theta_\tau \xi_2\right) \\ &= \left(\lambda_x \cos^2\theta_\tau + \lambda_{y_3} \sin^2\theta_\tau\right) v h \xi_1^* \xi_1 \\ &\quad + \left(\lambda_x \sin^2\theta_\tau + \lambda_{y_3} \cos^2\theta_\tau\right) v h \xi_2^* \xi_2 \\ &\quad + \left(v \sin\theta_\tau \cos\theta_\tau\right)\left(\lambda_{y_3} - \lambda_x\right)\left[h\xi_1^* \xi_2 + h\xi_2^* \xi_1\right].\end{aligned} \tag{B.3}$$

Let's define h_{ij} as follows

$$h_{11} \equiv \left(\lambda_x \cos^2\theta_\tau + \lambda_{y_3} \sin^2\theta_\tau\right) v, \tag{B.4}$$

$$h_{22} \equiv \left(\lambda_x \sin^2\theta_\tau + \lambda_{y_3} \cos^2\theta_\tau\right) v, \tag{B.5}$$

$$h_{12} = h_{21} \equiv \left(v \sin\theta_\tau \cos\theta_\tau\right)\left(\lambda_{y_3} - \lambda_x\right). \tag{B.6}$$

We can use Eq. (B.7) to rewrite the Yukawa terms in Eq. (B.1) in masss eigenstates

$$\begin{pmatrix} N \\ E^0 \end{pmatrix}_L = \begin{pmatrix} \cos\theta_L & \sin\theta_L \\ -\sin\theta_L & \cos\theta_L \end{pmatrix} \begin{pmatrix} n_{1L} \\ n_{2L} \end{pmatrix}, \quad \begin{pmatrix} N \\ E^0 \end{pmatrix}_R = \begin{pmatrix} \cos\theta_R & \sin\theta_R \\ -\sin\theta_R & \cos\theta_R \end{pmatrix} \begin{pmatrix} n_{1R} \\ n_{2R} \end{pmatrix}, \tag{B.7}$$

as

$$\overline{E_L^0} = -\sin\theta_L \overline{n_{1L}} + \cos\theta_L \overline{n_{2L}}, \tag{B.8}$$

$$E_R^0 = -\sin\theta_R n_{1R} + \cos\theta_R n_{2R}, \tag{B.9}$$

$$\overline{N_L} = \cos\theta_L \overline{n_{1L}} + \sin\theta_L \overline{n_{2L}}, \tag{B.10}$$

$$N_R = \cos\theta_R n_{1R} + \sin\theta_R n_{2R}, \tag{B.11}$$

so Eq. (B.1) becomes

$$\begin{aligned}
\frac{f_D}{\sqrt{2}}h\overline{N_L}E_R^0+\frac{f_F}{\sqrt{2}}h\overline{E_L^0}N_R+h.c. = &\frac{f_F}{\sqrt{2}}h\left(\cos\theta_L\overline{n_{1L}}+\sin\theta_L\overline{n_{2L}}\right)\left(-\sin\theta_R n_{1R}+\cos\theta_R n_{2R}\right)\\
&+\frac{f_F}{\sqrt{2}}h\left(-\sin\theta_L\overline{n_{1L}}+\cos\theta_L\overline{n_{2L}}\right)\left(\cos\theta_R n_{1R}+\sin\theta_R n_{2R}\right)+h.c.\\
=&\frac{-h}{\sqrt{2}}\left(f_D\cos\theta_L\sin\theta_R+f_F\sin\theta_L\cos\theta_R\right)\overline{n_1}n_1\\
&+\frac{\overline{n_1}}{\sqrt{2}}\left[(\cos\theta_L\cos\theta_R f_D-\sin\theta_L\sin\theta_R f_F)P_R\right.\\
&\qquad\left.-\left(\sin\theta_L\sin\theta_R f_D-\cos\theta_L\cos\theta_R f_F\right)P_L\right]n_2\\
&+\frac{h\overline{n_2}}{\sqrt{2}}\left[\left(\cos\theta_L\cos\theta_R f_F-\sin\theta_L\sin\theta_R f_D\right)P_R\right.\\
&\qquad\left.-\left(\sin\theta_L\sin\theta_R f_F-\cos\theta_L\cos\theta_R f_D\right)P_L\right]n_1\\
&+\frac{h}{\sqrt{2}}\left(f_D\sin\theta_L\cos\theta_R+f_F\cos\theta_L\sin\theta_R\right)\overline{n_2}n_2.
\end{aligned}\tag{B.12}$$

Let's also define h_{ij}^n as follows

$$h_{11}^n\equiv\frac{-1}{\sqrt{2}}\left(f_D\cos\theta_L\sin\theta_R+f_F\sin\theta_L\cos\theta_R\right)\tag{B.13}$$

$$h_{22}^n\equiv\frac{1}{\sqrt{2}}\left(f_D\sin\theta_L\cos\theta_R+f_F\cos\theta_L\sin\theta_R\right)\tag{B.14}$$

$$h_{12}^n\equiv\frac{1}{\sqrt{2}}\left[\left(\cos\theta_L\cos\theta_R f_D-\sin\theta_L\sin\theta_R f_F\right)P_R-\left(\sin\theta_L\sin\theta_R f_D-\cos\theta_L\cos\theta_R f_F\right)P_L\right]\tag{B.15}$$

$$h_{21}^n\equiv\frac{1}{\sqrt{2}}\left[\left(\cos\theta_L\cos\theta_R f_F-\sin\theta_L\sin\theta_R f_D\right)P_R-\left(\sin\theta_L\sin\theta_R f_F-\cos\theta_L\cos\theta_R f_D\right)P_L\right].\tag{B.16}$$

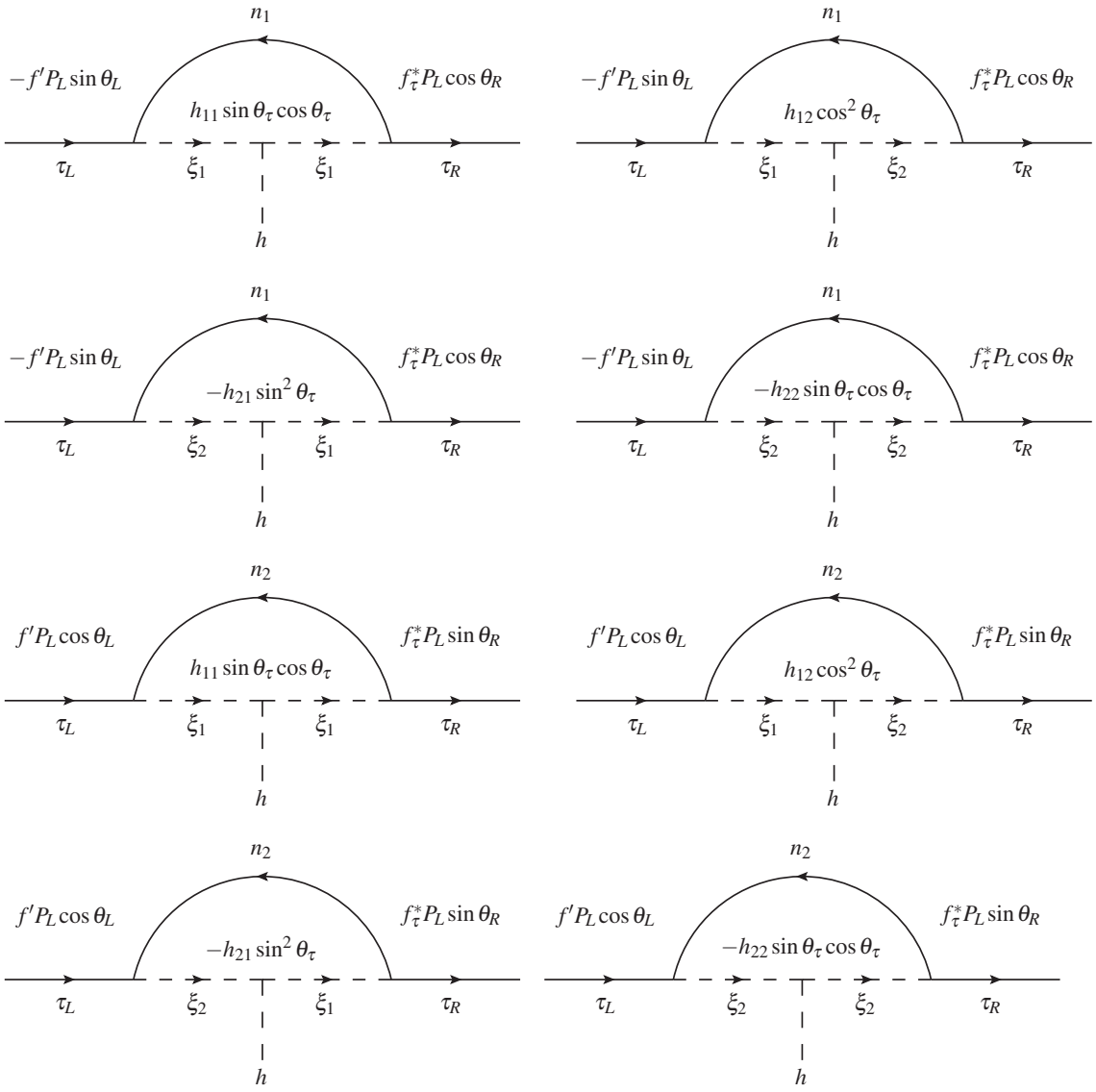

Figure B.1: Relevant diagrams to the effective Higgs Yukawa coupling from $\tau_L \to \tau_R$ involving $h\xi_i^*\xi_j$ terms.

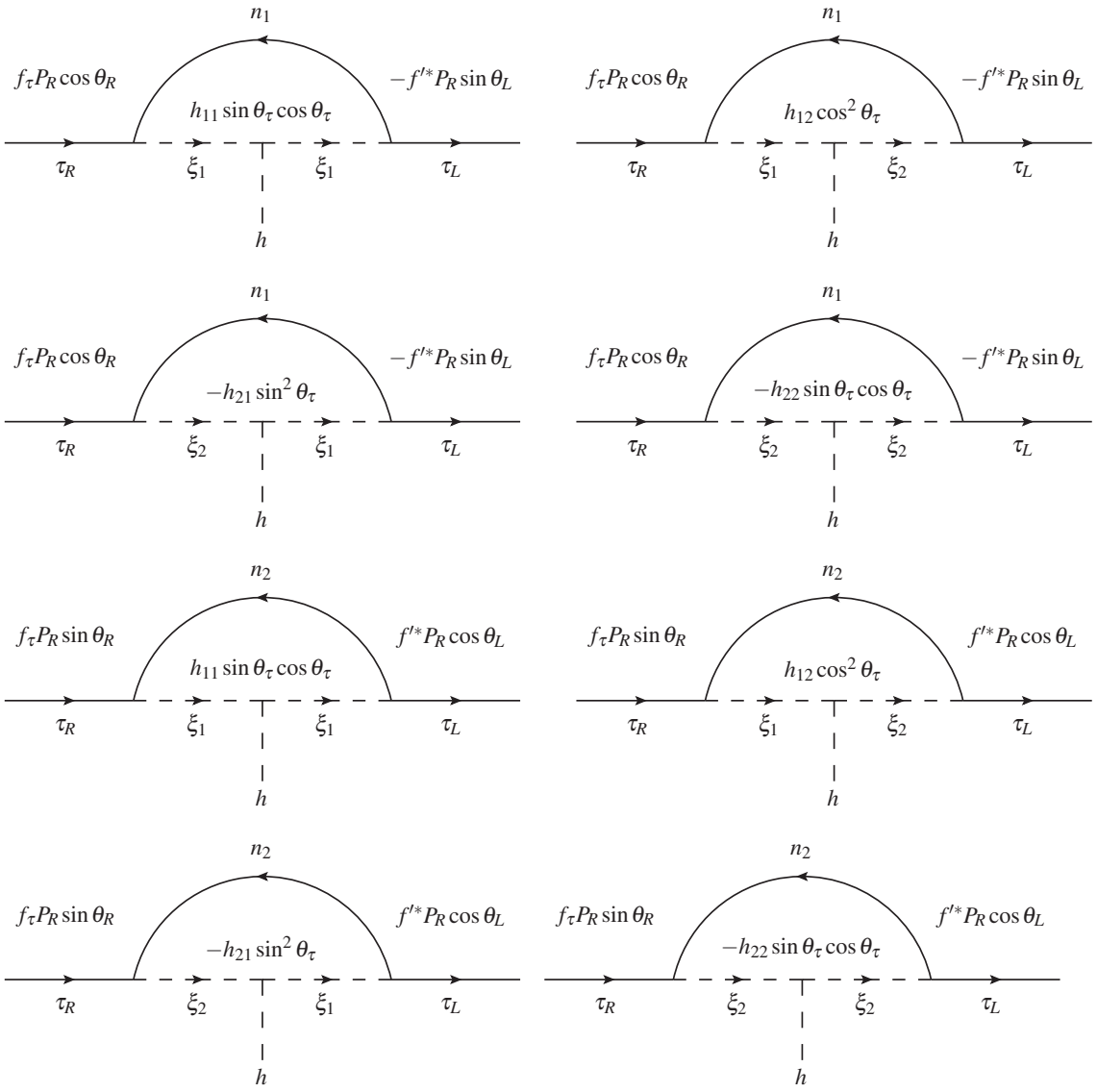

Figure B.2: Relevant diagrams to the effective Higgs Yukawa coupling from $\tau_R \to \tau_L$ involving $h\xi_i^*\xi_j$ terms.

B.1 Effective Higgs Yukawa Coupling: $h\xi_i^*\xi_j$ Terms

The amplitude of the first diagram in Fig. B.1 can be written as

$$\begin{aligned} i\mathcal{M} = \int \frac{d^4k}{(2\pi)^4} \bar{u}(p+q)\left(if_\tau^* P_L \cos\theta_R\right) \frac{i\left(\not{p} - \not{k} + m_{n_1}\right)}{(p-k)^2 - m_{n_1}^2 + i\epsilon} \left(-if' \sin\theta_L P_L\right) \\ \times \left(\sin\theta_\tau \cos\theta_\tau\right) \frac{i}{k^2 - m_{\xi_1}^2 + i\epsilon} \left(ih_{11}\right) \frac{i}{(k+q)^2 - m_{\xi_1}^2 + i\epsilon} u(p). \end{aligned} \tag{B.17}$$

Assuming that the couplings are real and adding the contributions from the similar diagram in $(R \to L)$ in Fig. B.2, the scalar part of the amplitude becomes

$$i\mathcal{M} = \int \frac{d^4k}{(2\pi)^4} \frac{\bar{u}(p+q)\left[f_\tau \cos\theta_R m_{n_1} f' \sin\theta_L \sin\theta_\tau \cos\theta_\tau h_{11}\right] u(p)}{\left[(p-k)^2 - m_{n_1}^2 + i\epsilon\right]\left[k^2 - m_{\xi_1}^2 + i\epsilon\right]\left[(k+q)^2 - m_{\xi_1}^2 + i\epsilon\right]}. \tag{B.18}$$

The denominator in Eq. (B.18) is the same as in Eq. (A.2), so it can be written as

$$\begin{aligned} I(m_n, m_\xi) &\equiv \int \frac{d^4k}{(2\pi)^4} \frac{1}{\left[(p-k)^2 - m_n^2 + i\epsilon\right]\left[k^2 - m_\xi^2 + i\epsilon\right]\left[(k+q)^2 - m_\xi^2 + i\epsilon\right]} \\ &= \iiint dxdydz \int \frac{d^4l}{(2\pi)^4} \frac{2}{\left(l^2 - \Delta + i\epsilon\right)^3} = \iiint dxdydz \frac{-i}{(4\pi)^2} \frac{1}{\Delta}, \end{aligned} \tag{B.19}$$

with

$$\Delta \approx (m_\xi^2 - m_n^2)(y+z) + m_n^2. \tag{B.20}$$

Then we have

$$I(m_n, x) = \frac{-i}{(4\pi)^2} \frac{x - 1 - \ln x}{m_n^2 (x-1)^2}, \tag{B.21}$$

with $x \equiv (m_\xi/m_n)^2$ and Eq. (B.18) becomes

$$i\mathcal{M} = \bar{u}(p+q)\left[\frac{-i}{(4\pi)^2} \frac{x_{11} - 1 - \ln x_{11}}{m_{n_1}^2 (x_{11}-1)^2} f_\tau \cos\theta_R m_{n_1} f' \sin\theta_L \sin\theta_\tau \cos\theta_\tau h_{11}\right] u(p) \tag{B.22}$$

The correction to the effective coupling to the Higgs boson from Eq. (B.22) is

$$f_{11}^\xi \supset \frac{f_\tau f' \cos\theta_R \sin\theta_L \sin\theta_\tau \cos\theta_\tau h_{11}}{16\pi^2 m_{n_1}} F(x_{11}, x_{11}), \tag{B.23}$$

where $F(x_{11},x_{11}) \equiv \dfrac{1}{x_{11}-1} - \dfrac{\ln x_{11}}{(x_{11}-1)^2}$. Let's do the integral for the diagram with Higgs connected to ξ_1 and ξ_2 in the first row of Fig. B.1 and B.2. The addition of these two diagrams is given by

$$i\mathcal{M} = \int \frac{d^4k}{(2\pi)^4} \frac{\bar{u}(p+q)\left[f_\tau \cos\theta_R m_{n_1} f' \sin\theta_L \cos^2\theta_\tau h_{12}\right] u(p)}{\left[(p-k)^2 - m_{n_1}^2 + i\epsilon\right]\left[k^2 - m_{\xi_1}^2 + i\epsilon\right]\left[(k+q)^2 - m_{\xi_2}^2 + i\epsilon\right]}. \tag{B.24}$$

Now we can write

$$\frac{1}{\left[(p-k)^2 - m_{n_1}^2 + i\epsilon\right]\left[k^2 - m_{\xi_1}^2 + i\epsilon\right]\left[(k+q)^2 - m_{\xi_2}^2 + i\epsilon\right]}, \tag{B.25}$$

as

$$\iiint dxdydz\delta(x+y+z-1)\frac{2}{D^3}, \tag{B.26}$$

however, this time we have

$$\begin{aligned} D &= x\left[k^2 + p^2 - 2k.p - m_{n_1}^2\right] + yk^2 - ym_{\xi_1}^2 + z\left[k^2 + q^2 + 2k.q\right] - zm_{\xi_2}^2 + i\epsilon \\ &= k^2 + 2(zq - xp).k + (p^2 - m_n^2)x - ym_{\xi_1}^2 + z(q^2 - m_{\xi_2}^2) + i\epsilon, \end{aligned} \tag{B.27}$$

so D can be written in terms of l and Δ as follows

$$D = l^2 - \Delta + i\epsilon, \tag{B.28}$$

$$l^\mu \equiv k^\mu + zq^\mu - xp^\mu, \tag{B.29}$$

$$\Delta \equiv z^2q^2 - z(q^2 - m_{\xi_2}^2) + x^2p^2 - 2xz(p.q) - x(p^2 - m_{n_1}^2) + ym_{\xi_1}^2. \tag{B.30}$$

Using $x+y+z=1$, and assuming $m_\tau \ll m_n, m_\xi$ in the non-relativistic limit we have

$$\Delta \approx zm_{\xi_2}^2 + (1-y-z)m_{n_1}^2 + ym_{\xi_1}^2. \tag{B.31}$$

After doing the integral over l, we get

$$I(m_n, m_{\xi_1}, m_{\xi_2}) \equiv \iint dydz \frac{-i}{(4\pi)^2}\frac{1}{\Delta} = \frac{-i}{(4\pi)^2}\frac{F(x_{11},x_{12})}{m_n^2}, \tag{B.32}$$

where

$$F(x_{11}, x_{12}) \equiv \frac{1}{x_{11} - x_{12}} \left[\frac{x_{11}}{x_{11} - 1} \ln x_{11} - \frac{x_{12}}{x_{12} - 1} \ln x_{12} \right]. \tag{B.33}$$

Then Eq. (B.24) becomes

$$i\mathcal{M} = \bar{u}(p+q) \left[f' f_\tau \cos\theta_R m_{n_1} \sin\theta_L \cos^2\theta_\tau h_{12} \right] \left(\frac{-i}{16\pi^2} \right) \frac{F(x_{11}, x_{12})}{m_{n_1}^2} u(p). \tag{B.34}$$

The correction to the effective coupling to the Higgs boson from Eq. (B.34) is

$$f_{12}^\xi \supset \frac{f' f_\tau \cos\theta_R \sin\theta_L \cos^2\theta_\tau h_{12}}{16\pi^2 m_{n_1}} F(x_{11}, x_{12}). \tag{B.35}$$

Likewise we can write

$$f_{21}^\xi \supset \frac{-f' f_\tau \cos\theta_R \sin\theta_L \sin^2\theta_\tau h_{21}}{16\pi^2 m_{n_1}} F(x_{12}, x_{11}) \tag{B.36}$$

$$f_{22}^\xi \supset \frac{-f_\tau f' \cos\theta_R \sin\theta_L \sin\theta_\tau \cos\theta_\tau h_{22}}{16\pi^2 m_{n_1}} F(x_{12}, x_{12}). \tag{B.37}$$

Now, we can add the lower diagrams with n_2 in the loops

$$f_{11}^\xi = \frac{h_{11} f_\tau f' \sin\theta_\tau \cos\theta_\tau}{16\pi^2} \left[\frac{\cos\theta_R \sin\theta_L}{m_{n_1}} F(x_{11}, x_{11}) - \frac{\cos\theta_L \sin\theta_R}{m_{n_2}} F(x_{21}, x_{21}) \right] \tag{B.38}$$

$$f_{12}^\xi = \frac{h_{12} f_\tau f' \cos^2\theta_\tau}{16\pi^2} \left[\frac{\cos\theta_R \sin\theta_L}{m_{n_1}} F(x_{11}, x_{12}) - \frac{\cos\theta_L \sin\theta_R}{m_{n_2}} F(x_{21}, x_{22}) \right] \tag{B.39}$$

$$f_{21}^\xi = \frac{h_{21} f_\tau f' \sin^2\theta_\tau}{16\pi^2} \left[\frac{\cos\theta_L \sin\theta_R}{m_{n_2}} F(x_{22}, x_{21}) - \frac{\cos\theta_R \sin\theta_L}{m_{n_1}} F(x_{12}, x_{11}) \right] \tag{B.40}$$

$$f_{22}^\xi = \frac{h_{22} f_\tau f' \sin\theta_\tau \cos\theta_\tau}{16\pi^2} \left[\frac{\cos\theta_L \sin\theta_R}{m_{n_2}} F(x_{22}, x_{22}) - \frac{\cos\theta_R \sin\theta_L}{m_{n_1}} F(x_{12}, x_{12}) \right] \tag{B.41}$$

B.2 Effective Higgs Yukawa Coupling: $h\overline{n}_i n_j$ Terms

The amplitude of the first diagram in Fig. B.3 can be written as

$$\begin{aligned} i\mathcal{M}_{LR} &= \int \frac{d^4k}{(2\pi)^4}\bar{u}(p+q)(if_\tau^* P_L\cos\theta_R)\frac{i(\not{k}+\not{q}+m_{n_1})}{(q+k)^2-m_{n_1}^2+i\epsilon}(ih_{11}^n\sin\theta_\tau\cos\theta_\tau) \\ &\times\frac{i(\not{k}+m_{n_1})}{k^2-m_{n_1}^2+i\epsilon}(-if'\sin\theta_L P_L)\frac{i}{(p-k)^2-m_{\xi_1}^2+i\epsilon}u(p) \\ &= \bar{u}(p+q)\int\frac{d^4k}{(2\pi)^4}\frac{[h_{11}^n f' f_\tau^*\sin\theta_L\cos\theta_R\sin\theta_\tau\cos\theta_\tau][(\not{k}+\not{q})\not{k}P_L+m_{n_1}^2P_L]}{[(q+k)^2-m_{n_1}^2+i\epsilon][k^2-m_{n_1}^2+i\epsilon][(p-k)^2-m_{\xi_1}^2+i\epsilon]}u(p) \end{aligned} \tag{B.42}$$

Note that: $\not{q} = \not{p}' - \not{p}$, so using Dirac equation we have, $\bar{u}(p+q)\not{q} = \bar{u}(p')[\not{p}' - \not{p}] = \bar{u}(p')[m_\tau - \not{p}]$. Also, we can write $\not{p}\not{k}u(p)$ as $\not{p}\not{k}u(p) = [2p.k - \not{k}\not{p}]u(p) = [2p.k - \not{k}m_\tau]u(p)$. Using $\not{k}\not{k} = k^2$ we have $i\mathcal{M}_{LR} = \bar{u}(p+q)\,\mathcal{O}_{\rm LR}\,u(p)$, where

$$\mathcal{O}_{\rm LR} = \int\frac{d^4k}{(2\pi)^4}\frac{[h_{11}^n f' f_\tau^*\sin\theta_L\cos\theta_R\sin\theta_\tau\cos\theta_\tau][(k^2-2p.k+m_{n_1}^2)P_L+m_\tau\not{k}]}{[(q+k)^2-m_{n_1}^2+i\epsilon][k^2-m_{n_1}^2+i\epsilon][(p-k)^2-m_{\xi_1}^2+i\epsilon]}. \tag{B.43}$$

The amplitude for the first diagram in Fig. B.4 is: $i\mathcal{M}_{RL} = \bar{u}(p+q)\,\mathcal{O}_{\rm RL}\,u(p)$, where

$$\mathcal{O}_{\rm RL} = \int\frac{d^4k}{(2\pi)^4}\frac{[h_{11}^n f'^* f_\tau\sin\theta_L\cos\theta_R\sin\theta_\tau\cos\theta_\tau][(k^2-2p.k+m_{n_1}^2)P_R+m_\tau\not{k}]}{[(q+k)^2-m_{n_1}^2+i\epsilon][k^2-m_{n_1}^2+i\epsilon][(p-k)^2-m_{\xi_1}^2+i\epsilon]}. \tag{B.44}$$

If we assume that the couplings are real, the addition of the amplitudes is given by

$$\mathcal{O} = \int\frac{d^4k}{(2\pi)^4}\frac{[h_{11}^n f' f_\tau\sin\theta_L\cos\theta_R\sin\theta_\tau\cos\theta_\tau]\left[k^2-2p.k+m_{n_1}^2+2m_\tau\not{k}\right]}{\left[(p-k)^2-m_{\xi_1}^2+i\epsilon\right]\left[k^2-m_{n_1}^2+i\epsilon\right]\left[(q+k)^2-m_{n_1}^2+i\epsilon\right]} \tag{B.45}$$

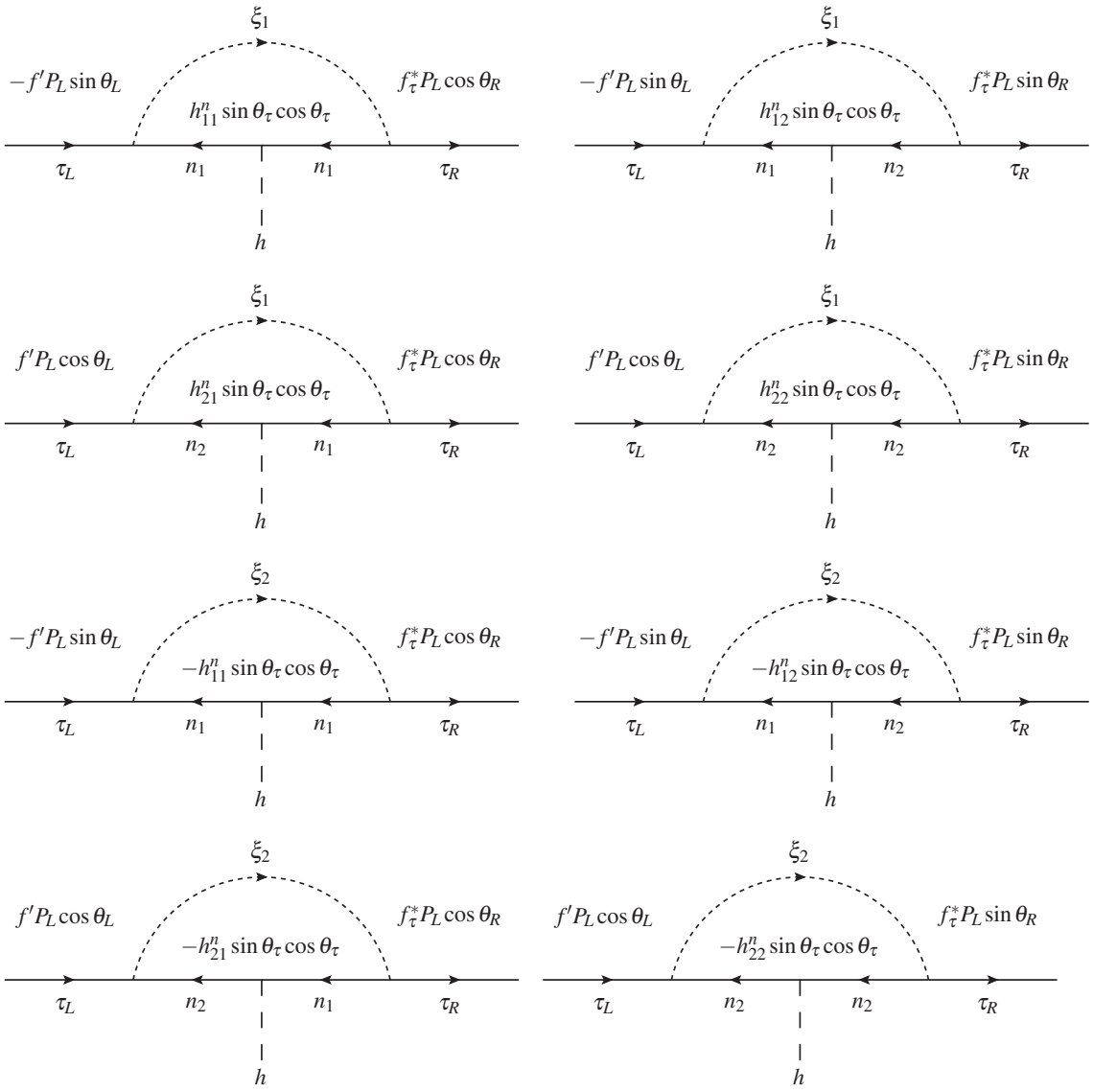

Figure B.3: Relevant diagrams to the effective Higgs Yukawa coupling from $\tau_L \to \tau_R$ involving $h\overline{n}_i n_j$ terms.

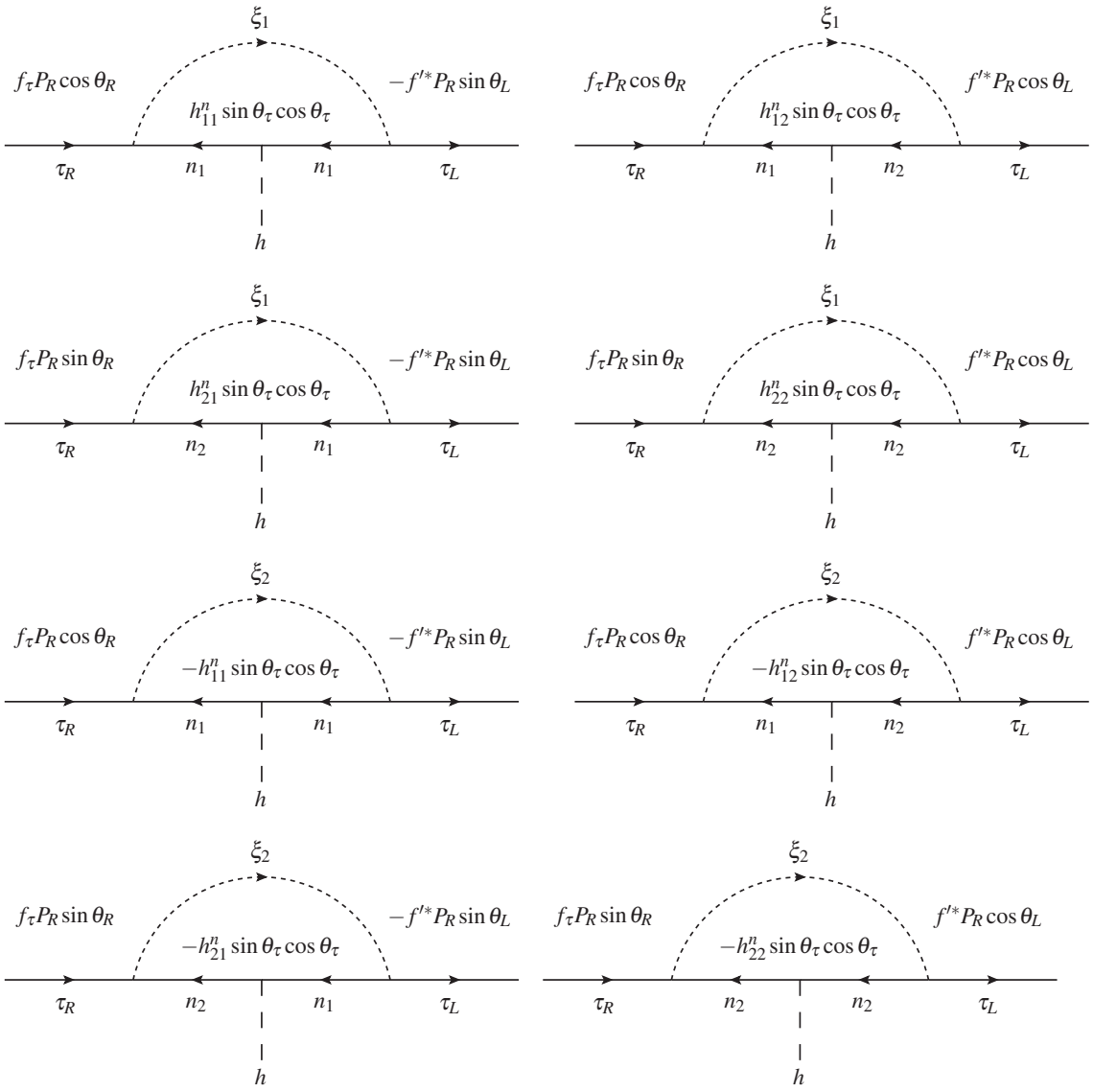

Figure B.4: Relevant diagrams to the effective Higgs Yukawa coupling from $\tau_R \to \tau_L$ involving $h\overline{n}_i n_j$ terms.

Now, we can write the integral

$$\frac{1}{[(p-k)^2 - m_{\xi_1}^2 + i\epsilon][k^2 - m_{n_1}^2 + i\epsilon][(k+q)^2 - m_{n_1}^2 + i\epsilon]}, \tag{B.46}$$

in terms of feynman parameters as follows

$$\iiint dx\, dy\, dz\, \delta(x+y+z-1)\frac{2}{D^3}, \tag{B.47}$$

with $D = x\left[(p-k)^2 - m_{\xi_1}^2 + i\epsilon\right] + y\left[k^2 - m_{n_1}^2 + i\epsilon\right] + z\left[(k+q)^2 - m_{n_1}^2 + i\epsilon\right].$

$$\begin{aligned} D &= x\left[k^2 + p^2 - 2k.p - m_{\xi_1}^2\right] + yk^2 - ym_{n_1}^2 + z\left[k^2 + q^2 + 2k.q\right] - zm_{n_1}^2 + i\epsilon \\ &= k^2 + 2\left(zq - xp\right).k + \left(p^2 - m_{\xi_1}^2\right)x - ym_{n_1}^2 + z\left(q^2 - m_{n_1}^2\right) + i\epsilon, \end{aligned} \tag{B.48}$$

such that, D can be written in terms of l and Δ as

$$D = l^2 - \Delta + i\epsilon, \tag{B.49}$$

$$l^\mu \equiv k^\mu + zq^\mu - xp^\mu, \tag{B.50}$$

$$\Delta \equiv z^2q^2 - z\left(q^2 - m_{n_1}^2\right) + x^2p^2 - 2xz\left(p.q\right) - x\left(p^2 - m_{\xi_1}^2\right) + ym_{n_1}^2. \tag{B.51}$$

Using $x + y + z = 1$, and assuming $m_\tau \ll m_n, m_\xi$ in the non-relativistic limit we have

$$\Delta \approx (m_{n_1}^2 - m_{\xi_1}^2)(y+z) + m_{\xi_1}^2. \tag{B.52}$$

The numerator may be written using the following relations

$$\longrightarrow \qquad k = l - zq + xp \tag{B.53}$$

$$\longrightarrow \qquad k^2 = l^2 + z^2q^2 + x^2p^2 - 2z\left(q.l\right) - 2xz\left(p.q\right) + 2x\left(l.p\right) \tag{B.54}$$

$$\longrightarrow \qquad -2p.k = -2p.l + 2z\left(q.p\right) - 2xp^2 \tag{B.55}$$

Assuming $m_\tau \ll m_n, m_\xi$, in the non-relativistic limit the numerator in Eq. (B.45) becomes

$$k^2 - 2p.k + m_{n_1}^2 + 2m_\tau \not{k} \approx l^2 + m_{n_1}^2, \tag{B.56}$$

so Eq. (B.45) can be written as

$$i\mathcal{M} = \bar{u}(p+q)h_{11}^{n} f' f_\tau \sin\theta_L \cos\theta_R \sin\theta_\tau \cos\theta_\tau \iint dydz \int \frac{d^4l}{(2\pi)^4} \frac{2\left(l^2 + m_{n_1}^2\right)}{\left(l^2 - \Delta + i\epsilon\right)^3} u(p). \tag{B.57}$$

The integral in Eq. (B.57) is divergent. However, we can combine the integrals from ξ_1 and ξ_2, and the sum will come out to be finite. Notice that there is a relative minus sign between them so

$$I(m_{n_1}, m_\xi) = \iint dydz \int \frac{d^4l}{8\pi^4} \frac{l^2 + m_{n_1}^2}{\left(l^2 - \Delta + i\epsilon\right)^3} \tag{B.58}$$

$$\longrightarrow I(m_{n_1}, m_{\xi_1}) + I(m_{n_1}, m_{\xi_2}) = \iint dxdy \int \frac{d^4l}{8\pi^4} \left[\frac{l^2 + m_{n_1}^2}{\left(l^2 - \Delta_{\xi_1} + i\epsilon\right)^3} - \frac{l^2 + m_{n_1}^2}{\left(l^2 - \Delta_{\xi_2} + i\epsilon\right)^3} \right]. \tag{B.59}$$

After doing Wick's rotation: $l^0 \equiv i l_E^0$, $\vec{l} \equiv \vec{l_E}$ we have

$$\begin{aligned} \int \frac{d^4l}{8\pi^4} \frac{l^2 + m_{n_1}^2}{\left(l^2 - \Delta + i\epsilon\right)^3} &= \frac{i}{(-1)^3} \int \frac{d^4l_E}{8\pi^4} \frac{-l_E^2 + m_{n_1}^2}{\left(l_E^2 + \Delta + i\epsilon\right)^3} = \frac{i}{8\pi^4} \int d^4l_E \frac{l_E^2 - m_{n_1}^2}{\left(l_E^2 + \Delta + i\epsilon\right)^3} \\ &= \frac{i}{8\pi^4} \int d\Omega_4 \int_0^\infty dl_E \frac{l_E^5 - m_{n_1}^2 l_E^3}{\left(l_E^2 + \Delta + i\epsilon\right)^3} = \frac{i}{4\pi^2} \int_0^\infty dl_E \frac{l_E^5 - m_{n_1}^2 l_E^3}{\left(l_E^2 + \Delta + i\epsilon\right)^3}. \end{aligned} \tag{B.60}$$

We take the integral in Eq. (B.60) from 0 to Λ, then we take the limit $\Lambda \to \infty$.

$$\int_0^\Lambda dl_E \frac{l_E^5}{(l_E^2 + \Delta + i\epsilon)^3} = \frac{-1}{4}(3 + 2\ln\Delta) + \frac{\Delta(3\Delta + 4\Lambda^2) + 2(\Lambda^2 + \Delta)^2 \ln(\Lambda^2 + \Delta)}{(\Lambda^2 + \Delta)^2}, \tag{B.61}$$

$$\int_0^\infty dl_E \frac{l_E^3}{(l_E^2 + \Delta + i\epsilon)^3} = \frac{1}{4\Delta}. \tag{B.62}$$

Now, we take the limit $\Lambda \to \infty$ of Eq. (B.61)

$$\lim_{\Lambda\to\infty} \int_0^\Lambda dl_E \left[\frac{l_E^5}{(l_E^2 + \Delta_{\xi_1} + i\epsilon)^3} - \frac{l_E^5}{(l_E^2 + \Delta_{\xi_2} + i\epsilon)^3} \right] = \frac{1}{2} \ln\left(\frac{\Delta_{\xi_2}}{\Delta_{\xi_1}}\right). \tag{B.63}$$

Eq. (B.59) becomes

$$\begin{aligned} I(m_{n_1}, m_{\xi_1}) + I(m_{n_1}, m_{\xi_2}) &= \iint dxdy \frac{i}{4\pi^2} \left[\frac{1}{2} \ln\left(\frac{\Delta_{\xi_2}}{\Delta_{\xi_1}}\right) - \frac{m_{n_1}^2}{4} \left(\frac{1}{\Delta_{\xi_1}} - \frac{1}{\Delta_{\xi_2}} \right) \right] \\ &= \frac{-i}{8\pi^2} \iint dxdy \left[\ln\left(\frac{\Delta_{\xi_1}}{\Delta_{\xi_2}}\right) - \frac{m_{n_1}^2}{2} \left(\frac{1}{\Delta_{\xi_2}} - \frac{1}{\Delta_{\xi_1}} \right) \right] \\ &= \frac{-i}{8\pi^2} \left[F_N(x_{11}, x_{11}) - F_N(x_{12}, x_{12}) \right], \end{aligned} \tag{B.64}$$

with

$$F_N(x,x) \equiv \frac{x(1+x)\ln x}{(1-x)^2} + \frac{2}{1-x}. \tag{B.65}$$

Therefore, Eq. (B.57) becomes

$$i\mathcal{M} = \bar{u}(p+q) \frac{-ih_{11}^n f' f_\tau \sin\theta_L \cos\theta_R \sin\theta_\tau \cos\theta_\tau}{16\pi^2} \left[F_N(x_{11}, x_{11}) - F_N(x_{12}, x_{12}) \right] u(p). \tag{B.66}$$

The amplitude for the second diagram in Fig. B.3 can be written as

$$\begin{aligned} i\mathcal{M}_{LR} = &\int \frac{d^4k}{(2\pi)^4} \bar{u}(p+q) \left(if_\tau^* P_L \sin\theta_R \right) \frac{i\left(\not{k} + \not{q} + m_{n_2}\right)}{(q+k)^2 - m_{n_2}^2 + i\epsilon} \left(ih_{12}^n \sin\theta_\tau \cos\theta_\tau \right) \\ &\times \frac{i\left(\not{k} + m_{n_1}\right)}{k^2 - m_{n_1}^2 + i\epsilon} \left(-if' \sin\theta_L P_L \right) \frac{i}{(p-k)^2 - m_{\xi_1}^2 + i\epsilon} u(p) \\ = &\bar{u}(p+q) \int \frac{d^4k}{(2\pi)^4} \frac{\left[f' f_\tau^* \sin\theta_L \sin\theta_R \sin\theta_\tau \cos\theta_\tau \right] \left[h_{12}^{nR} \left(\not{k} + \not{q}\right) \not{k} P_L + h_{12}^{nL} m_{n_2} m_{n_1} P_L \right]}{\left[(q+k)^2 - m_{n_1}^2 + i\epsilon \right] \left[k^2 - m_{n_1}^2 + i\epsilon \right] \left[(p-k)^2 - m_{\xi_1}^2 + i\epsilon \right]} u(p). \end{aligned} \tag{B.67}$$

Now, we write the amplitude for the third diagram in Fig. B.4 as $i\mathcal{M} = \bar{u}(p+q)\mathcal{O}_{\mathrm{RL}} u(p)$, where

$$\mathcal{O}_{\mathrm{RL}} = \int \frac{d^4k}{(2\pi)^4} \frac{\left[f' f_\tau^* \sin\theta_L \sin\theta_R \sin\theta_\tau \cos\theta_\tau \right] \left[h_{21}^{nL} \left(\not{k} + \not{q}\right) \not{k} P_R + h_{21}^{nR} m_{n_2} m_{n_1} P_R \right]}{\left[(q+k)^2 - m_{n_1}^2 + i\epsilon \right] \left[k^2 - m_{n_1}^2 + i\epsilon \right] \left[(p-k)^2 - m_{\xi_1}^2 + i\epsilon \right]}. \tag{B.68}$$

Since $h_{21}^{nL} = h_{12}^{nR}$ and $h_{21}^{nR} = h_{12}^{nL}$, addition of Eq. (B.67) and Eq. (B.68) becomes

$$\mathcal{O} = \int \frac{d^4k}{(2\pi)^4} \frac{\left[f' f_\tau^* \sin\theta_L \sin\theta_R \sin\theta_\tau \cos\theta_\tau \right] \left[h_{12}^{nR} \left(\not{k} + \not{q}\right) \not{k} + h_{12}^{nL} m_{n_2} m_{n_1} \right]}{\left[(q+k)^2 - m_{n_1}^2 + i\epsilon \right] \left[k^2 - m_{n_1}^2 + i\epsilon \right] \left[(p-k)^2 - m_{\xi_1}^2 + i\epsilon \right]}. \tag{B.69}$$

Then Eq. (B.52) changes to

$$\Delta_{\xi_1} \approx \left(m_{n_1}^2 - m_{\xi_1}^2\right) y + \left(m_{n_2}^2 - m_{\xi_1}^2\right) z + m_{\xi_1}^2 \tag{B.70}$$

Eqs. (B.58) to (B.63) still holds with the new Δ in Eq. (B.70), and $m_{n_1}^2$ replaced by $m_{n_1} m_{n_2}$.

The analogous to Eq. (B.64) is then given by

$$\begin{aligned} I(m_{n_1}, m_{n_2}, m_{\xi_1}) + & I(m_{n_1}, m_{n_2}, m_{\xi_2}) = \\ &= \iint dxdy \frac{i}{4\pi^2} \left[\frac{h_{12}^{nR}}{2} \ln\left(\frac{\Delta_{\xi_2}}{\Delta_{\xi_1}}\right) - \frac{h_{12}^{nL} m_{n_1} m_{n_2}}{4} \left(\frac{1}{\Delta_{\xi_1}} - \frac{1}{\Delta_{\xi_2}}\right) \right] \\ &= \frac{-i}{8\pi^2} \iint dxdy \left[h_{12}^{nR} \ln\left(\frac{\Delta_{\xi_1}}{\Delta_{\xi_2}}\right) - \frac{h_{12}^{nL} m_{n_1} m_{n_2}}{2} \left(\frac{1}{\Delta_{\xi_2}} - \frac{1}{\Delta_{\xi_1}}\right) \right]. \end{aligned} \tag{B.71}$$

The second part of the integral is

$$\frac{-i}{8\pi^2} \iint dxdy \frac{m_{n_1} m_{n_2}}{2} \frac{1}{\Delta_{\xi_1}} = \frac{-i}{16\pi^2} \frac{m_{n_2}}{m_{n_1}} K_1(x_{11}, x_{21}), \tag{B.72}$$

$$\frac{-i}{8\pi^2} \iint dxdy \frac{m_{n_1} m_{n_2}}{2} \frac{-1}{\Delta_{\xi_2}} = \frac{i}{16\pi^2} \frac{m_{n_2}}{m_{n_1}} K_1(x_{12}, x_{22}), \tag{B.73}$$

$$\longrightarrow \frac{i}{8\pi^2} \iint dxdy \frac{m_{n_1} m_{n_2}}{2} \left(\frac{1}{\Delta_{\xi_2}} - \frac{1}{\Delta_{\xi_1}}\right) = \frac{-i}{16\pi^2} \frac{m_{n_2}}{m_{n_1}} \left[K_1(x_{11}, x_{21}) - K_1(x_{12}, x_{22})\right]. \tag{B.74}$$

where,

$$K_1(x, y) \equiv \frac{y}{x - y} \left[\frac{1}{y - 1} \ln y - \frac{1}{x - 1} \ln x \right]. \tag{B.75}$$

The first part is given by

$$\frac{-i}{8\pi^2} \iint dxdy \ln\left(\frac{\Delta_{\xi_1}}{\Delta_{\xi_2}}\right) = \frac{-i}{16\pi^2} \left[K_2(x_{11}, x_{21}) - K_2(x_{12}, x_{22})\right], \tag{B.76}$$

where,

$$K_2(x, y) \equiv \frac{x}{x - y} \left[\frac{x - y - 1}{x - 1} \ln x + \frac{1}{y - 1} \ln y \right]. \tag{B.77}$$

Eq. (B.71) becomes

$$I(m_{n_1}, m_{n_2}, m_{\xi_1}) + I(m_{n_1}, m_{n_2}, m_{\xi_2}) = \frac{-i}{16\pi^2}\left[\frac{h_{12}^{nL} m_{n_2}}{m_{n_1}}\left[K_1(x_{11}, x_{21}) - K_1(x_{12}, x_{22})\right]\right.$$
$$\left. + h_{12}^{nR}\left[K_2(x_{11}, x_{21}) - K_2(x_{12}, x_{22})\right]\right]. \tag{B.78}$$

After plugging Eq. (B.78) into Eq. (B.71) we get the effective coupling generated by the second and sixth diagrams in Fig. B.3 and third and seventh diagrams in Fig. B.4

$$f_{12}^N = \frac{f' f_\tau \sin\theta_L \sin\theta_R \sin\theta_\tau \cos\theta_\tau}{16\pi^2}\left[\frac{h_{12}^{nL} m_{n_2}}{m_{n_1}}\left[K_1(x_{11}, x_{21}) - K_1(x_{12}, x_{22})\right]\right.$$
$$\left. + h_{12}^{nR}\left[K_2(x_{11}, x_{21}) - K_2(x_{12}, x_{22})\right]\right] \tag{B.79}$$

We can also find f_{11}^N from Eq. (B.66)

$$f_{11}^N = \frac{h_{11}^n f' f_\tau \sin\theta_L \cos\theta_R \sin\theta_\tau \cos\theta_\tau}{16\pi^2}\left[F_N(x_{11}, x_{11}) - F_N(x_{12}, x_{12})\right]. \tag{B.80}$$

The rest of the effective couplings can now be written by changing the indices and coefficients as follows

$$f_{21}^N = \frac{-f' f_\tau \cos\theta_L \cos\theta_R \sin\theta_\tau \cos\theta_\tau}{16\pi^2}\left[\frac{h_{21}^{nL} m_{n_1}}{m_{n_2}}\left[K_1(x_{21}, x_{11}) - K_1(x_{22}, x_{12})\right]\right.$$
$$\left. + h_{21}^{nR}\left[K_2(x_{21}, x_{11}) - K_2(x_{22}, x_{12})\right]\right] \tag{B.81}$$

$$f_{22}^N = \frac{-h_{22}^n f' f_\tau \cos\theta_L \sin\theta_R \sin\theta_\tau \cos\theta_\tau}{16\pi^2}\left[F_N(x_{22}, x_{22}) - F_N(x_{21}, x_{21})\right] \tag{B.82}$$

The total effective Yukawa coupling including the ones from Eqs. (B.38) to (B.41) is then given by

$$f_{h\tau\tau} = f_{11}^\xi + f_{12}^\xi + f_{21}^\xi + f_{22}^\xi + f_{11}^N + f_{12}^N + f_{21}^N + f_{22}^N. \tag{B.83}$$

B.3 The Higgs Yukawa Coupling in the Limit: $\theta_L = \theta_R$

If we set $\theta_L = \theta_R$, then we get the following relations for f_D nd f_F

$$\frac{f_D v}{\sqrt{2}} = m_{n_1} \cos\theta_L \sin\theta_R - m_{n_2} \cos\theta_R \sin\theta_L = (m_{n_1} - m_{n_2}) \cos\theta_L \sin\theta_L, \tag{B.84}$$

$$\frac{f_F v}{\sqrt{2}} = m_{n_1} \cos\theta_R \sin\theta_L - m_{n_2} \cos\theta_L \sin\theta_R = (m_{n_1} - m_{n_2}) \cos\theta_L \sin\theta_L. \tag{B.85}$$

Also, h^n_{ij} coefficients will be simplified as follows

$$h^n_{11} = -h^n_{22} = \frac{-f_D \sin 2\theta_L}{\sqrt{2}} = \frac{-(m_{n_1} - m_{n_2}) \sin^2 2\theta_L}{2v}, \tag{B.86}$$

$$h^{nL}_{12} = h^{nR}_{12} = h^{nR}_{21} = h^{nL}_{21} = \frac{f_D \cos 2\theta_L}{\sqrt{2}} = \frac{(m_{n_1} - m_{n_2}) \sin 2\theta_L \cos 2\theta_L}{2v}. \tag{B.87}$$

We find the ratio of the effective Yukawa coupling to tau mass in the case that λ_{y_3} and λ_x are set to zero to be

$$\begin{aligned}\frac{fv}{m_\tau} = (m_{n_1} - m_{n_2}) \Bigg(& \frac{[F_N(x_{12}, x_{12}) - F_N(x_{11}, x_{11}) - F_N(x_{22}, x_{22}) + F_N(x_{21}, x_{21})] \sin^2 2\theta_L}{2\left(m_{n_1}[H(x_{12}) - H(x_{11})] + m_{n_2}[H(x_{21}) - H(x_{22})]\right)} \\ & + \frac{[m_{n_1}[K_1(x_{22}, x_{12}) - K_1(x_{21}, x_{11})] + m_{n_2}[K_2(x_{22}, x_{12}) - K_2(x_{21}, x_{11})]] \cos^2\theta_L \cos 2\theta_L}{m_{n_2}\left(m_{n_1}[H(x_{12}) - H(x_{11})] + m_{n_2}[H(x_{21}) - H(x_{22})]\right)} \\ & + \frac{[m_{n_2}[K_1(x_{11}, x_{21}) - K_1(x_{12}, x_{22})] + m_{n_1}[K_2(x_{11}, x_{21}) - K_2(x_{12}, x_{22})]] \sin^2\theta_L \cos 2\theta_L}{m_{n_1}\left(m_{n_1}[H(x_{12}) - H(x_{11})] + m_{n_2}[H(x_{21}) - H(x_{22})]\right)} \Bigg)\end{aligned} \tag{B.88}$$

B.3.1 The Higgs Yukawa Coupling in the Limit: $\theta_L = \theta_R \longrightarrow 0$

If we set $\theta_L = \theta_R = 0$, the only non-zero term will come form Eq. (B.81), and we will have $f_D = f_F$. Using the definition of h in Eq. (B.16) we have

$$\begin{aligned}f_{h\tau\tau} = f^N_{21} = \frac{-f_D f' f_\tau \sin\theta_\tau \cos\theta_\tau}{16\pi^2\sqrt{2}} \Bigg[& \frac{m_{n_1}}{m_{n_2}} [K_1(x_{21}, x_{11}) - K_1(x_{22}, x_{12})] \\ & + K_2(x_{21}, x_{11}) - K_2(x_{22}, x_{12}) \Bigg]\end{aligned} \tag{B.89}$$

Recall the formula for tau mass (Eq. (A.77)):

$$m_\tau = (\frac{f' f_\tau \sin\theta_\tau \cos\theta_\tau}{16\pi^2}) \sin\theta_L \cos\theta_L \big(m_{n_1}[H(x_{12}) - H(x_{11})] + m_{n_2}[H(x_{21}) - H(x_{22})]\big). \tag{B.90}$$

We expect to retrieve the Standard Model Higgs coupling to tau, in the limit $\theta_{L,R} \longrightarrow 0$.

After taking this limit we get

$$\begin{aligned} \lim_{\theta_{L,R}\longrightarrow 0} \frac{fv}{m_\tau} &= \frac{(m_{n_1} - m_{n_2})\big[\frac{m_{n_1}}{m_{n_2}}[K_1(x_{22}, x_{12}) - K_1(x_{21}, x_{11})] + K_2(x_{22}, x_{12}) - K_2(x_{21}, x_{11})\big]}{m_{n_1}[H(x_{12}) - H(x_{11})] + m_{n_2}[H(x_{21}) - H(x_{22})]} \\ &= 1, \end{aligned} \tag{B.91}$$

which is what we expected.

Appendix C

Flavor Violating Processes:

$\mu \to e + \gamma$

The relevant terms for $\mu \to e + \gamma$ decay are given by ($q_e = -e$)

$$\mathcal{L} \supset f \left(\overline{E^0} \ , \quad E^+ \right)_R \left[\begin{pmatrix} \nu_e \\ e \end{pmatrix}_L s_1 + \begin{pmatrix} \nu_\mu \\ \mu \end{pmatrix}_L s_2 + \begin{pmatrix} \nu_\tau \\ \tau \end{pmatrix}_L s_3 \right] - e A_\nu E^+ \gamma^\nu E^- \qquad \text{(C.1)}$$

The corresponding diagrams are drawn in Fig. C.1. The amplitude for the first diagram

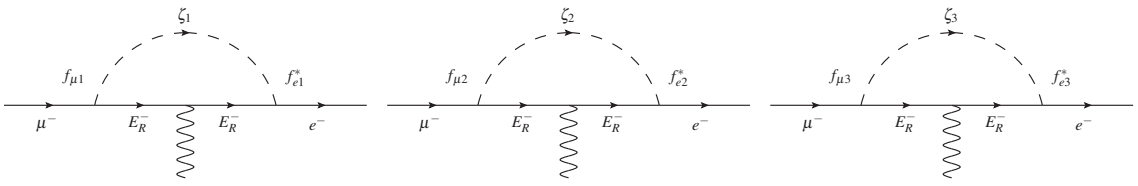

Figure C.1: Diagrams relevant to $\mu \to e + \gamma$ process.

can be written as

$$
\begin{aligned}
i\mathcal{M} = \int \frac{d^4k}{(2\pi)^4} \bar{u}_e(p-q)\,(if_{e1}^* P_R)\,\frac{i\left(\not{k}-\not{q}+m_{E_R}\right)}{(q-k)^2-m_{E_R}^2+i\epsilon}\,(-ie\epsilon_\nu^*\gamma^\nu)\,\frac{i\left(\not{k}+m_{E_R}\right)}{k^2-m_{E_R}^2+i\epsilon}\,(if_{\mu 1}P_L) \\
\times \frac{i}{(p-k)^2-m_{\zeta_1}^2+i\epsilon} u_\mu(p) \\
= \bar{u}_e(p-q)\,\mathcal{O}\,u_\mu(p),
\end{aligned}
\tag{C.2}
$$

where

$$
\mathcal{O} = \int \frac{d^4k}{(2\pi)^4} \frac{e f_{e1}^* f_{\mu 1}\left[\left(\not{k}-\not{q}\right)\not{\epsilon}^*\not{k}+\not{\epsilon}^* m_{E_R}^2\right]P_L}{\left[(q-k)^2-m_{E_R}^2+i\epsilon\right]\left[k^2-m_{E_R}^2+i\epsilon\right]\left[(p-k)^2-m_{\zeta_1}^2+i\epsilon\right]}. \tag{C.3}
$$

We can use feynman parameters like on P. 153

$$
\frac{1}{ABC} = \iiint dx\,dy\,dz\,\delta(x+y+z-1)\frac{2}{D^3}, \quad D = xA+yB+zC. \tag{C.4}
$$

Such that

$$
\frac{1}{\left[(p-k)^2-m_{\zeta_1}^2+i\epsilon\right]\left[k^2-m_{E_R}^2+i\epsilon\right]\left[(k-q)^2-m_{E_R}^2+i\epsilon\right]}, \tag{C.5}
$$

can be written as

$$
\iiint dx\,dy\,dz\,\delta(x+y+z-1)\frac{2}{D^3}, \tag{C.6}
$$

with $D = x\left[(p-k)^2-m_{\zeta_1}^2+i\epsilon\right]+y\left[k^2-m_{E_R}^2+i\epsilon\right]+z\left[(k-q)^2-m_{E_R}^2+i\epsilon\right].$

$$
\begin{aligned}
D &= x\left[k^2+p^2-2k.p-m_{\zeta_1}^2\right]+yk^2-ym_{E_R}^2+z\left[k^2+q^2-2k.q\right]-zm_{E_R}^2+i\epsilon \\
&= k^2-2(zq+xp).k+\left(p^2-m_{\zeta_1}^2\right)x-ym_{E_R}^2+z\left(q^2-m_{E_R}^2\right)+i\epsilon
\end{aligned}
\tag{C.7}
$$

Therefore, D can be written in terms of l and Δ as follows

$$D = l^2 - \Delta + i\epsilon, \tag{C.8}$$

$$l^\mu \equiv k^\mu - zq^\mu - xp^\mu = k^\mu - (z+x)p^\mu + zp'^\mu, \tag{C.9}$$

$$\Delta \equiv z^2q^2 - z\left(q^2 - m_{E_R}^2\right) + x^2p^2 + 2xz\,(p.q) - x\left(p^2 - m_{\zeta_1}^2\right) + ym_{E_R}^2 \approx xm_{\zeta_1}^2 + (y+z)m_{E_R}^2. \tag{C.10}$$

The first part of the numerator in Eq. (C.2) can be written as (we are ignoring $\not{\epsilon}^* m_{E_R}^2$ for now.)

$$\begin{aligned}\bar{u}_e(p')\left[\left(\not{k} - \not{q}\right)\not{\epsilon}^*\not{k}\right]P_L u_\mu(p) &= \bar{u}_e(p')\left[\not{l} - y\not{p} + (x+y)\not{p}'\right]\not{\epsilon}^*\left[\not{l} + (1-y)\not{p} - z\not{p}'\right]P_L u_\mu(p) \\ &= \bar{u}_e(p')\left[\not{l} - y\not{p} + (x+y)m_e\right]\not{\epsilon}^*\left[\not{l} - z\not{p}'\right]P_L u_\mu(p) + \bar{u}_e(p')\left[\not{l} - y\not{p} + (x+y)m_e\right]\not{\epsilon}^* \\ &\quad \times \left[(1-y)m_\mu\right]P_R u_\mu(p).\end{aligned} \tag{C.11}$$

We expand the terms in Eq. (C.11) to get

$$\not{l}\not{\epsilon}^*\not{l}P_L + zy\not{p}\not{\epsilon}^*\not{p}'P_L - z(x+y)m_e\not{\epsilon}^*\not{p}'P_L - y(1-y)\not{p}\not{\epsilon}^*m_\mu P_R + (x+y)m_e m_\mu(1-y)\not{\epsilon}^*P_R. \tag{C.12}$$

The first term in Eq. (C.12) is

$$\not{l}\not{\epsilon}^*\not{l}P_L = \left[2l.\epsilon^* - \not{\epsilon}^*\not{l}\right]\not{l}P_L = \left[2l.\epsilon^*\not{l} - \not{\epsilon}^* l^2\right]P_L. \tag{C.13}$$

The second term in Eq. (C.12) is

$$\begin{aligned}yz\left[\not{p}\not{\epsilon}^*\not{p}'\right]P_L &= yz\left[2p.\epsilon^* - \not{\epsilon}^*\not{p}\right]\not{p}'P_L = yz\left[2p.\epsilon^*\not{p}' - \not{\epsilon}^*\not{p}\not{p}'\right]P_L \\ &= yz\left[2p.\epsilon^*\not{p}' - \not{\epsilon}^*\left[2p.p' - \not{p}'\not{p}\right]\right]P_L \\ &= yz\left[2p.\epsilon^*\not{p}' - 2p.p'\not{\epsilon}^* + \left[2\epsilon^*.p' - \not{p}'\not{\epsilon}^*\right]\not{p}\right]P_L \\ &= yz\left[2p.\epsilon^*\not{p}' - 2p.p'\not{\epsilon}^* + 2\epsilon^*.p'\not{p} - \not{p}'\not{\epsilon}^*\not{p}\right]P_L.\end{aligned} \tag{C.14}$$

The third term in Eq. (C.12) is

$$-z(x+y)m_e\left[\not{\epsilon}^*\not{p}'\right]P_L = -z(x+y)m_e\left[2p'.\epsilon^* - \not{p}'\not{\epsilon}^*\right]P_L. \tag{C.15}$$

The fourth term in Eq. (C.12) is

$$-y(1-y)m_\mu\left[\not{p}\not{\epsilon}^*\right]P_R = -y(1-y)m_\mu\left[2p.\epsilon^* - \not{\epsilon}^*\not{p}\right]P_R. \tag{C.16}$$

After adding all of these terms together, Eq. (C.11) can now be written as

$$\begin{aligned}\bar{u}_e(p')\Big[&(2l.\epsilon^*\not{l} - \not{\epsilon}^* l^2)P_L + yz(2p.\epsilon^* m_e - 2p.p'\not{\epsilon}^*)P_L + yzm_\mu(2\epsilon^*.p' - m_e\not{\epsilon}^*)P_R \\ &- z(x+y)m_e(2p'.\epsilon^* - m_e\not{\epsilon}^*)P_L + m_\mu(1-y)((x+y)m_e\not{\epsilon}^* - 2y\epsilon^*.p)P_R \\ &+ y(1-y)m_\mu^2\not{\epsilon}^* P_L\Big]u_\mu(p).\end{aligned} \tag{C.17}$$

We rewrite Eq. (C.17) by making the following replacements:

$$P = p + p' \longrightarrow\ p = \frac{P+q}{2} \tag{C.18}$$

$$q = p - p' \longrightarrow\ p' = \frac{P-q}{2}, \tag{C.19}$$

to get

$$\begin{aligned}\bar{u}_e(p')\Big[&\left(2l.\epsilon^*\not{l} - \not{\epsilon}^* l^2\right)P_L + yz\left((P+q).\epsilon^* m_e - \frac{(P^2-q^2)}{2}\not{\epsilon}^*\right)P_L \\ &+ yzm_\mu\left(\epsilon^*.(P-q) - m_e\not{\epsilon}^*\right)P_R - z(x+y)m_e\left((P-q).\epsilon^* - m_e\not{\epsilon}^*\right)P_L \\ &+ m_\mu(1-y)\left((x+y)m_e\not{\epsilon}^* - y\epsilon^*.(P+q)\right)P_R + y(1-y)m_\mu^2\not{\epsilon}^* P_L\Big]u_\mu(p).\end{aligned} \tag{C.20}$$

We now Factor the terms proportional to γ_μ, P_μ and q_μ. We also add the term that we omitted in Eq. (C.11), i.e., $\not{\epsilon}^* m_{E_R}^2$ to get

$$\begin{aligned}
&\bar{u}_e(p')\left[(yz - z(x+y))\, m_e P_L + (yz - y(1-y))\, m_\mu P_R\right](\epsilon^*.P)u_\mu(p) \\
&+\bar{u}_e(p')\left[(yz + z(x+y))m_e P_L - (yz + y(1-y))m_\mu P_R\right](\epsilon^*.q)u_\mu(p) \\
&+\bar{u}_e(p')\left[\left(-\frac{l^2}{2} - \frac{yz(P^2-q^2)}{2} + z(x+y)m_e^2 + y(1-y)m_\mu^2 + m_{E_R}^2\right)P_R\right. \\
&\qquad \left. -(yz - (1-y)(x+y))\, m_e m_\mu\, P_L\right](\epsilon^*.\gamma)\, u_\mu(p).
\end{aligned} \tag{C.21}$$

Note that $\epsilon^*.q = 0$, so that only terms proportional to γ_μ and P_μ survive. Thus we simplify Eq. (C.21) further to get

$$\begin{aligned}
&\bar{u}_e(p')\left[\left(-\frac{l^2}{2} - \frac{yz(P^2-q^2)}{2} + z(x+y)m_e^2 + y(1-y)m_\mu^2 + m_{E_R}^2\right)P_R + xP_L\right](\epsilon^*.\gamma)\, u_\mu(p) \\
&+\bar{u}_e(p')\left[-zxm_e P_L - yxm_\mu P_R\right](\epsilon^*.P)\, u_\mu(p).
\end{aligned} \tag{C.22}$$

We make another replacement using the Gordon's identity:

$$\bar{u}_e(p')\left[P^\mu\right]P_R u_\mu(p) = \bar{u}_e(p')\left[i\sigma^{\mu\nu}q_\nu P_R + m_e\gamma^\mu P_R + m_\mu\gamma^\mu P_L\right]u_\mu(p) \tag{C.23}$$

$$\bar{u}_e(p')\left[P^\mu\right]P_L u_\mu(p) = \bar{u}_e(p')\left[i\sigma^{\mu\nu}q_\nu P_L + m_e\gamma^\mu P_L + m_\mu\gamma^\mu P_R\right]u_\mu(p). \tag{C.24}$$

Eq. (C.22) now becomes

$$\begin{aligned}
&\bar{u}_e(p')\left[\left(-\frac{l^2}{2} - \frac{yz(P^2-q^2)}{2} + z(x+y)m_e^2 + y(1-y)m_\mu^2 + m_{E_R}^2\right)P_R + xP_L\right](\epsilon^*.\gamma)\, u_\mu(p) \\
&+\bar{u}_e(p')\left[-zxm_e P_L - yxm_\mu P_R\right]\left(i\epsilon_\mu^*\sigma^{\mu\nu}q_\nu\right)u_\mu(p) \\
&+\bar{u}_e(p')\left[-zxm_e\left(m_e\gamma^\mu P_L + m_\mu\gamma^\mu P_R\right) - yxm_\mu\left(m_e\gamma^\mu P_R + m_\mu\gamma^\mu P_L\right)\right]\epsilon_\mu^* u_\mu(p),
\end{aligned} \tag{C.25}$$

after combining terms involving γ^μ, we get

$$\begin{aligned}
&\bar{u}_e(p')\Bigg[\left(-\frac{l^2}{2}-\frac{yz(P^2-q^2)}{2}+z(x+y)m_e^2+y(1-y)m_\mu^2+m_{E_R}^2-x(zm_e^2+ym_\mu^2)\right)P_R\\
&\qquad+x\left(1-m_em_\mu(y+z)\right)P_L\Bigg](\epsilon^*.\gamma)\,u_\mu(p)\\
&+\bar{u}_e(p')\left[-zxm_eP_L-yxm_\mu P_R\right]\left(i\epsilon_\mu^*\sigma^{\mu\nu}q_\nu\right)u_\mu(p),
\end{aligned}\tag{C.26}$$

and after simplifying it we get

$$\begin{aligned}
&\bar{u}_e(p')\left[\left(-\frac{l^2}{2}-\frac{yz(P^2-q^2)}{2}+m_{E_R}^2+yz(m_e^2+m_\mu^2)\right)P_R+x\left(1-m_em_\mu(y+z)\right)P_L\right]\\
&\qquad\times(\epsilon^*.\gamma)\,u_\mu(p)\\
&+\bar{u}_e(p')\left[-zxm_eP_L-yxm_\mu P_R\right]\left(i\epsilon_\mu^*\sigma^{\mu\nu}q_\nu\right)u_\mu(p).
\end{aligned}\tag{C.27}$$

We now focus on the integral of the $\sigma^{\mu\nu}q_\nu$ term only, since γ_μ terms cancel out the leg corrections

$$\begin{aligned}
i\mathcal{M}=&2ef_{e1}^*f_{\mu1}\bar{u}_e(p-q)\iiint dx\,dy\,dz\,\delta(x+y+z-1)\int\frac{d^4l}{(2\pi)^4}\frac{-zxm_eP_L-yxm_\mu P_R}{(l^2-\Delta+i\epsilon)^3}\\
&\left(i\epsilon_\mu^*\sigma^{\mu\nu}q_\nu\right)u_\mu(p)\\
=&2ef_{e1}^*f_{\mu1}\bar{u}_e(p-q)\iiint dxdydz\delta(x+y+z-1)\frac{-zxm_eP_L-yxm_\mu P_R}{32\pi^2\Delta}(\epsilon_\mu^*\sigma^{\mu\nu}q_\nu)u_\mu(p)\\
=&\frac{-ef_{e1}^*f_{\mu1}}{32\pi^2m_{E_R}^2}\bar{u}_e(p-q)\left[m_eG_\gamma(x_1)P_L+m_\mu G_\gamma(x_1)P_R\right]\epsilon_\mu^*\sigma^{\mu\nu}q_\nu u_\mu(p),
\end{aligned}\tag{C.28}$$

in which $x_1=\frac{m_{\zeta_1}^2}{m_{E_R}^2}$ and $G_\gamma(x)$ is given by

$$\frac{x_1}{2}G_\gamma(x_1)=\iint dxdy\frac{x(1-x-y)}{\Delta}=\frac{x_1\left(2x_1^3+3x_1^2-6x_1^2\ln x_1-6x_1+1\right)}{12(x_1-1)^4}.\tag{C.29}$$

Assuming $m_e \ll m_\mu$, the full amplitude and its conjugate for this process are given by

$$\mathcal{M} = \frac{iem_\mu}{32\pi^2 m_{E_R}^2}\bar{u}_e(p-q)[\epsilon_\mu^* \sigma^{\mu\nu} q_\nu P_R]u_\mu(p)[f_{e1}^* f_{\mu 1} G_\gamma(x_1) + f_{e2}^* f_{\mu 2} G_\gamma(x_2) + f_{e3}^* f_{\mu 3} G_\gamma(x_3)], \tag{C.30}$$

$$\mathcal{M}^\dagger = \frac{-iem_\mu}{32\pi^2 m_{E_R}^2}\bar{u}_\mu(p)[P_L \epsilon_\mu \sigma^{\mu\nu} q_\nu]u_e(p-q)[f_{e1} f_{\mu 1}^* G_\gamma(x_1) + f_{e2} f_{\mu 2}^* G_\gamma(x_2) + f_{e3} f_{\mu 3}^* G_\gamma(x_3)], \tag{C.31}$$

We can find the squared matrix element and sum over the electron spin and photon polarization as follows

$$\begin{aligned}
\overline{|\mathcal{M}|^2} =& \frac{e^2 m_\mu^2 |\sum_i f_{ei}^* f_{\mu i} G_\gamma(x_i)|^2}{2 \times 1024\pi^4 m_{E_R}^4} \sum_{\epsilon, s_e, s_\mu} [\bar{u}_e(p-q)[\epsilon_\alpha^* \sigma^{\alpha\beta} q_\beta P_R]u_\mu(p)\bar{u}_\mu(p)[P_L \epsilon_\mu \sigma^{\mu\nu} q_\nu]u_e(p-q)] \\
=& \frac{e^2 m_\mu^2 |\sum_i f_{ei}^* f_{\mu i} G_\gamma(x_i)|^2}{2048\pi^4 m_{E_R}^4} \sum_{\epsilon, s_e} [\bar{u}_e(p-q)[\epsilon_\alpha^* \sigma^{\alpha\beta} q_\beta P_R][\not{p} + m_\mu][P_L \epsilon_\mu \sigma^{\mu\nu} q_\nu]u_e(p-q)] \\
=& \frac{e^2 m_\mu^2 |\sum_i f_{ei}^* f_{\mu i} G_\gamma(x_i)|^2}{2048\pi^4 m_{E_R}^4} \sum_{\epsilon, s_e} \bar{u}_e(p-q)[\epsilon_\alpha^* \sigma^{\alpha\beta} q_\beta]\not{p}[P_L \epsilon_\mu \sigma^{\mu\nu} q_\nu]u_e(p-q)] \\
=& \frac{-e^2 m_\mu^2 |\sum_i f_{ei}^* f_{\mu i} G_\gamma(x_i)|^2}{2048\pi^4 m_{E_R}^4} Tr[(\not{p} - \not{q} + m_e)[g_{\alpha\mu} \sigma^{\alpha\beta} q_\beta]\not{p}[P_L \sigma^{\mu\nu} q_\nu]] \\
=& \frac{e^2 m_\mu^2 |\sum_i f_{ei}^* f_{\mu i} G_\gamma(x_i)|^2}{4 \times 2048\pi^4 m_{E_R}^4} Tr[(\not{p} - \not{q} + m_e)[(\gamma_\mu \gamma^\beta - \gamma^\beta \gamma_\mu) q_\beta]\not{p}[P_L(\gamma^\mu \gamma^\nu - \gamma^\nu \gamma^\mu) q_\nu]] \\
=& \frac{e^2 m_\mu^2 |\sum_i f_{ei}^* f_{\mu i} G_\gamma(x_i)|^2}{4 \times 2048\pi^4 m_{E_R}^4} Tr[(\not{p} - \not{q} + m_e)[8p.q\not{q} + 4\not{q}\not{p}\not{q}]P_L] \\
=& \frac{e^2 m_\mu^2 |\sum_i f_{ei}^* f_{\mu i} G_\gamma(x_i)|^2}{4 \times 2048\pi^4 m_{E_R}^4} [32(p.q)^2] = \frac{e^2 m_\mu^2 |\sum_i f_{ei}^* f_{\mu i} G_\gamma(x_i)|^2}{256\pi^4 m_{E_R}^4} (p.q)^2 \\
=& \frac{e^2 m_\mu^6 |\sum_i f_{ei}^* f_{\mu i} G_\gamma(x_i)|^2}{1024\pi^4 m_{E_R}^4},
\end{aligned} \tag{C.32}$$

in which the last equality holds in the CM refrence frame. The decay width can now be written as

$$\Gamma(\mu \to e\gamma) = \frac{p_f}{32\pi^2 m_\mu^2} \int \overline{|\mathcal{M}|^2} d\Omega = \frac{m_\mu^5}{4 \times 4096} \frac{e^2 |\sum_i f_{ei}^* f_{\mu i} G_\gamma(x_i)|^2}{\pi^5 m_{E_R}^4}, \tag{C.33}$$

and the branching ratio is given by

$$Br(\mu \to e\gamma) = \frac{192\pi^3 m_\mu^5}{4 \times 4096} \frac{e^2 |\sum_i f_{ei}^* f_{\mu i} G_\gamma(x_i)|^2}{G_F^2 m_\mu^5 \pi^5 m_{E_R}^4} = \frac{3}{256} \frac{e^2 |\sum_i f_{ei}^* f_{\mu i} G_\gamma(x_i)|^2}{G_F^2 \pi^2 m_{E_R}^4}. \tag{C.34}$$

Appendix D

Neutrino Textures from Seesaw

A list of possible neutrino textures driven from $m_\nu = m_D M_N^{-1} m_D^T$ is presented. The Dirac mass matrix, m_D must have *at least* three zeros as shown bellow. However, the other non-diagonal elements of m_D can be zero, without changing the texture of m_ν. We used Ref. [179] to check the status of each of these configurations.

$$N_R : \begin{pmatrix} \times & \times & \times \\ \times & \times & 0 \\ \times & 0 & 0 \end{pmatrix}, \quad m_D : \begin{pmatrix} \times & 0 & 0 \\ \times & \times & 0 \\ \times & \times & \times \end{pmatrix} \longrightarrow m_\nu : \begin{pmatrix} 0 & 0 & \times \\ 0 & \times & \times \\ \times & \times & \times \end{pmatrix} \tag{D.1}$$

This texture is suitable for a best fit to current neutrino-oscillation data with normal ordering of neutrino masses.

$$N_R : \begin{pmatrix} \times & \times & \times \\ \times & 0 & 0 \\ \times & 0 & \times \end{pmatrix}, \quad m_D : \begin{pmatrix} \times & 0 & 0 \\ \times & \times & \times \\ \times & 0 & \times \end{pmatrix} \longrightarrow m_\nu : \begin{pmatrix} 0 & \times & 0 \\ \times & \times & \times \\ 0 & \times & \times \end{pmatrix} \tag{D.2}$$

This texture is suitable for a 2σ fit to current neutrino-oscillation data with normal ordering of neutrino masses.

$$N_R : \begin{pmatrix} 0 & \times & 0 \\ \times & \times & \times \\ 0 & \times & \times \end{pmatrix}, \quad m_D : \begin{pmatrix} \times & \times & \times \\ 0 & \times & 0 \\ 0 & \times & \times \end{pmatrix} \longrightarrow m_\nu : \begin{pmatrix} \times & \times & \times \\ \times & 0 & 0 \\ \times & 0 & \times \end{pmatrix} \tag{D.3}$$

This texture is ruled out at by 2σ from the best fit to current neutrino-oscillation data.

$$N_R : \begin{pmatrix} 0 & 0 & \times \\ 0 & \times & \times \\ \times & \times & \times \end{pmatrix}, \quad m_D : \begin{pmatrix} \times & \times & \times \\ 0 & \times & \times \\ 0 & 0 & \times \end{pmatrix} \longrightarrow m_\nu : \begin{pmatrix} \times & \times & \times \\ \times & \times & 0 \\ \times & 0 & 0 \end{pmatrix} \tag{D.4}$$

This texture is ruled out at by 2σ from the best fit to current neutrino-oscillation data.

$$N_R : \begin{pmatrix} \times & \times & 0 \\ \times & \times & \times \\ 0 & \times & 0 \end{pmatrix}, \quad m_D : \begin{pmatrix} \times & \times & 0 \\ 0 & \times & 0 \\ \times & \times & \times \end{pmatrix} \longrightarrow m_\nu : \begin{pmatrix} \times & 0 & \times \\ 0 & 0 & \times \\ \times & \times & \times \end{pmatrix} \tag{D.5}$$

This texture is suitable for a best fit to current neutrino-oscillation data with normal ordering of neutrino masses.

$$N_R : \begin{pmatrix} \times & 0 & \times \\ 0 & 0 & \times \\ \times & \times & \times \end{pmatrix}, \quad m_D : \begin{pmatrix} \times & 0 & \times \\ \times & \times & \times \\ 0 & 0 & \times \end{pmatrix} \longrightarrow m_\nu : \begin{pmatrix} \times & \times & 0 \\ \times & \times & \times \\ 0 & \times & 0 \end{pmatrix} \tag{D.6}$$

This texture is suitable for a 2σ fit to current neutrino-oscillation data with inverse ordering of neutrino masses.